



저작자표시-비영리-변경금지 2.0 대한민국

이용자는 아래의 조건을 따르는 경우에 한하여 자유롭게

- 이 저작물을 복제, 배포, 전송, 전시, 공연 및 방송할 수 있습니다.

다음과 같은 조건을 따라야 합니다:



저작자표시. 귀하는 원저작자를 표시하여야 합니다.



비영리. 귀하는 이 저작물을 영리 목적으로 이용할 수 없습니다.



변경금지. 귀하는 이 저작물을 개작, 변형 또는 가공할 수 없습니다.

- 귀하는, 이 저작물의 재이용이나 배포의 경우, 이 저작물에 적용된 이용허락조건을 명확하게 나타내어야 합니다.
- 저작권자로부터 별도의 허가를 받으면 이러한 조건들은 적용되지 않습니다.

저작권법에 따른 이용자의 권리는 위의 내용에 의하여 영향을 받지 않습니다.

이것은 [이용허락규약\(Legal Code\)](#)을 이해하기 쉽게 요약한 것입니다.

[Disclaimer](#)

이학박사 학위논문

**Design, synthesis and evaluation of substituted
N-methyl-*N*-(pyrrolidin-3-yl)-7*H*-pyrrolo[2,3-
d]pyrimidin-4-amines as JAK1-selective
inhibitors for the treatment of rheumatoid
arthritis**

**류마티스 관절염 치료를 위한 JAK1 선택적
억제제로서의 *N*-메틸-*N*-(피롤리딘-3-일)-7*H*-
피롤로[2,3-*d*]피리미딘-4-아민의 설계, 합성 및
평가**

2 0 1 8년 2월

서울대학교 대학원

화학부 유기화학 전공

조 지 연

이학박사 학위논문

Design, synthesis and evaluation of substituted
N-methyl-*N*-(pyrrolidin-3-yl)-7*H*-pyrrolo[2,3-*d*]pyrimidin-4-amines
as JAK1-selective inhibitors for the treatment of rheumatoid
arthritis

지도교수 김 병 문

이 논문을 이학박사 학위논문으로 제출함
2017년 12월

서울대학교 대학원
화학부 유기화학전공
조 지 연

조지연의 이학박사 학위논문을 인준함
2018년 02월

위 원 장

홍 중 인 (인)

부위원장

김 병 문 (인)

위 원

홍 근 혁

위 원

이 홍 근

위 원

이 석 재

CONTENTS

Abstract	3
List of Figures	4
List of Schemes	6
List of Tables	7
I. Introduction	10
II. Strategy	13
III. Synthesis	16
IV. Results and Discussions	20
V. Conclusions	62
VI. Experimental Section	64
References	135
NMR Spectra	145
국문초록	239
감사의 글	240

Abstract

Design, synthesis and evaluation of substituted *N*-methyl-*N*-(pyrrolidin-3-yl)-7*H*-pyrrolo[2,3-*d*]pyrimidin-4-amines as JAK1-selective inhibitors for the treatment of rheumatoid arthritis*

Based on (*R*)-*N*-methyl-*N*-(5-azaspiro[2.4]heptan-7-yl)-7*H*-pyrrolo[2,3-*d*]pyrimidin-4-amine as a core scaffold, we identified (*R*)-3-(7-(methyl(7*H*-pyrrolo[2,3-*d*]pyrimidin-4-yl)amino)-5-azaspiro[2.4]heptan-5-yl)-3-oxopropanenitrile [(**R**)-**6c**] as a JAK1 selective inhibitor. The structural design was based on the combination of tofacitinib's 7-deazapurine and 5-azaspiro[2.4]heptan-7-amine. Compound (**R**)-**6c** exhibited 8.5 nM IC₅₀ on JAK1 with a selectivity index of 48 over JAK2. To optimize (**R**)-**6c** as a lead compound, we performed cell-based functional assays, human whole blood tests, *in vitro* ADME, hERG, kinase profiling, and pharmacokinetic tests. Rat *in vivo* studies verified that (**R**)-**6c** exhibited desired efficacies on CIA and AIA models.

Key words: JAK inhibitor, rheumatoid arthritis, JAK1-selective, collagen-induced arthritis mouse model, adjuvant-induced arthritis rat model

* The parts of the thesis were submitted as research articles in *MedChemComm* and *Bioorganic and Medicinal Chemistry* in 2017

List of Figures

Figure 1. Interactions of tofacitinib with JAK1 or JAK2.

Figure 2. Docking simulation of a) tofacitinib and b) compound **12a** at JAK2 (PDB ID: 3FUP) and c) overlay of the lowest conformations of tofacitinib (red color) and compound **12a** at JAK2.

Figure 3. Design strategy by changing the piperidine moiety A.

Figure 4. The kinome tree of (**R**)-**6c** and **12a** against 323 kinases at the 10 μ M concentration drawn by the web accessible Kinome Render program.

Figure 5. Plasma concentrations after oral administration and intravenous injection of (**R**)-**6** and **12a** in Beagle dogs, Sprague-Dawley rats, and ICR mice.

Figure 6. Plasma concentrations after oral administration and intravenous injection of the free base and the salt forms of (**R**)-**6c** and **12a** in Sprague-Dawley rats.

Figure 7. a) Clinical arthritis scores and b) paw volumes of (**R**)-**6c** and **12a** treatment on collagen-induced arthritis in DBA/1J mice for 18 days.

Figure 8. Effects of (**R**)-**6c** and **12a** treatment on collagen-induced arthritis in DBA/1J mice: a) the bone surface/volume ratios of right hind ankle joints measured by micro-CT, b) the histopathological semiquantitative scores of right hind ankle joints, c) the right hind ankle joint thicknesses, d-e) the articular surface cartilage thicknesses (tibia and talus) in right hind ankle joints, and f) the numbers of inflammatory cells infiltrated in the right hind ankle joints.

Figure 9. cytokine concentration changes in plasma by **(R)-6c** and **12a** treatment on collagen-induced arthritis in DBA/1J mice for 18 days: a) IL-1 β , b) IL-6, c) MCP-1, and d) TNF- α .

Figure 10. Effects of **(R)-6c** and **12a** treatment on adjuvant-induced arthritis in Lewis rats: a) the clinical arthritis scores and b) the volumes of right hind paws. The data were measured twice per week for 14 days.

List of Schemes

Scheme 1. Synthesis of inhibitors containing various heterocyclic core units replacing the aminopiperidine unit of tofacitinib and substituted *N*-methyl-*N*-(5-azaspiro[2.4]heptan-7-yl)-7*H*-pyrrolo[2,3-*d*]pyrimidin-4-amines.

Scheme 2. Synthesis of substituted (*R*)-*N*-alkyl-*N*-(pyrrolidin-3-yl)-7*H*-pyrrolo[2,3-*d*]pyrimidin-4-amines.

Scheme 3. Synthetic scheme of (*R*)-3-(7-(methyl(7*H*-pyrrolo[2,3-*d*]pyrimidin-4-yl)amino)-5-azaspiro[2.4]heptan-5-yl)-3-oxopropanenitrile, (*R*)-**6c**.

List of Tables

Table 1. Screening of the hydrophobic moieties (moiety A).

Table 2. Comparison of JAK1 IC₅₀ values of 3-(7-(methyl(7*H*-pyrrolo[2,3-*d*]pyrimidin-4-yl)amino)-5-azaspiro[2.4]heptan-5-yl)-3-oxopropanenitrile racemate and enantiomers.

Table 3. The IC₅₀ values of compound (***R***)-**6c** and **12a-c** against JAK1 and JAK2 and the selectivity indices of substituted (*R*)-*N*-methyl-*N*-(pyrrolidin-3-yl)-7*H*-pyrrolo[2,3-*d*]pyrimidin-4-amines according to the substitution at the 4-position of the pyrrolidine ring.

Table 4. The IC₅₀ values against JAK1 and JAK2 and the selectivity indices of substituted (*R*)-*N*-(pyrrolidin-3-yl)-7*H*-pyrrolo[2,3-*d*]pyrimidin-4-amines with varying R₁ and R₂ groups.

Table 5. The IC₅₀ values against JAK1 and JAK2 with the selectivity indices of substituted (*R*)-*N*-methyl-*N*-(5-azaspiro[2.4]heptan-7-yl)-7*H*-pyrrolo[2,3-*d*]pyrimidin-4-amines.

Table 6. The IC₅₀ values against JAK1 and JAK2 and the selectivity indices of substituted (*R*)-*N*-methyl-*N*-(pyrrolidin-3-yl)-7*H*-pyrrolo[2,3-*d*]pyrimidin-4-amines.

Table 7. The IC₅₀ values against cellular JAK1-JAK3 and JAK2 activity of substituted (*R*)-*N*-methyl-*N*-(pyrrolidin-3-yl)-7*H*-pyrrolo[2,3-*d*]pyrimidin-4-amines.

Table 8. Selectivity for individual JAK isozymes of substituted (*R*)-*N*-methyl-*N*-(pyrrolidin-3-yl)-7*H*-pyrrolo[2,3-*d*]pyrimidin-4-amines in cellular assays.

Table 9. Selectivity for JAK1 over JAK2 of substituted (*R*)-*N*-alkyl-*N*-

(pyrrolidin-3-yl)-7*H*-pyrrolo[2,3-*d*]pyrimidin-4-amines in human whole blood assays.

Table 10. Plasma stabilities.

Table 11. Plasma protein binding abilities and Log P values.

Table 12. Liver microsomal stabilities.

Table 13. Caco-2 permeabilities.

Table 14. The inhibition percentages against CYP₄₅₀ isoforms.

Table 15. Pharmacokinetic profiles of (*R*)-**6c**.

Table 16. Pharmacokinetic profiles of **12a**.

Table 17. Pharmacokinetic parameters of the free base and the salt forms of (*R*)-**6c** in Sprague-Dawley rats.

Table 18. Pharmacokinetic parameters of the free base and the salt forms of **12a** in Sprague-Dawley rats.

**Design, synthesis and evaluation of
substituted *N*-methyl-*N*-(pyrrolidin-
3-yl)-7*H*-pyrrolo[2,3-*d*]pyrimidin-4-
amines as JAK1-selective inhibitors
for the treatment of rheumatoid
arthritis**

I. Introduction

Rheumatoid arthritis (RA) is an autoimmune disease that affects approximately 1~2% of the worldwide population.¹⁻² Despite the high number afflicted by the disease, its pathogenesis and mechanism have still been elusive³ and target-oriented fundamental therapy for this disease has not yet been made available. Considerable work has been conducted for therapeutic targets⁴⁻⁵ and recently emerging molecular targets like cytokines,⁶⁻⁷ G-protein coupled receptors,⁸ and kinases⁹⁻¹⁰ have surfaced. The drugs and developing candidates against these targets are categorized as disease-modifying antirheumatic drugs (DMARDs).¹¹ The most commonly used drugs for this disease include conventional synthetic DMARDs, such as methotrexate, sulfasalazine, leflunomide, etc.¹² However, they cannot be used for long-term treatment due to the low therapeutic response and severe side effects. To overcome such limitations, researchers have developed biological DMARDs¹³ like etanercept, infliximab, and adalimumab. Although the biological DMARDs exhibit higher efficacies than synthetic ones, their applications also have several drawbacks due to the high cost, efficacy limitation on single administration,¹⁴ limited accessibility due to intravenous (i.v.) administration,¹⁵ etc.

To resolve the unmet medical needs in RA, many researchers have focused on developing new synthetic DMARDs equipped with high efficacy, low cost, and convenient administration regimen. As a result, Janus kinase (JAK)/signal transducer and activator of transcription (STAT) signal pathways have been identified as new therapeutic targets. JAK kinases had first been isolated in 1989¹⁶ and their roles were discovered in 1994.¹⁷ In the immune system, the sequential processes of this signaling proceeds as follows: 1) cytokines interact with extracellular membrane receptors, 2) a receptor pair is dimerized, 3) the dimer is combined with JAKs dependent upon the cytokines and the receptors, 4) the combined JAKs and dimer are phosphorylated, 5) STATs are introduced into the phosphorylated dimer, 6) the STATs are

phosphorylated (pSTAT) and separated from the dimer, 7) the separated STATs are dimerized and translocated into a nucleus, and 8) transcription of inflammation factors is triggered through the binding.¹⁸ The factors involved in the JAK-STAT signaling like the cytokines, receptors, STATs, and JAKs are related to many autoimmune diseases including rheumatoid arthritis, psoriasis, myelofibrosis, Crohn's disease, and ulcerative colitis. JAK3, out of four JAK isotypes, has received the most attention since it is mostly located in hematopoietic cells and affects the lymphoid cell function unlike others.¹⁹ In 2003, researchers at Pfizer reported tofacitinib as a JAK3 inhibitor.²⁰ Its median inhibitory concentrations (IC₅₀) measured by ELISA were described as 1 nM for JAK3, 20 nM for JAK2, and 112 nM for JAK1. However, other Pfizer workers published different inhibitory activities by peptide mobility shift assay in 2010,²¹ where the IC₅₀'s were 3.2, 4.1, 1.6, and 34.0 nM's for JAK1, JAK2, JAK3, and TYK2, respectively, rendering the tofacitinib a pan-JAK inhibitor. The fact that it suppresses all JAK-STAT signal pathways explains its excellent potencies in many preclinical²² and clinical trials²³⁻²⁵. Finally, tofacitinib became the first US Food and Drug Administration (FDA) approved oral drug for the treatment of rheumatoid arthritis in 2012²⁶ with the trade name Xeljanz.

Using Pan-JAK inhibitors like tofacitinib for treatment is accompanied by some drawbacks since they inhibit all JAK isoenzymes. In particular, preclinical studies²⁷⁻²⁹ and clinical trials³⁰⁻³¹ have revealed adverse effects derived from JAK2 inhibition like anemia, neutropenia, increased low and high density lipoprotein cholesterol levels, and elevated triglyceride levels. In the case of tofacitinib, similar adverse events have also been reported.^{24-25,32} As a result, European Medicines Agency (EMA) refused the marketing authorization in Europe.³³ To avoid the undesirable events mentioned above, selective inhibitors of isoenzymes, except for JAK2, for treatment of rheumatoid arthritis have been brought to researchers' attention.³⁴ Nowadays, the search for JAK1-selective inhibition has been given considerable attention since it has been revealed that JAK1 inhibition plays a principal role on the

efficacies of tofacitinib.³⁵ So, many researchers have been focusing on developing JAK1-selective inhibitors. The representative JAK1-selective inhibitors are filgotinib (GLPG0634),^{36,37-44} upadacitinib (ABT-494),⁴⁵⁻⁴⁹ solcitinib (GSK2586184),^{38,50-53} itacitinib (INCB039110),⁵⁴⁻⁵⁷ PF-04965842.⁵⁸⁻⁵⁹

Among various JAK1-selective inhibitors,⁶⁰ the most advanced is filgotinib in phase III clinical trials by Galapagos found in 2009,⁶¹⁻⁶² which is known to be highly selective for JAK1 over JAK2 by over 27.7 times. Its IC₅₀'s against IL-6/JAK1/pSTAT1 and GM-CSF/JAK2/pSTAT5 are 629 nM and 17453 nM, respectively.³⁶ From collagen-induced arthritis (CIA) mouse and rat models, its efficacy was shown to be similar to etanercept, a TNF- α blocker.⁶³ Through the phase IIa proof-of-concept study, the hypothesis was proven that rheumatoid arthritis can be ameliorated by treatment with JAK1-selective inhibitors.⁶⁴ Since 2016, Galapagos and Gilead have proceeded phase III clinical studies.⁶⁵⁻⁶⁷ Despite its advantages, the reported preclinical results indicated that it induced testicular toxicity in rats and dogs. Thus, the US FDA approved a lower male maximum clinical dosage than for the female one.⁶⁸ Therefore, new JAK1-selective drugs overcoming the toxicological weakness need to be developed. Another promising candidate compound in this class is upadacitinib in phase III by AbbVie.⁶⁹⁻⁷⁰ Although not much toxicological information on the preclinical and clinical trials of upadacitinib is available, its IC₅₀'s for JAK1 and JAK2 in cellular assay were reported to be 8 nM and 600 nM, respectively, indicating 74-fold selectivity.⁷¹

We have initiated our investigation on new JAK1-selective inhibitors based on the 5-azaspiro[2.4]heptan-7-amine core structure for subjugating the filgotinib limitation. New lead compounds were obtained, which met the criteria set by us for treating rheumatoid arthritis. In this paper, we describe the design, synthesis, and improved pharmaceutical efficacies of our inhibitors compared to filgotinib.

II. Strategy

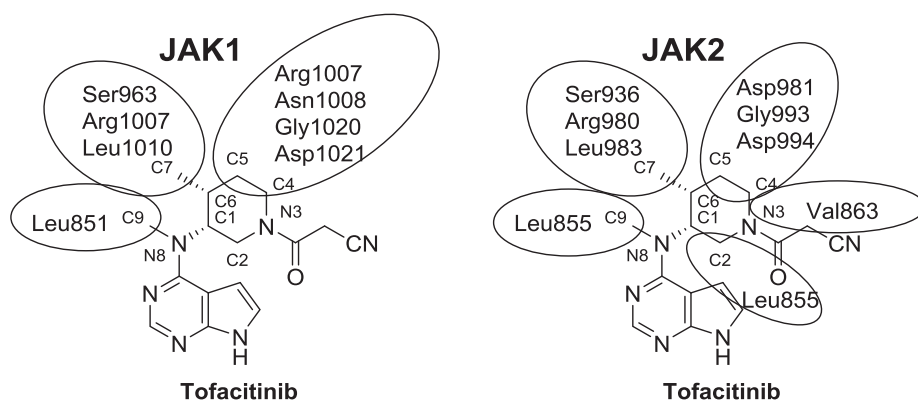


Figure 1 Interactions of tofacitinib with JAK1 or JAK2.

According to the tofacitinib's X-ray crystal structure reported by N. K. Williams et al.,⁷² the interactions between the piperidine moiety of tofacitinib and each isozyme including JAK1 and JAK2 appear to be the basis for binding affinity differentiation. Especially, the carbon atoms C4, C5, and C7 of the piperidine ring may play an important role: notable interactions are those of C4 and C5 with Arg1007, Asn1008, Gly1020, and Asp1021 at JAK1 (Asp981, Gly993, and Asp994 at JAK2) and C7 with Ser963, Arg1007, and Leu1010 at JAK1 (Ser936, Arg980, and Leu983 at JAK2). However, the C2 and N3 atoms appear to be involved in binding JAK2, but not JAK1. Therefore, we hypothesized that changing the piperidine moiety of tofacitinib can alter the binding affinity with JAK2 more than the one with JAK1.

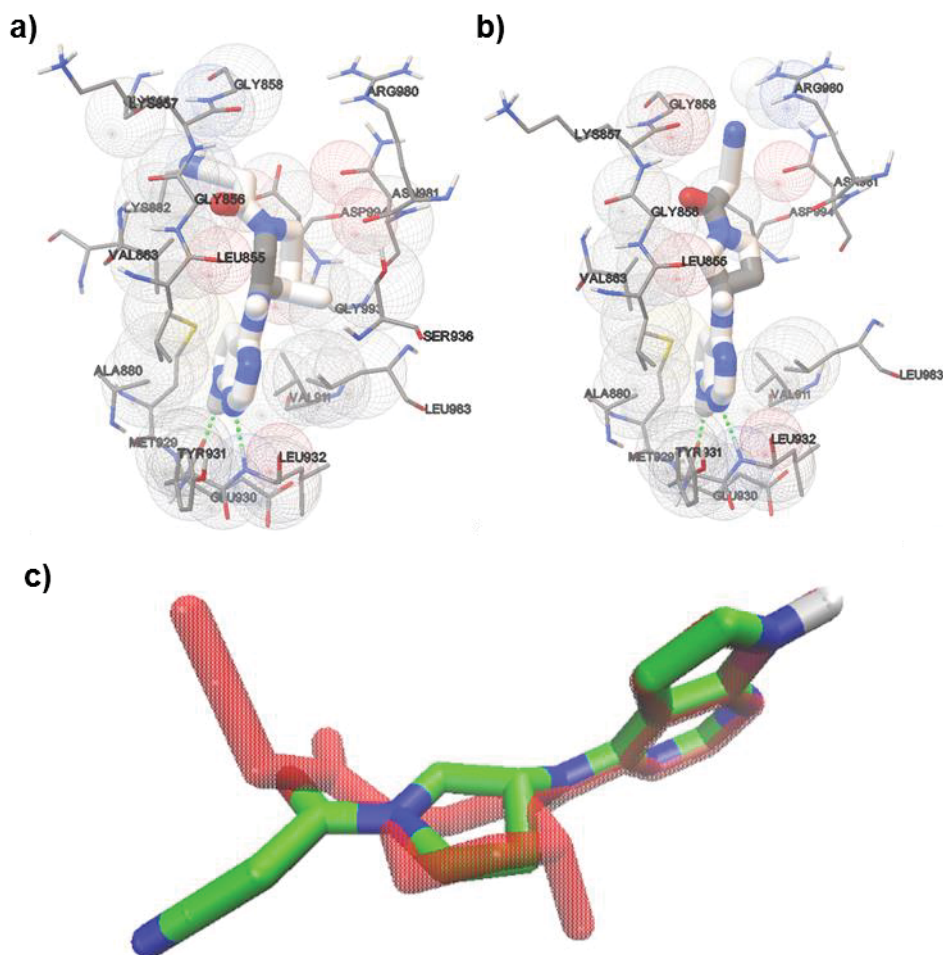


Figure 2 Docking simulation of a) tofacitinib and b) compound **12a** at JAK2 (PDB ID: 3FUP) and c) overlay of the lowest conformations of tofacitinib (red color) and compound **12a** at JAK2.

Based upon our hypothesis, we selected a pyrrolidine moiety in place of the piperidine of tofacitinib. A docking simulation using AutoDock 4.2 program⁷³ was performed to assess the effect of the pyrrolidine substitution at the piperidine site of the inhibitors. The estimated binding energies of tofacitinib and our representative compound **12a** at JAK1 (PDB ID: 3EYG) were -8.10 and -7.50 kcal/mol, respectively. And besides, estimated binding energies of -8.98 and -7.93 kcal/mol, respectively, for tofacitinib and compound

12a were obtained in the case of JAK2 binding (PDB ID: 3FUP, Figure 2). At JAK2, especially, the binding energy difference between tofacitinib and compound **12a** is influenced by their intermolecular energies composed of van der Waals, hydrogen bonding, electrostatic, and desolvation energies. Increasing intermolecular energy of compound **12a** seems to result from lacking the interactions with Ser963 and Leu983 at JAK2. From the above result, we expected that compound **12a** would exhibit lower binding affinity for JAK2 through the substitution into pyrrolidine moiety. In addition, since the methyl group of C9 at tofacitinib appears to interact with Leu855 at JAK2, replacing the methyl group by another alkyl group may also influence the binding affinity at JAK2. According to the docking results, we designed inhibitors possessing several substituted pyrrolidine moieties equipped with various alkyl groups at the bridging amino group of compound **12a**.

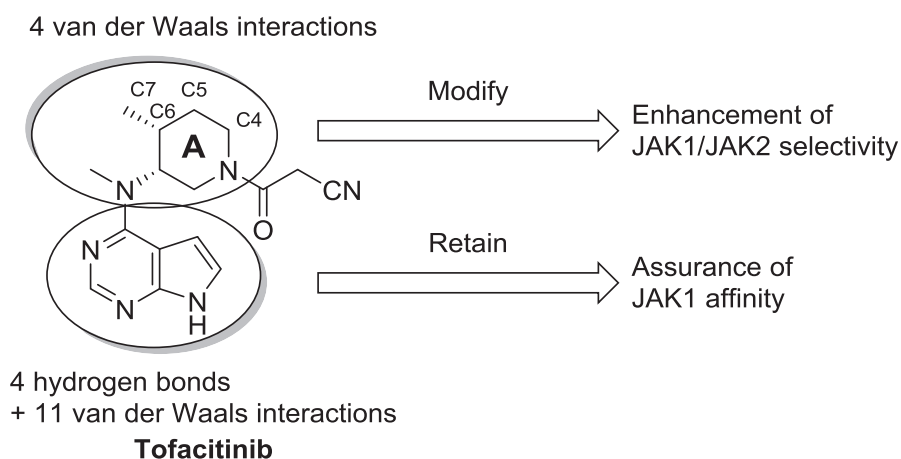
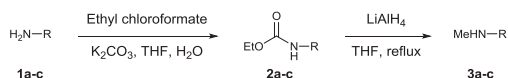


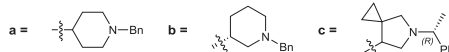
Figure 3 Design strategy by changing the piperidine moiety A.

III. Synthesis

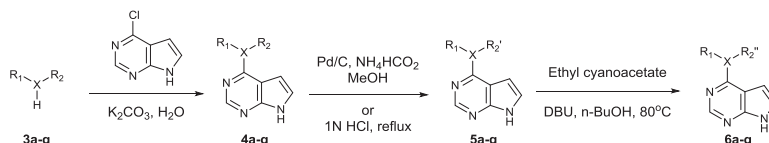
Methylation of primary amino groups



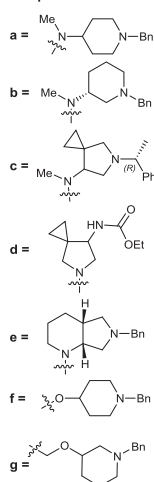
Compounds 1-3



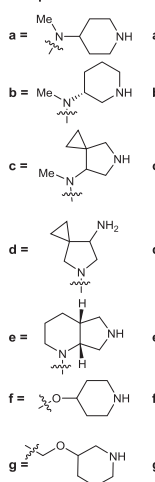
Synthesis of inhibitors



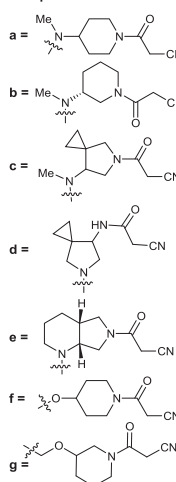
Compounds 3-4



Compounds 5



Compounds 6



Scheme 1 Synthesis of inhibitors containing various heterocyclic core units replacing the aminopiperidine unit of tofacitinib and substituted *N*-methyl-*N*-(5-azaspiro[2.4]heptan-7-yl)-7*H*-pyrrolo[2,3-*d*]pyrimidin-4-amines.

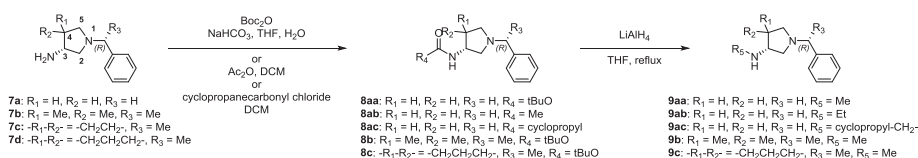
Various monocyclic and bicyclic nitrogen containing compounds **6a** – **6g** were synthesized for the selection of the most optimal scaffold at the position A in Figure 3 as shown in Scheme 1. Commercially available 4-amino-1-benzylpiperidine and (*R*)-3-amino-1-benzylpiperidine were converted to the *N*-ethyloxycarbonyl protected compounds, which were treated with lithium aluminium hydride to result in the formation of methylamine derivatives **3a** and

3b. The key pyrrolidine component of compound **6c**, 5-((*R*)-1-phenylethyl)-5-azaspiro[2.4]heptan-7-amine, was prepared according to the method reported by Y. Kimura and colleagues.⁷⁴ We obtained each diastereomer of 5-((*R*)-1-phenylethyl)-5-azaspiro[2.4]heptan-7-amine with the carbon 7 as an epimeric center. Methylated compound **3c** was obtained through the above method from 5-((*R*)-1-phenylethyl)-5-azaspiro[2.4]heptan-7-amine. Compound **3d** was synthesized through debenzoylation of **2c**. A bis(hydrochloric acid) salt form of bicyclic amine **3e**, (*R,R*)-6-benzyl-octahydro-pyrrolo[3,4-*b*]pyridine dihydrochloride was purchased from Sigma-Aldrich, USA. Commercially available compounds such as 4-hydroxypiperidine and *rac*-3-hydroxymethylpiperidine were converted to the corresponding benzylated amines, **3f** and **3g**.

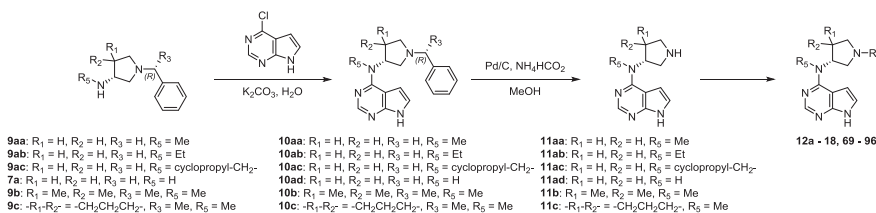
The obtained amines and alcohols, **3a** – **3g**, were used for the coupling with the 6-chloro-7-deazapurine in an aqueous solution, leading to compounds **4a** – **4g**. We then performed debenzoylation of **4a-c** and **4e-f** using palladium on carbon and ammonium formate to remove benzyl and (*R*)-1-phenylethyl protection groups, obtaining **5a-c** and **5e-f**. In the case of **5d**, *N*-ethyloxycarbonyl group of **4d** was deprotected with 1 N aqueous hydrochloric acid under reflux condition. From compounds **5a** – **5g**, the corresponding amide couplings were carried out with ethyl cyanoacetate and 1,8-diazabicyclo[5.4.0]undec-7-ene at 80 °C, leading to compounds **6a** – **6g** according to the reaction pathway shown in Scheme 1.

Since the inhibitor (*R*)-**6c** synthesized from 7(*R*)-5-((*R*)-1-phenylethyl)-7-amino-5-azaspiro[2.4]heptane (*R*)-**1c** showed the most promising inhibition selectivity between JAK1 and JAK2, we focused our efforts on compound (*R*)-**6c**. Amine (*R*)-**5c** was transformed to the final compounds **6c** and **19** – **68** through various reactions at the pyrrolidine nitrogen.

Alkylation of primary amino groups



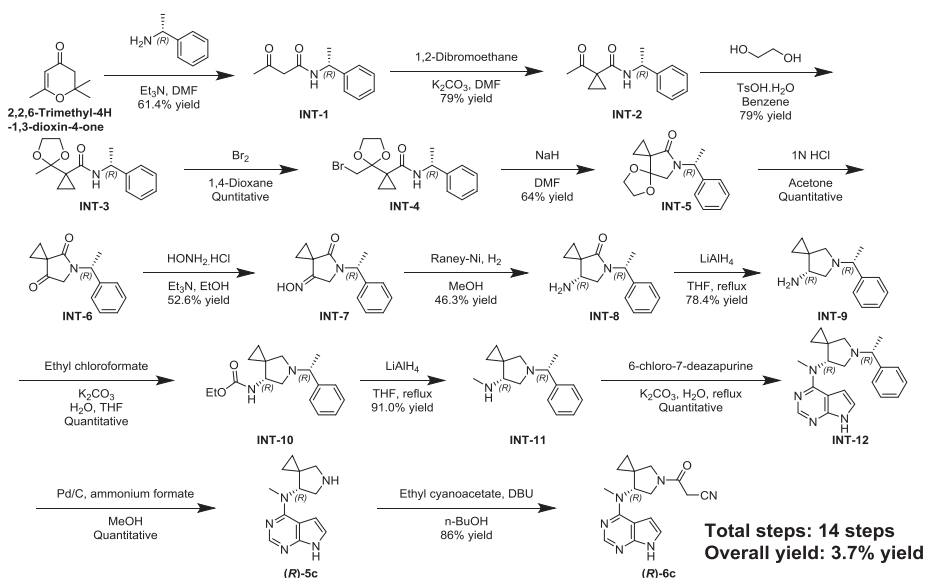
Synthesis of inhibitors



Scheme 2 Synthesis of substituted (*R*)-*N*-alkyl-*N*-(pyrrolidin-3-yl)-7*H*-pyrrolo[2,3-*d*]pyrimidin-4-amines.

For screening on the substituents at C4 atom of pyrrolidine moiety, four 3-aminopyrrolidine derivatives with varying R_1 and R_2 substituents at the 4-position were chosen for the studies, namely (*R*)-1-benzylpyrrolidin-3-amine (**7a**), (*R*)-4,4-dimethyl-1-((*R*)-1-phenylethyl)pyrrolidin-3-amine (**7b**), (*R*)-5-((*R*)-1-phenylethyl)-5-azaspiro[2.4]heptan-7-amine (**7c**), and (*R*)-6-((*R*)-1-phenylethyl)-6-azaspiro[3.4]octan-8-amine (**7d**). Except for the commercially available (*R*)-3-amino-1-benzylpyrrolidine (**7a**), compounds **7b**, **7c** and **7d** were synthesized according to published methods.⁷⁴⁻⁷⁵ Scheme 2 shows a synthetic sequence leading to the pyrrolidines **11aa** – **11d**, from which a variety of derivatives (**12a** – **18** and **69** – **96**) were prepared as potential JAK1 inhibitors: 1) the primary amino group of **7a-d** was protected from the reaction with di-*tert*-butyl dicarbonate, acetic anhydride, or cyclopropanecarbonyl chloride, 2) the *N*-ethoxycarbonyl-, *N*-acetyl- or *N*-cyclopropanecarbonyl-protected compounds **8aa** – **8d** were treated with $LiAlH_4$ to yield alkylated amines **9aa** – **9d**, 3) the alkylamine **9aa** – **9d** and the unprotected amine **7a** were allowed to react with 6-chloro-7-deazapurine to produce compounds **10aa** – **10d**, 4) hydrogenolysis using palladium on carbon and ammonium formate removed the benzyl group of **10aa** – **10ad** or 1-phenylethyl moiety of **10b** –

10d. The desired inhibitors **12a** and **69 – 96** were obtained from **11aa – 11d** through amide coupling, sulfonylation, alkylation, carbonylation, etc.



Scheme 3 Synthetic scheme of *(R)*-3-(7-(methyl(*7H*-pyrrolo[2,3-*d*]pyrimidin-4-yl)amino)-5-azaspiro[2.4]heptan-5-yl)-3-oxopropanenitrile, **(R)-6c**.

Although we found that compound **(R)-6c** from *(R)*-*N*-methyl-*N*-(5-azaspiro[2.4]heptan-7-yl)-*7H*-pyrrolo[2,3-*d*]pyrimidin-4-amine has a higher selectivity than compound **12a**, the reason that we tried to screen the derivatives from *(R)*-*N*-methyl-*N*-(pyrrolidin-3-yl)-*7H*-pyrrolo[2,3-*d*]pyrimidin-4-amine is the synthetic cost of compound **(R)-6c**. By Y. Kimura's method⁷⁴ we synthesized intermediate INT-9 which was not commercially available so that the total synthetic steps of **(R)-6c** consist of 14 steps. Moreover, the overall synthetic yield of **(R)-6c** became 3.7%. Because of long synthetic steps and low overall yield, the synthetic cost of compound **(R)-6c** was calculated as 150 million Korean won per 1 kg. So we selected compound **11aa** as an alternative scaffold because of commercially available *(R)*-1-benzylpyrrolidin-3-amine (**7a**).

IV. Results and Discussions

Enzyme assay

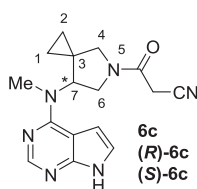
Table 1 Screening of the hydrophobic moieties (moiety A).

Compound		Inhibition% at 1 μ M	
		JAK1	JAK2
6a		49%	1%
6b		99%	83%
6c		95%	53%
6d		6%	10%
6e		54%	-7%
6f		35%	5%
6g		30%	10%

For the selection of a new scaffold, we first screened substituted piperidine and pyrrolidine scaffolds at the position A in Figure 3 (Table 1). Each compound was evaluated for inhibition against JAK1 and JAK2 at 1 μ M concentration. In the case of **6a** and **6f**, the inhibition abilities against JAK1 and JAK2 do not appear to be influenced by the connecting atom (nitrogen vs oxygen) at the C(4) position of piperidine. However, the amino-substitution position at the piperidine ring appeared to be an important factor for determining affinities for not only JAK1 but also JAK2. Between **6a** and **6b**, the substitution at the C(3) position of piperidine (**6b**) was more favoured for both JAK1 and JAK2 inhibitions than the substitution at the C(4) position (**6a**) was. The substitution with methoxy group (**6g**) was disfavoured for JAK1

affinity. In the case of **6e**, introducing (4*aR*,7*aR*)-octahydro-1*H*-pyrrolo[3,4-*b*]pyridine lowered the inhibition against JAK1. In introducing 5-azaspiro[2.4]heptan-7-amine moiety, the substitution position was important. While compound **6c** exhibited strong inhibition against JAK1, **6d** displayed very low inhibition against JAK1. Though both **6b** and **6c** showed strong inhibition against JAK1, **6b** showed high inhibition on JAK2 as well. Therefore, we selected **6c** as our scaffold for further SAR studies for finding inhibitors with high JAK1/JAK2 selectivity.

Table 2 Comparison of JAK1 IC₅₀ values of 3-(7-(methyl(7*H*-pyrrolo[2,3-*d*]pyrimidin-4-yl)amino)-5-azaspiro[2.4]heptan-5-yl)-3-oxopropanenitrile racemate and enantiomers.



Compound	Configuration at 7-position	JAK1 IC ₅₀ (nM)
6c	racemate	29
(R)-6c	(<i>R</i>)	8.5
(S)-6c	(<i>S</i>)	7.9x10 ²

Our further SAR study was based upon **5c** as a scaffold for derivatives on the pyrrolidine nitrogen. When a racemic mixture **6c** was tested against the JAK1 isozyme (Table 2), it showed an IC₅₀ value of 29 nM, proving that it could be used as a good lead for new JAK1 inhibitors. Then we investigated both enantiomers of **6c**. Compound **(R)-6c** exhibited 8.5 nM against JAK1, whereas 7.9x10² nM IC₅₀ was observed with the enantiomeric **(S)-6c**. As a result, for further SAR studies the (*R*)-configuration of 7-amino-5-azaspiro[2.4]heptane was chosen.

Table 3 The IC₅₀ values of compound **(R)-6c** and **12a-c** against JAK1 and JAK2 and the selectivity indices of substituted (*R*)-*N*-methyl-*N*-(pyrrolidin-3-yl)-7*H*-pyrrolo[2,3-*d*]pyrimidin-4-amines according to the substitution at the 4-position of the pyrrolidine ring.

Compound	A	IC ₅₀ (nM)		SI ^{a)}
		JAK1	JAK2	
12a		19	1.3x10 ²	6.8
12b		2.6x10 ²	5.9x10 ³	23
(R)-6c		8.5	4.1x10 ²	48
12c		16	4.5x10 ²	28
Tofacitinib		2.0	9.9	5.0

^{a)} SI: Selectivity Index = JAK2 IC₅₀ / JAK1 IC₅₀

The 7-deazapurine moiety of tofacitinib was considered to be critical in securing the ATP-binding site of JAK isozymes, therefore it was kept in our scaffold structure. First, to evaluate the effect of the substituents at the 4-position of the pyrrolidine ring, we prepared cyanoacetyl derivatives **(R)-6c**, and **12a-c** from the four parent pyrrolidine precursors, **(R)-5c**, **11aa**, **11b**, and **11c**. We then screened the inhibitory efficiencies of the derivatives substituted with dimethyl and spirocyclic moieties at the 4-position of the pyrrolidine core, which is believed to correspond to the 4-position of the piperidine of tofacitinib (Table 3). The unsubstituted inhibitor **12a** exhibited an IC₅₀ value of 19 nM for JAK1 and its selectivity index was 6.8, which was higher than that of

tofacitinib. The dimethyl-substituted **12b** was 10-fold less potent against JAK1 than that of compound **12a**, however, the spirocyclic derivatives (**R**)-**6c** and **12c** had similar levels of IC₅₀'s to compound **12a**. This may indicate that the binding site around the 4-position of the pyrrolidine is rather small in volume. We identified the fact that the derivative (**R**)-**6c** having (*R*)-5-benzyl-5-azaspiro[2.4]heptan-7-amine moiety showed the best selectivity of JAK1 over JAK2.

Table 4 The IC₅₀ values against JAK1 and JAK2 and the selectivity indices of substituted (*R*)-*N*-(pyrrolidin-3-yl)-7*H*-pyrrolo[2,3-*d*]pyrimidin-4-amines with varying R₁ and R₂ groups.

Compound	R ₁	R ₂	IC ₅₀ (nM)		SI ^{a)}
			JAK1	JAK2	
12a		Me	19	1.3x10 ²	6.8
13		Et	62	1.3x10 ³	21
14			1.6x10 ²	1.7x10 ³	11
15		H	5.1x10 ²	1.9x10 ³	3.7
16		Me	4.1	57	14
17		Et	19	1.1x10 ²	5.8
18			17	1.4x10 ³	82

^{a)} SI: Selectivity Index = JAK2 IC₅₀ / JAK1 IC₅₀

With the *N*-alkylated compounds in hand, we fixed the pyrrolidine nitrogen with either cyanoacetate or 3-cyanobenzenesulfonyl group as R₁ at 1-position and probed the inhibitory activities by changing the R₂ at 6-position from hydrogen to cyclopropylmethyl group. In both cyanoacetyl- and 3-cyanophenylsulfonyl-substituted pyrrolidine derivatives, increasing from

methyl to ethyl and to cyclopropylmethyl decreased the inhibitory activities against JAK1, although JAK2 inhibitions were not as much affected. In the case of compound **15**, where there is no alkyl substitution on the 3-amino group, quite low level of inhibition against JAK1 was observed. It turns out that the 3-cyanophenylsulfonyl substitution resulted in better inhibition on JAK1 than the cyanoacetyl one in all the cases examined, although mixed results were obtained in selectivity indices. After the results of Table 4, we chose methyl group as R₂ and (*R*)-*N*-methyl-*N*-(5-azaspiro[2.4]heptan-7-yl)-7*H*-pyrrolo[2,3-*d*]pyrimidin-4-amine as a scaffold for further SAR studies.

Table 5 The IC₅₀ values against JAK1 and JAK2 with the selectivity indices of substituted (*R*)-*N*-methyl-*N*-(5-azaspiro[2.4]heptan-7-yl)-7*H*-pyrrolo[2,3-*d*]pyrimidin-4-amines.

Compound	R	IC ₅₀ (nM)		SI ^{a)}
		JAK1	JAK2	
19		1.4x10 ³	3.0x10 ⁴	21
20		2.3x10 ²	1.5x10 ⁴	65
21		1.2x10 ²	9.8x10 ⁴	8.2x10 ²
(R)-6c		8.5	4.1x10 ²	48
22		21	2.5x10 ²	12
23		77	1.1x10 ³	14

^{a)} SI, Selectivity Index = JAK2 IC₅₀ / JAK1 IC₅₀

Table 6 The IC₅₀ values against JAK1 and JAK2 with the selectivity indices of substituted (*R*)-*N*-methyl-*N*-(5-azaspiro[2.4]heptan-7-yl)-7*H*-pyrrolo[2,3-*d*]pyrimidin-4-amines (continued).

Compound	R	IC ₅₀ (nM)		SI ^{a)}
		JAK1	JAK2	
24		1.7x10 ²	2.8x10 ³	16
25		1.7x10 ²	1.2x10 ³	7.1
26		5.2x10 ²	1.6x10 ⁴	31
27		6.7x10 ²	1.3x10 ⁴	19
28		1.8x10 ²	2.5x10 ³	14
29		53	9.3x10 ²	18
30		1.5x10 ²	6.3x10 ³	42
31		1.6x10 ²	7.8x10 ³	49
32		1.4x10 ²	6.5x10 ³	46
33		1.0x10 ²	7.4x10 ³	74

^{a)} SI, Selectivity Index = JAK2 IC₅₀ / JAK1 IC₅₀

Table 7 The IC₅₀ values against JAK1 and JAK2 with the selectivity indices of substituted (*R*)-*N*-methyl-*N*-(5-azaspiro[2.4]heptan-7-yl)-7*H*-pyrrolo[2,3-*d*]pyrimidin-4-amines (continued).

Compound	R	IC ₅₀ (nM)		SI ^{a)}
		JAK1	JAK2	
34		1.9x10 ²	4.5x10 ³	24
35		5.0x10 ²	9.1x10 ³	18
36		4.2x10 ²	1.1x10 ⁴	26
37		20	1.6x10 ²	8.0
38		34	1.2x10 ³	35
39		75	2.8x10 ³	37
40		69	4.4x10 ³	64
41		12	4.2x10 ²	35
42		23	1.0x10 ³	43
43		1.2x10 ²	4.7x10 ³	39

^{a)} SI, Selectivity Index = JAK2 IC₅₀ / JAK1 IC₅₀

Table 8 The IC₅₀ values against JAK1 and JAK2 with the selectivity indices of substituted (*R*)-*N*-methyl-*N*-(5-azaspiro[2.4]heptan-7-yl)-7*H*-pyrrolo[2,3-*d*]pyrimidin-4-amines (continued).

Compound	R	IC ₅₀ (nM)		SI ^{a)}
		JAK1	JAK2	
44		40	1.3x10 ³	33
45		54	2.8x10 ³	52
46		74	1.3x10 ³	18
47		85	1.3x10 ³	15
48		1.5x10 ³	9.1x10 ³	6.1
49		4.7x10 ²	1.1x10 ⁴	23
50		7.2	1.8x10 ²	25
51		20	1.3x10 ²	6.5
52		6.9	36	5.2

^{a)} SI, Selectivity Index = JAK2 IC₅₀ / JAK1 IC₅₀

Table 9 The IC₅₀ values against JAK1 and JAK2 with the selectivity indices of substituted (*R*)-*N*-methyl-*N*-(5-azaspiro[2.4]heptan-7-yl)-7*H*-pyrrolo[2,3-*d*]pyrimidin-4-amines (continued).

Compound	R	IC ₅₀ (nM)		SI ^{a)}
		JAK1	JAK2	
53		9.0	51	5.7
54		13	97	7.5
55		2.8	8.4	3.0
56		9.4	50	5.3
57		50	4.8x10 ²	9.6
58		5.8	59	10
59		9.8	1.1x10 ³	1.1x10 ²
60		26	4.7x10 ²	18
61		1.4	5.5	3.9

^{a)} SI, Selectivity Index = JAK2 IC₅₀ / JAK1 IC₅₀

Table 10 The IC₅₀ values against JAK1 and JAK2 with the selectivity indices of substituted (*R*)-*N*-methyl-*N*-(5-azaspiro[2.4]heptan-7-yl)-7*H*-pyrrolo[2,3-*d*]pyrimidin-4-amines (continued).

Compound	R	IC ₅₀ (nM)		SI ^{a)}
		JAK1	JAK2	
62		6.3	30	4.8
63		12	66	5.5
64		9.3	1.8x10 ²	19
65		16	1.4x10 ³	88
66		17	1.5x10 ²	8.8
67		15	1.5x10 ²	10
68		31	2.6x10 ²	8.4

^{a)} SI, Selectivity Index = JAK2 IC₅₀ / JAK1 IC₅₀

To find highly selective inhibitors for JAK1, we screened compounds possessing various substituent groups at the pyrrolidine nitrogen listed in Table 5 and comparing their IC₅₀ values against JAK1 and JAK2. For this study, (*R*)-**5c** was used as a starting material. In the cases of *N*(5)-alkylated compounds **19**, **20**, and **21**, inhibitor **21** has an *N*-benzyl group with a higher affinity to JAK1 than those with short alkyl amine groups, but was disfavored against JAK2

(1.2×10^2 nM in JAK1 vs. 9.8×10^4 nM in JAK2). The inhibitor with the benzylamine group displayed its selectivity index of 8.2×10^2 for JAK1 over JAK2.

In the cases of inhibitors with amide groups at the pyrrolidine nitrogen, those with cyanoacetyl and azidoacetyl substitutions (**(R)-6c** and **22**, respectively) were quite potent against JAK1 with the IC_{50} values of 8.5 and 21 nM, respectively. Amine compounds possessing aliphatic side chains (ethyl-, *n*-butyl- and benzyl- compounds, **19** – **21**, respectively) showed inferior inhibitory activities against JAK1 to that of **(R)-6c** with IC_{50} values over 100 nM's. A slightly larger isovaleric amide **23** exhibited comparable activity for JAK1 inhibition. It is interesting to note that two similarly-sized amides, isobutyramide **24** and cyclopropanecarboxamide **25**, exhibited similar JAK1 inhibitions. However, compound **24** showed a higher selectivity index against JAK2 than **25**. This tells us that there may be a more sensitive structural interaction in JAK2 with the amide motif. Amides substituted with a polar group like compounds **26** – **28** did not show significant inhibition against JAK1. Aroyl amides **30** – **36** also showed IC_{50} values in the 100-1000 nM ranges except for the small 2-furanoyl amide **29**, which gave 53 nM IC_{50} against JAK1. This indicates again that a large amide group at the pyrrolidine nitrogen is not tolerated well in the JAK1 binding site.

The transition from an amide to a thioamide lowered the inhibition activity against JAK1, but not so much against JAK2 that the inhibitor possessing 2-cyanoethanethioamide exhibited a lower selectivity index than that with 2-cyanoacetate (**(R)-6c** vs **37**). Introducing a urethane (**38**) into the pyrrolidine nitrogen resulted in considerable potency (IC_{50} = 34 nM) against JAK1 with a selectivity index of 35. Urea compounds (**39** – **48**), except for **43** and **48**, exhibited two-digit nanomolar IC_{50} 's against JAK1. For ureas made up with aliphatic amines, 1-butylurea **39** and 1-cyclohexylurea **40** showed similar affinities for JAK1 with IC_{50} values of 75 and 69 nM, respectively. However, compound **40** with a cyclic alkyl urea group was inferior in the JAK2 inhibition

with IC_{50} 's of 4.4×10^3 nM to the acyclic urea **39** with 2.8×10^3 IC_{50} . Comparing 1-cyclohexyl urea **40** and phenyl urea **41**, indicates that the inhibition abilities of the latter were higher in both JAK1 and JAK2 with IC_{50} 's of 12 nM and 4.2×10^2 nM, respectively. Halide-substituted phenyl ureas **42** – **47** did not show any improvements in inhibitory activities compared to the parent phenyl urea, **41**. When the phenyl group of the phenyl urea was substituted with an *ortho*-phenyl group (compound **48**), the inhibition of JAK1 and JAK2 decreased precipitously with IC_{50} values of 1.5×10^3 and 9.1×10^3 nM, respectively, presumably due to increased steric hindrance.

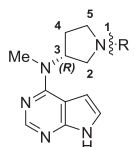
In the case of sulfonamides, most compounds displayed strong inhibition against the two enzymes. Some inhibitors showed single digit nanomolar range IC_{50} 's against JAK1. When amides and sulfonamides of similar sizes were compared, in all cases the inhibitors possessing a sulfonamide showed increased affinities for JAK1: the IC_{50} 's of **24** vs **51**, **30** vs **53**, **33** vs **58**, and **34** vs **59** were 1.7×10^2 vs 20, 1.5×10^2 vs 9.0, 1.0×10^2 vs 5.8, and 1.9×10^2 vs 9.8 nM, respectively. However, with the elevated affinities for JAK1, the sulfonamide inhibitors also increased their inhibition against JAK2, leading to lower selectivity indexes than those of amide inhibitors. The JAK1 affinity appeared to be quite sensitive towards the substituent on benzenesulfonamide (**54** – **62**): the *meta*-substitution gave the best inhibition whereas the *ortho*-substitution showed the lowest affinities for the JAK1 isozyme.

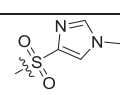
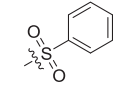
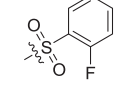
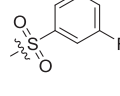
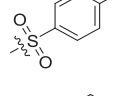
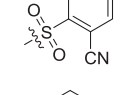
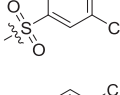
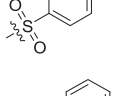
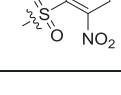
Table 11 The IC₅₀ values against JAK1 and JAK2 and the selectivity indices of substituted (*R*)-*N*-methyl-*N*-(pyrrolidin-3-yl)-7*H*-pyrrolo[2,3-*d*]pyrimidin-4-amines.

Compound	R	IC ₅₀ (nM)		SI ^{a)}
		JAK1	JAK2	
12a		19	1.3x10 ²	6.8
69		53	1.9x10 ³	36
70		7.4x10 ²	2.7x10 ⁴	36
71		10	1.7x10 ²	17
72		70	3.9x10 ³	56
73		1.1x10 ²	4.3x10 ³	39
74		22	5.5x10 ²	25
75		70	4.7x10 ³	67
76		1.4x10 ²	4.5x10 ³	32
77		79	2.4x10 ³	30
78		1.7x10 ²	4.8x10 ³	28
79		34	4.6x10 ²	14

^{a)} SI, Selectivity Index = JAK2 IC₅₀ / JAK1 IC₅₀

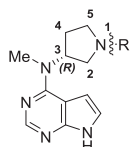
Table 12 The IC₅₀ values against JAK1 and JAK2 and the selectivity indices of substituted (*R*)-*N*-methyl-*N*-(pyrrolidin-3-yl)-7*H*-pyrrolo[2,3-*d*]pyrimidin-4-amines (continued).

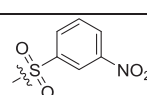
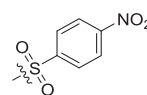
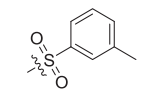
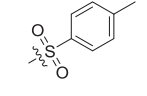
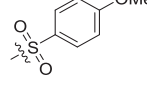
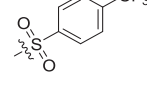
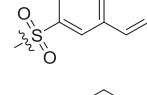
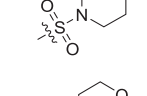
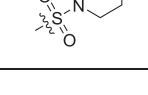


Compound	R	IC ₅₀ (nM)		SI ^{a)}
		JAK1	JAK2	
80		6.5x10 ²	1.9x10 ⁴	29
81		28	4.3x10 ²	15
82		25	1.3x10 ²	5.2
83		14	53	3.8
84		11	1.1x10 ²	10
85		52	3.7x10 ²	7.1
16		4.1	57	14
86		11	1.2x10 ³	1.1x10 ²
87		1.1x10 ²	1.1x10 ³	10

^{a)} SI, Selectivity Index = JAK2 IC₅₀ / JAK1 IC₅₀

Table 13 The IC₅₀ values against JAK1 and JAK2 and the selectivity indices of substituted (R)-N-methyl-N-(pyrrolidin-3-yl)-7H-pyrrolo[2,3-*d*]pyrimidin-4-amines (continued).



Compound	R	IC ₅₀ (nM)		SI ^{a)}
		JAK1	JAK2	
88		1.9	18	9.5
89		3.6	89	25
90		29	7.3x10 ²	25
91		19	1.8x10 ³	95
92		26	1.5x10 ³	58
93		9.5	3.4x10 ³	3.6x10 ²
94		13	6.9x10 ²	53
95		66	3.9x10 ³	59
96		2.7x10 ²	4.4x10 ³	16

^{a)} SI, Selectivity Index = JAK2 IC₅₀ / JAK1 IC₅₀

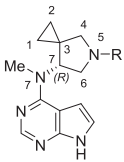
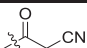
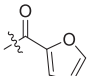
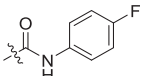
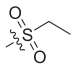
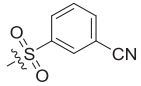
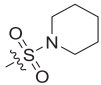
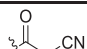
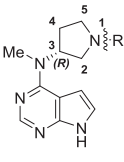
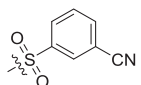
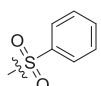
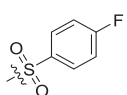
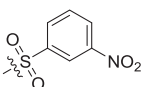
To find a new lead compound, we screened the inhibitory activities for JAK1 and JAK2 of compounds possessing a variety of substituents at the 1-nitrogen of pyrrolidine moiety (Table 6). First, a comparison between amide and alkylamine groups of similar size (**12a** vs **69**) was attempted and the amide group appeared to increase the affinity for JAK1 isozyme. This hypothesis also appears to apply to the urea functionality with compound **74** exhibiting 22 nM IC₅₀ value for JAK1. If the inhibitors contain an amide or urea side chain bulkier than the cyanomethyl group as in **12a**, their inhibitions for JAK1 isozyme were less effective (**70**, **72**, and **73**). However, in the case of **74**, its inhibitory activity was similar to that of compound **12a** although it has an *N*-phenyl side chain, which is larger than that of compound **12a**. With compounds **12a** and **71**, similar inhibitory activities were observed, which suggests that the planar or linear group at the side chain of amide offsets the ill effect the side chain length. The introduction of the sulfonamide on the 1-nitrogen of the pyrrolidine core improved the inhibitory activities for JAK1 (**70** vs **79**). Moreover, the arenesulfonamides (**16** and **81 – 94**) exhibited higher inhibitory activities than the sulfonamides having alkyl or heterocyclic groups (**75 – 80**). As for the substitutions at the benzene ring, inhibitors with substituents at *ortho*-position (**85** and **87**) showed lower inhibition than the *meta*- or *para*-counterparts, presumably due to steric interaction with JAK1 except for the fluorine substitution cases (**82 – 84**). In the case of the selectivity for JAK1 over JAK2, the inhibitors with substitution at *para*-position (**84**, **86**, and **89**) showed 2.5 to 7.9-fold improved JAK1 selectivity compared to those having *meta*-substitutions. Consequently, compounds **86** and **93** were the most selective for JAK1 over JAK2.

According to our enzyme assays, (*R*)-**6c** and **58** seemed to be more selective for JAK1 over JAK2 than filgotinib, of which the IC₅₀'s are 10, 28, 810, and 116 nM for JAK1, JAK2, JAK3, and TYK2, respectively.⁶³ Therefore, we selected two representative compounds, (*R*)-**6c** and **58**, for evaluation against JAK3 and TYK2. The IC₅₀ of (*R*)-**6c** on JAK3 and TYK2 were 1.1x10³

and 2.5×10^2 nM and the selectivity indices over JAK1 were 130 and 30, respectively. For **58**, 1.1×10^2 and 25 nM IC_{50} 's were observed for JAK3 and TYK2, respectively, with its selectivity indices as 19 and 4.3 for JAK3 and TYK2 over JAK1.

Cell-based functional assay

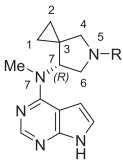
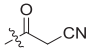
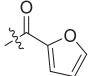
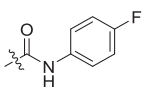
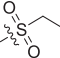
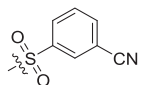
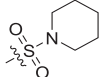
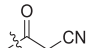
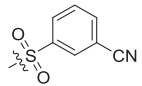
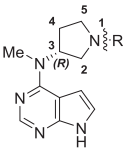
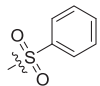
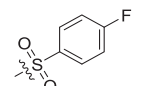
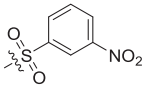
Table 14 The IC₅₀ values against cellular JAK1-JAK3 and JAK2 activity of substituted (*R*)-*N*-methyl-*N*-(pyrrolidin-3-yl)-7*H*-pyrrolo[2,3-*d*]pyrimidin-4-amines.

			IC ₅₀ (μM)		
Compound			JAK1/3		JAK2
			(THP-1, IL-4-pSTAT6)		(IL-3-Ba/F3 Proliferation)
Number	Scaffold	R	Facs Tube	96 well	
	Tofacitinib citrate		0.090	ND	~ 4.7
	Filgotinib		1.8	0.56	>10
(R)-6c			0.84	0.21	>10
29			11	4.3	>10
42			2.8	1.4	>10
50			ND	0.73	ND
58			1.1	0.24	>10
67			3.7	1.7	>10
12a			0.92	0.30	>10
16			0.61	0.20	>10
81			1.1	0.98	>10
84			<0.010	0.40	>10
88			0.13	0.040	>10

Encouraged by the enzyme assay results, we selected several compounds to see if they can inhibit JAK activity in a cell-based assay. We used the THP-1 cell to read the phosphorylation of STAT6, indicative of JAK activation.⁶³ When THP-1 cells are treated with IL-4 as a JAK-STAT pathway trigger, IL-4 receptors are dimerized. Consequently, one JAK1 and one JAK3 are recruited in the cytoplasmic domain. After the bound JAKs are phosphorylated and activated, STAT6 (pSTAT6) is phosphorylated. Thus, we performed FACS analysis to measure the pSTAT6 level in THP-1 cells upon IL-4 stimulation (Table 7). As expected, tofacitinib citrate, which strongly inhibits both JAK1 and JAK3 in the biochemical assay, showed potent inhibitory activity on the phosphorylation of STAT6 ($IC_{50} = 0.09 \mu M$). Compared to tofacitinib citrate, the JAK1-selective inhibitor filgotinib showed lower activity against JAK1-JAK3, which could be due to its relatively poor activity against JAK3 in the biochemical enzymatic assay ($IC_{50} = 810 \text{ nM}$). Among the compounds tested in this study, **(R)-6c**, **58**, **12a**, **16**, **81**, **84**, and **88** inhibited the phosphorylation of STAT6 with the IC_{50} values 0.84, 1.1, 0.92, 0.61, 1.1, <0.010, and 0.13 μM 's, respectively.

We evaluated the inhibitory activities of our representative compounds against JAK2 by performing the Ba/F3 cell proliferation assay. Ba/F3 cells proliferate upon the JAK2-STAT pathway activated by IL-3 stimulation.⁶³ Tofacitinib citrate exhibited an IC_{50} value of 4.7 μM , whereas our tested compounds except for **50** and filgotinib had IC_{50} values of >10 μM in this system. Taken together, these results suggest that our compounds possess higher selectivity for JAK1 or JAK3 than JAK2.

Table 15 Selectivity for individual JAK isozymes of substituted (*R*)-*N*-methyl-*N*-(pyrrolidin-3-yl)-7*H*-pyrrolo[2,3-*d*]pyrimidin-4-amines in cellular assays.

Compound			GI ₅₀ (μM)			
			TEL-JAKs-Ba/F3 (Proliferation)			
Number	Scaffold	R	JAK1	JAK2	JAK3	TYK2
	Tofacitinib citrate		1.0	4.3	3.1	> 10
	Filgotinib		7.0	>10	>10	> 10
(<i>R</i>)-6c			4.1	>10	>10	> 10
29			>10	>10	>10	> 10
42			>10	>10	>10	> 10
50			4.2	>10	>10	> 10
58			1.1	>10	>10	> 10
67			>10	>10	>10	> 10
12a			7.5	>10	>10	>10
16			1.0	>10	>10	>10
81			4.6	>10	>10	>10
84			4.2	>10	>10	>10
88			0.41	>10	>10	>10

We next examined 11 compounds, (*R*)-**6c**, **29**, **42**, **50**, **58**, **67**, **12a**, **16**, **81**, **84**, and **88**, in the selectivity for individual JAK isozymes by using Ba/F3

cell lines expressing constitutively active individual JAK isozymes (TEL-JAKs). We found that the tofacitinib citrate has growth inhibitory activity in cells expressing either JAK1, JAK2, or JAK3 with the median growth inhibitory concentrations (GI₅₀) of 1.0, 4.3, and 3.1 μ M, respectively, but not in cells expressing TYK2 (Table 8). However, filgotinib and our compounds including (**R**)-**6c**, **50**, **58**, **12a**, **16**, **81**, **84**, and **88** showed growth inhibitory activity only in cells expressing JAK1 with GI₅₀ values of 7.0, 4.1, 4.2, 1.1, 7.5, 1.0, 4.6, 4.2, and 0.41 μ M, respectively. These results suggest that our tested compounds (**R**)-**6c**, **50**, **58**, **12a**, **16**, **81**, **84**, and **88** are more potent for JAK1 than filgotinib.

Human whole blood tests

Table 16 Selectivity for JAK1 over JAK2 of substituted (*R*)-*N*-alkyl-*N*-(pyrrolidin-3-yl)-7*H*-pyrrolo[2,3-*d*]pyrimidin-4-amines in human whole blood assays.

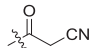
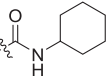
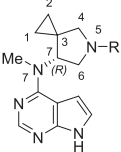
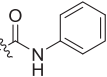
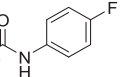
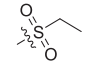
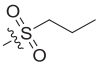
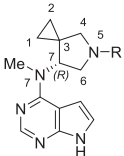
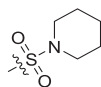
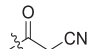
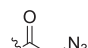
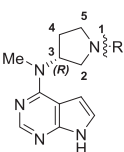
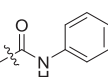
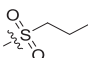
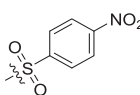
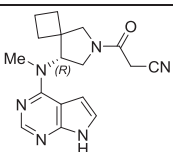
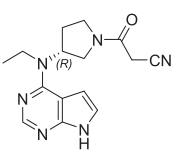
Number	Compound		IC ₅₀ (nM)		Selectivity index (JAK2/JAK1)
	Scaffold	R	JAK1 (IL-6/pSTAT1)	JAK2 (GM-CSF/pSTAT5)	
	Filgotinib		3.2x10 ² – 1.1x10 ³	7.8x10 ³ – 2.2x10 ⁴	9.1 – 25
	Baricitinib		8.0 – 40	17 – 1.4x10 ²	2.0 – 5.9
(R)-6c			1.7x10 ⁴	>2.0x10 ⁴	>1.2
40			1.5x10 ⁴	>2.0x10 ⁴	>1.4
41			6.3x10 ³	>2.0x10 ⁴	>3.2
42			1.2x10 ⁴	>2.0x10 ⁴	>1.6
50			4.4x10 ²	2.4x10 ³	5.5
52			5.6x10 ²	>2.0x10 ⁴	>36

Table 17 Selectivity for JAK1 over JAK2 of substituted (*R*)-*N*-alkyl-*N*-(pyrrolidin-3-yl)-7*H*-pyrrolo[2,3-*d*]pyrimidin-4-amines in human whole blood assays (continued).

Number	Compound Scaffold	R	IC ₅₀ (nM)		Selectivity index (JAK2/JAK1)
			JAK1 (IL-6/pSTAT1)	JAK2 (GM-CSF/pSTAT5)	
67			4.8x10 ³	>2.0x10 ⁴	>4.1
12a			2.5x10 ²	7.4x10 ²	2.9
71			2.4x10 ²	1.5x10 ⁴	60
74			3.6x10 ³	>2.0x10 ⁴	>5.5
79			4.3x10 ²	>2.0x10 ⁴	>47
89			3.0x10 ²	1.5x10 ⁴	51
12c			4.3x10 ²	6.0x10 ³	14
13			5.8x10 ²	7.0x10 ⁴	12

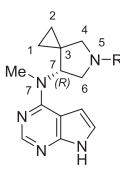
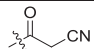
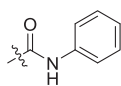
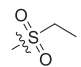
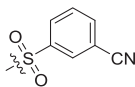
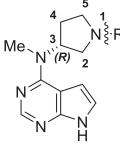
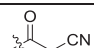
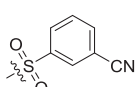
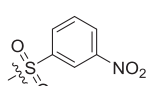
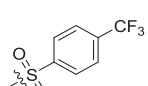
To identify the inhibition of the JAK-STAT signal pathway by our compounds in human blood environment, we performed human whole blood tests for 18 compounds. We selected two pathways: IL-6/JAK1/pSTAT1 and GM-CSF/JAK2/pSTAT5. For screening JAK1 inhibition in human blood, whole blood is treated with IL-6 and the pathway activated by IL-6 was

inhibited through JAK1 inhibition by inhibitors so that the inhibition percentage against the phosphorylation of STAT1 displays the inhibition portion of the pathway by JAK1 inhibitors. Similarly, the inhibition against the phosphorylation of STAT5 activated by GM-CSF shows the result from JAK2 inhibition of the pathway. As the result, we can obtain the selectivity indices for JAK1 over JAK2 in human whole blood environment.

We used filgotinib, JAK1-selective inhibitor, and baricitinib, JAK1/JAK2 inhibitor, as positive controls. The selectivity for JAK1 over JAK2 of filgotinib was distributed from 9.1 to 25.0. Of our test compounds, the tests of **18**, **44**, **93**, and **94** were not carried out because of low water solubility. Of other compounds, 6 compounds, **52**, **71**, **79**, **89**, **12c**, and **13** showing the selectivity indices ranged from 12 to 60 were more selective for JAK1 over JAK2 than filgotinib. However, our representative compound (**R**)-**6c** had the IC_{50} value of 1.6×10^4 nM for inhibition of IL-6/JAK1/pSTAT1 pathway so that we could not calculate the selectivity index. So we guessed that this system was not appropriate for identifying the selectivity of compound (**R**)-**6c**. In the case of compound **12a**, it showed the lower JAK1 IC_{50} value of 2.5×10^2 nM than filgotinib did, but it had a lower selectivity index of 2.9 than filgotinib.

In vitro ADME studies

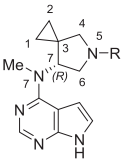
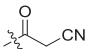
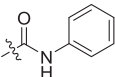
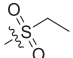
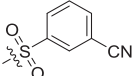
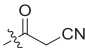

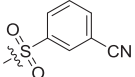
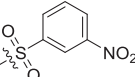
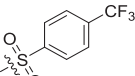
Table 18 Plasma stabilities.

Compound			Human		Rat	
			(% remaining)		(% remaining)	
Number	Scaffold	R	30 min	120 min	30 min	120 min
(R)-6c			95.0	98.5	98.4	89.6
41			> 100	> 100	> 100	95.5
50			> 100	> 100	> 100	> 100
58			96.6	98.6	> 100	> 100
12a			96.3	99.8	> 100	> 100
16			94.8	96.9	> 100	> 100
88			90.6	93.0	> 100	> 100
93			> 100	> 100	98.9	99.8

Several *in vitro* ADME profiles for selected JAK1 inhibitors, **(R)-6c**, **41**, **50**, **58**, **12a**, **16**, **88**, and **93**, were investigated for plasma stability, protein binding, liver microsomal stability, Caco-2 permeability, and CYP inhibition. First, over 90% of all test compounds except for **(R)-6c** in rat plasma during 120 minutes remained in human and rat plasma for 120 minutes in plasma stability tests (Table 10). In the comparison between derivatives of *(R)*-*N*-alkyl-*N*-(pyrrolidin-3-yl)-7*H*-pyrrolo[2,3-*d*]pyrimidin-4-amine and *(R)*-*N*-methyl-*N*-(5-azaspiro[2.4]heptan-7-yl)-7*H*-pyrrolo[2,3-*d*]pyrimidin-4-amine (**(R)-6c** vs **12a**, and **58** vs **16**), whether the spiro moiety at pyrrolidine ring exist cannot

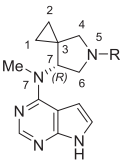
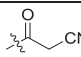
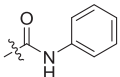
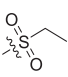
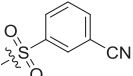
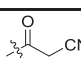
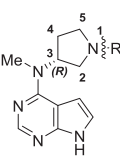
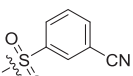
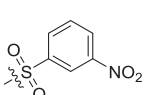
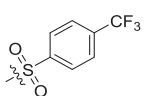
affect their plasma stability. Therefore, it can be concluded that most compounds are kept as their parent drug structures in plasma.

Table 19 Plasma protein binding abilities and Log P values.

Number	Compound		% bound		LogP (neutral X)
	Scaffold	R	Human	Rat	
(R)-6c			29.8	18.7	1.69
41			92.5	88.1	3.07 (cLogP)
50			44.4	49.5	2.07
58			87.4	85.8	3.69
12a			14.7	17.7	0.61
16			83.1	82.7	2.73
88			90.4	91.9	3.03
93			98.7	95.9	3.58 (cLogP)

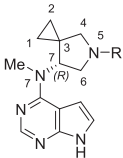
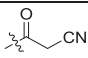
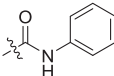
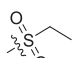
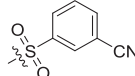
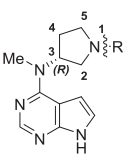
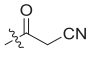
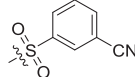
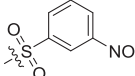
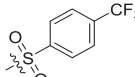
In human plasma protein binding tests (Table 11), the bound proportion of **(R)-6c** was 29.8%, which was similar to that of tofacitinib citrate and filgotinib, 39% and 31.8%, respectively.^{33, 36} Compounds, **50**, **58**, **16**, **88**, and **93**, all of which have sulfonamide groups, showed higher protein binding of over 44.4%. The results correlate well with their lipophilicities: the LogP values of their neutral forms gradually increase in the order of amides **12a** and **(R)-6c**, aliphatic sulfonamide **50**, and aromatic sulfonamides **16** and **55**.

Table 20 Liver microsomal stabilities.

Compound			% Remaining after 30 min (%)			
Number	Scaffold	R	Human	Dog	Rat	Mouse
(R)-6c			94.6	99.9	84.8	84.9
41			67.3	62.2	41.6	18.5
50			79.7	56.1	22.9	33.9
58			6.0	5.5	2.4	3.2
12a			97.6	92.8	92.8	> 100
16			26.3	31.6	3.7	10.0
88			13.4	10.4	2.5	3.1
93			21.0	14.2	11.4	8.4

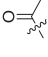
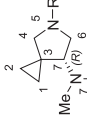
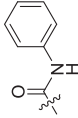
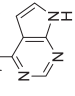
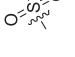
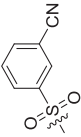
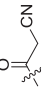
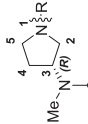
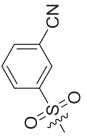
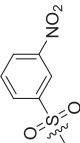
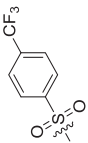
To probe the stability of the selected compounds in the liver first-pass, liver microsomal stabilities were examined (Table 12). The remaining compounds **(R)-6c** and **12a** (94.6 and 97.6%, respectively) after 30 minute incubation in human liver microsomes were similar to those of filgotinib (87% after 60 minute incubation).³⁶ While compound **50** possessing an ethanesulfonamide group was less stable than filgotinib, with 79.7% remaining after 30 minutes, the benzenesulfonamide-containing compounds, **58**, **16**, **88**, and **93** were heavily metabolized in human liver microsomes and only below 26.3% remained after 30 min incubation.

Table 21 Caco-2 permeabilities.

Compound			P _{app} , (x10 ⁻⁵ cm/sec)		Efflux ratio	Remark
Number	Scaffold	R	A to B	B to A		
(R)-6c			0.66	1.9	2.8	moderate
41			2.6	2.1	0.80	high
50			2.5	2.6	1.0	High
58			1.3	1.6	1.2	high
12a			0.38	0.77	2.0	moderate
16			1.7	2.3	1.4	high
88			1.4	1.9	1.3	high
93			0.19	0.42	2.3	moderate

Moderate permeabilities were observed for **(R)-6c**, **12a**, **93**, and filgotinib in Caco-2 permeability tests with the permeability coefficients 0.66, 0.38, 0.19 and 0.37x10⁻⁵ cm/sec, respectively (Table 13).³⁶ On the other hand, **41**, **50**, **58**, **16**, and **88** had high permeability coefficients ranged from 1.3x10⁻⁵ cm/sec to 2.6x10⁻⁵ cm/sec. As the results, the sulfonamide groups and the urea group at R group position, except for compound **93**, improved passive cell permeability from A to B. The efflux ratios of all test compounds were below 3.0 and they did not seem to be heavily affected by the efflux mechanism.

Table 22 The inhibition percentages against CYP₄₅₀ isoforms.

Compound		CYP ₄₅₀ isoforms (% of control activity @ 10 μM)									
Number	Scaffold	R	1A2	2A6	2B6	2C8	2C9	2C19	2D6	2E1	3A4
(R)-6c			92.5	92.0	91.5	81.0	84.4	66.0	91.6	50.3	89.7
41			70.1	85.8	92.5	63.6	60.7	92.1	95.8	48.7	73.5
50			99.9	96.7	> 100	> 100	90.7	93.8	> 100	63.9	95.4
58			65.7	87.2	92.0	66.2	50.4	55.8	90.3	59.8	33.2
12a			89.3	99.1	> 100	> 100	> 100	91.8	> 100	57.7	98.2
16			69.2	85.7	> 100	> 100	62.3	76.2	98.9	66.0	55.3
88			71.6	85.1	90.1	> 100	56.4	65.0	94.1	63.5	50.2
93			85.1	79.7	86.5	78.1	63.0	58.0	70.3	51.8	76.7

To probe drug-drug interaction possibilities, we screened 8 test compounds against representative CYP₄₅₀ isoforms at 10 μ M concentrations for each compound (Table 14). In the cases of **(R)-6c** and **12a**, CYP 2C19 and 2E1 were influenced at the same concentrations. Compound **50** seemed to inhibit only CYP 2E1 isoform at the concentration. However, the treatments of the benzenesulfonamide-containing **41**, **58**, **16**, **88**, and **93** were likely to affect many isoforms including CYP 1A2, 2C8, 2C9, 2C19, 2E1, and 3A4, which may lead to possible interactions with many drugs. The CYP 2E1 isoform, which test compounds commonly inhibited, has substrates for some anaesthetics like halothane, enflurane, methoxyflurane, sevoflurane, etc.⁷⁶ Representative substrates of CYP 2C19 comprise of proton pump inhibitors including esomeprazole, lansoprazole, etc. In the case of the proton pump inhibitors, their prescription frequencies are decreasing in recent times, so that the combined prescription would not be a problem.

Due to high plasma protein binding, low liver microsomal stability, and high CYP₄₅₀ inhibition rates, we excluded compounds with sulfonamide groups from further studies. Therefore, **(R)-6c** and **12a** were chosen for studies on hERG, kinase profiling, and *in vivo* efficacy tests.

Human ether-a-go-go related gene (hERG) potassium channel assays and kinase profiling

Next, we investigated the hERG binding of **(R)-6c** and **12a** for its cardiotoxicity prediction. The binding test was carried out with HEK293 cells according to the automated patch clamp method. Compound **(R)-6c** and **12a** showed with IC₅₀ of 1.2×10^2 and 93 μ M, respectively. Under the same conditions, filgotinib gave IC₅₀ of 85 μ M. In the case of tofacitinib citrate, IC₅₀ was reported above 100 μ M.⁷⁷ From these results, **(R)-6c** appears to be superior to filgotinib in the cardiotoxicity predicted by the hERG assay.

Kinase inhibitors targeting an ATP-binding site have a probability of

inhibiting other kinases in addition to the targeted one, which can result in some predictable side effects. Therefore, we screened (**R**)-**6c** and **12a** against 323 kinases at the 10 μ M concentration. Under this condition, only four JAK family kinases including JAK1, JAK2, JAK3, and TYK2 showed over 90% inhibition by compound (**R**)-**6c**. The kinases with 80 – 90% inhibition were only ROCK-IIs derived from rats and humans. In the case of compound **12a**, the kinases inhibited to over 90% were only three kinases, JAK1, JAK2, and TYK2. And the kinases with 80 – 90% inhibition included 6 kinases: JAK3, ROCK-II (human), ROCK-II (rat), DCAMKL3, CLK1, and Flt4. On the other hand, it was reported that tofacitinib citrate inhibits 26 kinases above 90%,²⁰ so it is likely that (**R**)-**6c** and **12a** would have less side effects than tofacitinib citrate.

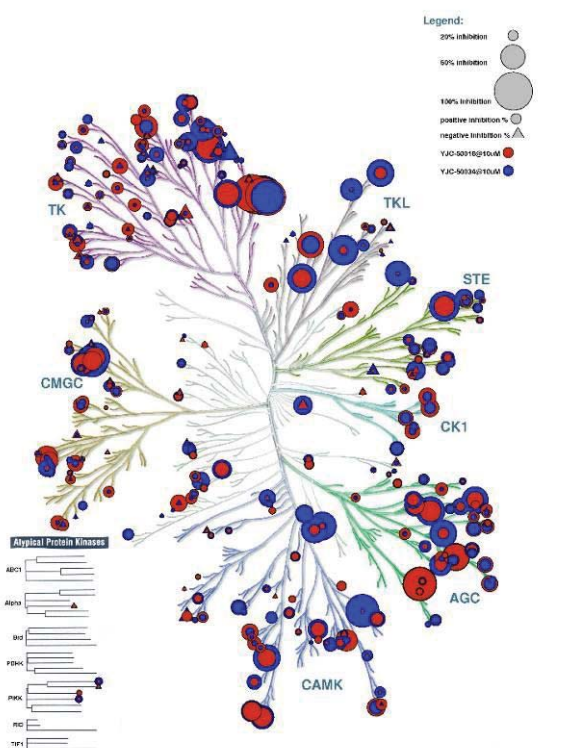


Figure 4 The kinome tree of (**R**)-**6c** and **12a** against 323 kinases at the 10 μ M concentration drawn by the web accessible Kinome Render program.⁷⁸

Pharmacokinetics

Table 23 Pharmacokinetic profiles of (*R*)-**6c**.

Species	Beagle dog		S. D. rat		ICR mouse	
Route	P.O.	I.V.	P.O.	I.V.	P.O.	I.V.
N	4M	4M	4M	4M	4M	4M
Dose (mg/kg)	5	3	10	5	10	5
C _{max} (ng/mL)	1.9x10 ³		1.0x10 ³		1.8x10 ³	
T _{max} (h)	1.8		0.30		1.3	
t _{1/2} (h)	3.3	3.0	2.1	1.2	1.7	0.9
AUC _{0→inf} (ng·h/mL)	1.5x10 ⁴	5.2x10 ³	2.1x10 ³	9.2x10 ²	4.8x10 ³	6.8x10 ²
AUC _{0→t} (ng·h/mL)	1.4x10 ⁴	5.0x10 ³	1.9x10 ³	9.0x10 ²	4.7x10 ³	6.0x10 ²
MRT (h)	7.3	4.7	3.1	1.1	2.9	1.3
F (%)	1.7x10 ²		1.1x10 ²		1.9x10 ²	

Table 24 Pharmacokinetic profiles of **12a**.

Species	Beagle dog		S. D. rat		ICR mouse	
Route	P.O.	I.V.	P.O.	I.V.	P.O.	I.V.
N	4M	4M	4M	4M	4M	4M
Dose (mg/kg)	5	3	10	5	10	5
C _{max} (ng/mL)	1.9x10 ³		1.9x10 ³		1.0x10 ³	
T _{max} (h)	1.1		0.30		0.30	
t _{1/2} (h)	1.7	1.6	2.1	0.70	2.1	0.9
AUC _{0→inf} (ng·h/mL)	6.5x10 ³	2.2x10 ³	4.3x10 ³	9.5x10 ²	2.1x10 ³	6.8x10 ²
AUC _{0→t} (ng·h/mL)	6.4x10 ³	2.1x10 ³	4.1x10 ³	9.3x10 ²	1.9x10 ³	5.1x10 ²
MRT (h)	3.1	2.4	2.9	0.9	3.1	1.4
F (%)	1.8x10 ²		2.2x10 ²		1.9x10 ²	

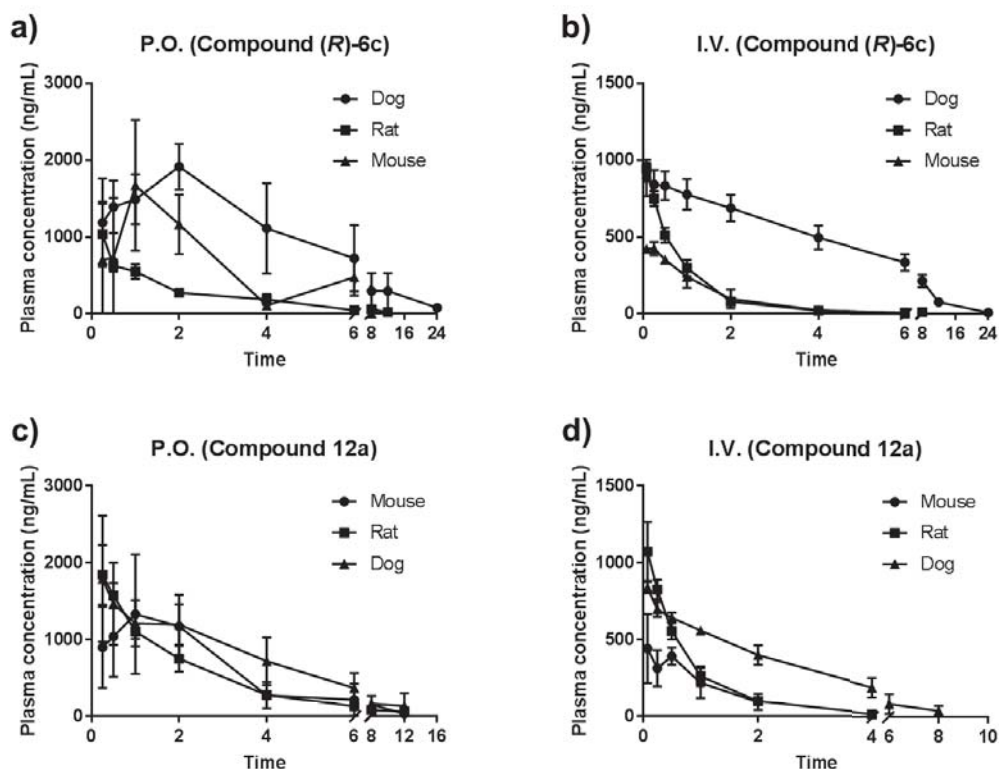


Figure 5 Plasma concentrations after oral administration and intravenous injection of **(R)-6** and **12a** in Beagle dogs, Sprague-Dawley rats, and ICR mice.

To address oral bioavailability of our representative compounds, **(R)-6c** and **12a**, we then carried out the pharmacokinetic tests in dogs, rats, and mice. The vehicles for oral administration and intravenous injection were corn oil and the solution of 10% ethanol and 90% PEG400, respectively, because of low solubility of **(R)-6c** and **12a** in water. In the case of pharmacokinetics through intravenous injection, the drug exposure generally tended to be decreased so that the bioavailability at all species became over 100%, which is similar to the results reported by K. W. Ward *et al.*⁷⁹ and R. Weaver *et al.*⁸⁰

In the case of oral administration at 10 mg/kg dosage in male Sprague Dawley rats, compound **(R)-6c** showed 2.1 hours of half-life ($t_{1/2}$), 4.3×10^3 ng·h/mL of area under curve from 0 to infinite ($AUC_{0 \rightarrow \infty}$), 1.9×10^3 ng/mL of

maximum concentration (C_{\max}), and 0.30 hour of the time to reach the maximum concentration (T_{\max}). Compound **12a** had similar profiles to compound (**R**)-**6c** except for C_{\max} and AUC which had about twice the values of compound (**R**)-**6c**. Though the profiles of $t_{1/2}$, C_{\max} , and T_{\max} were similar to the reported tofacitinib's ones ($t_{1/2} = 2.0$ h, $C_{\max} = 2.4 \times 10^3$ ng/mL, $T_{\max} = 0.31$ h), (**R**)-**6c** and **12a** surpassed tofacitinib with $AUC_{0 \rightarrow \infty}$ value of 2.8×10^3 ng·h/mL on drug exposure.⁷⁷ In comparison with the reported profiles of filgotinib through oral treatment at 5 mg/kg dosage, filgotinib has a longer half-life ($t_{1/2} = 3.9$ h), but a lower drug exposure ($AUC_{0 \rightarrow t} = 1.7 \times 10^3$ ng·h/mL) than compound **12a**,³⁶ although direct comparison with filgotinib and **12a** is impossible because of their different oral administration dosages. Compound (**R**)-**6c** and **12a** showed a superior drug exposure to tofacitinib ($AUC_{0 \rightarrow \infty} = 2.3 \times 10^3$ ng·h/mL)⁷⁷ in the PK study in male beagle dogs at 5 mg/kg dosage. However, PK profiles of (**R**)-**6c** and **12a** in dogs are inferior to the reported values of filgotinib, which features 5.2 hours of half-life ($t_{1/2}$) and 1.4×10^4 ng·h/mL of $AUC_{0 \rightarrow t}$.³⁶

Table 25 Pharmacokinetic parameters of the free base and the salt forms of **(R)-6c** in Sprague-Dawley rats.

(R)-6c									
Sample		Free base			Hydrochloride			Citrate	
Salt form		P.O.	I.V.		P.O.	I.V.		P.O.	I.V.
Route									
N (S.D. Rat)		4M	4M		4M	4M		4M	4M
Dose (mg/kg)		10	5		10	5		10	5
C _{max} (ng/mL)		1.0x10 ³			1.3 x10 ³			1.0x10 ³	
T _{max} (h)		0.30			0.40			0.40	
t _{1/2} (h)		2.1	1.2		1.1	0.60		1.0	1.0
AUC _{0→∞} (ng·h/mL)		2.1x10 ³	9.2x10 ²		2.4x10 ³	1.9x10 ³		1.9x10 ³	1.4x10 ³
AUC _{0→t} (ng·h/mL)		1.9x10 ³	9.0x10 ²		2.4x10 ³	1.8x10 ³		1.9x10 ³	1.4x10 ³
MRT (h)		3.1	1.1		1.6	0.7		1.5	0.9
F (%)		1.1x10 ²			65			68	

Table 26 Pharmacokinetic parameters of the free base and the salt forms of **12a** in Sprague-Dawley rats.

Sample 12a									
Salt form		Free base			Hydrochloride			Citrate	
Route		P.O.	I.V.		P.O.	I.V.		P.O.	I.V.
N (S.D. Rat)		4M	4M		4M	4M		4M	4M
Dose (mg/kg)		10	5		10	5		10	5
C _{max} (ng/mL)		1.9x10 ³			1.3x10 ³			2.0x10 ³	3.4x10 ³
T _{max} (h)		0.30			0.60			0.50	
t _{1/2} (h)		2.1	0.70		2.9	4.1		3.2	7.7
AUC _{0→∞} (ng·h/mL)		4.3x10 ³	9.5x10 ²		2.8x10 ³	2.1x10 ³		3.8x10 ³	4.6x10 ³
AUC _{0→t} (ng·h/mL)		4.1x10 ³	9.3x10 ²		2.7x10 ³	2.0x10 ³		3.8x10 ³	4.6x10 ³
MRT (h)		2.9	0.90		2.7	2.4		2.4	1.9
F (%)		2.2x10 ²			67			41	
								2.8	1.4
								35	

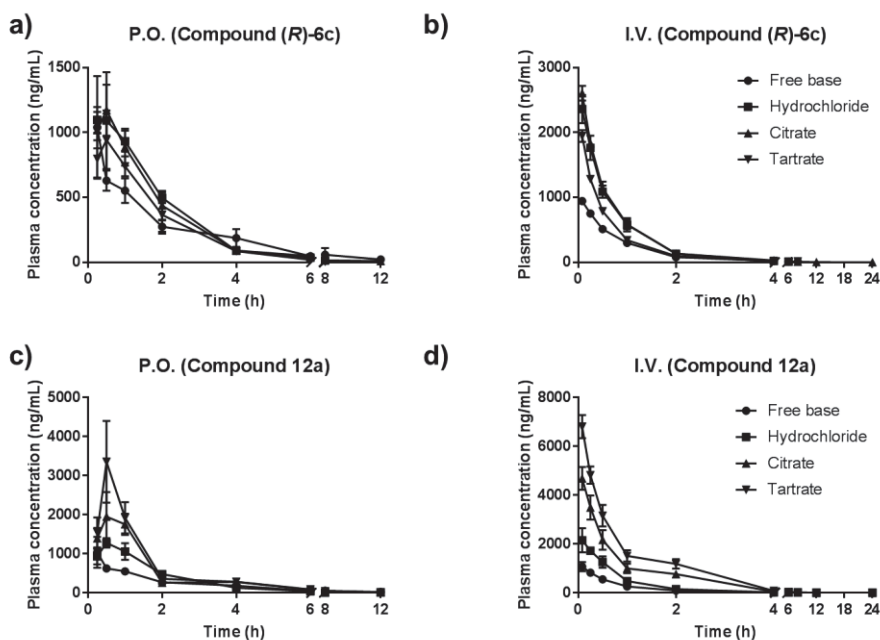


Figure 6 Plasma concentrations after oral administration and intravenous injection of the free base and the salt forms of **(R)-6c** and **12a** in Sprague-Dawley rats.

To improve exposures of **(R)-6c** and **12a** in the *in vivo* model, we made several different salts using hydrochloride, citric acid, and tartaric acid. For hydrochloride and citrate salts, their drug exposures were increased compared to the free base form. However, the tartrate salt of **(R)-6** and the hydrochloride and citrate salts of **12a** were less exposed than the free base in the oral administration. Moreover, the citrate form of **(R)-6c** and three salts of **12a** had the additive advantage that their half-lives were elongated to 2.9 – 4.2 hours. Hence, the citrate of **(R)-6c** and the tartrate of **12a** appear to be the preferred formulations in oral administration.

In vivo efficacy studies on (R)-6c and 12a

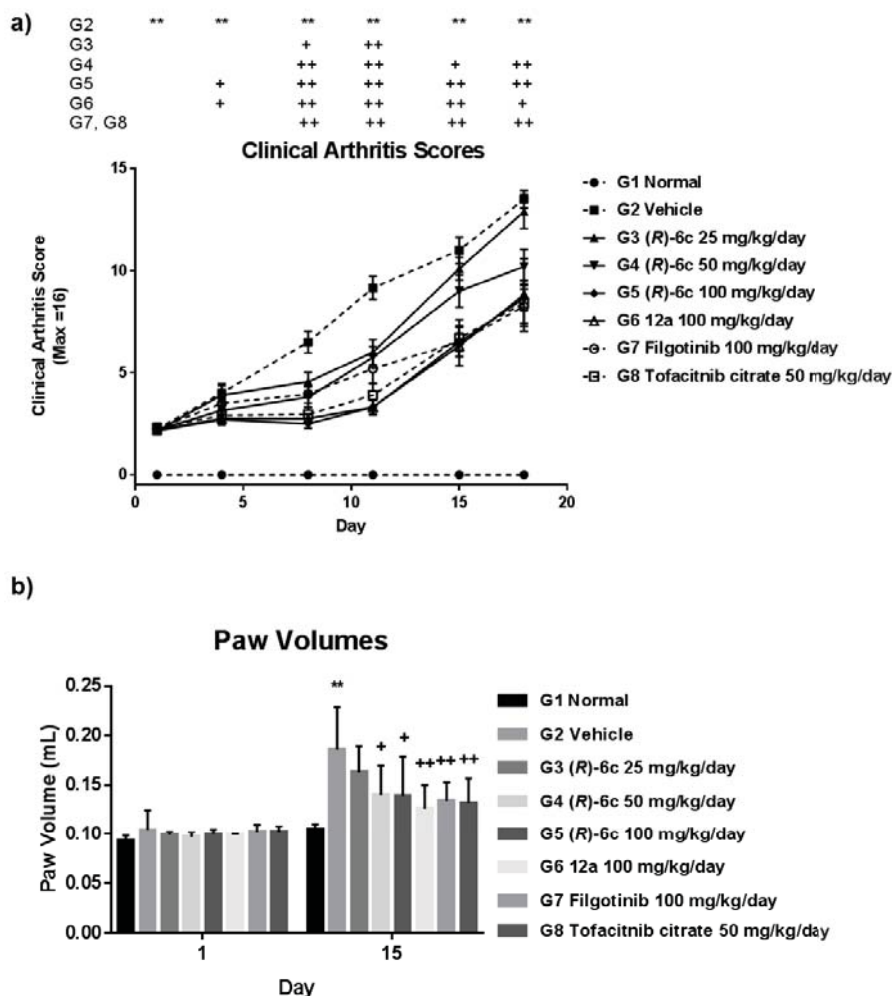


Figure 7 a) Clinical arthritis scores and b) paw volumes of (R)-6c and 12a treatment on collagen-induced arthritis in DBA/1J mice for 18 days. The significance symbols are ** = significantly different between G1 and G2 ($P < 0.01$), + = significantly different from G2 ($P < 0.05$), and ++ = significantly different from G2 ($P < 0.01$).

Both collagen-induced arthritis (CIA) and adjuvant-induced arthritis (AIA) are well-established animal models for the testing and development of new RA therapeutics.⁸¹⁻⁸² We used these to evaluate the efficacies for the treatment with (R)-6c and 12a in a free base form. In the mouse CIA study, the effect of (R)-6c and 12a treatments were evaluated by using the following

indices: clinical arthritis score, paw volume, serum cytokine concentration, bone surface/volume ratio, and histopathological data of ankles. Filgotinib (100 mg/kg/day)⁶³ and tofacitinib citrate (50 mg/kg/day)²² were used as positive controls. Treatment with **(R)-6c** (25, 50 or 100 mg/kg/day) and **12a** (100 mg/kg/day) resulted in significant attenuation of arthritis in DBA1/J mice when compared to vehicle treatment (Figure 7). In the clinical arthritis scores, the treatments of **(R)-6c** and **12a** at 100 mg/kg/day dosage seemed to be faster relieve the symptom than filgotinib's one. However, the results of the treatments of **(R)-6c** and **12a** in clinical scores and paw volume at day 18 showed no significant difference between two test articles and two positive controls.

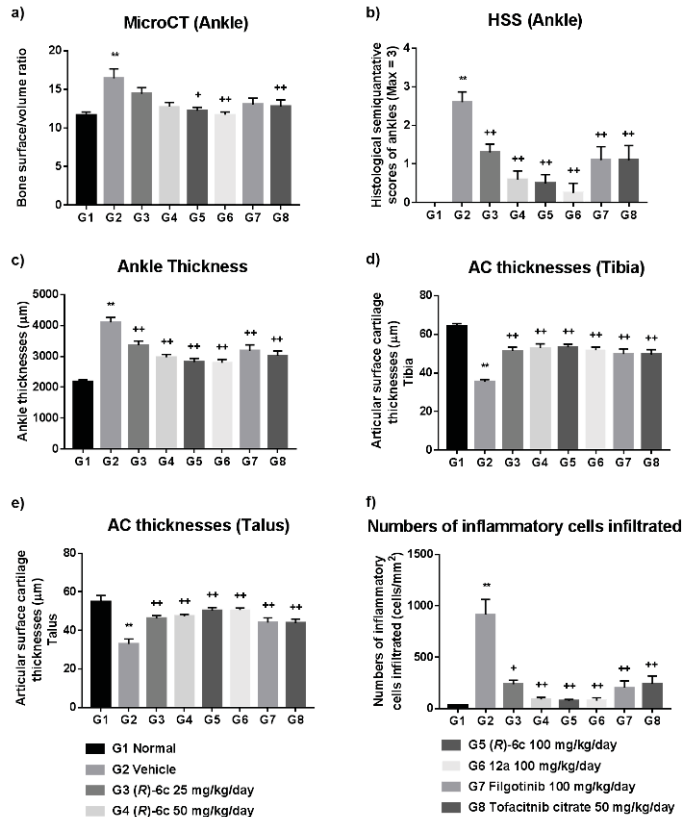


Figure 8 Effects of **(R)-6c** and **12a** treatment on collagen-induced arthritis in DBA1/J mice: a) the bone surface/volume ratios of right hind ankle joints measured by micro-CT, b) the histopathological semiquantitative scores of right hind ankle joints, c) the

right hind ankle joint thicknesses, d-e) the articular surface cartilage thicknesses (tibia and talus) in right hind ankle joints, and f) the numbers of inflammatory cells infiltrated in the right hind ankle joints. The significance symbols are ** = significantly different between G1 and G2 ($P < 0.01$), + = significantly different from G2 ($P < 0.05$), and ++ = significantly different from G2 ($P < 0.01$).

We performed the micro-CT assay and the histopathological assays for further studies on the effects of compound **(R)-6c** and **12a**. We measured the bone surface/volume ratios of right hind ankle joints measured by micro-CT, and identified the following histopathological factors: the histopathological semiquantitative scores of right hind ankle joints, the right hind ankle joint thicknesses, the articular surface cartilage thicknesses (tibia and talus) in right hind ankle joints, and the numbers of inflammatory cells infiltrated in the right hind ankle joints. As the results, all treatments of **(R)-6c** and **12a** except for one at 25 mg/kg/day displayed higher alleviation efficacy than two positive controls. So, in the faces of micro-CT analysis and histopathological assay, **(R)-6c**, a JAK1-selective inhibitor, seemed to have better efficacy than tofacitinib citrate, a pan-JAK inhibitor, at same dosages.

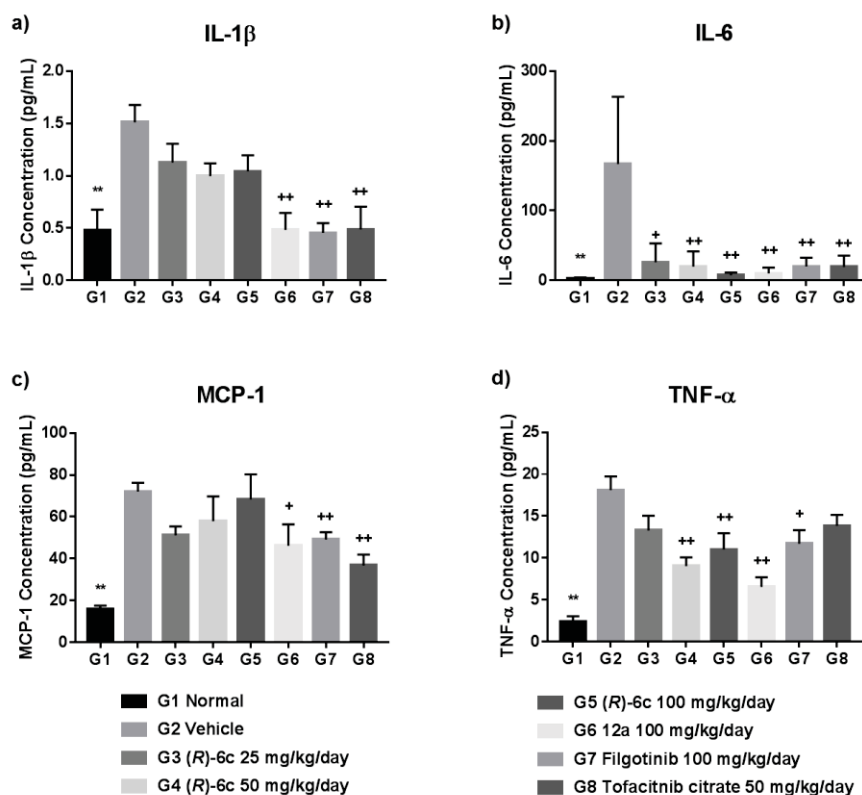
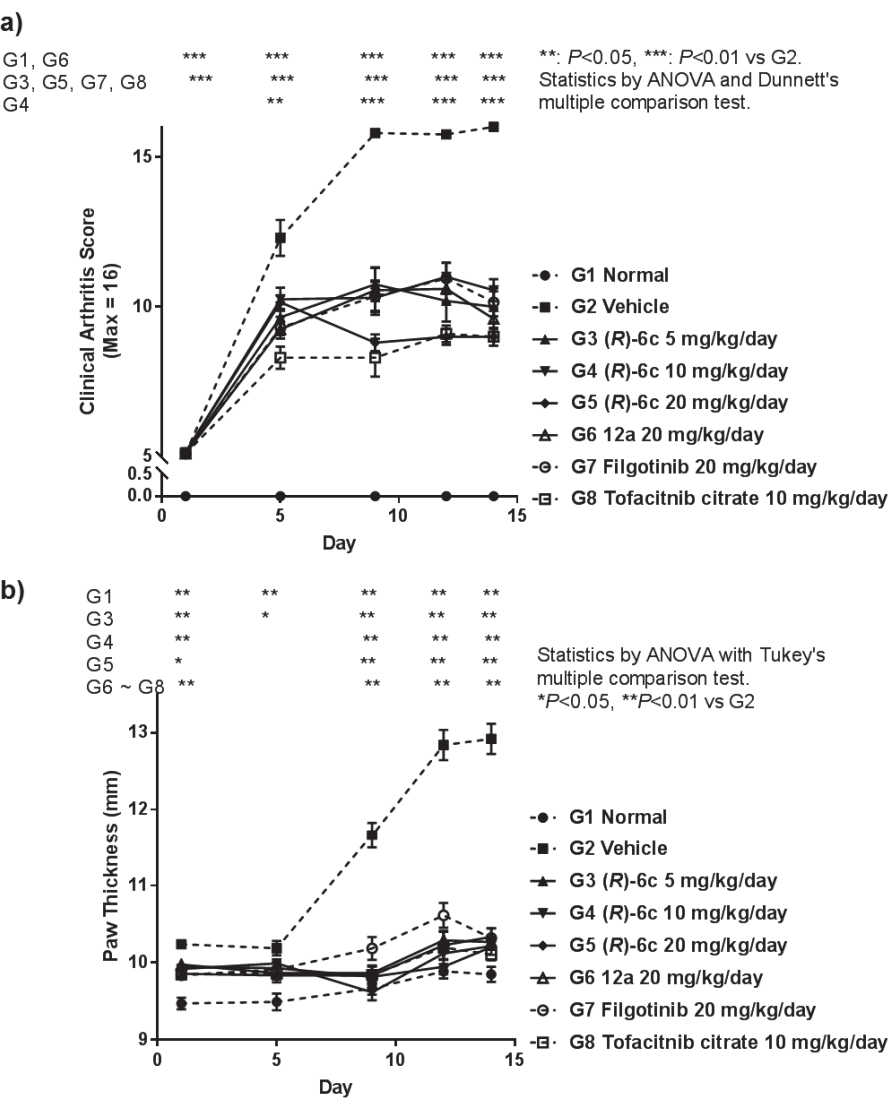


Figure 9 cytokine concentration changes in plasma by (R)-6c and 12a treatment on collagen-induced arthritis in DBA/1J mice for 18 days: a) IL-1 β , b) IL-6, c) MCP-1, and d) TNF- α . The significance symbols are ** = significantly different between G1 and G2 ($P < 0.01$), + = significantly different from G2 ($P < 0.05$), and ++ = significantly different from G2 ($P < 0.01$).

We identified concentration changes of cytokines, including IL-1 β , IL-6, MCP-1 and TNF- α , related to rheumatoid arthritis in plasma through the treatments of (R)-6c and 12a for 18 days. As a result, compound (R)-6c and 12a clearly influenced IL-6 and TNF- α levels in plasma. On these cytokines, treatments of (R)-6c and 12a at all dosages more alleviated cytokine levels than positive controls' ones. The treatment of 12a seemed to decrease the levels of

IL-1 β and MCP-1 in plasma although its alleviation was inferior to one of tofacitinib citrate. However, compound (*R*)-**6c** could not significantly affect IL-6 and TNF- α levels in plasma. As the results, compound (*R*)-**6c** and **12a** may alleviate the clinical and histopathological symptoms in mouse CIA model through lowering IL-6 level.



Statistics by ANOVA with Tukey's multiple comparison test.

* $P < 0.05$, ** $P < 0.01$ vs G2

Figure 10 Effects of (*R*)-**6c** and **12a** treatment on adjuvant-induced arthritis in Lewis rats: a) the clinical arthritis scores and b) the volumes of right hind paws. The data were measured twice per week for 14 days.

In the rat AIA study, all treatments with test articles significantly suppressed the arthritis symptoms versus vehicle treatment for 14 days. The treatment with 20 mg/kg/day of **(R)-6c** demonstrated nearly equal efficacy as that of tofacitinib citrate (10 mg/kg/day). Their clinical arthritis scores reached the same 9.0 value at day 14 and paw thicknesses were similar (**(R)-6c** at 10.20 mm and tofacitinib citrate at 10.10 mm). However, filgotinib (20 mg/kg/day) and **(R)-6c** in lower concentrations (5 and 10 mg/kg) showed slightly inferior clinical arthritis scores (10.32, 10.21, and 10.33, respectively) to the former case. Treatment with compound **12a** (20 mg/kg/day) significantly attenuated arthritis symptoms to a similar extent as filgotinib (20 mg/kg/day) treatment and significantly reduced paw swelling to a similar extent as tofacitinib citrate (10 mg/kg/day) treatment.

V. Conclusions

We have shown the efficacy of **(R)-6c** and **12a** through *in vitro* and *in vivo* tests. In the enzyme assays, the JAK1 IC₅₀ value of **(R)-6c** was 8.5 nM and the selectivity indices of JAK2, JAK3, and TYK2 over JAK1 were 48.5, 128.5, and 29.6, respectively. And compound **12a** also showed a better JAK1-selectivity than tofacitinib citrate (IC₅₀ value of 19 nM and selectivity index of 6.8). In the cell based functional assay, it inhibited the JAK1 isozyme more effectively than filgotinib, but less so than tofacitinib citrate. In the kinase profiling, the inhibitory activities on other kinases except for JAK series were less than those of tofacitinib citrate. From the above *in vitro* tests, we obtained highly JAK1-selective profiles for our inhibitor, which presumably would lead to lower toxicity than tofacitinib citrate.

In the *in vitro* ADME tests, its profiles were similar to those of tofacitinib citrate and filgotinib. The compound **(R)-6c** and **12a** showed good human plasma stability along with two positive controls to exhibit similar profiles on the bound percentages on human plasma protein and the stability against human liver microsomes. Thus, there was a moderate permeability coefficient from A to B in Caco-2 permeability tests like filgotinib, but less efflux ratio so that it seems to be more highly permeable to cells than filgotinib. In the CYP₄₅₀ isozyme screening, the compound showed inhibition of 2C19 and 2E1 isoforms at 10 µM concentrations. In pharmacokinetic studies in rats through oral administration, the profiles of the free base were at acceptable levels.

In the *in vivo* studies, we observed that a double dose of **(R)-6c** and **12a**, JAK1-selective inhibitors, gave similar or superior efficacies to that of tofacitinib citrate, a pan-JAK inhibitor. Moreover, **(R)-6c** and **12a** relieved the arthritis symptoms more than an equivalent dose of filgotinib, the JAK1-selective inhibitor belonging to the same category, did. Taken together, our present study indicates that **(R)-6c** and **12a** have desirable physicochemical

properties and efficacy via selective inhibition of the JAK1 pathway. These findings suggest that (*R*)-**6c** and **12a** have therapeutic potential for the treatment of rheumatoid arthritis.

VI. Experimental Section

Synthesis

All reagents for the syntheses were obtained from commercially available sources and used without any further purification. A diastereomeric pair of the key starting material, 5-((*R*)-1-phenylethyl)-5-azaspiro[2.4]heptan-7-amine, was purchased from custom-synthesis through Sundia Meditech, China. All final products were purified by flash column chromatography and Merck silica gel 60 (0.040 – 0.063 mm) was used for flash column chromatography. The structures of the compounds were identified through ^1H and ^{13}C NMR spectroscopy and high resolution mass spectrometry (MS). NMR spectra were taken from Agilent NMR system 400 MHz DD2MR400, Bruker Biospin AVANCE II 400, and Varian NMR System 500 MHz. Bruker Compact Ultra High Resolution ESI Q-TOF mass spectrometer was used for the MS data. The purities of synthesized compounds were analyzed through the use of 256 nm-wavelength absorption spectra on Agilent HPLC 1100 and 1260 infinity with 6120 Quadrupole LC/MS detector. Additionally, their optical rotation data were obtained by JASCO's P-1030 Polarimeter.

Synthesis of ethyl ((R)-5-((R)-1-phenylethyl)-5-azaspiro[2.4]heptan-7-yl)carbamate, (R)-2c

Potassium carbonate (25.9 g, 187 mmol) in 140 mL of deionized water was added to a (*R*)-5-((*R*)-1-phenylethyl)-5-azaspiro[2.4]heptan-7-amine (**R**)-**1c** (20.1 g, 92.9 mmol) solution in 250 mL of tetrahydrofuran and stirred at room temperature for 10 minutes. Ethyl chloroformate (9.46 mL, 99.4 mmol) was then added and the mixture was stirred at room temperature overnight. After the reaction, the solution was evaporated and the residue was extracted with dichloromethane three times. The combined organic layers were dried over anhydrous sodium sulfate and the solid was filtered off. The filtered solution was evaporated. Removing the solvent in vacuo provided 26.7 g of

ethyl ((*R*)-5-((*R*)-1-phenylethyl)-5-azaspiro[2.4]heptan-7-yl)carbamate (quantitatively yield). ¹H NMR (400 MHz, CDCl₃) δ 7.27 (m, 5H), 5.20 (d, *J* = 8.9 Hz, 1H), 4.04 (dd, *J* = 14.2, 7.1 Hz, 2H), 3.82 (ddd, *J* = 8.7, 5.8, 2.8 Hz, 1H), 3.21 (dd, *J* = 13.1, 6.5 Hz, 1H), 2.84 (dd, *J* = 9.6, 6.0 Hz, 1H), 2.78 (d, *J* = 8.9 Hz, 1H), 2.46 (dd, *J* = 9.6, 2.5 Hz, 1H), 2.30 (d, *J* = 8.8 Hz, 1H), 1.34 (d, *J* = 6.6 Hz, 3H), 1.20 (t, *J* = 7.1 Hz, 3H), 0.75 (m, 2H), 0.59 (m, 1H), 0.47 (m, 1H). ¹³C NMR (100 MHz, CDCl₃) δ 156.4, 144.8, 128.5, 127.2, 125.5, 77.5, 77.2, 76.9, 65.6, 61.0, 60.8, 60.7, 56.1, 26.4, 22.7, 14.7, 14.2, 8.9.

Synthesis of (R)-N-methyl-5-((R)-1-phenylethyl)-5-azaspiro[2.4]heptan-7-amine, (R)-3c

An ethyl ((*R*)-5-((*R*)-1-phenylethyl)-5-azaspiro[2.4]heptan-7-yl)carbamate (**R**)-**2c** (26.6 g, 92.2 mmol) solution in 345 mL of tetrahydrofuran was placed in a 1 L round bottom flask. After it was cooled at -40 °C, lithium aluminum hydride (7.01 g, 185 mmol) was slowly added and stirred. The reaction mixture was refluxed for 4 hours then cooled down to -40 °C. The reaction was quenched with 40 mL of deionized water, 40 mL of 15% sodium hydroxide solution, and 40 mL of deionized water. Then, celite 545 was added and the mixture was stirred for 30 minutes before being filtered through a celite 545 pad. The filtered solution was evaporated and extracted with dichloromethane three times. Combined organic layers were dried over anhydrous sodium sulfate and the solid was filtered off. And the filtered solution was evaporated. Removing the solvent in vacuo provided 19.4 g of (*R*)-*N*-methyl-5-((*R*)-1-phenylethyl)-5-azaspiro[2.4]heptan-7-amine (91.0% yield). ¹H NMR (400 MHz, CDCl₃) δ 7.27 (m, 5H), 3.22 (q, *J* = 6.6 Hz, 1H), 3.11 (dd, *J* = 9.4, 6.1 Hz, 1H), 2.86 (t, *J* = 5.5 Hz, 1H), 2.61 (d, *J* = 8.9 Hz, 1H), 2.39 (m, 1H), 2.30 (d, *J* = 4.9 Hz, 3H), 2.28 (d, *J* = 9.0 Hz, 1H), 1.37 (d, *J* = 6.6 Hz, 3H), 0.78 (m, 1H), 0.56 (dd, *J* = 8.6, 7.1 Hz, 2H), 0.35 (m, 1H). ¹³C NMR (100 MHz, CDCl₃) δ 145.4, 128.4, 127.3, 127.0, 66.2, 63.8, 61.9, 59.8, 34.4, 25.9, 23.0, 14.1, 7.3.

Synthesis of N-methyl-N-((R)-5-((R)-1-phenylethyl)-5-azaspiro[2.4]heptan-7-yl)-7H-pyrrolo[2,3-d]pyrimidin-4-amine, (R)-4c

A (R)-N-methyl-5-((R)-1-phenylethyl)-5-azaspiro[2.4]heptan-7-amine (**(R)-3c**) (18.3 g, 79.4 mmol) solution in 330 mL of deionized water was placed in a 500 mL round bottom flask. Consequently, 6-chloro-7-deazapurine (12.8 g, 83.3 mmol) and potassium carbonate (22.0 g, 159 mmol) were added and refluxed for 18 hours. After the reaction, it was cooled at room temperature and the aqueous mixture was extracted with 250 mL of dichloromethane three times. Combined organic layers were dried over anhydrous sodium sulfate and the solid was filtered off while the filtered solution was evaporated. Removing the solvent in vacuo provided 27.7 g of N-methyl-N-((R)-5-((R)-1-phenylethyl)-5-azaspiro[2.4]heptan-7-yl)-7H-pyrrolo[2,3-d]pyrimidin-4-amine (quantitatively yield). ¹H NMR (400 MHz, CDCl₃) δ 12.24 (s, 1H), 8.20 (s, 1H), 7.36 (d, *J* = 7.1 Hz, 2H), 7.30 (t, *J* = 7.4 Hz, 2H), 7.22 (dd, *J* = 13.4, 6.2 Hz, 1H), 7.03 (t, *J* = 3.7 Hz, 1H), 6.53 (d, *J* = 3.4 Hz, 1H), 5.52 (s, 1H), 3.49 (s, 3H), 3.18 (dd, *J* = 13.0, 6.5 Hz, 1H), 2.87 (t, *J* = 9.5 Hz, 2H), 2.73 (dd, *J* = 10.5, 2.8 Hz, 1H), 2.45 (d, *J* = 8.8 Hz, 1H), 1.38 (d, *J* = 6.5 Hz, 3H), 0.94 (m, 1H), 0.63 (m, 2H), 0.47 (m, 1H). ¹³C NMR (100 MHz, CDCl₃) δ 158.0, 151.8, 150.6, 145.5, 128.6, 127.1, 127.1, 120.2, 102.7, 102.2, 66.2, 62.1, 59.7, 58.6, 33.8, 24.5, 23.2, 12.6, 11.6.

Synthesis of (R)-N-methyl-N-(5-azaspiro[2.4]heptan-7-yl)-7H-pyrrolo[2,3-d]pyrimidin-4-amine, (R)-5c

A N-methyl-N-((R)-5-((R)-1-phenylethyl)-5-azaspiro[2.4]heptan-7-yl)-7H-pyrrolo[2,3-d]pyrimidin-4-amine (**(R)-4c**) (27.7 g, 79.7 mmol) solution in 890 mL of methanol was placed in a 2 L round bottom flask. Then, 10w/w% palladium on charcoal (14.0 g, 5 wt%) and 10.1 g of ammonium formate (10.1 g, 160 mmol) were added and the reaction mixture was stirred at 60~70 °C overnight. After the reaction, it was filtered through a celite 545 pad before the

solution was evaporated. Removing the solvent in vacuo provided 22.2 g of (*R*)-*N*-methyl-*N*-(5-azaspiro[2.4]heptan-7-yl)-7*H*-pyrrolo[2,3-*d*]pyrimidin-4-amine (quantitatively yield). ¹H NMR (400 MHz, CDCl₃) δ 12.13 (s, 1H), 8.25 (s, 1H), 7.08 (t, *J* = 6.0 Hz, 1H), 6.54 (d, *J* = 3.4 Hz, 1H), 5.35 (m, 1H), 4.52 (s, 1H), 3.64 (dd, *J* = 12.2, 8.2 Hz, 1H), 3.48 (t, *J* = 8.4 Hz, 1H), 3.41 (s, 3H), 3.27 (d, *J* = 10.9 Hz, 1H), 2.96 (m, 1H), 0.91 (d, *J* = 9.8 Hz, 1H), 0.71 (m, 2H), 0.62 (d, *J* = 10.1 Hz, 1H). ¹³C NMR (100 MHz, CDCl₃) δ 157.9, 151.8, 150.5, 120.7, 103.1, 102.1, 62.4, 56.2, 51.3, 34.8, 25.1, 14.9, 9.4.

*Syntheses of the 3-(7-(methyl(7*H*-pyrrolo[2,3-*d*]pyrimidin-4-yl)amino)-5-azaspiro[2.4]heptan-5-yl)-3-oxopropanenitrile enantiomers*

In a 5 mL round bottom flask, (*R*)-*N*-methyl-*N*-(5-azaspiro[2.4]heptan-7-yl)-7*H*-pyrrolo[2,3-*d*]pyrimidin-4-amine (**R**)-**5c** (210 mg, 0.863 mmol) was placed and solved with 2.50 mL of *n*-butanol. Ethyl cyanoacetate (0.918 mL, 8.63 mmol) was added before 1,8-diazabicyclo[5.4.0]undec-7-ene (0.0654 mL, 0.437 mmol), then heated at 80 °C for 24 hours. The reaction solution was evaporated and the residue was purified with flash column chromatography (methanol:dichloromethane=2:98). Finally, collected fragments were evaporated. Removing the solvent in vacuo provided 238 mg of (*R*)-3-(7-(methyl(7*H*-pyrrolo[2,3-*d*]pyrimidin-4-yl)amino)-5-azaspiro[2.4]heptan-5-yl)-3-oxopropanenitrile (88.8% yield).

In the cases of racemic mixture and (*S*)-enantiomer, the racemic mixture and the (*S*)-enantiomer of 5-(1-phenylethyl)-5-azaspiro[2.4]heptan-7-amine were purchased at Sundia Meditech, China, and the desired products were synthesized from them by the processes similar to the synthesis of (*R*)-form.

*(R)-3-(7-(Methyl(7*H*-pyrrolo[2,3-*d*]pyrimidin-4-yl)amino)-5-azaspiro[2.4]heptan-5-yl)-3-oxopropanenitrile, (R)-6c*

100% purity by HPLC. ¹H NMR (500 MHz, CDCl₃) δ 12.16 (s, 1H), 8.26 (d, *J* = 6.0 Hz, 1H), 7.13 (s, 1H), 6.56 (d, *J* = 8.6 Hz, 1H), 5.44 (dd, *J* = 41.1, 5.6 Hz, 1H), 4.26 – 4.00 (m, 1H), 3.98 – 3.70 (m, 2H), 3.58 – 3.32 (m, 6H), 1.16 – 0.94 (m, 1H), 0.82 (dd, *J* = 21.5, 10.3 Hz, 3H). ¹³C NMR (100 MHz, CDCl₃) δ 159.9, 157.5, 151.9, 150.3, 120.9, 113.8, 103.1, 101.8, 77.4, 77.1, 76.8, 61.5, 54.8, 51.3, 33.5, 25.7, 22.6, 16.7, 8.1. HRMS (ESI) calcd for C₁₆H₁₉N₆O: 311.1620. Obsd 311.1616. [α]_D +51.6° (*c* 1.49, CHCl₃).

*3-(7-(Methyl(7H-pyrrolo[2,3-*d*]pyrimidin-4-yl)amino)-5-azaspiro[2.4]heptan-5-yl)-3-oxopropanenitrile, 6c*

Yield: 70.0 mg (79.2%). 96.8% purity by HPLC. ¹H NMR (500 MHz, CDCl₃) δ 12.09 (s, 1H), 8.26 (d, *J* = 6.1 Hz, 1H), 7.13 (s, 1H), 6.56 (d, *J* = 8.9 Hz, 1H), 5.56 – 5.27 (m, 1H), 4.25 – 4.02 (m, 1H), 4.00 – 3.70 (m, 2H), 3.60 – 3.29 (m, 6H), 1.15 – 0.94 (m, 1H), 0.82 (dd, *J* = 19.5, 9.6 Hz, 3H). ¹³C NMR (125 MHz, CDCl₃) δ 159.5, 157.3, 151.7, 150.1, 120.5, 113.3, 102.8, 101.6, 61.4, 54.6, 52.6, 33.2, 25.4, 22.5, 16.5, 8.0. HRMS (ESI) calcd for C₁₆H₁₉N₆O: 311.1620. Obsd: 311.1616.

*(S)-3-(7-(Methyl(7H-pyrrolo[2,3-*d*]pyrimidin-4-yl)amino)-5-azaspiro[2.4]heptan-5-yl)-3-oxopropanenitrile, (S)-6c*

Yield: 117 mg (80.1%). 97.4% purity by HPLC. ¹H NMR (500 MHz, CDCl₃) δ 12.18 (s, 1H), 8.26 (s, 1H), 7.12 (s, 1H), 6.55 (s, 1H), 5.38 (t, *J* = 37.8 Hz, 1H), 4.10 (d, *J* = 42.3 Hz, 1H), 3.82 (dd, *J* = 74.7, 15.0 Hz, 2H), 3.63 – 3.18 (m, 6H), 1.02 (d, *J* = 32.1 Hz, 1H), 0.78 (s, 3H). ¹³C NMR (125 MHz, CDCl₃) δ 160.0, 157.5, 151.9, 150.2, 120.9, 113.9, 103.1, 101.8, 61.5, 54.8, 51.3, 33.4, 25.7, 22.6, 16.7, 8.1. HRMS (ESI) calcd for C₁₆H₁₉N₆O: 311.1620. Obsd: 311.1616. [α]_D +35.6° (*c* 0.980, CHCl₃).

In the cases of **6a**, **6b** and **6d** – **6g**, the desired products were synthesized with 4-amino-1-benzylpiperidine, (*R*)-3-amino-1-

benzylpiperidine, ethyl (5-benzyl-5-azaspiro[2.4]heptan-7-yl)carbamate, (*R,R*)-6-benzyl-octahydro-pyrrolo[3,4-*b*]pyridine dihydrochloride, 4-hydroxypiperidine, and 3-hydroxymethylpiperidine, respectively, instead of (*R*)-5-((*R*)-1-phenylethyl)-5-azaspiro[2.4]heptan-7-amine according to the aforementioned process (vide supra).

*3-(4-(Methyl(7H-pyrrolo[2,3-*d*]pyrimidin-4-yl)amino)piperidin-1-yl)-3-oxopropanenitrile, 6a*

Yield: 6.2 mg (3.2%). 91.1% purity by HPLC. ¹H NMR (400 MHz, DMSO-*d*₆) δ 12.65 (s, 1H), 8.38 (s, 1H), 7.43 (s, 1H), 6.90 (d, *J* = 1.6 Hz, 1H), 4.75 (s, 1H), 4.52 (d, *J* = 12.8 Hz, 1H), 4.08 (s, 2H), 3.81 (d, *J* = 13.6 Hz, 1H), 3.27 – 3.20 (m, 3H), 2.82 – 2.75 (m, 1H), 2.03 – 1.91 (m, 1H), 1.77 (s, 2H), 1.23 – 1.18 (m, 2H). LRMS (ESI) calcd for C₁₅H₁₉N₆O: 299.2. Obsd: 299.1.

*(R)-3-(3-(Methyl(7H-pyrrolo[2,3-*d*]pyrimidin-4-yl)amino)piperidin-1-yl)-3-oxopropanenitrile, 6b*

Yield: 42.0 mg (36.2%). 97.2% purity by HPLC. ¹H NMR (400 MHz, CDCl₃) δ 10.41 (d, *J* = 84 Hz, 1H), 8.32 (s, 1H), 7.13 – 7.12 (m, 1H), 6.62 – 6.59 (m, 1H), 4.79 – 4.72 (m, 1H), 4.67 (d, *J* = 11.2 Hz, 1H), 3.91 – 3.55 (m, 3H), 3.38 (s, 2H), 3.27 (s, 1H), 3.12 (q, *J* = 13.2, 11.2 Hz, 1H), 2.65 – 2.58 (m, 1H), 2.11 – 2.08 (m, 1H), 2.02 – 1.69 (m, 3H). LRMS (ESI) calcd for C₁₅H₁₉N₆O: 299.2. Obsd: 299.1.

*N-(5-(7H-Pyrrolo[2,3-*d*]pyrimidin-4-yl)-5-azaspiro[2.4]heptan-7-yl)-2-cyanoacetamide, 6d*

Yield: 30.0 mg (44.0%). 100% purity by HPLC. ¹H NMR (400 MHz, DMSO-*d*₆) δ 11.62 (s, 1H), 8.68 (d, *J* = 7.2 Hz, 1H), 8.18 (s, 1H), 7.13 (s, 1H), 6.55 (s, 1H), 3.99 (s, 2H), 3.85 (d, *J* = 10.0 Hz, 1H), 3.64 (s, 2H), 3.62 – 3.55 (m, 1H), 3.16 – 3.10 (m, 1H), 0.84 – 0.70 (m, 4H). LRMS (ESI) calcd for C₁₅H₁₇N₆O: 297.1. Obsd: 297.1.

3-((4aR,7aR)-1-(7H-Pyrrolo[2,3-d]pyrimidin-4-yl)octahydro-6H-pyrrolo[3,4-b]pyridin-6-yl)-3-oxopropanenitrile, 6e

Yield: 50.0 mg (63.3%). 97.0% purity by HPLC. ¹H NMR (400 MHz, CDCl₃) δ 10.04 (s, 1H), 8.36 (d, *J* = 2.8 Hz, 1H), 7.15 – 7.08 (m, 1H), 6.58 – 6.54 (m, 1H), 5.65 – 5.51 (m, 1H), 4.65 – 4.57 (m, 1H), 4.01 – 3.49 (m, 4H), 3.46 (d, *J* = 3.6 Hz, 2H), 3.41 – 3.20 (m, 1H), 2.53 – 2.39 (m, 1H), 2.01 – 1.94 (m, 2H), 1.80 – 1.69 (m, 1H), 1.54 – 1.42 (m, 1H). LRMS (ESI) calcd for C₁₆H₁₉N₆O: 311.2. Obsd: 311.1.

3-(4-((7H-Pyrrolo[2,3-d]pyrimidin-4-yl)oxy)piperidin-1-yl)-3-oxopropanenitrile, 6f

Yield: 35.4 mg (49.4%). 100% purity by HPLC. ¹H NMR (400 MHz, CDCl₃) δ 12.03 (s, 1H), 8.34 (s, 1H), 7.35 (t, *J* = 3.2 Hz, 1H), 6.47 (q, *J* = 3.6, 2.0 Hz, 1H), 5.58 – 5.43 (m, 1H), 4.08 (s, 2H), 3.90 – 3.86 (m, 1H), 3.63 – 3.59 (m, 1H), 3.47 – 3.32 (m, 2H), 2.09 – 2.00 (m, 2H), 1.82 – 1.77 (m, 1H), 1.69 – 1.61 (m, 1H). LRMS (ESI) calcd for C₁₄H₁₆N₅O₂: 286.1. Obsd: 286.1.

3-(3-(((7H-Pyrrolo[2,3-d]pyrimidin-4-yl)oxy)methyl)piperidin-1-yl)-3-oxopropanenitrile, 6g

Yield: 54.9 mg (30.0%). 89.2% purity by HPLC. ¹H NMR (400 MHz, DMSO-*d*₆) δ 12.03 (s, 1H), 8.34 (s, 1H), 7.36 (s, 1H), 6.54 – 6.46 (m, 1H), 4.43 – 4.39 (m, 1H), 4.35 – 4.26 (m, 2H), 4.06 – 4.02 (m, 2H), 3.07 – 3.01 (m, 1H), 2.76 – 2.67 (m, 2H), 1.98 – 1.91 (m, 1H), 1.90 – 1.84 (m, 1H), 1.74 – 1.66 (m, 1H), 1.45 – 1.37 (m, 2H). LRMS (ESI) calcd for C₁₅H₁₈N₅O₂: 300.1. Obsd: 300.1.

Synthesis of (R)-N-(5-ethyl-5-azaspiro[2.4]heptan-7-yl)-N-methyl-7H-pyrrolo[2,3-d]pyrimidin-4-amine, 19

In a 5 mL round-bottom flask, (R)-N-methyl-N-(5-azaspiro[2.4]heptan-7-yl)-7H-pyrrolo[2,3-d]pyrimidin-4-amine (**R**)-**5c** (70.0 mg, 0.288 mmol) was

placed and solved with 1.00 mL of dichloromethane. The solution was treated with bromoethane (0.0320 mL, 0.432 mmol) and *N,N*-diisopropylethylamine (0.100 mL, 0.574 mmol) was added. The reaction solution was stirred at room temperature overnight then evaporated. The residue was purified by flash column chromatography (methanol:dichloromethane=2:98) and collected fragments were evaporated. Removing the solvent in vacuo provided 23.9 mg of (*R*)-*N*-(5-ethyl-5-azaspiro[2.4]heptan-7-yl)-*N*-methyl-7*H*-pyrrolo[2,3-*d*]pyrimidin-4-amine (30.7% yield). 100% purity by HPLC. ¹H NMR (400 MHz, CDCl₃) δ 11.99 (s, 1H), 8.24 (s, 1H), 7.06 (d, *J* = 3.2 Hz, 1H), 6.57 (s, 1H), 5.58 (s, 1H), 3.46 (d, *J* = 2.8 Hz, 3H), 3.08 (s, 1H), 2.94 (s, 1H), 2.80 (d, *J* = 5.9 Hz, 1H), 2.58 (d, *J* = 5.4 Hz, 2H), 1.19 – 1.12 (m, 3H), 0.90 (dd, *J* = 21.8, 5.3 Hz, 2H), 0.68 (s, 2H), 0.50 (d, *J* = 5.7 Hz, 1H). ¹³C NMR (100 MHz, CDCl₃) δ 157.9, 151.8, 150.5, 120.0, 102.6, 102.0, 63.3, 59.9, 58.3, 50.4, 33.9, 24.1, 13.4, 13.2, 10.4. HRMS (ESI) calcd for C₁₅H₂₂N₅: 272.1875. Obsd: 272.1872. [α]_D +43.2° (*c* 0.560, CHCl₃).

In the cases of **20** and **21**, the desired products were synthesized through substitution reactions with *n*-butyl bromide and benzyl bromide, respectively, instead of ethyl bromide according to the aforementioned process (vide supra).

(R)-*N*-(5-Butyl-5-azaspiro[2.4]heptan-7-yl)-*N*-methyl-7*H*-pyrrolo[2,3-*d*]pyrimidin-4-amine, **20**

Yield: 35.0 mg (40.7%). 100% purity by HPLC. ¹H NMR (400 MHz, CDCl₃) δ 11.46 (s, 1H), 8.24 (s, 1H), 7.06 (d, *J* = 3.5 Hz, 1H), 6.58 (d, *J* = 3.4 Hz, 1H), 5.55 (s, 1H), 3.48 (s, 3H), 3.02 (s, 2H), 2.86 (s, 1H), 2.67 – 2.40 (m, 3H), 1.65 – 1.47 (m, 2H), 1.38 (dq, *J* = 14.4, 7.3 Hz, 2H), 0.94 (t, *J* = 7.3 Hz, 4H), 0.69 (s, 2H), 0.52 (t, *J* = 10.2 Hz, 1H). ¹³C NMR (100 MHz, CDCl₃) δ 157.8, 151.9, 150.7, 119.9, 102.6, 102.2, 63.4, 60.0, 58.6, 56.2, 34.1, 30.3, 24.0, 20.6, 14.0, 13.1, 10.6. HRMS (ESI) calcd for C₁₇H₂₆N₅: 300.2188. Obsd: 300.2188. [α]_D +55.6° (*c* 0.410, CHCl₃).

(R)-N-(5-Benzyl-5-azaspiro[2.4]heptan-7-yl)-N-methyl-7H-pyrrolo[2,3-d]pyrimidin-4-amine, 21

Yield: 40.0 mg (38.8%). 100% purity by HPLC. ¹H NMR (400 MHz, CDCl₃) δ 11.52 (s, 1H), 8.21 (s, 1H), 7.44 – 7.21 (m, 5H), 7.03 (d, *J* = 3.5 Hz, 1H), 6.56 (d, *J* = 3.4 Hz, 1H), 5.57 (s, 1H), 3.64 (dd, *J* = 31.2, 12.9 Hz, 2H), 3.52 (s, 3H), 3.01 – 2.87 (m, 2H), 2.76 (d, *J* = 8.9 Hz, 1H), 2.51 (d, *J* = 8.9 Hz, 1H), 1.01 – 0.90 (m, 1H), 0.70 – 0.56 (m, 2H), 0.51 – 0.40 (m, 1H). ¹³C NMR (100 MHz, CDCl₃) δ 157.9, 151.8, 150.7, 138.9, 128.6, 128.3, 127.0, 119.7, 102.2, 63.3, 60.6, 59.1, 33.7, 24.4, 12.5, 11.2. HRMS (ESI) calcd for C₂₀H₂₄N₅: 334.2032. Obsd: 334.2025. [α]_D +52.9° (*c* 3.07, CHCl₃).

Synthesis of (R)-3-methyl-1-(7-(methyl(7H-pyrrolo[2,3-d]pyrimidin-4-yl)amino)-5-azaspiro[2.4]heptan-5-yl)butan-1-one, 23

In a 5 mL round-bottom flask, *(R)-N-methyl-N-(5-azaspiro[2.4]heptan-7-yl)-7H-pyrrolo[2,3-d]pyrimidin-4-amine (R)-5c* (60.0 mg, 0.247 mmol) was placed and solved with 1.00 mL of *N,N*-dimethylformamide. The solution was treated with isovaleryl chloride (46.6 mg, 0.386 mmol) and *N,N*-diisopropylethylamine (0.0860 mL, 0.494 mmol) was added. The reaction solution was stirred at room temperature overnight and then evaporated. The residue was purified by column chromatography (methanol:dichloromethane=2:98) and collected fragments were evaporated. Removing the solvent in vacuo provided 32.0 mg of *(R)-3-methyl-1-(7-(methyl(7H-pyrrolo[2,3-d]pyrimidin-4-yl)amino)-5-azaspiro[2.4]heptan-5-yl)butan-1-one* (39.1% yield). 100% purity by HPLC. ¹H NMR (500 MHz, CDCl₃) δ 12.06 (d, *J* = 16.4 Hz, 1H), 8.27 (d, *J* = 8.9 Hz, 1H), 7.11 (d, *J* = 9.6 Hz, 1H), 6.56 (d, *J* = 9.9 Hz, 1H), 5.37 (t, *J* = 38.6 Hz, 1H), 4.05 (ddd, *J* = 43.9, 27.1, 11.7 Hz, 2H), 3.82 (dd, *J* = 66.1, 11.9 Hz, 1H), 3.65 (dd, *J* = 178.8, 11.3 Hz, 1H), 3.45 – 3.33 (m, 3H), 2.20 (d, *J* = 13.8 Hz, 3H), 0.99 (s, 6H), 0.78 (t, *J* = 21.2 Hz, 4H). ¹³C NMR (125 MHz, CDCl₃) δ 171.0, 157.5, 151.8, 150.2,

120.4, 102.8, 101.6, 61.6, 55.1, 52.5, 43.3, 33.1, 25.4, 24.8, 22.6, 16.6, 8.0. HRMS (ESI) calcd for C₁₈H₂₆N₅O: 328.2137. Obsd: 328.2126. [α]_D +45.2° (c 1.21, CHCl₃).

In the cases of **24**, **25**, and **29** – **36**, the desired products were synthesized through substitution reactions with isobutyryl chloride, cyclopropane carbonyl chloride, 2-furoyl chloride, benzoyl chloride, nicotinoyl chloride hydrochloride, isonicotinoyl chloride hydrochloride, 3-cyanobenzoyl chloride, 4-cyanobenzoyl chloride, 2-(trifluoromethyl)benzoyl chloride, and 3-(trifluoromethyl)benzoyl chloride, respectively, instead of isovaleryl chloride according to the aforementioned process (vide supra).

(R)-2-Methyl-1-(7-(methyl(7H-pyrrolo[2,3-d]pyrimidin-4-yl)amino)-5-azaspiro[2.4]heptan-5-yl)propan-1-one, 24

Yield: 38.0 mg (42.2%). 100% purity by HPLC. ¹H NMR (500 MHz, CDCl₃) δ 12.06 (d, *J* = 17.4 Hz, 1H), 8.27 (d, *J* = 9.1 Hz, 1H), 7.11 (d, *J* = 10.0 Hz, 1H), 6.56 (d, *J* = 10.8 Hz, 1H), 5.37 (dd, *J* = 42.3, 38.0 Hz, 1H), 4.23 – 3.74 (m, 3H), 3.43 (t, *J* = 21.8 Hz, 4H), 2.79 – 2.56 (m, 1H), 1.16 (dd, *J* = 9.8, 5.6 Hz, 6H), 1.10 – 0.94 (m, 1H), 0.79 (td, *J* = 25.2, 8.8 Hz, 3H). ¹³C NMR (125 MHz, CDCl₃) δ 175.4, 157.2, 151.9, 150.3, 120.4, 102.9, 101.7, 61.6, 54.2, 50.3, 32.8, 32.0, 24.9, 18.7, 16.8, 8.0. HRMS (ESI) calcd for C₁₇H₂₄N₅O: 314.1981. Obsd: 314.1971. [α]_D +50.0° (c 1.12, CHCl₃).

(R)-Cyclopropyl(7-(methyl(7H-pyrrolo[2,3-d]pyrimidin-4-yl)amino)-5-azaspiro[2.4]heptan-5-yl)methanone, 25

Yield: 41.0 mg (46.1%). 93.1% purity by HPLC. ¹H NMR (500 MHz, CDCl₃) δ 12.28 (d, *J* = 15.5 Hz, 1H), 8.28 (d, *J* = 10.3 Hz, 1H), 7.12 (d, *J* = 10.0 Hz, 1H), 6.56 (d, *J* = 14.6 Hz, 1H), 5.44 (d, *J* = 15.0 Hz, 1H), 4.40 – 4.24 (m, 1H), 4.11 – 3.92 (m, 2H), 3.74 (dd, *J* = 141.4, 10.9 Hz, 2H), 3.45 (t, *J* = 21.3 Hz, 3H), 1.63 (d, *J* = 40.6 Hz, 1H), 1.16 – 0.94 (m, 3H), 0.80 (s, 4H). ¹³C NMR (125 MHz, CDCl₃) δ 172.1, 157.7, 152.0, 150.4, 120.6, 103.0, 101.8,

61.5, 54.5, 52.3, 33.2, 22.9, 16.8, 12.4, 12.3, 7.7. HRMS (ESI) calcd for $C_{17}H_{22}N_5O$: 312.1824. Obsd: 312.1823. $[\alpha]_D +60.0^\circ$ (*c* 1.31, $CHCl_3$).

(R)-Furan-2-yl(7-(methyl(7*H*-pyrrolo[2,3-*d*]pyrimidin-4-yl)amino)-5-azaspiro[2.4]heptan-5-yl)methanone, **29**

Yield: 60.0 mg (54.0%). 99.2% purity by HPLC. 1H NMR (400 MHz, $CDCl_3$) δ 11.49 (s, 1H), 8.28 (s, 1H), 7.52 (s, 1H), 7.15 (d, *J* = 2.5 Hz, 1H), 7.10 (d, *J* = 3.4 Hz, 1H), 6.58 (d, *J* = 2.6 Hz, 1H), 6.51 (s, 1H), 5.48 (s, 1H), 4.60 – 4.41 (m, 1H), 4.25 (d, *J* = 10.0 Hz, 2H), 4.18 – 4.02 (m, 1H), 3.72 (dd, *J* = 70.6, 11.6 Hz, 1H), 3.44 (s, 2H), 1.06 (s, 1H), 0.83 (dd, *J* = 22.6, 14.3 Hz, 3H). ^{13}C NMR (100 MHz, $CDCl_3$) δ 157.8, 157.6, 151.5, 150.2, 144.4, 144.3, 120.5, 116.6, 111.5, 102.9, 102.1, 61.8, 58.5, 51.8, 33.3, 25.5, 16.7, 8.0. HRMS (ESI) calcd for $C_{18}H_{20}N_5O_2$: 338.1617. Obsd: 338.1616. $[\alpha]_D +56.0^\circ$ (*c* 0.360, $CHCl_3$).

(R)-(7-(Methyl(7*H*-pyrrolo[2,3-*d*]pyrimidin-4-yl)amino)-5-azaspiro[2.4]heptan-5-yl)(phenyl)methanone, **30**

Yield: 77.7 mg (67.8%). 95.5% purity by HPLC. 1H NMR (400 MHz, $CDCl_3$) δ 12.45 (s, 1H), 8.25 (d, *J* = 25.1 Hz, 1H), 7.54 (s, 2H), 7.39 (s, 2H), 7.28 (s, 1H), 7.06 (s, 1H), 6.53 (d, *J* = 21.5 Hz, 1H), 5.45 (d, *J* = 74.9 Hz, 1H), 4.40 – 3.97 (m, 2H), 3.89 – 3.54 (m, 2H), 3.42 (d, *J* = 20.4 Hz, 3H), 1.01 (s, 1H), 0.79 (dd, *J* = 26.4, 14.3 Hz, 2H), 0.63 (s, 1H). ^{13}C NMR (100 MHz, $CDCl_3$) δ 169.5, 157.5, 151.9, 150.1, 136.1, 130.1, 128.4, 127.0, 120.7, 102.9, 101.7, 61.4, 57.5, 50.6, 33.2, 22.9, 16.5, 8.5. HRMS (ESI) calcd for $C_{20}H_{22}N_5O$: 348.1824. Obsd: 348.1819. $[\alpha]_D +22.5^\circ$ (*c* 2.85, $CHCl_3$).

(R)-(7-(Methyl(7*H*-pyrrolo[2,3-*d*]pyrimidin-4-yl)amino)-5-azaspiro[2.4]heptan-5-yl)(pyridin-3-yl)methanone, **31**

Yield: 32.0 mg (32.0%). 100% purity by HPLC. 1H NMR (500 MHz, $CDCl_3$) δ 11.87 (s, 1H), 8.83 (s, 1H), 8.68 (d, *J* = 12.5 Hz, 1H), 8.25 (d, *J* = 31.9 Hz, 1H), 7.90 (s, 1H), 7.47 – 7.31 (m, 1H), 7.10 (d, *J* = 12.4 Hz, 1H), 6.56

(d, $J = 27.7$ Hz, 1H), 5.40 (dd, $J = 73.5, 68.8$ Hz, 1H), 4.37 – 4.03 (m, 2H), 3.94 – 3.59 (m, 2H), 3.43 (t, $J = 15.8$ Hz, 3H), 1.05 (d, $J = 8.0$ Hz, 1H), 0.96 – 0.73 (m, 2H), 0.67 (s, 1H). ^{13}C NMR (100 MHz, CDCl_3) δ 166.9, 157.5, 152.0, 151.1, 150.4, 148.0, 135.0, 131.9, 123.4, 120.6, 103.0, 101.8, 61.5, 54.5, 50.7, 33.4, 22.6, 16.5, 8.4. HRMS (ESI) calcd for $\text{C}_{19}\text{H}_{21}\text{N}_6\text{O}$: 349.1777. Obsd: 349.1764. $[\alpha]_{\text{D}} +15.1^\circ$ (c 1.12, CHCl_3).

(R)-(7-(Methyl(7H-pyrrolo[2,3-*d*]pyrimidin-4-yl)amino)-5-azaspiro[2.4]heptan-5-yl)(pyridin-4-yl)methanone, **32**

Yield: 41.0 mg (28.7%). 94.1% purity by HPLC. ^1H NMR (500 MHz, CDCl_3) δ 12.14 (s, 1H), 8.72 (d, $J = 15.1$ Hz, 2H), 8.25 (d, $J = 31.9$ Hz, 1H), 7.41 (s, 2H), 7.11 (d, $J = 12.7$ Hz, 1H), 6.55 (d, $J = 24.5$ Hz, 1H), 5.46 (d, $J = 111.2$ Hz, 1H), 4.19 (dt, $J = 26.7, 13.8$ Hz, 2H), 3.64 (d, $J = 12.1$ Hz, 1H), 3.56 (dd, $J = 220.1, 10.6$ Hz, 1H), 3.44 (d, $J = 14.5$ Hz, 3H), 1.04 (d, $J = 6.5$ Hz, 1H), 0.95 – 0.72 (m, 2H), 0.67 (s, 1H). ^{13}C NMR (125 MHz, CDCl_3) δ 166.9, 157.5, 152.0, 150.4, 150.3, 143.5, 121.1, 120.7, 103.0, 101.7, 61.4, 57.2, 50.6, 33.4, 22.6, 16.6, 8.5. HRMS (ESI) calcd for $\text{C}_{19}\text{H}_{21}\text{N}_6\text{O}$: 349.1777. Obsd: 349.1772. $[\alpha]_{\text{D}} +24.5^\circ$ (c 1.16, CHCl_3).

(R)-3-(7-(Methyl(7H-pyrrolo[2,3-*d*]pyrimidin-4-yl)amino)-5-azaspiro[2.4]heptane-5-carbonyl)benzonitrile, **33**

Yield: 87.8 mg (71.4%). 97.7% purity by HPLC. ^1H NMR (400 MHz, CDCl_3) δ 12.28 (s, 1H), 8.27 (d, $J = 23.4$ Hz, 1H), 7.85 (s, 1H), 7.79 (d, $J = 7.2$ Hz, 1H), 7.76 – 7.64 (m, 1H), 7.62 – 7.46 (m, 1H), 7.11 (d, $J = 5.6$ Hz, 1H), 6.56 (d, $J = 18.0$ Hz, 1H), 5.46 (d, $J = 82.3$ Hz, 1H), 4.39 – 4.02 (m, 2H), 3.65 (t, $J = 12.3$ Hz, 1H), 3.58 (dd, $J = 185.8, 10.4$ Hz, 1H), 3.44 (d, $J = 14.8$ Hz, 3H), 1.05 (d, $J = 10.3$ Hz, 1H), 0.97 – 0.74 (m, 2H), 0.68 (s, 1H). ^{13}C NMR (100 MHz, CDCl_3) δ 166.9, 157.5, 152.0, 150.2, 137.3, 133.5, 131.4, 130.8, 129.5, 120.8, 117.9, 112.8, 103.1, 101.7, 61.5, 54.5, 50.8, 33.4, 22.6, 16.6, 8.4.

HRMS (ESI) calcd for C₂₁H₂₁N₆O: 373.1777. Obsd: 373.1772. [α]_D +10.9° (c 0.963, CHCl₃).

(R)-4-(7-(Methyl(7H-pyrrolo[2,3-d]pyrimidin-4-yl)amino)-5-azaspiro[2.4]heptane-5-carbonyl)benzonitrile, **34**

Yield: 78.0 mg (72.9%). 100% purity by HPLC. ¹H NMR (500 MHz, CDCl₃) δ 12.35 (s, 1H), 8.26 (d, *J* = 32.1 Hz, 1H), 7.78 – 7.67 (m, 2H), 7.64 (d, *J* = 6.7 Hz, 2H), 7.11 (d, *J* = 12.4 Hz, 1H), 6.55 (d, *J* = 25.3 Hz, 1H), 5.45 (d, *J* = 116.1 Hz, 1H), 4.19 (dt, *J* = 98.3, 17.9 Hz, 2H), 3.64 (d, *J* = 12.2 Hz, 1H), 3.55 (dd, *J* = 225.6, 10.4 Hz, 1H), 3.44 (d, *J* = 17.0 Hz, 3H), 1.03 (d, *J* = 6.0 Hz, 1H), 0.97 – 0.72 (m, 2H), 0.66 (s, 1H). ¹³C NMR (125 MHz, CDCl₃) δ 167.4, 157.5, 152.0, 150.2, 140.3, 132.4, 127.8, 120.8, 118.0, 113.8, 103.0, 101.7, 61.5, 57.3, 50.7, 33.4, 22.6, 16.6, 8.5. HRMS (ESI) calcd for C₂₁H₂₁N₆O: 373.1777. Obsd: 373.1766. [α]_D +15.7° (c 2.54, CHCl₃).

(R)-(7-(Methyl(7H-pyrrolo[2,3-d]pyrimidin-4-yl)amino)-5-azaspiro[2.4]heptan-5-yl)(2-(trifluoromethyl)phenyl)methanone, **35**

Yield: 82.9 mg (69.7%). 98.8% purity by HPLC. ¹H NMR (400 MHz, CDCl₃) δ 12.19 (s, 1H), 8.30 (d, *J* = 32.9 Hz, 1H), 7.71 (dd, *J* = 13.4, 7.9 Hz, 1H), 7.66 – 7.56 (m, 1H), 7.52 (dt, *J* = 14.8, 7.6 Hz, 1H), 7.42 (d, *J* = 7.4 Hz, 1H), 7.09 (dd, *J* = 9.7, 3.5 Hz, 1H), 6.57 (dd, *J* = 18.0, 3.1 Hz, 1H), 5.69 – 5.31 (m, 1H), 4.07 (ddd, *J* = 19.1, 12.6, 7.8 Hz, 1H), 3.87 (dd, *J* = 163.0, 12.6 Hz, 1H), 4.18 – 3.35 (m, 1H), 3.45 (s, 3H), 3.31 (dd, *J* = 158.2, 10.8 Hz, 1H), 1.04 (dd, *J* = 11.7, 6.7 Hz, 1H), 0.94 – 0.68 (m, 2H), 0.68 – 0.56 (m, 1H). ¹³C NMR (100 MHz, CDCl₃) δ 167.0, 157.5, 151.8, 150.0, 135.4 (d, *J* = 26.1 Hz), 132.3, 129.3 (d, *J* = 4.1 Hz), 127.1 (d, *J* = 12.0 Hz), 126.9 – 126.6 (m), 123.6 (q, *J* = 273.8 Hz), 120.7, 103.2, 101.9, 61.2, 56.6, 50.2, 33.3, 24.8, 16.8, 8.3. HRMS (ESI) calcd for C₂₁H₂₁F₃N₅O: 416.1698. Obsd: 416.1695. [α]_D +25.1° (c 1.71, CHCl₃).

(R)-(7-(Methyl(7*H*-pyrrolo[2,3-*d*]pyrimidin-4-yl)amino)-5-azaspiro[2.4]heptan-5-yl)(3-(trifluoromethyl)phenyl)methanone, **36**

Yield: 55.0 mg (46.2%). 98.4% purity by HPLC. ¹H NMR (400 MHz, CDCl₃) δ 11.67 (s, 1H), 8.27 (s, 1H), 7.82 (s, 1H), 7.71 (dd, *J* = 17.7, 7.8 Hz, 2H), 7.62 – 7.46 (m, 1H), 7.09 (s, 1H), 6.58 (d, *J* = 20.8 Hz, 1H), 5.48 (d, *J* = 77.8 Hz, 1H), 4.39 – 4.01 (m, 2H), 3.66 (t, *J* = 13.7 Hz, 1H), 3.59 (dd, *J* = 173.8, 10.5 Hz, 1H), 3.46 (d, *J* = 18.1 Hz, 3H), 1.05 (d, *J* = 10.5 Hz, 1H), 0.98 – 0.73 (m, 2H), 0.68 (s, 1H). ¹³C NMR (100 MHz, CDCl₃) δ 167.8, 157.5, 151.4, 149.9, 136.8, 131.0 (q, *J* = 32.8 Hz), 130.4, 129.1, 126.9, 124.1, 123.6 (q, *J* = 273.0 Hz), 120.7, 103.4, 102.0, 61.5, 54.5, 50.7, 33.4, 22.8, 16.6, 8.4. HRMS (ESI) calcd for C₂₁H₂₁F₃N₅O: 416.1698. Obsd: 416.1692. [α]_D +20.7° (*c* 0.730, CHCl₃).

Synthesis of (R)-2-azido-1-(7-(methyl(7*H*-pyrrolo[2,3-*d*]pyrimidin-4-yl)amino)-5-azaspiro[2.4]heptan-5-yl)ethan-1-one, **22**

In a 10 mL round-bottom flask, 2-azidoacetic acid (208 mg, 2.06 mmol) was placed and solved with 6.0 mL of *N,N*-dimethylformamide. *N,N'*-dicyclohexylcarbodiimide (423 mg, 2.05 mmol) and *N,N*-diisopropylethylamine (0.716 mL, 4.11 mmol) were added and the reaction mixture was stirred for 15 minutes. In a second 25 mL round-bottom flask, (*R*)-*N*-methyl-*N*-(5-azaspiro[2.4]heptan-7-yl)-7*H*-pyrrolo[2,3-*d*]pyrimidin-4-amine (**R**)-**5c** (300 mg, 1.23 mmol) was placed and the reaction mixture of 2-azidoacetic acid was transferred to this second flask. The reaction mixture was refluxed overnight and then cooled at room temperature before being filtered through a celite 545 pad and the solution evaporated. The residue was purified with column chromatography (methanol:dichloromethane=2:98) and collected fragments were evaporated. Removing the solvent in vacuo provided 41.0 mg of (*R*)-2-azido-1-(7-(methyl(7*H*-pyrrolo[2,3-*d*]pyrimidin-4-yl)amino)-5-azaspiro[2.4]heptan-5-yl)ethan-1-one (11.9% yield). 100% purity by HPLC. ¹H

NMR (500 MHz, CDCl₃) δ 11.80 (s, 1H), 8.23 (d, J = 22.5 Hz, 1H), 7.10 (d, J = 17.0 Hz, 1H), 6.56 (s, 1H), 5.55 – 5.22 (m, 1H), 4.17 – 3.94 (m, 1H), 3.90 (d, J = 16.4 Hz, 2H), 3.81 – 3.47 (m, 2H), 3.38 (dd, J = 33.1, 19.3 Hz, 4H), 1.03 (d, J = 46.0 Hz, 1H), 0.91 – 0.58 (m, 3H). ¹³C NMR (125 MHz, CDCl₃) δ 165.7, 157.5, 151.9, 150.4, 120.8, 103.1, 101.8, 61.7, 54.5, 51.6, 51.0, 33.4, 22.4, 16.8, 8.1. HRMS (ESI) calcd for C₁₅H₁₉N₈O: 327.1682. Obsd: 327.1673. [α]_D +37.3° (*c* 1.49, CHCl₃).

In the cases of **26** – **28**, the desired products were synthesized through amide coupling reactions with *N*-acetylglycine, 3-(methylamino)-3-oxopropanoic acid, and 1-acetyl-4-piperidinecarboxylic acid, respectively, instead of 2-azidoacetic acid according to the aforementioned process (vide supra).

(R)-*N*-(2-(7-(Methyl(7*H*-pyrrolo[2,3-*d*]pyrimidin-4-yl)amino)-5-azaspiro[2.4]heptan-5-yl)-2-oxoethyl)acetamide, **26**

Yield: 62.1 mg (44.0%). 98.6% purity by HPLC. ¹H NMR (400 MHz, CDCl₃) δ 12.07 (s, 1H), 8.26 (s, 1H), 7.30 (s, 1H), 7.12 (s, 1H), 6.55 (s, 1H), 5.43 (d, J = 11.0 Hz, 1H), 4.09 (d, J = 15.0 Hz, 2H), 3.88 (ddd, J = 47.9, 37.2, 16.8 Hz, 2H), 3.45 (dd, J = 42.9, 13.8 Hz, 3H), 2.04 (s, 3H), 1.26 (s, 2H), 1.15 – 0.96 (m, 1H), 0.96 – 0.61 (m, 3H). ¹³C NMR (100 MHz, CDCl₃) δ 170.5, 167.0, 157.5, 151.9, 150.2, 120.9, 103.1, 101.7, 61.3, 54.4, 51.2, 42.0, 33.3, 24.6, 22.8, 16.6, 8.1. HRMS (ESI) calcd for C₁₇H₂₃N₆O₂: 343.1882. Obsd: 343.1879. [α]_D +42.2° (*c* 1.00, CHCl₃).

(R)-*N*-Methyl-3-(7-(methyl(7*H*-pyrrolo[2,3-*d*]pyrimidin-4-yl)amino)-5-azaspiro[2.4]heptan-5-yl)-3-oxopropanamide, **27**

Yield: 39.1 mg (13.0%). 100% purity by HPLC. ¹H NMR (400 MHz, CDCl₃) δ 11.96 (d, J = 30.6 Hz, 1H), 8.24 (dd, J = 6.6, 1.8 Hz, 1H), 8.13 (s, 1H), 7.11 (s, 1H), 6.54 (s, 1H), 5.51 – 5.34 (m, 1H), 4.13 (ddd, J = 21.2, 12.6, 7.5 Hz, 1H), 4.00 – 3.80 (m, 2H), 3.49 (t, J = 11.6 Hz, 1H), 3.40 (d, J = 14.5

Hz, 3H), 3.35 (t, J = 19.8 Hz, 2H), 2.83 (dd, J = 4.5, 2.1 Hz, 3H), 1.11 – 0.94 (m, 1H), 0.90 – 0.68 (m, 3H). ^{13}C NMR (100 MHz, CDCl_3) δ 167.0, 166.7, 157.5, 152.0, 150.4, 120.8, 103.0, 101.7, 59.3, 55.6, 52.7, 41.3, 33.3, 26.1, 22.9, 16.3, 8.1. HRMS (ESI) calcd for $\text{C}_{17}\text{H}_{23}\text{N}_6\text{O}_2$: 343.1882. Obsd: 343.1872. $[\alpha]_{\text{D}}^{25} +37.2^\circ$ (c 1.30, CHCl_3).

(R)-1-(4-(7-(Methyl(7*H*-pyrrolo[2,3-*d*]pyrimidin-4-yl)amino)-5-azaspiro[2.4]heptane-5-carbonyl)piperidin-1-yl)ethan-1-one, **28**

Yield: 104 mg (64.0%). 95.3% purity by HPLC. ^1H NMR (400 MHz, CDCl_3) δ 12.29 (s, 1H), 8.36 – 8.21 (m, 1H), 7.13 (dd, J = 9.8, 2.7 Hz, 1H), 6.62 – 6.51 (m, 1H), 5.54 – 5.31 (m, 1H), 4.62 (dd, J = 17.9, 8.6 Hz, 1H), 4.19 (dd, J = 9.8, 6.5 Hz, 1H), 4.11 – 3.76 (m, 3H), 3.54 – 3.46 (m, 1H), 3.46 – 3.33 (m, 3H), 3.19 – 3.01 (m, 1H), 2.75 – 2.51 (m, 2H), 2.17 – 2.02 (m, 3H), 1.97 – 1.63 (m, 4H), 1.15 – 0.95 (m, 1H), 0.92 – 0.71 (m, 3H). ^{13}C NMR (100 MHz, CDCl_3) δ 172.6, 168.8, 157.5, 152.0, 150.3, 120.8, 103.1, 101.7, 61.9, 58.9, 50.6, 45.7, 40.9, 40.2, 33.4, 24.9, 21.4, 16.0, 8.1. HRMS (ESI) calcd for $\text{C}_{21}\text{H}_{29}\text{N}_6\text{O}_2$: 397.2352. Obsd: 397.2343. $[\alpha]_{\text{D}}^{25} +45.2^\circ$ (c 1.63, CHCl_3).

Synthesis of (R)-3-(7-(methyl(7*H*-pyrrolo[2,3-*d*]pyrimidin-4-yl)amino)-5-azaspiro[2.4]heptan-5-yl)-3-thioxopropanenitrile, **37**

In a 5 mL round-bottom flask, (*R*)-3-(7-(methyl(7*H*-pyrrolo[2,3-*d*]pyrimidin-4-yl)amino)-5-azaspiro[2.4]heptan-5-yl)-3-oxopropanenitrile (**R**)-**6c** (44.7 mg, 0.144 mmol) was placed and solved with 1.40 mL of dichloromethane. The solution was treated with Lawesson's reagent (32.0 mg, 0.0791 mmol) and stirred for 3 days before being evaporated. The residue was purified with column chromatography (methanol:dichloromethane=2:98) and collected fragments were evaporated. Removing the solvent in vacuo provided 37.0 mg of (*R*)-3-(7-(methyl(7*H*-pyrrolo[2,3-*d*]pyrimidin-4-yl)amino)-5-azaspiro[2.4]heptan-5-yl)-3-thioxopropanenitrile (78.7% yield). 100% purity

by HPLC. ^1H NMR (400 MHz, CDCl_3) δ 12.07 (s, 1H), 8.27 (d, $J = 3.4$ Hz, 1H), 7.20 – 7.08 (m, 1H), 6.57 (dd, $J = 5.7, 3.7$ Hz, 1H), 5.45 (tt, $J = 186.7, 93.9$ Hz, 1H), 4.42 – 4.25 (m, 1H), 4.20 (dd, $J = 131.3, 13.0$ Hz, 1H), 4.01 (dd, $J = 162.4, 14.4$ Hz, 1H), 3.98 – 3.85 (m, 2H), 3.90 (dd, $J = 211.1, 11.8$ Hz, 1H), 3.44 (t, $J = 19.7$ Hz, 3H), 1.16 – 1.00 (m, 1H), 0.97 – 0.74 (m, 3H). ^{13}C NMR (100 MHz, CDCl_3) δ 184.8, 157.4, 152.0, 150.2, 121.0, 114.1, 103.2, 101.8, 62.3, 59.1, 57.0, 34.2, 33.7, 25.2, 16.9, 8.1. HRMS (ESI) calcd for $\text{C}_{16}\text{H}_{19}\text{N}_6\text{S}$: 327.1392. Obsd: 327.1380. $[\alpha]_{\text{D}} +48.8^\circ$ (c 1.23, CHCl_3).

Synthesis of isobutyl (R)-7-(methyl(7H-pyrrolo[2,3-d]pyrimidin-4-yl)amino)-5-azaspiro[2.4]heptane-5-carboxylate, 38

In a 5 mL round-bottom flask, (*R*)-*N*-methyl-*N*-(5-azaspiro[2.4]heptan-7-yl)-7H-pyrrolo[2,3-d]pyrimidin-4-amine (**R**)-**5c** (100 mg, 0.411 mmol) was placed and solved with 1.00 mL of *N,N*-dimethylformamide. The solution was treated with isobutyl chloroformate (84.2 mg, 0.616 mmol) and *N,N*-diisopropylethylamine (0.138 mL, 0.792 mmol) was added. The reaction solution was stirred at room temperature overnight and evaporated. The residue was purified by column chromatography (methanol:dichloromethane=2:98) and collected fragments were evaporated. Removing the solvent in vacuo provided 107.0 mg of isobutyl (*R*)-7-(methyl(7H-pyrrolo[2,3-d]pyrimidin-4-yl)amino)-5-azaspiro[2.4]heptane-5-carboxylate (76.4% yield). 100% purity by HPLC. ^1H NMR (500 MHz, CDCl_3) δ 12.56 (s, 1H), 8.28 (s, 1H), 7.11 (s, 1H), 6.55 (s, 1H), 5.41 (s, 1H), 4.08 – 3.97 (m, 1H), 3.91 (d, $J = 4.7$ Hz, 2H), 3.85 – 3.66 (m, 2H), 3.42 (s, 3H), 3.39 – 3.29 (m, 1H), 2.02 – 1.87 (m, 1H), 1.01 (s, 1H), 0.94 (s, 6H), 0.75 (d, $J = 9.4$ Hz, 3H). ^{13}C NMR (125 MHz, CDCl_3) δ 157.7, 154.9, 152.0, 150.3, 120.6, 102.9, 101.8, 71.4, 61.0, 54.6, 51.1, 33.0, 28.0, 23.6, 19.1, 16.5, 8.1. HRMS (ESI) calcd for $\text{C}_{18}\text{H}_{26}\text{N}_5\text{O}_2$: 344.2087. Obsd: 344.2077. $[\alpha]_{\text{D}} +33.2^\circ$ (c 4.45, CHCl_3).

Synthesis of (R)-N-butyl-7-(methyl(7H-pyrrolo[2,3-d]pyrimidin-4-yl)amino)-5-azaspiro[2.4]heptane-5-carboxamide, 39

In a 5 mL round-bottom flask, (*R*)-*N*-methyl-*N*-(5-azaspiro[2.4]heptan-7-yl)-7*H*-pyrrolo[2,3-*d*]pyrimidin-4-amine (**R**)-**5c** (49.2 mg, 0.202 mmol) was placed and solved with 2.00 mL of dichloromethane. *N,N*-diisopropylethylamine (0.0370 mL, 0.212 mmol) was added and the mixture was treated with 0.0241 mL of butyl isocyanate (0.0241 mL, 0.214 mmol). The reaction solution was stirred for 2 hours before being evaporated. The residue was purified by column chromatography (methanol:dichloromethane=2:98) and collected fragments were evaporated. Removing the solvent in vacuo provided 67.7 mg of (*R*)-*N*-butyl-7-(methyl(7*H*-pyrrolo[2,3-*d*]pyrimidin-4-yl)amino)-5-azaspiro[2.4]heptane-5-carboxamide (97.8% yield). 100% purity by HPLC. ¹H NMR (400 MHz, CDCl₃) δ 12.31 (s, 1H), 8.26 (s, 1H), 7.10 (s, 1H), 6.54 (s, 1H), 5.38 (d, *J* = 5.5 Hz, 1H), 4.46 (s, 1H), 3.98 (dd, *J* = 10.4, 7.6 Hz, 1H), 3.71 (dd, *J* = 31.5, 10.3 Hz, 2H), 3.41 (s, 3H), 3.33 (d, *J* = 9.8 Hz, 1H), 3.26 (d, *J* = 5.1 Hz, 2H), 1.50 (dt, *J* = 14.5, 7.2 Hz, 2H), 1.34 (td, *J* = 14.5, 7.2 Hz, 2H), 0.99 (d, *J* = 7.7 Hz, 1H), 0.92 (t, *J* = 7.2 Hz, 3H), 0.85 (s, 1H), 0.75 (s, 2H). ¹³C NMR (100 MHz, CDCl₃) δ 157.6, 156.6, 151.5, 150.0, 120.7, 102.9, 101.9, 61.0, 54.4, 51.1, 40.4, 33.1, 32.5, 24.1, 20.0, 16.7, 13.8, 8.1. HRMS (ESI) calcd for C₁₈H₂₇N₆O: 343.2246. Obsd: 343.2241. [α]_D +43.2° (*c* 2.89, CHCl₃).

In the cases from **40** to **48**, the desired products were synthesized through substitution reactions with cyclohexyl isocyanate, phenyl isocyanate, isocyanic acid 4-fluorophenyl ester, isocyanic acid 2,4-dichlorophenyl ester, 3,4-dichlorophenyl isocyanate, 2,5-dichlorophenyl isocyanate, 2,3-dichlorophenyl isocyanate, 3-chloro-4-methylphenyl isocyanate, and 2-biphenyl isocyanate, respectively, instead of butyl isocyanate according to the aforementioned process (vide supra).

(R)-N-Cyclohexyl-7-(methyl(7H-pyrrolo[2,3-d]pyrimidin-4-yl)amino)-5-azaspiro[2.4]heptane-5-carboxamide, 40

Yield: 59.1 mg (78.4%). 96.4% purity by HPLC. ¹H NMR (400 MHz, CDCl₃) δ 12.25 (s, 1H), 8.28 (s, 1H), 7.10 (d, *J* = 2.1 Hz, 1H), 6.56 (s, 1H), 5.39 (d, *J* = 5.8 Hz, 1H), 4.18 (d, *J* = 7.6 Hz, 1H), 3.97 (dd, *J* = 10.8, 7.5 Hz, 1H), 3.66 (t, *J* = 10.8 Hz, 2H), 3.53 (dd, *J* = 163.5, 9.8 Hz, 2H), 3.43 (s, 3H), 1.97 (d, *J* = 11.4 Hz, 2H), 1.70 (d, *J* = 9.8 Hz, 2H), 1.60 (d, *J* = 12.8 Hz, 1H), 1.36 (td, *J* = 14.2, 2.5 Hz, 2H), 1.22 – 1.04 (m, 3H), 1.03 – 0.93 (m, 1H), 0.76 (s, 3H). ¹³C NMR (100 MHz, CDCl₃) δ 157.6, 155.9, 151.5, 150.0, 120.6, 103.0, 101.9, 61.0, 54.4, 51.1, 49.2, 34.1, 33.1, 25.6, 25.0, 24.0, 16.7, 8.1. HRMS (ESI) calcd for C₂₀H₂₉N₆O: 369.2403. Obsd: 369.2398. [α]_D +39.1° (*c* 2.39, CHCl₃).

(R)-7-(Methyl(7*H*-pyrrolo[2,3-*d*]pyrimidin-4-yl)amino)-*N*-phenyl-5-azaspiro[2.4]heptane-5-carboxamide, **41**

Yield: 70.6 mg (94.8%). 98.5% purity by HPLC. ¹H NMR (400 MHz, CDCl₃) δ 11.63 (s, 1H), 8.29 (s, 1H), 7.44 (d, *J* = 7.2 Hz, 2H), 7.29 (s, 2H), 7.09 (s, 1H), 7.02 (t, *J* = 7.2 Hz, 1H), 6.52 (d, *J* = 45.2 Hz, 2H), 5.43 (s, 1H), 4.11 (s, 1H), 3.84 (dd, *J* = 21.3, 10.0 Hz, 2H), 3.68 – 3.25 (m, 1H), 3.46 (s, 3H), 1.04 (d, *J* = 8.6 Hz, 1H), 0.95 – 0.69 (m, 3H). ¹³C NMR (100 MHz, CDCl₃) δ 157.5, 153.7, 150.9, 149.6, 138.8, 128.9, 123.1, 120.7, 119.7, 103.1, 102.2, 61.2, 54.6, 51.4, 33.3, 24.0, 16.8, 8.2. HRMS (ESI) calcd for C₂₀H₂₃N₆O: 363.1933. Obsd: 363.1928. [α]_D +38.0° (*c* 0.707, CHCl₃).

(R)-*N*-(4-Fluorophenyl)-7-(methyl(7*H*-pyrrolo[2,3-*d*]pyrimidin-4-yl)amino)-5-azaspiro[2.4]heptane-5-carboxamide, **42**

Yield: 50.8 mg (46.6%). 99.2% purity by HPLC. ¹H NMR (400 MHz, DMSO-*d*₆) δ 12.03 (s, 1H), 8.41 – 8.28 (m, 1H), 8.18 (s, 1H), 7.52 (dd, *J* = 6.9, 5.2 Hz, 2H), 7.26 (s, 1H), 7.07 (t, *J* = 7.9 Hz, 2H), 6.72 (s, 1H), 5.20 (s, 1H), 4.03 (dd, *J* = 11.1, 7.4 Hz, 1H), 3.80 (t, *J* = 10.6 Hz, 2H), 3.49 (d, *J* = 68.5 Hz, 10H), 3.37 (s, 9H), 0.95 (d, *J* = 10.2 Hz, 1H), 0.84 (d, *J* = 13.6 Hz, 2H), 0.68 (d, *J* = 10.1 Hz, 1H). ¹³C NMR (101 MHz, DMSO-*d*₆) δ 157.7 (d, *J* = 237.8 Hz), 154.2, 149.9, 148.6, 137.1 (d, *J* = 2.4 Hz), 122.2, 121.5 (d, *J* = 7.6 Hz),

115.2 (d, $J = 22.0$ Hz), 102.9, 102.5, 61.6, 54.5, 51.5, 33.6, 24.2, 16.5, 8.2. HRMS (ESI) calcd for $C_{20}H_{22}FN_6O$: 381.1839. Obsd: 381.1835. $[\alpha]_D +54.3^\circ$ (c 0.223, MeOH).

(R)-N-(2,4-Dichlorophenyl)-7-(methyl(7H-pyrrolo[2,3-d]pyrimidin-4-yl)amino)-5-azaspiro[2.4]heptane-5-carboxamide, **43**

Yield: 82.7 mg (67.2%). 97.3% purity by HPLC. 1H NMR (400 MHz, $CDCl_3$) δ 12.01 (s, 1H), 8.28 (d, $J = 8.9$ Hz, 2H), 7.40 – 7.31 (m, 1H), 7.22 (dd, $J = 8.9, 2.1$ Hz, 1H), 7.13 (d, $J = 2.6$ Hz, 1H), 6.82 (s, 1H), 6.59 (s, 1H), 5.53 (d, $J = 6.3$ Hz, 1H), 4.16 (dd, $J = 10.9, 7.5$ Hz, 1H), 3.87 (dd, $J = 23.7, 10.4$ Hz, 2H), 3.48 (s, 3H), 3.42 (s, 1H), 1.08 (d, $J = 10.3$ Hz, 1H), 0.84 (s, 3H). ^{13}C NMR (100 MHz, $CDCl_3$) δ 157.6, 152.6, 151.5, 150.0, 134.4, 128.3, 127.9, 127.4, 122.3, 121.2, 120.7, 103.0, 102.0, 60.7, 54.4, 51.1, 33.2, 24.1, 16.8, 8.2. HRMS (ESI) calcd for $C_{20}H_{21}Cl_2N_6O$: 431.1154. Obsd: 431.1146. $[\alpha]_D +47.8^\circ$ (c 0.970, $CHCl_3$).

(R)-N-(3,4-Dichlorophenyl)-7-(methyl(7H-pyrrolo[2,3-d]pyrimidin-4-yl)amino)-5-azaspiro[2.4]heptane-5-carboxamide, **44**

Yield: 34.7 mg (38.0%). 99.1% purity by HPLC. 1H NMR (400 MHz, $CDCl_3$) δ 11.85 (d, $J = 18.4$ Hz, 1H), 8.24 (s, 1H), 7.64 (s, 1H), 7.26 (d, $J = 4.1$ Hz, 2H), 7.07 (d, $J = 2.2$ Hz, 1H), 6.72 (d, $J = 12.8$ Hz, 1H), 6.52 (d, $J = 2.7$ Hz, 1H), 5.37 (d, $J = 4.8$ Hz, 1H), 4.05 (dd, $J = 10.6, 7.0$ Hz, 1H), 3.79 (dd, $J = 25.3, 10.5$ Hz, 2H), 3.40 (s, 4H), 1.00 (s, 1H), 0.82 (d, $J = 42.1$ Hz, 3H). ^{13}C NMR (100 MHz, $CDCl_3$) δ 157.6, 153.2, 151.8, 150.3, 138.5, 132.4, 130.2, 125.9, 121.2, 120.6, 118.9, 103.0, 101.9, 61.0, 54.6, 51.5, 33.2, 23.8, 16.8, 8.2. HRMS (ESI) calcd for $C_{20}H_{21}Cl_2N_6O$: 431.1154. Obsd: 431.1148. $[\alpha]_D +48.5^\circ$ (c 0.850, $CHCl_3$).

(R)-N-(2,5-Dichlorophenyl)-7-(methyl(7H-pyrrolo[2,3-d]pyrimidin-4-yl)amino)-5-azaspiro[2.4]heptane-5-carboxamide, **45**

Yield: 77.6 mg (86.0%). 98.4% purity by HPLC. ¹H NMR (400 MHz, CDCl₃) δ 12.32 (s, 1H), 8.36 (d, *J* = 53.7 Hz, 2H), 7.12 (s, 1H), 7.07 (dd, *J* = 124.5, 8.5 Hz, 2H), 6.88 (s, 1H), 6.57 (s, 1H), 5.53 (d, *J* = 5.8 Hz, 1H), 4.24 – 4.07 (m, 1H), 3.87 (dd, *J* = 21.7, 10.3 Hz, 2H), 3.48 (s, 1H), 3.46 (s, 3H), 1.07 (d, *J* = 8.7 Hz, 1H), 0.83 (s, 3H). ¹³C NMR (100 MHz, CDCl₃) δ 157.6, 152.4, 152.1, 150.3, 136.5, 133.5, 129.3, 122.9, 120.7, 120.2, 119.9, 103.0, 101.8, 60.6, 54.4, 51.0, 33.2, 24.1, 16.7, 8.1. HRMS (ESI) calcd for C₂₀H₂₁Cl₂N₆O: 431.1154. Obsd: 431.1148. [α]_D +34.6° (*c* 2.36, DMSO).

*(R)-N-(2,3-Dichlorophenyl)-7-(methyl(7H-pyrrolo[2,3-*d*]pyrimidin-4-yl)amino)-5-azaspiro[2.4]heptane-5-carboxamide, 46*

Yield: 72.2 mg (78.2%). 98.8% purity by HPLC. ¹H NMR (400 MHz, CDCl₃) δ 12.36 (s, 1H), 8.45 – 8.16 (m, 2H), 7.23 – 7.06 (m, 3H), 6.97 (s, 1H), 6.58 (s, 1H), 5.54 (d, *J* = 5.8 Hz, 1H), 4.17 (dd, *J* = 10.8, 7.6 Hz, 1H), 3.88 (dd, *J* = 19.3, 10.4 Hz, 2H), 3.50 (s, 1H), 3.47 (s, 3H), 1.07 (d, *J* = 8.0 Hz, 1H), 0.86 (d, *J* = 18.6 Hz, 3H). ¹³C NMR (100 MHz, CDCl₃) δ 157.6, 152.6, 151.7, 150.0, 137.3, 132.3, 127.7, 123.7, 120.8, 120.4, 118.4, 103.1, 101.9, 60.7, 54.4, 51.1, 33.2, 24.2, 16.7, 8.2. HRMS (ESI) calcd for C₂₀H₂₁Cl₂N₆O: 431.1154. Obsd: 431.1148. [α]_D +31.7° (*c* 3.17, CHCl₃).

*(R)-N-(3-Chloro-4-methylphenyl)-7-(methyl(7H-pyrrolo[2,3-*d*]pyrimidin-4-yl)amino)-5-azaspiro[2.4]heptane-5-carboxamide, 47*

Yield: 82.1 mg (93.8%). 98.3% purity by HPLC. ¹H NMR (400 MHz, CDCl₃) δ 12.26 (s, 1H), 8.24 (s, 1H), 7.49 (s, 1H), 7.20 (d, *J* = 6.6 Hz, 1H), 7.13 – 6.98 (m, 2H), 6.87 (s, 1H), 6.49 (s, 1H), 5.36 (s, 1H), 4.04 (s, 1H), 3.79 (d, *J* = 8.2 Hz, 2H), 3.42 (d, *J* = 32.5 Hz, 1H), 3.36 (s, 3H), 2.25 (s, 3H), 0.97 (d, *J* = 8.3 Hz, 1H), 0.72 (s, 3H). ¹³C NMR (100 MHz, CDCl₃) δ 157.5, 153.8, 151.5, 150.0, 137.9, 134.1, 130.7, 130.3, 120.7, 120.5, 118.4, 103.0, 101.9, 61.0, 54.5, 51.3, 33.2, 23.9, 19.3, 16.6, 8.1. HRMS (ESI) calcd for C₂₁H₂₄ClN₆O: 411.1700. Obsd: 411.1694. [α]_D +41.1° (*c* 3.38, CHCl₃).

(R)-N-([1,1'-Biphenyl]-2-yl)-7-(methyl(7H-pyrrolo[2,3-d]pyrimidin-4-yl)amino)-5-azaspiro[2.4]heptane-5-carboxamide, 48

Yield: 29.7 mg (32.5%). 97.9% purity by HPLC. ¹H NMR (400 MHz, CDCl₃) δ 11.27 (s, 1H), 8.24 (s, 1H), 8.20 (d, *J* = 8.3 Hz, 1H), 7.51 – 7.30 (m, 6H), 7.21 (d, *J* = 7.2 Hz, 1H), 7.10 (dd, *J* = 9.2, 5.5 Hz, 2H), 6.55 (d, *J* = 2.9 Hz, 1H), 6.38 (s, 1H), 5.34 (d, *J* = 6.4 Hz, 1H), 3.82 (dd, *J* = 10.9, 7.5 Hz, 1H), 3.64 (d, *J* = 10.0 Hz, 1H), 3.48 (d, *J* = 10.1 Hz, 1H), 3.38 (s, 3H), 3.20 (d, *J* = 9.9 Hz, 1H), 1.04 – 0.95 (m, 1H), 0.78 – 0.59 (m, 3H). ¹³C NMR (101 MHz, CDCl₃) δ 157.4, 153.4, 149.6, 148.6, 138.5, 135.8, 131.5, 129.6, 129.2, 129.1, 128.5, 128.0, 123.0, 120.9, 120.6, 102.5, 61.1, 54.2, 50.9, 31.9, 22.7, 16.8, 8.1. HRMS (ESI) calcd for C₂₆H₂₇N₆O: 439.2246. Obsd: 439.2242. [α]_D +29.2° (*c* 0.587, CHCl₃).

Synthesis of (R)-N-(3,5-bis(trifluoromethyl)phenyl)-7-(methyl(7H-pyrrolo[2,3-d]pyrimidin-4-yl)amino)-5-azaspiro[2.4]heptane-5-carbothioamide, 49

In a 5 mL round-bottom flask, *(R)-N*-methyl-*N*-(5-azaspiro[2.4]heptan-7-yl)-7H-pyrrolo[2,3-d]pyrimidin-4-amine (**R**)-**5c** (49.8 mg, 0.205 mmol) was placed and solved with 2.00 mL of dichloromethane. *N,N*-diisopropylethylamine (0.0374 mL, 0.215 mmol) was added and the mixture was treated with 3,5-bis(trifluoromethyl)phenyl isothiocyanate (0.0400 mL, 0.219 mmol). The reaction solution was stirred for 2 hours before being evaporated. The residue was purified by column chromatography (methanol:dichloromethane=2:98) and collected fragments were evaporated. Removing the solvent in vacuo provided 109.8 mg of *(R)-N*-(3,5-bis(trifluoromethyl)phenyl)-7-(methyl(7H-pyrrolo[2,3-d]pyrimidin-4-yl)amino)-5-azaspiro[2.4]heptane-5-carbothioamide (quantitatively yield). 99.5% purity by HPLC. ¹H NMR (400 MHz, CDCl₃) δ 12.02 (s, 1H), 8.27 (s, 1H), 7.97 (s, 2H), 7.69 (s, 1H), 7.62 (s, 1H), 7.08 (s, 1H), 6.55 (s, 1H), 5.42 (s,

1H), 4.30 (s, 1H), 4.15 (s, 2H), 3.72 (s, 1H), 3.43 (s, 3H), 1.03 (s, 1H), 0.83 (s, 3H). ¹³C NMR (101 MHz, CDCl₃) δ 177.8, 157.5, 151.4, 149.7, 140.7, 131.6 (q, *J* = 33.6 Hz), 124.8, 123.0 (q, *J* = 272.9 Hz), 120.9, 118.6, 103.4, 102.0, 61.0, 55.3, 33.4, 29.7, 23.3, 16.8, 8.0. HRMS (ESI) calcd for C₂₂H₂₁F₆N₆S: 515.1453. Obsd: 515.1446. [α]_D +51.4° (*c* 3.37, CHCl₃).

*Synthesis of (R)-N-(5-(ethylsulfonyl)-5-azaspiro[2.4]heptan-7-yl)-N-methyl-7H-pyrrolo[2,3-*d*]pyrimidin-4-amine, 50*

In a 5 mL round bottom flask, (*R*)-*N*-methyl-*N*-(5-azaspiro[2.4]heptan-7-yl)-7*H*-pyrrolo[2,3-*d*]pyrimidin-4-amine (**R**)-**5c** (70.0 mg, 0.288 mmol) was placed and solved with 0.700 mL of *N,N*-dimethylformamide. The solution was treated with ethanesulfonyl chloride (55.5 mg, 0.432 mmol) and *N,N*-diisopropylethylamine (0.208 mL, 1.19 mmol) was added. Then, the reaction solution was stirred at room temperature overnight before being evaporated. The residue was purified by flash column chromatography (methanol:dichloromethane=2:98) and collected fragments were evaporated. Removing the solvent in vacuo provided 80.0 mg of (*R*)-*N*-(5-(ethylsulfonyl)-5-azaspiro[2.4]heptan-7-yl)-*N*-methyl-7*H*-pyrrolo[2,3-*d*]pyrimidin-4-amine (82.5% yield). 100% purity by HPLC. ¹H NMR (500 MHz, CDCl₃) δ 12.42 (s, 1H), 8.26 (s, 1H), 7.12 (s, 1H), 6.56 (s, 1H), 5.55 (s, 1H), 3.92 (t, *J* = 9.1 Hz, 1H), 3.68 (d, *J* = 9.9 Hz, 2H), 3.48 (s, 3H), 3.33 (d, *J* = 9.8 Hz, 1H), 3.14 – 3.03 (m, 2H), 1.42 (t, *J* = 7.0 Hz, 3H), 1.03 (d, *J* = 9.9 Hz, 1H), 0.77 (d, *J* = 11.9 Hz, 2H), 0.73 (d, *J* = 10.9 Hz, 1H). ¹³C NMR (125 MHz, CDCl₃) δ 157.7, 152.0, 150.2, 120.7, 103.0, 101.8, 60.5, 55.9, 52.4, 44.2, 33.5, 24.4, 15.4, 9.2, 7.9. HRMS (ESI) calcd for C₁₅H₂₂N₅O₂S: 336.1494. Obsd: 336.1485. [α]_D +34.7° (*c* 3.25, CHCl₃).

In the cases from **51** to **68**, the desired products were synthesized through substitution reactions with 2-propanesulfonyl chloride, 1-propanesulfonyl chloride, benzenesulfonyl chloride, 2-fluorobenzene-1-

sulfonyl chloride, 3-fluorobenzene-1-sulfonyl chloride, 4-fluorobenzenesulfonyl chloride, 2-cyanobenzenesulfonyl chloride, 3-cyanobenzenesulfonyl chloride, 4-cyanobenzenesulfonyl chloride, 2-nitrobenzenesulfonyl chloride, 3-nitrobenzenesulfonyl chloride, 4-nitrobenzenesulfonyl chloride, 3-toluenesulfonyl chloride, 4-methoxybenzenesulfonyl chloride, 4-(trifluoromethyl)benzenesulfonyl chloride, 2-naphthalenesulfonyl chloride, piperidine-1-sulfonyl chloride, and morpholine-4-sulfonyl chloride, respectively, instead of ethylsulfonyl chloride according to the aforementioned process (vide supra).

(R)-N-(5-(Isopropylsulfonyl)-5-azaspiro[2.4]heptan-7-yl)-N-methyl-7H-pyrrolo[2,3-d]pyrimidin-4-amine, 51

Yield: 54.0 mg (54.0%). 100% purity by HPLC. ¹H NMR (500 MHz, CDCl₃) δ 12.17 (s, 1H), 8.26 (s, 1H), 7.11 (s, 1H), 6.57 (s, 1H), 5.51 (s, 1H), 3.99 (t, *J* = 8.2 Hz, 1H), 3.71 (d, *J* = 8.7 Hz, 2H), 3.48 (s, 3H), 3.38 (d, *J* = 9.6 Hz, 1H), 3.28 (d, *J* = 4.9 Hz, 1H), 1.40 (s, 6H), 1.03 (d, *J* = 8.7 Hz, 1H), 0.85 – 0.69 (m, 3H). ¹³C NMR (125 MHz, CDCl₃) δ 157.6, 151.9, 150.3, 120.5, 102.9, 101.8, 60.6, 56.4, 53.4, 52.9, 33.5, 24.4, 16.6, 15.5, 8.9. HRMS (ESI) calcd for C₁₆H₂₄N₅O₂S: 350.1651. Obsd: 350.1639. [α]_D +36.0° (*c* 1.82, CHCl₃).

(R)-N-Methyl-N-(5-(propylsulfonyl)-5-azaspiro[2.4]heptan-7-yl)-7H-pyrrolo[2,3-d]pyrimidin-4-amine, 52

Yield: 71.0 mg (71.0%). 99.4% purity by HPLC. ¹H NMR (400 MHz, CDCl₃) δ 12.17 (s, 1H), 8.29 (s, 1H), 7.12 (d, *J* = 3.3 Hz, 1H), 6.59 (s, 1H), 5.65 – 5.46 (m, 1H), 3.91 (dd, *J* = 10.9, 7.6 Hz, 1H), 3.77 – 3.61 (m, 2H), 3.49 (s, 3H), 3.32 (d, *J* = 9.8 Hz, 1H), 3.11 – 2.94 (m, 2H), 1.91 (dd, *J* = 15.4, 7.6 Hz, 2H), 1.09 (t, *J* = 7.4 Hz, 3H), 1.07 – 0.98 (m, 1H), 0.76 (dt, *J* = 11.3, 9.9 Hz, 3H). ¹³C NMR (100 MHz, CDCl₃) δ 157.7, 151.8, 150.1, 120.7, 103.1, 101.9, 60.5, 55.8, 52.3, 51.3, 33.6, 24.4, 17.0, 15.4, 13.1, 9.2. HRMS (ESI) calcd for C₁₆H₂₄N₅O₂S: 350.1651. Obsd: 350.1650. [α]_D +34.9° (*c* 1.97, CHCl₃).

(R)-N-Methyl-N-(5-(phenylsulfonyl)-5-azaspiro[2.4]heptan-7-yl)-7H-pyrrolo[2,3-d]pyrimidin-4-amine, 53

Yield: 70.0 mg (63.6%). 99.4% purity by HPLC. ¹H NMR (500 MHz, CDCl₃) δ 12.22 (s, 1H), 8.11 (s, 1H), 7.75 (s, 2H), 7.56 (s, 1H), 7.48 (s, 2H), 7.00 (s, 1H), 6.42 (s, 1H), 5.34 (s, 1H), 3.51 (s, 2H), 3.43 (d, *J* = 8.4 Hz, 1H), 3.24 (s, 3H), 2.99 (d, *J* = 8.3 Hz, 1H), 0.79 (s, 1H), 0.64 (s, 1H), 0.52 (s, 2H). ¹³C NMR (125 MHz, CDCl₃) δ 157.6, 152.0, 150.2, 135.1, 133.0, 129.1, 127.9, 120.6, 102.9, 101.8, 59.9, 56.0, 52.7, 33.3, 23.9, 14.5, 9.6. HRMS (ESI) calcd for C₁₉H₂₂N₅O₂S: 384.1494. Obsd: 384.1483. [α]_D -3.5° (*c* 2.73, CHCl₃).

(R)-N-(5-((2-Fluorophenyl)sulfonyl)-5-azaspiro[2.4]heptan-7-yl)-N-methyl-7H-pyrrolo[2,3-d]pyrimidin-4-amine, 54

Yield: 57.0 mg (49.6%). 97.3% purity by HPLC. ¹H NMR (400 MHz, CDCl₃) δ 11.84 (s, 1H), 8.21 (s, 1H), 7.91 (t, *J* = 7.3 Hz, 1H), 7.68 – 7.56 (m, 1H), 7.39 – 7.20 (m, 2H), 7.09 (d, *J* = 3.4 Hz, 1H), 6.54 (d, *J* = 3.0 Hz, 1H), 5.47 (d, *J* = 5.4 Hz, 1H), 3.82 (dd, *J* = 10.9, 7.8 Hz, 1H), 3.77 – 3.67 (m, 1H), 3.48 (dd, *J* = 160.2, 9.9 Hz, 2H), 3.41 (s, 3H), 0.98 – 0.89 (m, 1H), 0.76 (dt, *J* = 13.1, 6.5 Hz, 1H), 0.72 – 0.61 (m, 2H). ¹³C NMR (100 MHz, CDCl₃) δ 159.1 (d, *J* = 255.8 Hz), 157.6, 151.7, 150.2, 135.2 (d, *J* = 8.4 Hz), 131.5, 125.0 (d, *J* = 14.8 Hz), 124.5 (d, *J* = 3.8 Hz), 120.6, 117.3 (d, *J* = 22.0 Hz), 102.9, 102.0, 60.3, 55.7, 52.3, 33.4, 24.2, 14.9, 9.3. HRMS (ESI) calcd for C₁₉H₂₁FN₅O₂S: 402.1400. Obsd: 402.1393. [α]_D -7.2° (*c* 0.803, CHCl₃).

(R)-N-(5-((3-Fluorophenyl)sulfonyl)-5-azaspiro[2.4]heptan-7-yl)-N-methyl-7H-pyrrolo[2,3-d]pyrimidin-4-amine, 55

Yield: 46.0 mg (39.9%). 99.6% purity by HPLC. ¹H NMR (400 MHz, CDCl₃) δ 11.90 (s, 1H), 8.20 (s, 1H), 7.67 – 7.62 (m, 1H), 7.56 (dt, *J* = 13.4, 6.6 Hz, 2H), 7.36 (ddd, *J* = 10.0, 5.3, 1.5 Hz, 1H), 7.10 (d, *J* = 3.5 Hz, 1H), 6.53 (d, *J* = 3.4 Hz, 1H), 5.44 (t, *J* = 5.0 Hz, 1H), 3.62 (d, *J* = 5.2 Hz, 2H), 3.37 (s, 3H), 3.33 (dd, *J* = 185.2, 9.6 Hz, 2H), 0.96 – 0.85 (m, 1H), 0.77 (dd, *J* = 10.2,

4.9 Hz, 1H), 0.69 – 0.54 (m, 2H). ^{13}C NMR (100 MHz, CDCl_3) δ 162.5 (d, J = 252.1 Hz), 157.6, 151.7, 150.1, 137.4 (d, J = 6.5 Hz), 130.9 (d, J = 7.7 Hz), 123.6 (d, J = 3.4 Hz), 120.6, 120.2 (d, J = 21.2 Hz), 115.1 (d, J = 24.1 Hz), 102.9, 101.9, 60.0, 56.0, 52.8, 33.4, 23.9, 14.6, 9.7. HRMS (ESI) calcd for $\text{C}_{19}\text{H}_{21}\text{FN}_5\text{O}_2\text{S}$: 402.1400. Obsd: 402.1391. $[\alpha]_{\text{D}}$ -6.7° (c 0.880, CHCl_3).

(R)-N-(5-((4-Fluorophenyl)sulfonyl)-5-azaspiro[2.4]heptan-7-yl)-N-methyl-7H-pyrrolo[2,3-d]pyrimidin-4-amine, 56

Yield: 59.0 mg (51.3%). 96.3% purity by HPLC. ^1H NMR (500 MHz, CDCl_3) δ 12.06 (s, 1H), 8.11 (d, J = 3.9 Hz, 1H), 7.78 (ddd, J = 8.8, 4.6, 2.0 Hz, 2H), 7.22 – 7.11 (m, 2H), 7.02 (d, J = 3.5 Hz, 1H), 6.44 (d, J = 3.4 Hz, 1H), 5.35 (s, 1H), 3.51 (d, J = 5.1 Hz, 2H), 3.44 (d, J = 9.6 Hz, 1H), 3.28 (s, 3H), 2.98 (d, J = 9.6 Hz, 1H), 0.87 – 0.77 (m, 1H), 0.71 – 0.61 (m, 1H), 0.60 – 0.48 (m, 2H). ^{13}C NMR (125 MHz, CDCl_3) δ 164.8 (d, J = 255.8 Hz), 157.1, 151.5, 149.8, 130.9, 130.1 (d, J = 9.0 Hz), 120.1, 115.9 (d, J = 21.4 Hz), 102.4, 101.4, 59.5, 55.6, 52.3, 33.0, 23.4, 14.1, 9.2. HRMS (ESI) calcd for $\text{C}_{19}\text{H}_{21}\text{FN}_5\text{O}_2\text{S}$: 402.1400. Obsd: 402.1388. $[\alpha]_{\text{D}}$ -3.0° (c 2.17, CHCl_3).

(R)-2-((7-(Methyl(7H-pyrrolo[2,3-d]pyrimidin-4-yl)amino)-5-azaspiro[2.4]heptan-5-yl)sulfonyl)benzonitrile, 57

Yield: 56.0 mg (47.9%). 99.2% purity by HPLC. ^1H NMR (500 MHz, CDCl_3) δ 12.05 (s, 1H), 8.12 (s, 1H), 8.00 (d, J = 7.5 Hz, 1H), 7.83 (d, J = 7.3 Hz, 1H), 7.66 (dt, J = 22.3, 7.4 Hz, 2H), 7.02 (d, J = 3.1 Hz, 1H), 6.45 (d, J = 3.0 Hz, 1H), 5.41 (d, J = 4.8 Hz, 1H), 3.74 (dd, J = 10.9, 7.7 Hz, 1H), 3.68 (d, J = 9.8 Hz, 1H), 3.61 (dd, J = 11.0, 2.7 Hz, 1H), 3.32 (s, 3H), 3.29 (d, J = 9.8 Hz, 1H), 0.88 (t, J = 7.0 Hz, 1H), 0.72 (dd, J = 8.7, 5.5 Hz, 1H), 0.69 – 0.57 (m, 2H). ^{13}C NMR (100 MHz, CDCl_3) δ 157.6, 151.9, 150.2, 140.0, 135.6, 133.0, 132.9, 130.3, 120.7, 116.4, 110.9, 103.0, 101.8, 60.3, 56.1, 52.6, 33.5, 24.1, 14.9, 9.3. HRMS (ESI) calcd for $\text{C}_{20}\text{H}_{21}\text{N}_6\text{O}_2\text{S}$: 409.1447. Obsd: 409.1435. $[\alpha]_{\text{D}}$ +2.2° (c 1.91, CHCl_3).

(R)-3-((7-(Methyl(7*H*-pyrrolo[2,3-*d*]pyrimidin-4-yl)amino)-5-azaspiro[2.4]heptan-5-yl)sulfonyl)benzonitrile, **58**

Yield: 62.0 mg (53.0%). 100% purity by HPLC. ¹H NMR (500 MHz, CDCl₃) δ 12.03 (s, 1H), 8.19 (s, 1H), 8.14 (s, 1H), 8.06 (d, *J* = 7.9 Hz, 1H), 7.91 (d, *J* = 7.7 Hz, 1H), 7.70 (t, *J* = 7.8 Hz, 1H), 7.11 (d, *J* = 2.8 Hz, 1H), 6.52 (d, *J* = 2.8 Hz, 1H), 5.40 (s, 1H), 3.65 (t, *J* = 5.1 Hz, 2H), 3.60 (d, *J* = 9.8 Hz, 1H), 3.36 (s, 3H), 3.10 (d, *J* = 9.7 Hz, 1H), 0.90 (dd, *J* = 9.8, 4.4 Hz, 1H), 0.83 – 0.74 (m, 1H), 0.73 – 0.58 (m, 2H). ¹³C NMR (100 MHz, CDCl₃) δ 157.5, 151.9, 150.2, 137.5, 136.0, 131.6, 131.2, 130.2, 120.7, 117.1, 113.8, 103.0, 101.8, 60.1, 56.1, 52.8, 33.5, 23.8, 14.8, 9.6. HRMS (ESI) calcd for C₂₀H₂₁N₆O₂S: 409.1447. Obsd: 409.1435. [α]_D -7.5° (c 1.82, CHCl₃).

(R)-4-((7-(Methyl(7*H*-pyrrolo[2,3-*d*]pyrimidin-4-yl)amino)-5-azaspiro[2.4]heptan-5-yl)sulfonyl)benzonitrile, **59**

Yield: 62.0 mg (53.0%). 94.1% purity by HPLC. ¹H NMR (400 MHz, CDCl₃) δ 10.59 (s, 1H), 8.18 (s, 1H), 8.00 – 7.90 (m, 2H), 7.89 – 7.81 (m, 2H), 7.08 (dd, *J* = 3.5, 1.8 Hz, 1H), 6.52 (d, *J* = 2.4 Hz, 1H), 5.36 (dd, *J* = 5.7, 4.4 Hz, 1H), 3.65 (s, 1H), 3.64 (d, *J* = 1.9 Hz, 1H), 3.59 (d, *J* = 9.7 Hz, 1H), 3.34 (s, 3H), 3.10 (d, *J* = 9.7 Hz, 1H), 0.91 (ddd, *J* = 10.2, 6.2, 4.0 Hz, 1H), 0.82 – 0.75 (m, 1H), 0.73 – 0.59 (m, 2H). ¹³C NMR (100 MHz, CDCl₃) δ 157.5, 151.9, 150.2, 134.0, 132.9, 128.3, 120.8, 117.2, 116.7, 103.0, 101.8, 60.2, 56.0, 52.9, 33.5, 23.8, 14.9, 9.5. HRMS (ESI) calcd for C₂₀H₂₁N₆O₂S: 409.1447. Obsd: 409.1433. [α]_D -12.7° (c 1.66, CHCl₃).

(R)-*N*-Methyl-*N*-(5-((2-nitrophenyl)sulfonyl)-5-azaspiro[2.4]heptan-7-yl)-7*H*-pyrrolo[2,3-*d*]pyrimidin-4-amine, **60**

Yield: 68.8 mg (76.5%). 96.9% purity by HPLC. ¹H NMR (400 MHz, CDCl₃) δ 12.38 (s, 1H), 8.23 (s, 1H), 8.00 (d, *J* = 7.3 Hz, 1H), 7.69 (dd, *J* = 16.0, 7.9 Hz, 2H), 7.62 (d, *J* = 7.3 Hz, 1H), 7.10 (s, 1H), 6.53 (s, 1H), 5.50 (d, *J* = 6.2 Hz, 1H), 4.03 – 3.87 (m, 1H), 3.75 (d, *J* = 9.6 Hz, 2H), 3.39 (s, 3H),

3.38 – 3.27 (m, 1H), 0.96 (d, J = 5.5 Hz, 1H), 0.91 – 0.59 (m, 3H). ^{13}C NMR (100 MHz, CDCl_3) δ 157.6, 152.0, 150.2, 148.4, 133.9, 131.6, 130.8, 124.1, 120.7, 103.0, 101.8, 60.4, 55.9, 52.6, 33.4, 24.2, 15.1, 9.2. HRMS (ESI) calcd for $\text{C}_{19}\text{H}_{21}\text{N}_6\text{O}_4\text{S}$: 429.1345. Obsd: 429.1340. $[\alpha]_{\text{D}} +6.1^\circ$ (c 2.21, CHCl_3).

(R)-N-Methyl-N-(5-((3-nitrophenyl)sulfonyl)-5-azaspiro[2.4]heptan-7-yl)-7H-pyrrolo[2,3-d]pyrimidin-4-amine, **61**

Yield: 61.6 mg (68.5%). 94.8% purity by HPLC. ^1H NMR (400 MHz, CDCl_3) δ 10.49 (s, 1H), 8.67 (d, J = 1.4 Hz, 1H), 8.49 (d, J = 8.2 Hz, 1H), 8.16 (d, J = 3.4 Hz, 2H), 7.78 (td, J = 8.1, 3.3 Hz, 1H), 7.06 (s, 1H), 6.52 (s, 1H), 5.47 – 5.32 (m, 1H), 3.79 – 3.57 (m, 3H), 3.37 (d, J = 3.2 Hz, 3H), 3.14 (d, J = 9.7 Hz, 1H), 0.90 (dd, J = 6.2, 3.2 Hz, 1H), 0.84 – 0.74 (m, 1H), 0.74 – 0.58 (m, 2H). ^{13}C NMR (100 MHz, CDCl_3) δ 157.5, 152.0, 150.6, 148.4, 138.1, 133.2, 130.5, 127.4, 122.7, 120.3, 102.8, 102.1, 60.1, 56.1, 52.9, 33.6, 23.8, 14.8, 9.6. HRMS (ESI) calcd for $\text{C}_{19}\text{H}_{21}\text{N}_6\text{O}_4\text{S}$: 429.1345. Obsd: 429.1339. $[\alpha]_{\text{D}} -6.4^\circ$ (c 0.117, CHCl_3).

(R)-N-Methyl-N-(5-((4-nitrophenyl)sulfonyl)-5-azaspiro[2.4]heptan-7-yl)-7H-pyrrolo[2,3-d]pyrimidin-4-amine, **62**

Yield: 52.1 mg (58.0%). 97.1% purity by HPLC. ^1H NMR (400 MHz, CDCl_3) δ 11.61 (s, 1H), 8.50 – 8.30 (m, 2H), 8.19 (d, J = 3.4 Hz, 1H), 8.02 (s, 2H), 7.09 (s, 1H), 6.50 (s, 1H), 5.36 (d, J = 3.5 Hz, 1H), 3.67 (s, 2H), 3.65 – 3.56 (m, 1H), 3.36 (d, J = 3.5 Hz, 3H), 3.19 – 3.05 (m, 1H), 0.83 – 0.75 (m, 1H), 0.67 (dd, J = 14.9, 9.8 Hz, 3H). ^{13}C NMR (100 MHz, CDCl_3) δ 157.5, 152.0, 150.3, 150.2, 141.6, 128.9, 124.3, 120.6, 103.0, 101.9, 60.2, 56.1, 52.9, 33.5, 23.8, 14.9, 9.5. HRMS (ESI) calcd for $\text{C}_{19}\text{H}_{21}\text{N}_6\text{O}_4\text{S}$: 429.1345. Obsd: 429.1338. $[\alpha]_{\text{D}} -19.0^\circ$ (c 1.38, CHCl_3).

*(R)-N-Methyl-N-(5-(*m*-tolylsulfonyl)-5-azaspiro[2.4]heptan-7-yl)-7H-pyrrolo[2,3-d]pyrimidin-4-amine*, **63**

Yield: 124 mg (81.6%). 98.0% purity by HPLC. ¹H NMR (400 MHz, CDCl₃) δ 12.57 (s, 1H), 8.22 (d, *J* = 4.7 Hz, 1H), 7.65 (s, 2H), 7.43 (s, 2H), 7.10 (s, 1H), 6.50 (s, 1H), 5.41 (s, 1H), 3.61 (s, 2H), 3.52 (dd, *J* = 9.3, 4.4 Hz, 1H), 3.33 (d, *J* = 4.3 Hz, 3H), 3.08 (dd, *J* = 9.3, 4.5 Hz, 1H), 2.42 (d, *J* = 4.3 Hz, 3H), 0.87 (d, *J* = 4.6 Hz, 1H), 0.75 (d, *J* = 9.6 Hz, 1H), 0.61 (d, *J* = 2.9 Hz, 2H). ¹³C NMR (100 MHz, CDCl₃) δ 157.6, 151.9, 150.1, 139.3, 134.9, 133.8, 129.0, 128.2, 125.0, 120.7, 102.9, 101.8, 60.0, 56.0, 52.8, 33.3, 23.9, 21.4, 14.4, 9.7. HRMS (ESI) calcd for C₂₀H₂₄N₅O₂S: 398.1651. Obsd: 398.1645. [α]_D -5.6° (c 3.88, CHCl₃).

(R)-N-(5-((4-Methoxyphenyl)sulfonyl)-5-azaspiro[2.4]heptan-7-yl)-N-methyl-7H-pyrrolo[2,3-d]pyrimidin-4-amine, 64

Yield: 99.5 mg (83.8%). 96.3% purity by HPLC. ¹H NMR (400 MHz, CDCl₃) δ 11.94 (s, 1H), 8.19 (s, 1H), 7.78 (d, *J* = 8.8 Hz, 2H), 7.09 (d, *J* = 3.4 Hz, 1H), 7.02 (d, *J* = 8.8 Hz, 2H), 6.53 (d, *J* = 3.1 Hz, 1H), 5.43 (t, *J* = 4.7 Hz, 1H), 3.89 (s, 3H), 3.56 (d, *J* = 4.9 Hz, 2H), 3.36 (s, 3H), 3.27 (dd, *J* = 174.5, 9.5 Hz, 2H), 0.95 – 0.84 (m, 1H), 0.78 – 0.68 (m, 1H), 0.62 (t, *J* = 7.5 Hz, 2H). ¹³C NMR (100 MHz, CDCl₃) δ 163.2, 157.6, 151.7, 150.2, 130.1, 126.6, 120.5, 114.2, 102.9, 102.0, 59.9, 56.0, 55.6, 52.7, 33.4, 23.9, 14.3, 9.9. HRMS (ESI) calcd for C₂₀H₂₄N₅O₃S: 414.1600. Obsd: 414.1591. [α]_D -14.2° (c 0.983, CHCl₃).

(R)-N-Methyl-N-(5-((4-(trifluoromethyl)phenyl)sulfonyl)-5-azaspiro[2.4]heptan-7-yl)-7H-pyrrolo[2,3-d]pyrimidin-4-amine, 65

Yield: 70.5 mg (54.2%). 97.5% purity by HPLC. ¹H NMR (400 MHz, CDCl₃) δ 11.77 (s, 1H), 8.23 (s, 1H), 7.90 (dd, *J* = 54.7, 8.2 Hz, 4H), 7.10 (d, *J* = 3.1 Hz, 1H), 6.54 (s, 1H), 5.41 (dd, *J* = 6.0, 3.1 Hz, 1H), 3.65 (dd, *J* = 15.1, 4.8 Hz, 2H), 3.37 (s, 3H), 3.34 (dd, *J* = 191.6, 9.6 Hz, 2H), 0.99 – 0.87 (m, 1H), 0.82 – 0.72 (m, 1H), 0.71 – 0.57 (m, 2H). ¹³C NMR (100 MHz, CDCl₃) δ 157.5, 151.5, 149.9, 139.1, 134.7 (q, *J* = 33.1 Hz), 128.3, 126.3 (q, *J* = 3.6 Hz), 123.2

(q, $J = 272.9$ Hz), 120.7, 103.1, 102.0, 60.2, 56.0, 52.8, 33.5, 23.9, 14.7, 9.7. HRMS (ESI) calcd for $C_{20}H_{21}F_3N_5O_2S$: 452.1368. Obsd: 452.1361. $[\alpha]_D -6.8^\circ$ (c 0.970, $CHCl_3$).

(R)-N-Methyl-N-(5-(naphthalen-2-ylsulfonyl)-5-azaspiro[2.4]heptan-7-yl)-7H-pyrrolo[2,3-d]pyrimidin-4-amine, **66**

Yield: 124 mg (99.0%). 98.5% purity by HPLC. 1H NMR (400 MHz, $CDCl_3$) δ 12.58 (s, 1H), 8.42 (s, 1H), 8.19 (d, $J = 1.7$ Hz, 1H), 7.96 (d, $J = 8.1$ Hz, 2H), 7.93 – 7.77 (m, 2H), 7.62 (dt, $J = 16.4, 7.3$ Hz, 2H), 7.06 (s, 1H), 6.43 (s, 1H), 5.39 (s, 1H), 3.67 (d, $J = 3.8$ Hz, 2H), 3.36 (dd, $J = 171.8, 9.6$ Hz, 2H), 3.30 (s, 3H), 0.81 (d, $J = 7.0$ Hz, 1H), 0.71 (d, $J = 4.6$ Hz, 1H), 0.57 (t, $J = 6.5$ Hz, 2H). ^{13}C NMR (100 MHz, $CDCl_3$) δ 157.5, 151.9, 150.1, 134.9, 132.3, 132.1, 129.3, 129.2, 128.9, 127.9, 127.6, 123.1, 120.7, 102.9, 101.8, 60.0, 56.1, 52.9, 33.4, 23.9, 14.5, 9.7. HRMS (ESI) calcd for $C_{23}H_{24}N_5O_2S$: 434.1651. Obsd: 434.1644. $[\alpha]_D -17.1^\circ$ (c 4.58, $CHCl_3$).

(R)-N-Methyl-N-(5-(piperidin-1-ylsulfonyl)-5-azaspiro[2.4]heptan-7-yl)-7H-pyrrolo[2,3-d]pyrimidin-4-amine, **67**

Yield: 73.0 mg (65.2%). 95.4% purity by HPLC. 1H NMR (400 MHz, $CDCl_3$) δ 11.36 (s, 1H), 8.25 (s, 1H), 7.09 (s, 1H), 6.58 (s, 1H), 5.56 (d, $J = 5.8$ Hz, 1H), 3.92 – 3.76 (m, 1H), 3.54 (d, $J = 9.5$ Hz, 2H), 3.48 (s, 4H), 3.28 (d, $J = 4.5$ Hz, 4H), 1.61 (dd, $J = 26.6, 3.9$ Hz, 6H), 1.03 (d, $J = 9.7$ Hz, 1H), 0.76 (d, $J = 9.9$ Hz, 2H), 0.69 (d, $J = 9.9$ Hz, 1H). ^{13}C NMR (100 MHz, $CDCl_3$) δ 157.7, 152.0, 150.6, 120.3, 102.8, 102.0, 60.2, 56.6, 52.9, 47.2, 33.5, 25.5, 24.0, 23.8, 15.1, 9.5. HRMS (ESI) calcd for $C_{18}H_{27}N_6O_2S$: 391.1916. Obsd: 391.1913. $[\alpha]_D +32.7^\circ$ (c 0.297, $CHCl_3$).

(R)-N-Methyl-N-(5-(morpholinomethylsulfonyl)-5-azaspiro[2.4]heptan-7-yl)-7H-pyrrolo[2,3-d]pyrimidin-4-amine, **68**

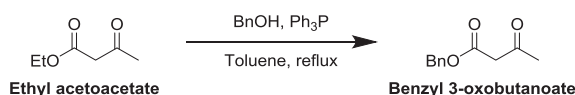
Yield: 44.0 mg (38.9%). 94.6% purity by HPLC. 1H NMR (400 MHz, $CDCl_3$) δ 12.33 (s, 1H), 8.27 (d, $J = 2.8$ Hz, 1H), 7.13 (s, 1H), 6.57 (s, 1H), 5.63

– 5.51 (m, 1H), 3.90 (ddd, $J = 10.6, 7.6, 2.7$ Hz, 1H), 3.75 (dd, $J = 5.8, 3.1$ Hz, 4H), 3.65 – 3.55 (m, 2H), 3.48 (d, $J = 2.8$ Hz, 3H), 3.37 – 3.22 (m, 5H), 1.04 (d, $J = 9.6$ Hz, 1H), 0.85 – 0.75 (m, 2H), 0.75 – 0.65 (m, 1H). ^{13}C NMR (100 MHz, CDCl_3) δ 157.7, 152.0, 150.3, 120.7, 102.9, 101.8, 66.4, 60.2, 56.8, 53.1, 46.4, 33.5, 24.0, 15.3, 9.3. HRMS (ESI) calcd for $\text{C}_{17}\text{H}_{25}\text{N}_6\text{O}_3\text{S}$: 393.1709. Obsd: 393.1704. $[\alpha]_{\text{D}} +32.9^\circ$ (c 1.57, CHCl_3).

Synthesis of (R)-4,4-dimethyl-1-((R)-1-phenylethyl)pyrrolidin-3-amine,

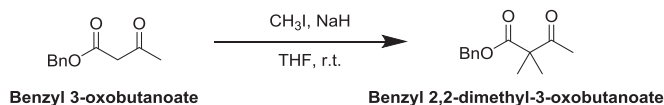
7b

Benzyl 3-oxobutanoate



Benzyl alcohol (4.78 mL, 46.0 mmol) was added to ethyl acetoacetate (6.00 g, 46.1 mmol) solution in 60.0 mL of toluene. The solution was treated with triphenylphosphine (1.21 g, 4.61 mmol) and then refluxed for 12 hours. The mixture was concentrated under reduced pressure. The residue was purified with flash column chromatography (ethyl acetate:*n*-hexane = 1:20). Removing the solvent in vacuo provided 6.69 g of benzyl 3-oxobutanoate (75.1% yield). ^1H NMR (400 MHz, CDCl_3) δ 7.39 – 7.23 (m, 5H), 5.17 (s, 2H), 3.50 (s, 2H), 2.24 (s, 3H).

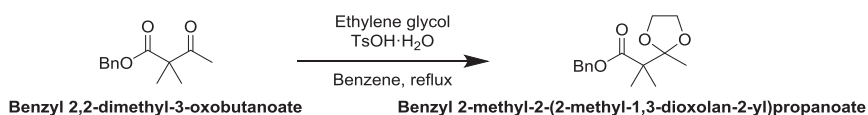
Benzyl 2,2-dimethyl-3-oxobutanoate



Sodium hydride, 60wt% (3.48 g, 87.0 mmol) was slowly added to benzyl 3-oxobutanoate (6.69 g, 34.8 mmol) solution in 67.0 mL of tetrahydrofuran at 0 °C. The mixture was stirred at room temperature for 1 hour. Iodomethane (6.48 mL, 104 mmol) was slowly added at 0 °C. The reaction mixture was stirred at room temperature for 12 hours. The mixture was

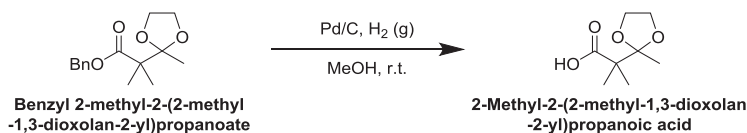
concentrated under reduced pressure. To the residue were added 100 mL of brine and 50 mL of saturated ammonium chloride solution. The aqueous mixture was extracted with 100 mL of ethyl acetate three times. The combined organic layers were dried over anhydrous sodium sulfate, filtered and concentrated. The residue was purified with flash column chromatography (ethyl acetate:*n*-hexane = 1:8). Removing the solvent in vacuo provided 6.69 g of benzyl 2,2-dimethyl-3-oxobutanoate (90.1% yield). ¹H NMR (400 MHz, CDCl₃) δ 7.39 – 7.30 (m, 5H), 5.17 (s, 2H), 2.08 (s, 3H), 1.38 (s, 6H).

Benzyl 2-methyl-2-(2-methyl-1,3-dioxolan-2-yl)propanoate



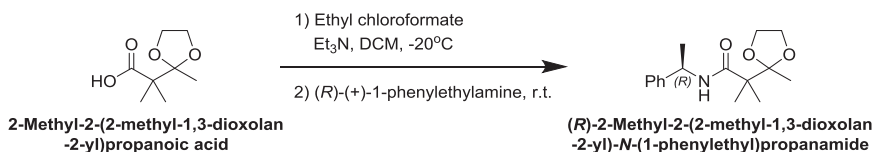
Ethylene glycol (4.90 mL, 87.6 mmol) and *p*-toluenesulfonic acid monohydrate (0.410 g, 2.16 mmol) were added to benzyl 2,2-dimethyl-3-oxobutanoate (9.69 g, 44.0 mmol) solution in 195 mL of benzene. The reaction flask was equipped with a Dean-Stark trap. The reaction solution was refluxed stirred for 24 hours. The solution was concentrated under reduced pressure. To the residue were added 200 mL of brine and 100 mL of saturated sodium bicarbonate solution. The aqueous mixture was extracted with 100 mL of ethyl acetate three times. The combined organic layers were dried over anhydrous sodium sulfate, filtered and concentrated. The residue was purified with flash column chromatography (ethyl acetate:*n*-hexane = 1:10). Removing the solvent in vacuo provided 9.47 g of benzyl 2-methyl-2-(2-methyl-1,3-dioxolan-2-yl)propanoate (81.6% yield). ¹H NMR (400 MHz, CDCl₃) δ 7.39 – 7.26 (m, 5H), 5.15 (s, 2H), 3.99 – 3.93 (m, 2H), 3.89 – 3.84 (m, 2H), 1.33 (s, 3H), 1.29 (s, 6H).

2-Methyl-2-(2-methyl-1,3-dioxolan-2-yl)propanoic acid



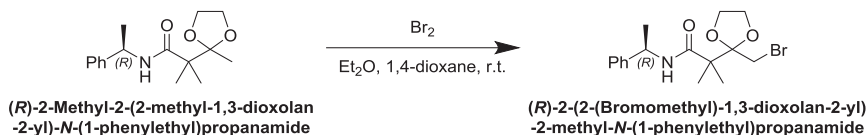
Palladium on charcoal (9.47 g, 10wt/wt%) was added to benzyl 2-methyl-2-(2-methyl-1,3-dioxolan-2-yl)propanoate (9.47 g, 35.8 mmol) solution in 95.0 mL of methanol. The reaction flask was equipped with a hydrogen gas balloon. The reaction mixture was vigorously stirred for 24 hours. The mixture was filtered through a celite 545 pad. Removing the solvent in vacuo provided 5.94 g of 2-methyl-2-(2-methyl-1,3-dioxolan-2-yl)propanoic acid (95.2% yield). ^1H NMR (400 MHz, CDCl_3) δ 4.09 – 4.01 (m, 4H), 1.37 (s, 3H), 1.29 (s, 6H).

(R)-2-Methyl-2-(2-methyl-1,3-dioxolan-2-yl)-N-(1-phenylethyl)propanamide



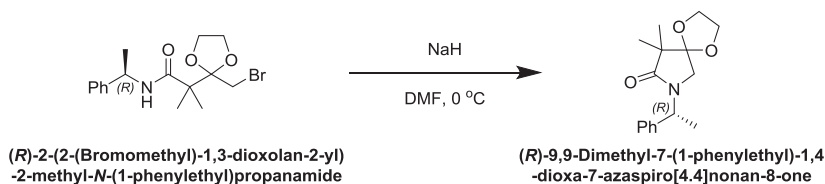
Triethylamine (9.51 mL, 68.2 mmol) was added to 2-methyl-2-(2-methyl-1,3-dioxolan-2-yl)propanoic acid (5.94 g, 21.4 mmol) solution in 53.0 mL of dichloromethane at -20 °C. Ethyl chloroformate (3.59 mL, 37.7 mmol) was slowly added at -20 °C. The reaction solution was stirred at -20 °C for 40 minutes. To the reaction solution was dropwise added (R)-(+)-phenylethylamine (4.78 mL, 37.6 mmol) at -20 °C. After the addition, the reaction solution was stirred at room temperature for 12 hours. To the reaction solution was poured 50.0 mL of deionized water and then the organic layer was separated. The organic layer was dried over anhydrous sodium sulfate, filtered and concentrated. The residue was purified with flash column chromatography (ethyl acetate:*n*-hexane = 1:8). Removing the solvent in vacuo provided 1.89 g of (R)-2-methyl-2-(2-methyl-1,3-dioxolan-2-yl)-N-(1-phenylethyl)propanamide (20.0% yield). ^1H NMR (400 MHz, CDCl_3) δ 7.35 – 7.21 (m, 5H), 7.11 (d, J = 6.8 Hz, 1H), 5.14 – 5.04 (m, 1H), 4.04 – 3.97 (m, 2H), 3.96 – 3.90 (m, 2H), 1.47 (d, J = 6.8 Hz, 3H), 1.24 (s, 3H), 1.23 (s, 3H), 1.20 (s, 3H).

(R)-2-(2-(Bromomethyl)-1,3-dioxolan-2-yl)-2-methyl-N-(1-phenylethyl)propanamide

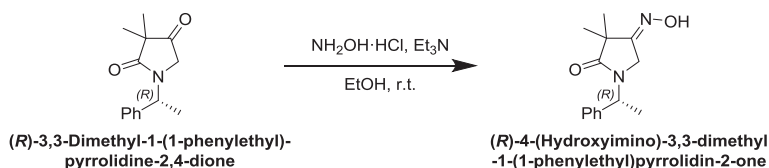


A solution of bromine (0.590 mL, 11.5 mmol) in 30.0 mL of 1,4-dioxane was slowly added to (R)-2-methyl-2-(2-methyl-1,3-dioxolan-2-yl)-N-(1-phenylethyl)propanamide (1.89 g, 6.81 mmol) in 18.0 mL of diethyl ether and 8.00 mL of 1,4-dioxane at 0 °C. The reaction solution was stirred at room temperature for 12 hours. The solution was concentrated under reduced pressure. The residue was extracted with 18.0 mL of ethyl acetate, 18.0 mL of brine, and 18.0 mL of saturated sodium thiosulfate solution. The organic layer was dried over anhydrous sodium sulfate, filtered and concentrated. The residue was purified with flash column chromatography (ethyl acetate:*n*-hexane = 1:10). Removing the solvent in vacuo provided 2.29 g of (R)-2-(2-(bromomethyl)-1,3-dioxolan-2-yl)-2-methyl-N-(1-phenylethyl)propanamide (94.2% yield). ¹H NMR (400 MHz, CDCl₃) δ 7.36 – 7.22 (m, 5H), 7.02 (d, *J* = 7.6 Hz, 1H), 5.11 – 5.01 (m, 1H), 4.43 – 4.36 (m, 2H), 4.14 – 4.05 (m, 2H), 3.62 (d, *J* = 11.2 Hz, 1H), 3.51 (d, *J* = 10.0 Hz, 1H), 1.54 (d, *J* = 7.6 Hz, 3H), 1.25 (s, 6H).

(R)-9,9-Dimethyl-7-(1-phenylethyl)-1,4-dioxo-7-azaspiro[4.4]nonan-8-one

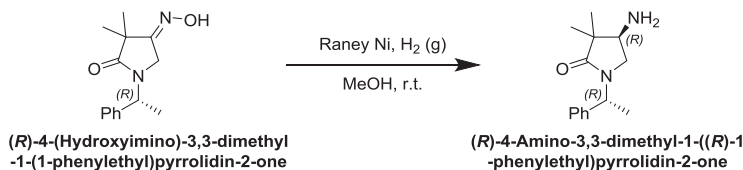


An (R)-2-methyl-2-(2-methyl-1,3-dioxolan-2-yl)-N-(1-phenylethyl)propanamide (2.29 g, 6.43 mmol) was solved in 22.0 mL of *N,N*-dimethylformamide. The solution was treated with sodium hydride, 60wt% (440 mg, 11.0 mmol) at 0 °C. The reaction mixture was stirred at 0 °C for 3



Hydroxylamine hydrochloride (395 mg, 5.68 mmol), and triethylamine (0.782 mL, 5.61 mmol) were added to *(R)*-3,3-dimethyl-1-(1-phenylethyl)pyrrolidine-2,4-dione (840 mg, 3.63 mmol) solution in 9.00 mL of ethanol. The reaction solution was stirred at room temperature for 5 hours. The reaction solution was concentrated under reduced pressure. The residue was purified with flash column chromatography (ethyl acetate:*n*-hexane = 1:3). Removing the solvent in vacuo provided 730 mg of *(R)*-4-(hydroxyimino)-3,3-dimethyl-1-(1-phenylethyl)pyrrolidin-2-one (94.1% yield). ¹H NMR (400 MHz, CDCl₃) δ 7.37 – 7.26 (m, 5H), 7.26 (s, 1H), 5.65 (q, *J* = 7.2 Hz, 1H), 4.10 (d, *J* = 16.8 Hz, 1H), 3.71 (d, *J* = 16.4 Hz, 1H), 1.55 (s, 3H), 1.34 (s, 3H), 1.30 (s, 3H).

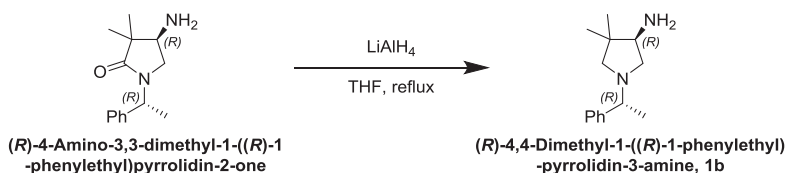
(R)-4-Amino-3,3-dimethyl-1-((*R*)-1-phenylethyl)pyrrolidin-2-one



Raney[®]-nickel slurry (1.56 mL, Raney[®] 2400) was added to *(R)*-4-(hydroxyimino)-3,3-dimethyl-1-(1-phenylethyl)pyrrolidin-2-one (730 mg, 2.96 mmol) solution in 36.5 mL of methanol. The reaction flask was equipped with a hydrogen gas balloon. The reaction mixture was vigorously stirred for 12 hours. The mixture was filtered through a celite 545 pad. The filtered solution was concentrated under reduced pressure. The residue was purified with flash column chromatography (methanol:dichloromethane = 2:98). Removing the solvent in vacuo provided 264 mg of *(R)*-4-amino-3,3-dimethyl-1-((*R*)-1-phenylethyl)pyrrolidin-2-one (38.4% yield). ¹H NMR (400 MHz, CDCl₃) δ 7.31 – 7.26 (m, 5H), 5.50 (q, *J* = 6.8 Hz, 1H), 3.09 – 3.03 (m, 2H),

2.83 – 2.76 (m, 1H), 1.50 (d, $J = 6.8$, 3H), 1.12 (s, 3H), 1.03 (s, 3H). Also was obtained 300 mg of (*S*)-4-amino-3,3-dimethyl-1-((*R*)-1-phenylethyl)pyrrolidin-2-one (38.4% yield). ^1H NMR (400 MHz, CDCl_3) δ 7.31 – 7.26 (m, 5H), 5.50 (q, $J = 6.8$ Hz, 1H), 3.10 – 3.03 (m, 2H), 2.83 – 2.76 (m, 1H), 1.50 (d, $J = 6.8$ Hz, 3H), 1.12 (s, 3H), 1.03 (s, 3H).

(*R*)-4,4-Dimethyl-1-((*R*)-1-phenylethyl)-pyrrolidin-3-amine, **7b**



Lithium aluminum hydride (189 mg, 4.98 mmol) was slowly added to (*R*)-4-amino-3,3-dimethyl-1-((*R*)-1-phenylethyl)pyrrolidin-2-one (264 mg, 1.14 mmol) solution in 13.0 mL of tetrahydrofuran at 0 °C. The reaction solution was refluxed for 12 hours and then cooled down to 0 °C. The reaction was quenched with 1.15 mL of deionized water, 1.15 mL of 15% sodium hydroxide solution, and 3.45 mL of deionized water. Then, celite 545 was added and the mixture was stirred for 30 minutes before being filtered through a celite 545 pad. The filtered solution was concentrated under reduced pressure and the residue was extracted with 10.0 mL of brine and 10.0 mL of ethyl acetate. The organic layer was dried over anhydrous sodium sulfate and filtered. Removing the solvent in vacuo provided 240 mg of (*R*)-4,4-dimethyl-1-((*R*)-1-phenylethyl)-pyrrolidin-3-amine, **1b** (96.8% yield). ^1H NMR (400 MHz, CDCl_3) δ 7.38 – 7.16 (m, 5H), 3.26 (q, $J = 6.8$ Hz, 1H), 3.08 (dd, $J = 9.2$, 7.2 Hz, 1H), 2.98 (t, $J = 7.2$ Hz, 1H), 2.36 (s, 2H), 2.20 (dd, $J = 9.6$, 6.8 Hz, 1H), 1.30 (d, $J = 6.4$ Hz, 3H), 1.03 (s, 3H), 0.92 (s, 3H).

*Synthesis of tert-butyl (R)-(1-benzylpyrrolidin-3-yl)carbamate, **8aa***

Sodium bicarbonate (5.92 g, 70.5 mmol) in 118 mL of deionized water was added to (3*R*)-(+)-benzylaminopyrrolidine **7a** (5.00 g, 28.4 mmol) solution in 118 mL of acetonitrile and the mixture was stirred at room temperature for

10 minutes. Di-*tert*-butyl dicarbamate (6.22 g, 28.5 mmol) was then added and the mixture was stirred at room temperature overnight. After the reaction, the solution was concentrated under reduced pressure and the residue was extracted with dichloromethane three times. Combined organic layers were dried over anhydrous sodium sulfate, filtered and concentrated. The residue was purified with flash column chromatography (methanol:dichloromethane = 2:98). Removing the solvent in vacuo provided 4.24 g of *tert*-butyl (*R*)-(1-benzylpyrrolidin-3-yl)carbamate (65.2% yield). ¹H NMR (400 MHz, CDCl₃) δ 7.36 – 7.26 (m, 5H), 4.86 (bs, 1H), 4.18 (bs, 1H), 3.61 (s, 2H), 2.79 (bs, 1H), 2.65 – 2.61 (m, 1H), 2.54 (d, *J* = 8.0 Hz, 1H), 2.34 – 2.25 (m, 2H), 1.61 – 1.51 (m, 1H), 1.46 (s, 9H). [α]_D +2.5° (*c* 0.620, CHCl₃).

In the cases of **8b** and **8c**, the desired products were synthesized from (*R*)-4,4-dimethyl-1-((*R*)-1-phenylethyl)pyrrolidin-3-amine (**7b**) and (*R*)-6-((*R*)-1-phenylethyl)-6-azaspiro[3.4]octan-8-amine (**7c**), respectively, instead of (3*R*)-(+)-benzylaminopyrrolidine **7a** according to the aforementioned process (vide supra).

tert-Butyl ((*R*)-4,4-dimethyl-1-((*R*)-1-phenylethyl)pyrrolidin-3-yl)carbamate, **8b**

Yield: 335 mg (95.7%). ¹H NMR (400 MHz, CDCl₃) δ 7.29 – 7.20 (m, 5H), 4.61 (d, *J* = 10.4 Hz, 1H), 3.79 – 3.74 (m, 1H), 3.23 (m, 1H), 2.89 (q, *J* = 9.6, 7.2 Hz, 1H), 2.51 (d, *J* = 9.2 Hz, 1H), 2.31 – 2.19 (m, 2H), 1.43 (s, 9H), 1.30 (d, *J* = 6.4 Hz, 3H), 1.10 (s, 3H), 0.98 (s, 3H). [α]_D +7.4° (*c* 0.153, CHCl₃).

tert-Butyl ((*R*)-6-((*R*)-1-phenylethyl)-6-azaspiro[3.4]octan-8-yl)carbamate, **8c**

Yield: 563 mg (quantitative yield). ¹H NMR (400 MHz, CDCl₃) δ 7.32 – 7.22 (m, 5H), 4.71 (d, *J* = 8.8 Hz, 1H), 3.95 – 3.90 (m, 1H), 3.21 (q, *J* = 6.4 Hz, 1H), 2.77 – 2.70 (m, 2H), 2.51 (d, *J* = 9.6 Hz, 1H), 2.21 (dd, *J* = 10.0, 3.6

Hz, 1H), 2.07 – 2.02 (m, 2H), 1.89 – 1.73 (m, 4H), 1.45 (s, 9H), 1.31 (d, $J = 6.4$ Hz, 3H). $[\alpha]_{\text{D}} +8.4^{\circ}$ (c 0.387, CHCl_3).

In the cases of **8ab** and **8ac**, the desired products were synthesized through substitution reactions with acetic anhydride and cyclopropanecarbonyl chloride instead of di-*tert*-butyl dicarbamate according to the aforementioned process (vide supra).

(R)-N-(1-Benzylpyrrolidin-3-yl)acetamide, 8ab

Yield: 2.12 g (85.0%). ^1H NMR (400 MHz, CDCl_3) δ 7.34 – 7.24 (m, 5H), 5.93 (s, 1H), 4.46 – 4.42 (m, 1H), 3.60 (s, 2H), 2.90 – 2.86 (m, 1H), 2.62 – 2.51 (m, 2H), 2.30 – 2.22 (m, 2H), 1.93 (s, 3H), 1.64 – 1.60 (m, 1H). $[\alpha]_{\text{D}} +19.7^{\circ}$ (c 0.410, CHCl_3).

(R)-N-(1-Benzylpyrrolidin-3-yl)cyclopropanecarboxamide, 8ac

Yield: 3.02 g (quantitative yield). ^1H NMR (400 MHz, CDCl_3) δ 8.39 (d, $J = 5.2$ Hz, 1H), 7.62 – 7.48 (m, 5H), 4.96 (s, 1H), 4.28 – 4.21 (bs, 2H), 3.81 (s, 1H), 3.52 (d, $J = 11.2$ Hz, 1H), 3.05 – 2.88 (m, 2H), 2.54 – 2.47 (m, 1H), 2.30 – 2.23 (m, 1H), 0.94 – 0.91 (m, 2H), 0.89 – 0.84 (m, 1H), 0.78 – 0.75 (m, 2H). $[\alpha]_{\text{D}} +16.3^{\circ}$ (c 0.397, CHCl_3).

Synthesis of (R)-1-benzyl-N-methylpyrrolidin-3-amine, 9aa

A *tert*-butyl (*R*)-(1-benzylpyrrolidin-3-yl)carbamate **8aa** (3.20 g, 11.6 mmol) solution in 58.0 mL of tetrahydrofuran was placed in a 100 mL round bottom flask. After it was cooled at -40°C , lithium aluminum hydride (2.64 g, 69.6 mmol) was slowly added to the stirred mixture. The reaction mixture was refluxed for 4 hours and then cooled down to -40°C . The reaction was quenched with 2.70 mL of deionized water, 2.70 mL of 15% sodium hydroxide solution, and 8.10 mL of deionized water. Then, celite 545 was added and the mixture

was stirred for 30 minutes before being filtered through a celite 545 pad. The filtered solution was concentrated under reduced pressure and the residue was extracted with dichloromethane three times. Combined organic layers were dried over anhydrous sodium sulfate, filtered and concentrated. The residue was purified with flash column chromatography (methanol:dichloromethane :ammonium hydroxide = 5:90:5). Removing the solvent in vacuo provided 2.17 g of (*R*)-1-benzyl-*N*-methylpyrrolidin-3-amine (98.6% yield). ¹H NMR (400 MHz, CDCl₃) δ 7.34 – 7.24 (m, 5H), 3.62 (s, 2H), 3.25 – 3.19 (m, 1H), 2.74 (dd, *J* = 9.4, 6.8 Hz, 1H), 2.64 (dt, *J* = 8.6, 6.0 Hz, 1H), 2.52 (dt, *J* = 8.4, 6.0 Hz, 1H), 2.41 – 2.37 (m, 1H), 2.38 (s, 3H), 2.19 – 2.09 (m, 1H), 2.02 (bs, 1H), 1.63 – 1.56 (m, 1H).

In the cases from **9ab** to **9c**, the desired products were synthesized from **8ab** – **8c**, respectively, instead of (*R*)-(1-benzylpyrrolidin-3-yl)carbamate **8aa** according to the aforementioned process (vide supra).

(R)-1-Benzyl-*N*-ethylpyrrolidin-3-amine, **9ab**

Yield: 1.61 g (94.0%). ¹H NMR (400 MHz, CDCl₃) δ 7.31 – 7.27 (m, 5H), 3.64 (s, 2H), 3.51 (d, *J* = 12.8 Hz, 1H), 2.67 – 2.58 (m, 2H), 2.53 – 2.50 (m, 1H), 2.29 – 2.25 (m, 2H), 2.06 – 1.95 (m, 2H), 1.69 – 1.60 (m, 2H), 1.13 – 1.04 (m, 3H).

(R)-1-Benzyl-*N*-(cyclopropylmethyl)pyrrolidin-3-amine, **9ac**

Yield: 1.68 g (64.0%). ¹H NMR (400 MHz, CDCl₃) δ 7.34 – 7.29 (m, 5H), 3.62 (d, *J* = 7.2 Hz, 2H), 3.66 – 3.33 (m, 1H), 2.80 – 2.76 (m, 1H), 2.65 – 2.55 (m, 2H), 2.44 – 2.38 (m, 2H), 2.36 – 2.32 (m, 2H), 1.61 – 1.55 (m, 2H), 0.97 – 0.93 (m, 1H), 0.51 – 0.47 (m, 2H), 0.12 – 0.09 (m, 2H).

(R)-*N*,4,4-Trimethyl-1-((*R*)-1-phenylethyl)pyrrolidin-3-amine, **9b**

Yield: 238 mg (97.9%). ¹H NMR (400 MHz, CDCl₃) δ 7.38 – 7.07 (m, 5H), 3.26 (q, *J* = 13.2, 6.4 Hz, 1H), 3.08 (q, *J* = 9.2, 7.2 Hz, 1H), 2.73 (t, *J* =

7.2 Hz, 1H), 2.37 (s, 3H), 2.36 (d, $J = 4.4$ Hz, 1H), 2.31 – 2.26 (m, 1H), 2.24 – 2.17 (m, 1H), 1.30 (d, $J = 6.4$ Hz, 3H), 1.06 (s, 3H), 0.96 (s, 3H).

(R)-*N*-Methyl-6-((*R*)-1-phenylethyl)-6-azaspiro[3.4]octan-8-amine, **9c**

Yield: 308 mg (75.0%). ^1H NMR (400 MHz, CDCl_3) δ 7.33 – 7.23 (m, 5H), 3.24 (q, $J = 6.4$ Hz, 1H), 3.03 (dd, $J = 9.6, 6.4$ Hz, 1H), 2.81 (t, $J = 6.4$ Hz, 1H), 2.66 (d, $J = 9.2$ Hz, 1H), 2.55 (d, $J = 9.2$ Hz, 1H), 2.41 (s, 3H), 2.21 (s, 1H), 2.17 (dd, $J = 9.6, 5.6$ Hz, 1H), 1.99 – 1.95 (m, 1H), 1.90 – 1.63 (m, 4H), 1.34 (d, $J = 6.4$ Hz, 4H).

Synthesis of (*R*)-*N*-(1-benzylpyrrolidin-3-yl)-*N*-methyl-7*H*-pyrrolo[2,3-*d*]pyrimidin-4-amine, **10aa**

A solution of (*R*)-1-benzyl-*N*-methylpyrrolidin-3-amine **9aa** (420 mg, 2.21 mmol) in 11.0 mL of deionized water was placed in a 50 mL round bottom flask. Consequently, 6-chloro-7-deazapurine (372 mg, 2.42 mmol) and potassium carbonate (609 mg, 4.41 mmol) were added and the mixture was refluxed for 18 hours. After the reaction, it was cooled at room temperature and the aqueous mixture was extracted with 20 mL of dichloromethane three times. Combined organic layers were dried over anhydrous sodium sulfate, filtered and concentrated. The residue was purified with flash column chromatography (methanol:dichloromethane = 2:98). Removing the solvent in vacuo provided 507 mg of (*R*)-*N*-(1-benzylpyrrolidin-3-yl)-*N*-methyl-7*H*-pyrrolo[2,3-*d*]pyrimidin-4-amine (74.8% yield). ^1H NMR (400 MHz, CDCl_3) δ 10.40 (s, 1H), 8.29 (s, 1H), 7.51 – 7.20 (m, 5H), 7.03 (s, 1H), 6.59 (d, $J = 2.2$ Hz, 1H), 5.66 (s, 1H), 3.65 (dd, $J = 62.5, 12.9$ Hz, 2H), 3.42 (s, 3H), 2.98 (dd, $J = 13.5, 7.8$ Hz, 1H), 2.83 (dd, $J = 10.3, 3.4$ Hz, 1H), 2.69 – 2.53 (m, 1H), 2.44 – 2.21 (m, 2H), 1.96 – 1.83 (m, 1H).

In the cases of **10ab**, **10ac**, **10ad**, **10b**, and **10c**, the desired products were synthesized from **9ab**, **9ac**, **7a**, **9b**, and **9c**, respectively, instead of (*R*)-1-

benzyl-*N*-methylpyrrolidin-3-amine **9aa** according to the aforementioned process (vide supra).

(R)-*N*-(1-Benzylpyrrolidin-3-yl)-*N*-ethyl-7*H*-pyrrolo[2,3-*d*]pyrimidin-4-amine, **10ab**

Yield: 296 mg (10.0%). ¹H NMR (400 MHz, CDCl₃) δ 10.84 (s, 1H), 8.31 (s, 1H), 7.39 – 7.33 (m, 5H), 7.06 (d, *J* = 3.6 Hz, 1H), 6.51 (d, *J* = 3.6 Hz, 1H), 5.57 (bs, 1H), 3.93 – 3.85 (m, 2H), 3.78 – 3.75 (m, 1H), 3.65 – 3.58 (m, 1H), 2.98 (bs, 1H), 2.84 (bs, 1H), 2.70 (bs, 1H), 2.49 – 2.33 (m, 2H), 2.01 – 1.93 (m, 1H), 1.36 (t, *J* = 7.2 Hz, 3H).

(R)-*N*-(1-Benzylpyrrolidin-3-yl)-*N*-(cyclopropylmethyl)-7*H*-pyrrolo[2,3-*d*]pyrimidin-4-amine, **10ac**

Yield: 313 mg (12.4%). ¹H NMR (400 MHz, CDCl₃) δ 9.59 – 9.54 (bs, 1H), 8.30 (s, 1H), 7.36 – 7.30 (bs, 5H), 7.03 (bs, 1H), 6.69 (bs, 1H), 5.54 (bs, 1H), 3.78 – 3.68 (m, 3H), 3.63 (bs, 1H), 3.00 (bs, 1H), 2.62 (bs, 1H), 2.39 (bs, 2H), 2.01 (bs, 1H), 1.64 (bs, 1H), 0.62 – 0.54 (m, 1H), 0.44 – 0.41 (m, 1H), 0.39 – 0.36 (m, 1H).

(R)-*N*-(1-Benzylpyrrolidin-3-yl)-7*H*-pyrrolo[2,3-*d*]pyrimidin-4-amine, **10ad**

Yield: 292 mg (58.5%). ¹H NMR (400 MHz, CDCl₃) δ 11.20 (s, 1H), 8.36 (s, 1H), 7.37 – 7.26 (m, 5H), 7.05 (d, *J* = 3.6 Hz, 1H), 6.40 (d, *J* = 3.2 Hz, 1H), 5.80 (d, *J* = 8.0 Hz, 1H), 4.89 (s, 1H), 3.71 (s, 2H), 3.02 – 3.00 (m, 1H), 2.88 (d, *J* = 8.4 Hz, 1H), 2.81 – 2.76 (m, 1H), 2.51 – 2.39 (m, 2H), 1.92 – 1.83 (m, 1H).

N-((*R*)-4,4-Dimethyl-1-((*R*)-1-phenylethyl)pyrrolidin-3-yl)-*N*-methyl-7*H*-pyrrolo[2,3-*d*]pyrimidin-4-amine, **10b**

Yield: 106 mg (30.7%). ¹H NMR (400 MHz, CDCl₃) δ 9.03 (s, 1H), 8.21 (s, 1H), 7.38 – 7.19 (m, 5H), 6.96 (q, *J* = 3.6, 2.0 Hz, 1H), 6.61 (q, *J* = 3.2, 1.6 Hz, 1H), 5.14 (d, *J* = 8.4 Hz, 1H), 3.48 (s, 3H), 3.18 (q, *J* = 13.2, 6.4 Hz, 1H), 2.98 (d, *J* = 9.2 Hz, 1H), 2.68 (d, *J* = 12.0 Hz, 1H), 2.48 (q, *J* = 11.2, 8.4 Hz, 1H), 2.10 (d, *J* = 8.8 Hz, 1H), 1.39 (d, *J* = 6.4 Hz, 3H), 1.35 (s, 3H), 0.98 (s, 3H).

N-Methyl-N-((R)-6-((R)-1-phenylethyl)-6-azaspiro[3.4]octan-8-yl)-7H-pyrrolo[2,3-d]pyrimidin-4-amine, 10c

Yield: 272 mg (60.0%). ¹H NMR (400 MHz, CDCl₃) δ 9.06 (s, 1H), 8.25 (s, 1H), 7.37 – 7.22 (m, 5H), 6.98 (dd, *J* = 3.6, 2.4 Hz, 1H), 6.61 (dd, *J* = 3.6, 2.0 Hz, 1H), 5.48 (s, 1H), 3.29 (s, 3H), 3.18 (d, *J* = 6.8 Hz, 2H), 2.65 – 2.46 (m, 4H), 1.98 – 1.91 (m, 2H), 1.87 – 1.80 (m, 2H), 1.73 – 1.69 (m, 1H), 1.40 (d, *J* = 6.4 Hz, 3H).

Synthesis of (R)-N-methyl-N-(pyrrolidin-3-yl)-7H-pyrrolo[2,3-d]pyrimidin-4-amine, 11aa

A (R)-N-(1-benzylpyrrolidin-3-yl)-N-methyl-7H-pyrrolo[2,3-d]pyrimidin-4-amine **10aa** (638 mg, 2.08 mmol) solution in 20.8 mL of methanol was placed in a 100 mL round bottom flask. Then, 10w/w% palladium on charcoal (638 mg, 5 wt%) and 10.1 g of ammonium formate (262 mg, 4.15 mmol) were added and the reaction mixture was stirred at 60 – 70 °C overnight. After the reaction, it was filtered through a celite 545 pad before the solution was concentrated under reduced pressure. The residue was purified with flash column chromatography (methanol:dichloromethane:ammonium hydroxide = 10:88:2). Removing the solvent in vacuo provided 325 mg of (R)-N-methyl-N-(pyrrolidin-3-yl)-7H-pyrrolo[2,3-d]pyrimidin-4-amine (72.0% yield). ¹H NMR (400 MHz, CDCl₃) δ 12.16 (bs, 1H), 8.33 (s, 1H), 7.09 (d, *J* = 3.5 Hz, 1H), 6.58 (d, *J* = 3.4 Hz, 1H), 5.62 – 5.42 (m, 1H), 3.42 – 3.32 (m, 3H), 3.29 (dd, *J* = 11.5, 8.4 Hz, 1H), 3.24 – 3.12 (m, 1H), 3.10 – 3.01 (m, 1H), 2.98

(dd, $J = 11.5, 6.2$ Hz, 1H), 2.66 (bs, 1H), 2.26 – 2.10 (m, 1H), 1.91 (td, $J = 14.9, 7.6$ Hz, 1H).

In the cases from **11ab** to **11c**, the desired products were synthesized from **10ab** – **10c**, respectively, instead of (*R*)-*N*-(1-benzylpyrrolidin-3-yl)-*N*-methyl-7*H*-pyrrolo[2,3-*d*]pyrimidin-4-amine **10aa** according to the aforementioned process (vide supra).

(R)-*N*-Ethyl-*N*-(pyrrolidin-3-yl)-7*H*-pyrrolo[2,3-*d*]pyrimidin-4-amine, **11ab**

Yield: 189 mg (88.8%). ^1H NMR (400 MHz, CDCl_3) δ 10.30 – 10.01 (bs, 1H), 8.31 (s, 1H), 7.09 (d, $J = 3.6$ Hz, 1H), 6.51 (d, $J = 3.6$ Hz, 1H), 5.10 – 5.04 (m, 1H), 3.81 (q, $J = 7.2$ Hz, 2H), 3.51 (s, 1H), 3.35 – 3.29 (m, 2H), 3.14 – 3.04 (m, 2H), 2.26 – 2.20 (m, 1H), 2.10 – 2.01 (m, 1H), 1.40 (t, $J = 7.2$ Hz, 3H).

(R)-*N*-(Cyclopropylmethyl)-*N*-(pyrrolidin-3-yl)-7*H*-pyrrolo[2,3-*d*]pyrimidin-4-amine, **11ac**

Yield: 162 mg (70.7%). ^1H NMR (400 MHz, CDCl_3) δ 10.40 – 10.10 (bs, 1H), 8.32 (d, $J = 4.4$ Hz, 1H), 7.10 (d, $J = 3.6$ Hz, 1H), 6.67 (d, $J = 3.6$ Hz, 1H), 4.95 – 4.91 (m, 1H), 3.76 – 3.60 (m, 2H), 3.39 – 3.34 (m, 1H), 3.26 – 3.24 (m, 2H), 3.04 – 2.97 (m, 1H), 2.24 – 2.12 (m, 2H), 1.25 – 1.13 (m, 2H), 0.69 – 0.62 (m, 2H), 0.45 – 0.39 (m, 2H).

(R)-*N*-(Pyrrolidin-3-yl)-7*H*-pyrrolo[2,3-*d*]pyrimidin-4-amine, **11ad**

Yield: 191 mg (94.8%). ^1H NMR (400 MHz, $\text{DMSO-}d_6$) δ 11.47 (s, 1H), 8.08 (s, 1H), 7.31 (d, $J = 6.8$ Hz, 1H), 7.05 (d, $J = 3.2$ Hz, 1H), 5.73 (d, $J = 3.6$ Hz, 1H), 4.63 – 4.50 (m, 1H), 3.12 – 3.07 (m, 1H), 3.02 – 2.95 (m, 1H), 2.87 – 2.81 (m, 1H), 2.75 (dd, $J = 11.2, 3.2$ Hz, 1H), 2.10 – 2.01 (m, 1H), 1.75 – 1.67 (m, 1H).

*(R)-N-(4,4-Dimethylpyrrolidin-3-yl)-N-methyl-7H-pyrrolo[2,3-
d]pyrimidin-4-amine, 11b*

Yield: 58.2 mg (79.1%). ¹H NMR (400 MHz, CDCl₃) δ 9.57 (d, *J* = 24.8 Hz, 1H), 8.24 (d, *J* = 14.8 Hz, 1H), 7.01 – 6.98 (m, 1H), 6.67 – 6.61 (m, 1H), 5.34 – 5.23 (m, 1H), 3.56 – 3.40 (m, 3H), 3.19 – 3.16 (m, 1H), 2.97 – 2.55 (m, 2H), 2.32 (s, 1H), 1.33 (d, *J* = 25.2 Hz, 3H), 0.94 (d, *J* = 12.0 Hz, 3H).

*(R)-N-Methyl-N-(6-azaspiro[3.4]octan-8-yl)-7H-pyrrolo[2,3-
d]pyrimidin-4-amine, 11c*

Yield: 163 mg (84.5%). ¹H NMR (400 MHz, CDCl₃) δ 10.62 (s, 1H), 8.29 (s, 1H), 7.07 (d, *J* = 3.6 Hz, 1H), 6.62 (d, *J* = 4.0 Hz, 1H), 5.40 (s, 1H), 3.43 (dd, *J* = 12.4, 8.4 Hz, 1H), 3.30 (s, 3H), 3.26 – 3.19 (m, 2H), 3.09 (dd, *J* = 12.4, 5.2 Hz, 1H), 2.37 – 2.32 (m, 2H), 2.03 (d, *J* = 7.2 Hz, 1H), 1.95 – 1.88 (m, 2H), 1.86 – 1.81 (m, 2H).

*Syntheses of (R)-3-(3-(methyl(7H-pyrrolo[2,3-d]pyrimidin-4-
yl)amino)pyrrolidin-1-yl)-3-oxopropanenitrile, 12a*

To an *(R)-N-methyl-N-(pyrrolidin-3-yl)-7H-pyrrolo[2,3-d]pyrimidin-4-amine 11aa* (103 mg, 0.474 mmol) solution in 4.70 mL of *n*-butanol in a 10 mL round bottom flask, ethyl cyanoacetate (0.505 mL, 4.75 mmol) and 1,8-diazabicyclo[5.4.0]undec-7-ene (0.0355 mL, 0.237 mmol) were added and the mixture was heated at 80 °C for 24 hours. The reaction solution was concentrated under reduced pressure and the residue was purified with flash column chromatography (methanol:dichloromethane = 2:98). Removing the solvent in vacuo provided 101 mg of *(R)-3-(3-(methyl(7H-pyrrolo[2,3-d]pyrimidin-4-yl)amino)pyrrolidin-1-yl)-3-oxopropanenitrile* (74.8% yield). 98.7% purity by HPLC.

¹H NMR (400 MHz, CDCl₃) δ 10.98 (s, 1H), 8.33 (s, 1H), 7.13 (d, *J* = 3.6 Hz, 1H), 6.60 (d, *J* = 3.6 Hz, 1H), 5.76 (m, 1H), 3.90 (dt, *J* = 14.9, 8.0 Hz, 1H), 3.70 (ddd, *J* = 26.4, 16.1, 8.3 Hz, 1H), 3.51 (m, 4H), 3.35 (d, *J* = 14.8 Hz,

3H), 2.27 (m, 2H). ^{13}C NMR (100 MHz, CDCl_3) δ 160.3, 157.8, 152.3, 150.9, 120.9, 113.8, 103.6, 102.1, 55.0, 48.0, 45.2, 32.5, 26.9, 26.0. HRMS (ESI) calcd for $\text{C}_{14}\text{H}_{17}\text{N}_6\text{O}$: 285.1464. Obsd: 285.1452. $[\alpha]_{\text{D}} +42.6^\circ$ (c 1.00, CHCl_3).

In the cases of **12b**, **12c**, **13**, and **14**, the desired products were synthesized from **11b**, **11c**, **11ab**, and **11ac**, respectively, instead of (*R*)-*N*-methyl-*N*-(pyrrolidin-3-yl)-7*H*-pyrrolo[2,3-*d*]pyrimidin-4-amine **11aa** according to the aforementioned process (vide supra).

(R)-3-(3,3-Dimethyl-4-(methyl(7*H*-pyrrolo[2,3-*d*]pyrimidin-4-yl)amino)pyrrolidin-1-yl)-3-oxopropanenitrile, **12b**

Yield: 41.4 mg (57.1%). 97.7% purity by HPLC. ^1H NMR (400 MHz, CDCl_3) δ 12.19 (s, 1H), 8.31 (s, 1H), 7.14 (s, 1H), 6.61 (s, 1H), 5.69 (dd, J = 39.2, 6.0 Hz, 1H), 4.03 (m, 1H), 3.82 (dd, J = 34.5, 12.6 Hz, 1H), 3.54 (m, 3H), 3.41 (m, 1H), 3.34 (d, J = 10.4 Hz, 3H), 1.25 (d, J = 2.8 Hz, 3H), 1.04 (m, 3H). ^{13}C NMR (100 MHz, CDCl_3) δ 160.4, 158.0, 152.3, 150.3, 120.8, 113.9, 103.1, 102.2, 62.2, 59.9, 49.1, 44.6, 33.9, 28.1, 26.0, 21.6. HRMS (ESI) calcd for $\text{C}_{16}\text{H}_{21}\text{N}_6\text{O}$: 313.1777. Obsd: 313.1772. $[\alpha]_{\text{D}} -8.93^\circ$ (c 0.864, CHCl_3).

(R)-3-(8-(Methyl(7*H*-pyrrolo[2,3-*d*]pyrimidin-4-yl)amino)-6-azaspiro[3.4]octan-6-yl)-3-oxopropanenitrile, **12c**

Yield: 23.7 mg (19.0%). 95.0% purity by HPLC. ^1H NMR (400 MHz, CDCl_3) δ 11.84 (s, 1H), 8.36 (s, 1H), 7.15 (s, 1H), 6.62 (s, 1H), 5.96 (dd, J = 19.0, 6.3 Hz, 1H), 3.94 (ddd, J = 39.2, 19.0, 12.0 Hz, 2H), 3.73 (m, 2H), 3.50 (d, J = 5.8 Hz, 2H), 3.28 (d, J = 4.9 Hz, 3H), 2.23 (m, 1H), 1.99 (m, 5H). ^{13}C NMR (100 MHz, CDCl_3) δ 160.0, 158.2, 152.4, 150.6, 120.8, 113.7, 103.1, 102.3, 62.0, 58.9, 49.9, 47.7, 35.7, 33.6, 26.4, 26.0, 16.3. HRMS (ESI) calcd for $\text{C}_{17}\text{H}_{21}\text{N}_6\text{O}$: 325.1777. Obsd: 325.1770. $[\alpha]_{\text{D}} +7.04^\circ$ (c 0.557, CHCl_3).

(R)-3-(3-(Ethyl(7*H*-pyrrolo[2,3-*d*]pyrimidin-4-yl)amino)pyrrolidin-1-yl)-3-oxopropanenitrile, **13**

Yield: 50.9 mg (55.0%). 96.1% purity by HPLC. ¹H NMR (400 MHz, DMSO-*d*₆) δ 11.66 (s, 1H), 8.11 (d, *J* = 2.5 Hz, 1H), 7.16 (s, 1H), 6.48 (m, 1H), 5.35 (ddd, *J* = 54.1, 16.5, 8.3 Hz, 1H), 3.95 (dd, *J* = 19.0, 8.5 Hz, 1H), 3.87 (dd, *J* = 18.9, 3.9 Hz, 1H), 3.70 (m, 1H), 3.62 (dd, *J* = 9.2, 6.9 Hz, 3H), 3.45 (dd, *J* = 17.5, 8.8 Hz, 1H), 3.24 (m, 1H), 2.16 (m, 1H), 2.07 (m, 1H), 1.19 (dd, *J* = 11.2, 6.1 Hz, 3H). ¹³C NMR (100 MHz, DMSO-*d*₆) δ 161.3, 156.1, 151.8, 150.5, 121.5, 116.0, 101.7, 101.1, 54.4, 47.4, 44.2, 28.5, 26.8, 25.5, 15.7. HRMS (ESI) calcd for C₁₅H₁₉N₆O: 299.1620. Obsd: 299.1617. [α]_D +78.5° (*c* 1.09, DMSO).

(R)-3-(3-((Cyclopropylmethyl)(7*H*-pyrrolo[2,3-*d*]pyrimidin-4-yl)amino)pyrrolidin-1-yl)-3-oxopropanenitrile, **14**

Yield: 38.4 mg (54.0%). 95.3% purity by HPLC. ¹H NMR (400 MHz, CDCl₃) δ 12.03 (d, *J* = 14.0 Hz, 1H), 8.35 (d, *J* = 5.1 Hz, 1H), 7.17 (d, *J* = 5.0 Hz, 1H), 6.67 (m, 1H), 5.30 (ddt, *J* = 25.0, 16.8, 8.3 Hz, 1H), 3.93 (m, 2H), 3.63 (m, 3H), 3.49 (m, 3H), 2.33 (ddt, *J* = 17.5, 12.0, 9.6 Hz, 2H), 1.18 (m, 1H), 0.69 (t, *J* = 8.9 Hz, 2H), 0.36 (m, 2H). ¹³C NMR (100 MHz, CDCl₃) δ 160.3, 157.1, 152.3, 150.4, 121.4, 114.0, 103.2, 101.8, 56.6, 50.4, 48.9, 45.1, 29.6, 26.0, 11.9, 5.1, 4.9. HRMS (ESI) calcd for C₁₇H₂₁N₆O: 325.1777. Obsd: 325.1775. [α]_D +24.5° (*c* 1.08, CHCl₃).

Synthesis of (R)-3-((3-(methyl(7*H*-pyrrolo[2,3-*d*]pyrimidin-4-yl)amino)pyrrolidin-1-yl)sulfonyl)benzonitrile, **16**

To an (*R*)-*N*-methyl-*N*-(pyrrolidin-3-yl)-7*H*-pyrrolo[2,3-*d*]pyrimidin-4-amine **11aa** (70.0 mg, 0.322 mmol) solution in 1.50 mL of dichloromethane in a 5 mL round bottom flask, 3-cyanobenzenesulfonyl chloride (68.6 mg, 0.340 mmol) and *N,N*-diisopropylethylamine (0.0590 mL, 0.339 mmol) were

added. Then, the reaction solution was stirred at room temperature overnight before being concentrated under reduced pressure. The residue was purified by flash column chromatography (methanol:dichloromethane=2:98). Removing the solvent in vacuo provided 88.6 mg of (*R*)-3-((3-(methyl(7*H*-pyrrolo[2,3-*d*]pyrimidin-4-yl)amino)pyrrolidin-1-yl)sulfonyl)benzonitrile (72.4% yield). 97.0% purity by HPLC.

¹H NMR (400 MHz, DMSO-*d*6) δ 11.68 (s, 1H), 8.32 (d, *J* = 7.8 Hz, 1H), 8.23 (d, *J* = 7.7 Hz, 1H), 8.17 (d, *J* = 8.0 Hz, 1H), 8.06 (t, *J* = 4.6 Hz, 1H), 7.88 (td, *J* = 7.8, 2.2 Hz, 1H), 7.14 (d, *J* = 2.1 Hz, 1H), 6.48 (s, 1H), 5.27 (m, 1H), 3.51 (dd, *J* = 7.6, 4.4 Hz, 1H), 3.44 (m, 1H), 3.36 (s, 3H), 3.23 (m, 1H), 3.17 (s, 1H), 2.03 (dd, *J* = 15.0, 7.6 Hz, 2H). ¹³C NMR (100 MHz, DMSO-*d*6) δ 156.8, 151.7, 150.4, 137.1, 136.8, 131.9, 131.0, 130.9, 121.2, 117.6, 112.9, 102.5, 101.3, 54.0, 48.7, 46.8, 31.7, 27.5. HRMS (ESI) calcd for C₁₈H₁₉N₆O₂S: 383.1290. Obsd: 383.1285. [α]_D -45.7° (*c* 0.530, CHCl₃).

In the cases of **15**, **17**, and **18**, the desired products were synthesized from **11ad**, **11ab**, and **11ac**, respectively, instead of (*R*)-*N*-methyl-*N*-(pyrrolidin-3-yl)-7*H*-pyrrolo[2,3-*d*]pyrimidin-4-amine **11aa** according to the aforementioned process (vide supra).

(R)-3-((3-((7*H*-Pyrrolo[2,3-*d*]pyrimidin-4-yl)amino)pyrrolidin-1-yl)sulfonyl)benzonitrile, **15**

Yield: 42.0 mg (38.2%). 97.6% purity by HPLC. ¹H NMR (400 MHz, DMSO-*d*6) δ 11.49 (s, 1H), 8.14 (s, 1H), 8.06 (s, 1H), 7.98 (d, *J* = 7.7 Hz, 1H), 7.92 (d, *J* = 7.5 Hz, 1H), 7.58 (t, *J* = 7.7 Hz, 1H), 7.13 (d, *J* = 4.1 Hz, 1H), 7.03 (s, 1H), 6.36 (s, 1H), 4.38 (d, *J* = 4.3 Hz, 1H), 3.49 (m, 2H), 3.31 (m, 1H), 3.25 (m, 1H), 2.06 (dd, *J* = 12.3, 6.2 Hz, 1H), 1.88 (m, 1H). ¹³C NMR (100 MHz, DMSO-*d*6) δ 155.2, 151.1, 150.2, 137.2, 136.4, 131.6, 130.7, 130.4, 121.0, 117.5, 112.7, 102.6, 98.7, 53.3, 50.0, 46.7, 30.3. HRMS (ESI) calcd for C₁₇H₁₇N₆O₂S: 369.1134. Obsd: 369.1128. [α]_D -27.4° (*c* 1.09, DMSO).

(R)-3-((3-(*Ethyl*(7*H*-pyrrolo[2,3-*d*]pyrimidin-4-yl)amino)pyrrolidin-1-yl)sulfonyl)benzonitrile, **17**

Yield: 84.3 mg (73.3%). 95.1% purity by HPLC. ¹H NMR (400 MHz, CDCl₃) δ 11.64 (s, 1H), 8.17 (d, *J* = 14.8 Hz, 2H), 8.11 (d, *J* = 7.9 Hz, 1H), 7.92 (d, *J* = 7.6 Hz, 1H), 7.72 (t, *J* = 7.8 Hz, 1H), 7.13 (d, *J* = 3.0 Hz, 1H), 6.42 (d, *J* = 3.0 Hz, 1H), 5.23 (m, 1H), 3.71 (m, 4H), 3.33 (m, 1H), 3.26 (m, 1H), 2.20 (m, 2H), 1.34 (t, *J* = 6.9 Hz, 3H). ¹³C NMR (100 MHz, CDCl₃) δ 156.5, 152.1, 150.4, 138.6, 136.1, 131.7, 131.2, 130.4, 121.2, 117.4, 114.0, 102.7, 101.5, 55.6, 49.5, 47.0, 40.6, 28.9, 16.0. HRMS (ESI) calcd for C₁₉H₂₁N₆O₂S: 397.1447. Obsd: 397.1442. [α]_D -63.5° (c 0.568, CHCl₃).

(R)-3-((3-((Cyclopropylmethyl)(7*H*-pyrrolo[2,3-*d*]pyrimidin-4-yl)amino)pyrrolidin-1-yl)sulfonyl)benzonitrile, **18**

Yield: 62.2 mg (61.0%). 95.0% purity by HPLC. ¹H NMR (400 MHz, CDCl₃) δ 11.91 (s, 1H), 8.19 (s, 1H), 8.11 (d, *J* = 7.7 Hz, 1H), 8.04 (s, 1H), 7.93 (d, *J* = 7.4 Hz, 1H), 7.73 (t, *J* = 7.3 Hz, 1H), 7.15 (s, 1H), 6.60 (s, 1H), 5.05 (m, 1H), 3.66 (m, 2H), 3.60 (d, *J* = 4.9 Hz, 2H), 3.48 (m, 1H), 3.31 (dd, *J* = 15.4, 7.6 Hz, 1H), 2.26 (d, *J* = 7.2 Hz, 2H), 1.12 (s, 1H), 0.65 (d, *J* = 2.7 Hz, 2H), 0.33 (d, *J* = 2.1 Hz, 2H). ¹³C NMR (100 MHz, CDCl₃) δ 156.6, 152.0, 149.9, 138.3, 136.0, 131.8, 131.3, 130.3, 121.2, 117.4, 113.9, 103.2, 101.8, 56.9, 51.3, 49.7, 47.4, 29.2, 11.7, 4.8. HRMS (ESI) calcd for C₂₁H₂₃N₆O₂S: 423.1603. Obsd: 423.1598. [α]_D -31.5° (c 1.49, CHCl₃).

Synthesis of (R)-3-(3-(methyl(7*H*-pyrrolo[2,3-*d*]pyrimidin-4-yl)amino)pyrrolidin-1-yl)propanenitrile, **69**

To an (*R*)-*N*-methyl-*N*-(pyrrolidin-3-yl)-7*H*-pyrrolo[2,3-*d*]pyrimidin-4-amine **11aa** (60.0 mg, 0.276 mmol) solution in 1.00 mL of dichloromethane in a 5 mL round-bottom flask, 3-bromopropionitrile (0.0240 mL, 0.289 mmol)

and *N,N*-diisopropylethylamine (0.0720 mL, 0.413 mmol) were added. The reaction mixture was stirred at room temperature overnight and then concentrated under reduced pressure. The residue was purified by column chromatography (methanol:dichloromethane=2:98). Removing the solvent in vacuo provided 55.3 mg of (*R*)-3-(3-(methyl(7*H*-pyrrolo[2,3-*d*]pyrimidin-4-yl)amino)pyrrolidin-1-yl)propanenitrile (74.7% yield). 100% purity by HPLC.

¹H NMR (400 MHz, CDCl₃) δ 12.32 (s, 1H), 8.32 (s, 1H), 7.10 (d, *J* = 3.4 Hz, 1H), 6.58 (d, *J* = 3.3 Hz, 1H), 5.73 (s, 1H), 3.42 (s, 3H), 3.06 (t, *J* = 7.1 Hz, 1H), 2.94 (dd, *J* = 9.9, 3.1 Hz, 1H), 2.83 (m, 1H), 2.72 (m, 1H), 2.64 (t, *J* = 9.2 Hz, 1H), 2.56 (t, *J* = 6.8 Hz, 2H), 2.34 (m, 2H), 1.93 (dt, *J* = 13.0, 10.0 Hz, 1H). ¹³C NMR (100 MHz, CDCl₃) δ 157.6, 151.8, 150.6, 120.4, 118.8, 103.1, 102.1, 57.2, 54.4, 53.7, 50.8, 32.4, 29.3, 17.7. HRMS (ESI) calcd for C₁₄H₁₉N₆: 271.1671. Obsd: 271.1665. [α]_D +35.3° (*c* 1.07, CHCl₃).

In the cases of compound **70**, the desired products were synthesized through substitution reactions with *n*-butyl bromide instead of 3-bromopropionitrile according to the aforementioned process (vide supra).

(R)-*N*-(1-Butylpyrrolidin-3-yl)-*N*-methyl-7*H*-pyrrolo[2,3-*d*]pyrimidin-4-amine, **70**

Yield: 90.0 mg (83.3%). 100% purity by HPLC. ¹H NMR (400 MHz, DMSO-*d*₆) δ 11.69 (s, 1H), 8.11 (s, 1H), 7.11 (d, *J* = 3.1 Hz, 1H), 6.58 (d, *J* = 3.2 Hz, 1H), 5.53 (dt, *J* = 15.1, 7.7 Hz, 1H), 3.25 (s, 4H), 3.08 (m, 2H), 2.81 (m, 3H), 2.16 (m, 1H), 1.95 (m, 1H), 1.50 (dt, *J* = 15.2, 7.4 Hz, 2H), 1.25 (dq, *J* = 14.5, 7.3 Hz, 2H), 0.82 (t, *J* = 7.3 Hz, 3H). ¹³C NMR (100 MHz, DMSO-*d*₆) δ 156.7, 151.6, 150.4, 121.1, 102.5, 101.5, 54.5, 54.3, 53.7, 52.9, 32.7, 28.2, 27.1, 19.7, 13.6. HRMS (ESI) calcd for C₁₅H₂₄N₅: 274.2032. Obsd: 274.2027. [α]_D +10.6° (*c* 3.42, DMSO).

Synthesis of (R)-2-azido-1-(3-(methyl(7H-pyrrolo[2,3-d]pyrimidin-4-yl)amino)pyrrolidin-1-yl)ethan-1-one, 71

To a 2-azidoacetic acid (247 mg, 2.44 mmol) solution in 8.0 mL of *N,N*-dimethylformamide in a 25 mL round-bottom flask, *N,N'*-dicyclohexylcarbodiimide (503 mg, 2.44 mmol) and *N,N*-diisopropylethylamine (0.850 mL, 4.88 mmol) were added and the reaction mixture was stirred for 15 minutes. In a second 25 mL round-bottom flask, (*R*)-*N*-methyl-*N*-(pyrrolidin-3-yl)-7*H*-pyrrolo[2,3-*d*]pyrimidin-4-amine **11aa** (265 mg, 1.22 mmol) was placed and the reaction mixture of 2-azidoacetic acid was transferred to this second flask. The reaction mixture was refluxed overnight and then cooled at room temperature. The mixture was filtered through a celite 545 pad and the solution was concentrated under reduced pressure. The residue was purified with column chromatography (methanol:dichloromethane=2:98). Removing the solvent in vacuo provided 41.0 mg of (*R*)-2-azido-1-(3-(methyl(7*H*-pyrrolo[2,3-*d*]pyrimidin-4-yl)amino)pyrrolidin-1-yl)ethan-1-one (5.27% yield). 96.2% purity by HPLC.

¹H NMR (400 MHz, CDCl₃) δ 11.97 (d, *J* = 32.0 Hz, 1H), 8.34 (d, *J* = 1.9 Hz, 1H), 7.15 (dd, *J* = 6.5, 3.6 Hz, 1H), 6.59 (s, 1H), 5.75 (m, 1H), 3.92 (m, 3H), 3.79 (dd, *J* = 19.2, 10.6 Hz, 1H), 3.57 (tt, *J* = 11.9, 8.2 Hz, 2H), 3.34 (m, 3H), 2.21 (m, 2H). ¹³C NMR (100 MHz, CDCl₃) δ 166.2, 157.8, 152.3, 150.7, 121.1, 103.6, 101.8, 55.0, 51.3, 46.7, 44.6, 32.3, 26.7. HRMS (ESI) calcd for C₁₃H₁₇N₈O: 301.1525. Obsd: 301.1522. [α]_D +33.2° (*c* 0.753, CHCl₃).

Synthesis of (R)-3-methyl-1-(3-(methyl(7H-pyrrolo[2,3-d]pyrimidin-4-yl)amino)pyrrolidin-1-yl)butan-1-one, 72

To an (*R*)-*N*-methyl-*N*-(pyrrolidin-3-yl)-7*H*-pyrrolo[2,3-*d*]pyrimidin-4-amine **11aa** (70.0 mg, 0.322 mmol) solution in 1.00 mL of dichloromethane in a 5 mL round-bottom flask, isovaleryl chloride (38.8 mg, 0.322 mmol) and *N,N*-diisopropylethylamine (0.0590 mL, 0.339 mmol) were added. The reaction

mixture was stirred at room temperature overnight and then concentrated under reduced pressure. The residue was purified by column chromatography (methanol:dichloromethane=2:98). Removing the solvent in vacuo provided 66.7 mg of (*R*)-3-methyl-1-(3-(methyl(7*H*-pyrrolo[2,3-*d*]pyrimidin-4-yl)amino)pyrrolidin-1-yl)butan-1-one (68.7% yield). 98.7% purity by HPLC.

¹H NMR (400 MHz, CDCl₃) δ 11.67 (s, 1H), 8.38 (s, 1H), 7.14 (s, 1H), 6.60 (s, 1H), 5.72 (m, 1H), 3.81 (m, 2H), 3.49 (m, 2H), 3.34 (d, *J* = 11.5 Hz, 3H), 2.18 (m, 4H), 1.50 (d, *J* = 35.8 Hz, 1H), 0.94 (d, *J* = 44.9 Hz, 6H). ¹³C NMR (100 MHz, CDCl₃) δ 171.6, 157.7, 151.9, 150.2, 121.1, 103.5, 101.7, 54.9, 47.8, 45.4, 43.8, 32.1, 29.7, 25.5, 22.8. HRMS (ESI) calcd for C₁₆H₂₄N₅O: 302.1981. Obsd: 302.1977. [α]_D +29.6° (*c* 1.47, CHCl₃).

Synthesis of isobutyl (R)-3-(methyl(7H-pyrrolo[2,3-d]pyrimidin-4-yl)amino)pyrrolidine-1-carboxylate, 73

To an (*R*)-*N*-methyl-*N*-(pyrrolidin-3-yl)-7*H*-pyrrolo[2,3-*d*]pyrimidin-4-amine **11aa** (70.0 mg, 0.322 mmol) solution in 1.00 mL of dichloromethane in a 5 mL round-bottom flask, isobutyl chloroformate (44.0 mg, 0.322 mmol) and *N,N*-diisopropylethylamine (0.0560 mL, 0.321 mmol) were added. The reaction solution was stirred at room temperature overnight and then concentrated under reduced pressure. The residue was purified by column chromatography (methanol:dichloromethane=2:98). Removing the solvent in vacuo provided 41.0 mg of isobutyl (*R*)-3-(methyl(7*H*-pyrrolo[2,3-*d*]pyrimidin-4-yl)amino)pyrrolidine-1-carboxylate (40.2% yield). 97.7% purity by HPLC.

¹H NMR (400 MHz, CDCl₃) δ 11.83 (s, 1H), 8.33 (s, 1H), 7.11 (d, *J* = 2.8 Hz, 1H), 6.58 (d, *J* = 3.3 Hz, 1H), 5.72 (d, *J* = 6.3 Hz, 1H), 3.90 (d, *J* = 6.5 Hz, 2H), 3.76 (d, *J* = 9.2 Hz, 1H), 3.69 (m, 1H), 3.45 (m, 2H), 3.33 (s, 3H), 2.15 (dd, *J* = 21.9, 12.3 Hz, 2H), 1.95 (d, *J* = 6.1 Hz, 1H), 0.94 (d, *J* = 6.2 Hz, 6H). ¹³C NMR (100 MHz, CDCl₃) δ 157.9, 155.5, 152.0, 150.6, 120.8, 103.4,

102.0, 71.5, 54.7, 46.8, 44.8, 32.0, 28.2, 19.2, 9.5. HRMS (ESI) calcd for $C_{16}H_{24}N_5O_2$: 318.1930. Obsd: 318.1924. $[\alpha]_D +23.7^\circ$ (c 0.550, $CHCl_3$).

Synthesis of (R)-3-(methyl(7H-pyrrolo[2,3-d]pyrimidin-4-yl)amino)-N-phenylpyrrolidine-1-carboxamide, 74

To an (R)-N-methyl-N-(pyrrolidin-3-yl)-7H-pyrrolo[2,3-d]pyrimidin-4-amine **11aa** (70.0 mg, 0.322 mmol) solution in 1.00 mL of dichloromethane in a 5 mL round-bottom flask, *N,N*-diisopropylethylamine (0.0590 mL, 0.339 mmol) was added and the mixture was treated with phenyl isocyanate (0.0350 mL, 0.322 mmol). The reaction solution was stirred for 2 hours before being concentrated under reduced pressure. The residue was purified by column chromatography (methanol:dichloromethane = 2:98). Removing the solvent in vacuo provided 81.5 mg of (R)-3-(methyl(7H-pyrrolo[2,3-d]pyrimidin-4-yl)amino)-N-phenylpyrrolidine-1-carboxamide (75.4% yield). 99.8% purity by HPLC.

1H NMR (400 MHz, DMSO-*d*6) δ 11.72 (s, 1H), 8.22 (s, 1H), 8.18 (s, 1H), 7.54 (d, J = 8.1 Hz, 2H), 7.23 (t, J = 7.8 Hz, 2H), 7.18 (d, J = 2.3 Hz, 1H), 6.92 (t, J = 7.2 Hz, 1H), 6.64 (d, J = 3.1 Hz, 1H), 5.56 (m, 1H), 3.75 (m, 1H), 3.67 (m, 1H), 3.45 (m, 2H), 3.25 (s, 3H), 2.16 (m, 2H). ^{13}C NMR (100 MHz, DMSO-*d*6) δ 157.1, 154.1, 151.8, 150.6, 140.5, 128.3, 121.7, 121.1, 119.5, 102.6, 101.6, 54.2, 46.8, 44.4, 31.6, 27.6. HRMS (ESI) calcd for $C_{18}H_{21}N_6O$: 337.1777. Obsd: 337.1772. $[\alpha]_D +43.6^\circ$ (c 2.44, DMSO).

Synthesis of (R)-N-methyl-N-(1-(methanesulfonyl)pyrrolidin-3-yl)-7H-pyrrolo[2,3-d]pyrimidin-4-amine, 75

To an (R)-N-methyl-N-(pyrrolidin-3-yl)-7H-pyrrolo[2,3-d]pyrimidin-4-amine **11aa** (70.0 mg, 0.322 mmol) solution in 1.00 mL of dichloromethane in a 5 mL round bottom flask, methanesulfonyl chloride (36.9 mg, 0.322 mmol) and *N,N*-diisopropylethylamine (0.0590 mL, 0.339 mmol) were added. Then,

the reaction solution was stirred at room temperature overnight before being concentrated under reduced pressure. The residue was purified by flash column chromatography (methanol:dichloromethane=2:98). Removing the solvent in vacuo provided 40.0 mg of (*R*)-*N*-methyl-*N*-(1-(methylsulfonyl)pyrrolidin-3-yl)-7*H*-pyrrolo[2,3-*d*]pyrimidin-4-amine (42.1% yield). 96.9% purity by HPLC.

¹H NMR (400 MHz, DMSO-*d*₆) δ 11.70 (s, 1H), 8.15 (d, *J* = 1.3 Hz, 1H), 7.17 (d, *J* = 2.9 Hz, 1H), 6.62 (d, *J* = 2.7 Hz, 1H), 5.58 (m, 1H), 3.52 (t, *J* = 9.0 Hz, 1H), 3.46 (m, 1H), 3.31 (dd, *J* = 17.4, 8.7 Hz, 1H), 3.23 (dd, *J* = 10.0, 4.4 Hz, 4H), 2.98 (d, *J* = 1.3 Hz, 3H), 2.14 (m, 2H). ¹³C NMR (100 MHz, DMSO-*d*₆) δ 157.0, 151.8, 150.5, 121.1, 102.6, 101.5, 54.2, 48.4, 46.3, 33.4, 31.8, 27.9. HRMS (ESI) calcd for C₁₂H₁₈N₅O₂S: 296.1181. Obsd: 296.1175. [α]_D +23.0° (c 1.20, DMSO).

In the cases from **76** to **96**, the desired products were synthesized through substitution reactions with trifluoromethanesulfonyl chloride, ethanesulfonyl chloride, 2-propanesulfonyl chloride, 1-propanesulfonyl chloride, 1-methyl-1*H*-imidazole-4-sulfonyl chloride, benzenesulfonyl chloride, 2-fluorobenzene-1-sulfonyl chloride, 3-fluorobenzene-1-sulfonyl chloride, 4-fluorobenzenesulfonyl chloride, 2-cyanobenzenesulfonyl chloride, 4-cyanobenzenesulfonyl chloride, 2-nitrobenzenesulfonyl chloride, 3-nitrobenzenesulfonyl chloride, 4-nitrobenzenesulfonyl chloride, 3-toluenesulfonyl chloride, 4-toluenesulfonyl chloride, 4-methoxybenzenesulfonyl chloride, 4-(trifluoromethyl)benzenesulfonyl chloride, 2-naphthalenesulfonyl chloride, piperidine-1-sulfonyl chloride, and morpholine-4-sulfonyl chloride, respectively, instead of methanesulfonyl chloride according to the aforementioned process (vide supra).

(R)-*N*-Methyl-*N*-(1-((trifluoromethyl)sulfonyl)pyrrolidin-3-yl)-7*H*-pyrrolo[2,3-*d*]pyrimidin-4-amine, **76**

Yield: 72.0 mg (64.3%). 97.4% purity by HPLC. ^1H NMR (400 MHz, CDCl_3) δ 12.77 (s, 1H), 8.37 (d, $J = 8.8$ Hz, 1H), 7.18 (m, 1H), 6.59 (m, 1H), 5.84 (m, 1H), 3.89 (m, 2H), 3.62 (m, 1H), 3.53 (m, 1H), 3.36 (d, $J = 8.7$ Hz, 3H), 2.29 (dd, $J = 17.0, 8.6$ Hz, 2H). ^{13}C NMR (100 MHz, CDCl_3) δ 157.6, 152.2, 150.3, 121.3, 120.4 (q, $J = 323.8$ Hz), 103.7, 101.6, 54.7, 48.9, 47.7, 32.4, 28.5. HRMS (ESI) calcd for $\text{C}_{12}\text{H}_{15}\text{F}_3\text{N}_5\text{O}_2\text{S}$: 350.0899. Obsd: 350.0893. $[\alpha]_{\text{D}} +19.4^\circ$ (c 2.79, CHCl_3).

(R)-N-(1-(Ethylsulfonyl)pyrrolidin-3-yl)-N-methyl-7H-pyrrolo[2,3-d]pyrimidin-4-amine, 77

Yield: 53.4 mg (53.6%). 98.2% purity by HPLC. ^1H NMR (400 MHz, CDCl_3) δ 11.30 (s, 1H), 8.34 (s, 1H), 7.13 (s, 1H), 6.61 (s, 1H), 5.80 (m, 1H), 3.70 (dd, $J = 19.4, 10.1$ Hz, 2H), 3.43 (d, $J = 10.3$ Hz, 2H), 3.38 (s, 3H), 3.08 (q, $J = 7.3$ Hz, 2H), 2.28 (s, 1H), 2.19 (m, 1H), 1.43 (t, $J = 7.3$ Hz, 3H). ^{13}C NMR (100 MHz, CDCl_3) δ 157.6, 151.6, 149.9, 121.1, 103.8, 102.0, 54.9, 48.6, 46.6, 44.6, 29.8, 28.8, 8.1. HRMS (ESI) calcd for $\text{C}_{13}\text{H}_{20}\text{N}_5\text{O}_2\text{S}$: 310.1338. Obsd: 310.1335. $[\alpha]_{\text{D}} +13.1^\circ$ (c 1.24, CHCl_3).

(R)-N-(1-(Isopropylsulfonyl)pyrrolidin-3-yl)-N-methyl-7H-pyrrolo[2,3-d]pyrimidin-4-amine, 78

Yield: 36.0 mg (34.6%). 99.1% purity by HPLC. ^1H NMR (400 MHz, CDCl_3) δ 12.23 (s, 1H), 8.35 (s, 1H), 7.14 (d, $J = 3.2$ Hz, 1H), 6.59 (d, $J = 2.6$ Hz, 1H), 5.78 (m, 1H), 3.75 (m, 2H), 3.46 (m, 2H), 3.36 (s, 3H), 3.28 (dt, $J = 13.6, 6.8$ Hz, 1H), 2.26 (m, 1H), 2.16 (m, 1H), 1.41 (d, $J = 6.8$ Hz, 6H). ^{13}C NMR (100 MHz, CDCl_3) δ 157.8, 152.2, 150.6, 120.9, 103.5, 101.9, 55.0, 53.6, 49.0, 47.2, 32.3, 28.9, 16.8. HRMS (ESI) calcd for $\text{C}_{14}\text{H}_{22}\text{N}_5\text{O}_2\text{S}$: 324.1494. Obsd: 324.1487. $[\alpha]_{\text{D}} +18.2^\circ$ (c 0.950, CHCl_3).

(R)-N-Methyl-N-(1-(propylsulfonyl)pyrrolidin-3-yl)-7H-pyrrolo[2,3-d]pyrimidin-4-amine, 79

Yield: 49.0 mg (54.9%). 97.1% purity by HPLC. ¹H NMR (400 MHz, CDCl₃) δ 12.36 (s, 1H), 8.34 (s, 1H), 7.15 (s, 1H), 6.58 (s, 1H), 5.78 (m, 1H), 3.67 (m, 2H), 3.41 (d, *J* = 9.3 Hz, 2H), 3.36 (s, 3H), 3.01 (m, 2H), 2.27 (s, 1H), 2.19 (m, 1H), 1.90 (dd, *J* = 14.5, 7.2 Hz, 2H), 1.09 (t, *J* = 7.1 Hz, 3H). ¹³C NMR (100 MHz, CDCl₃) δ 157.7, 152.1, 150.5, 121.0, 103.5, 101.8, 54.8, 51.5, 48.5, 46.5, 32.3, 28.7, 17.1, 13.3. HRMS (ESI) calcd for C₁₄H₂₂N₅O₂S: 324.1494. Obsd: 324.1488. [α]_D +11.3° (*c* 1.52, CHCl₃).

(R)-N-Methyl-N-(1-((1-methyl-1H-imidazol-4-yl)sulfonyl)pyrrolidin-3-yl)-7H-pyrrolo[2,3-d]pyrimidin-4-amine, 80

Yield: 17.0 mg (22.4%). 98.4% purity by HPLC. ¹H NMR (400 MHz, DMSO-*d*₆) δ 11.70 (s, 1H), 8.10 (s, 1H), 7.89 (s, 2H), 7.16 (s, 1H), 6.52 (s, 1H), 5.31 (dd, *J* = 15.6, 7.8 Hz, 1H), 3.74 (s, 3H), 3.50 (m, 2H), 3.27 (m, 2H), 3.12 (s, 3H), 1.99 (dd, *J* = 15.6, 8.0 Hz, 2H). ¹³C NMR (100 MHz, DMSO-*d*₆) δ 156.8, 151.6, 150.3, 140.2, 135.8, 126.1, 121.2, 102.4, 101.4, 54.2, 48.7, 46.9, 33.6, 31.4, 27.7. HRMS (ESI) calcd for C₁₅H₂₀N₇O₂S: 362.1399. Obsd: 362.1393. [α]_D +12.5° (*c* 0.477, DMSO).

(R)-N-Methyl-N-(1-(phenylsulfonyl)pyrrolidin-3-yl)-7H-pyrrolo[2,3-d]pyrimidin-4-amine, 81

Yield: 101 mg (84.2%). 99.3% purity by HPLC. ¹H NMR (400 MHz, CDCl₃) δ 12.18 (s, 1H), 8.26 (s, 1H), 7.87 (dd, *J* = 7.0, 1.4 Hz, 2H), 7.65 (m, 1H), 7.58 (m, 2H), 7.10 (d, *J* = 3.0 Hz, 1H), 6.50 (d, *J* = 2.9 Hz, 1H), 5.60 (m, 1H), 3.64 (dd, *J* = 12.1, 5.7 Hz, 1H), 3.45 (dd, *J* = 13.6, 5.3 Hz, 1H), 3.35 (m, 1H), 3.27 (d, *J* = 2.1 Hz, 3H), 3.12 (dt, *J* = 16.6, 4.7 Hz, 1H), 2.17 (ddd, *J* = 12.3, 10.0, 7.7 Hz, 1H), 2.05 (m, 1H). ¹³C NMR (100 MHz, CDCl₃) δ 157.6, 152.1, 150.5, 135.8, 133.1, 129.3, 127.9, 120.9, 103.4, 101.8, 54.4, 49.3, 47.2,

32.2, 28.5. HRMS (ESI) calcd for C₁₇H₂₀N₅O₂S: 358.1338. Obsd: 358.1333. [α]_D -29.2° (c 1.21, CHCl₃).

(R)-N-(1-((2-Fluorophenyl)sulfonyl)pyrrolidin-3-yl)-N-methyl-7H-pyrrolo[2,3-d]pyrimidin-4-amine, 82

Yield: 96.8 mg (80.6%). 99.4% purity by HPLC. ¹H NMR (400 MHz, CDCl₃) δ 12.58 (s, 1H), 8.29 (s, 1H), 7.91 (t, *J* = 6.8 Hz, 1H), 7.60 (d, *J* = 5.0 Hz, 1H), 7.27 (m, 2H), 7.11 (s, 1H), 6.51 (s, 1H), 5.68 (m, 1H), 3.73 (d, *J* = 8.2 Hz, 1H), 3.63 (t, *J* = 9.1 Hz, 1H), 3.40 (m, 1H), 3.34 (d, *J* = 8.5 Hz, 1H), 3.28 (s, 3H), 2.20 (s, 1H), 2.10 (dd, *J* = 19.9, 9.1 Hz, 1H). ¹³C NMR (100 MHz, CDCl₃) δ 160.3, 157.7, 157.5, 152.0, 150.3, 135.2 (d, *J* = 8.4 Hz), 131.4, 125.4 (d, *J* = 14.9 Hz), 124.6 (d, *J* = 3.6 Hz), 121.0, 117.4 (d, *J* = 22.0 Hz), 102.5 (d, *J* = 172.3 Hz), 54.5, 48.4, 46.6, 32.1, 28.5. HRMS (ESI) calcd for C₁₇H₁₉FN₅O₂S: 376.1243. Obsd: 376.1236. [α]_D -18.5° (c 3.38, CHCl₃).

(R)-N-(1-((3-Fluorophenyl)sulfonyl)pyrrolidin-3-yl)-N-methyl-7H-pyrrolo[2,3-d]pyrimidin-4-amine, 83

Yield: 101 mg (84.0%). 100% purity by HPLC. ¹H NMR (400 MHz, CDCl₃) δ 12.64 (s, 1H), 8.27 (s, 1H), 7.65 (d, *J* = 7.5 Hz, 1H), 7.55 (dd, *J* = 14.7, 6.6 Hz, 2H), 7.33 (m, 1H), 7.11 (d, *J* = 2.8 Hz, 1H), 6.49 (d, *J* = 2.9 Hz, 1H), 5.59 (dd, *J* = 14.9, 7.4 Hz, 1H), 3.63 (t, *J* = 7.3 Hz, 1H), 3.47 (t, *J* = 9.3 Hz, 1H), 3.33 (dd, *J* = 10.2, 6.6 Hz, 1H), 3.26 (s, 3H), 3.13 (dd, *J* = 16.7, 9.1 Hz, 1H), 2.15 (m, 1H), 2.06 (m, 1H). ¹³C NMR (100 MHz, CDCl₃) δ 163.8, 161.3, 157.4, 152.0, 150.2, 137.9 (d, *J* = 6.5 Hz), 131.1 (d, *J* = 7.7 Hz), 123.5 (d, *J* = 3.2 Hz), 121.0 (s), 120.2 (d, *J* = 21.2 Hz), 115.0 (d, *J* = 24.1 Hz), 102.5 (d, *J* = 172.4 Hz), 54.3, 49.1, 47.0, 32.1, 28.3. HRMS (ESI) calcd for C₁₇H₁₉FN₅O₂S: 376.1243. Obsd: 376.1239. [α]_D -39.8° (c 3.38, CHCl₃).

(R)-N-(1-((4-Fluorophenyl)sulfonyl)pyrrolidin-3-yl)-N-methyl-7H-pyrrolo[2,3-d]pyrimidin-4-amine, 84

Yield: 93.5 mg (77.8%). 98.0% purity by HPLC. ¹H NMR (400 MHz, CDCl₃) δ 11.08 (s, 1H), 8.24 (s, 1H), 7.89 (dd, *J* = 8.4, 5.1 Hz, 2H), 7.26 (dd, *J* = 9.2, 7.5 Hz, 2H), 7.09 (d, *J* = 2.7 Hz, 1H), 6.52 (d, *J* = 2.9 Hz, 1H), 5.61 (m, 1H), 3.65 (t, *J* = 7.5 Hz, 1H), 3.38 (dt, *J* = 10.1, 6.9 Hz, 2H), 3.31 (d, *J* = 8.7 Hz, 3H), 3.11 (m, 1H), 2.18 (d, *J* = 4.7 Hz, 1H), 2.08 (dd, *J* = 14.9, 6.4 Hz, 1H). ¹³C NMR (100 MHz, CDCl₃) δ 166.8, 164.2, 157.6, 152.1, 150.5, 132.1, 130.6 (d, *J* = 9.6 Hz), 120.9, 116.6 (d, *J* = 22.5 Hz), 90.4, 54.4, 49.2, 47.2, 32.3, 28.5. HRMS (ESI) calcd for C₁₇H₁₉FN₅O₂S: 376.1243. Obsd: 376.1237. [α]_D -35.9° (*c* 0.670, CHCl₃).

(R)-2-((3-(Methyl(7H-pyrrolo[2,3-d]pyrimidin-4-yl)amino)pyrrolidin-1-yl)sulfonyl)benzonitrile, 85

Yield: 68.8 mg (56.0%). 98.3% purity by HPLC. ¹H NMR (400 MHz, CDCl₃) δ 12.29 (s, 1H), 8.28 (d, *J* = 3.7 Hz, 1H), 8.11 (dd, *J* = 7.4, 2.8 Hz, 1H), 7.91 (m, 1H), 7.74 (m, 2H), 7.12 (s, 1H), 6.55 (s, 1H), 5.73 (d, *J* = 6.8 Hz, 1H), 3.80 (t, *J* = 8.8 Hz, 1H), 3.67 (td, *J* = 10.1, 3.5 Hz, 1H), 3.43 (m, 2H), 3.32 (d, *J* = 3.5 Hz, 3H), 2.22 (ddd, *J* = 18.3, 11.1, 4.5 Hz, 2H). ¹³C NMR (100 MHz, CDCl₃) δ 157.6, 152.1, 150.4, 140.7, 135.7, 133.2, 133.0, 130.4, 121.0, 116.5, 110.8, 103.5, 101.8, 54.6, 48.7, 47.2, 32.3, 28.5. HRMS (ESI) calcd for C₁₈H₁₉N₆O₂S: 383.1290. Obsd: 383.1287. [α]_D -12.6° (*c* 2.34, CHCl₃).

(R)-4-((3-(Methyl(7H-pyrrolo[2,3-d]pyrimidin-4-yl)amino)pyrrolidin-1-yl)sulfonyl)benzonitrile, 86

Yield: 80.5 mg (65.8%). 100% purity by HPLC. ¹H NMR (400 MHz, DMSO-*d*₆) δ 11.66 (s, 1H), 8.09 (m, 2H), 8.03 (d, *J* = 3.0 Hz, 1H), 7.98 (dd, *J* = 4.7, 3.8 Hz, 2H), 7.09 (d, *J* = 1.3 Hz, 1H), 6.43 (s, 1H), 5.24 (m, 1H), 3.44 (m, 2H), 3.17 (ddd, *J* = 18.1, 10.9, 5.2 Hz, 2H), 3.06 (d, *J* = 2.8 Hz, 3H), 1.96

(m, 2H). ^{13}C NMR (100 MHz, DMSO-*d*6) δ 156.8, 151.7, 150.4, 139.8, 133.6, 128.2, 121.1, 117.7, 115.6, 102.6, 101.4, 54.1, 48.7, 46.8, 31.7, 27.6. HRMS (ESI) calcd for $\text{C}_{18}\text{H}_{19}\text{N}_6\text{O}_2\text{S}$: 383.1290. Obsd: 383.1284. $[\alpha]_{\text{D}} -10.7^\circ$ (*c* 2.72, DMSO).

(R)-N-Methyl-N-(1-((2-nitrophenyl)sulfonyl)pyrrolidin-3-yl)-7H-pyrrolo[2,3-d]pyrimidin-4-amine, 87

Yield: 101 mg (78.1%). 97.5% purity by HPLC. ^1H NMR (400 MHz, CDCl_3) δ 11.92 (s, 1H), 8.30 (s, 1H), 8.05 (dd, *J* = 7.3, 1.7 Hz, 1H), 7.72 (m, 2H), 7.64 (dd, *J* = 7.5, 1.6 Hz, 1H), 7.12 (d, *J* = 3.2 Hz, 1H), 6.56 (d, *J* = 3.3 Hz, 1H), 5.75 (dd, *J* = 15.9, 7.8 Hz, 1H), 3.76 (m, 2H), 3.46 (ddd, *J* = 17.0, 9.8, 7.2 Hz, 2H), 3.32 (s, 3H), 2.26 (m, 1H), 2.18 (m, 1H). ^{13}C NMR (100 MHz, CDCl_3) δ 157.7, 152.2, 150.6, 148.5, 133.9, 131.8, 131.6, 131.1, 124.2, 120.9, 103.5, 101.9, 54.7, 48.6, 47.0, 32.3, 28.7. HRMS (ESI) calcd for $\text{C}_{17}\text{H}_{19}\text{N}_6\text{O}_4\text{S}$: 403.1188. Obsd: 403.1182. $[\alpha]_{\text{D}} +12.6^\circ$ (*c* 2.17, CHCl_3).

(R)-N-Methyl-N-(1-((3-nitrophenyl)sulfonyl)pyrrolidin-3-yl)-7H-pyrrolo[2,3-d]pyrimidin-4-amine, 88

Yield: 104 mg (81.0%). 99.6% purity by HPLC. ^1H NMR (400 MHz, CDCl_3) δ 10.63 (s, 1H), 8.70 (s, 1H), 8.50 (d, *J* = 7.9 Hz, 1H), 8.22 (s, 1H), 8.19 (d, *J* = 8.1 Hz, 1H), 7.80 (t, *J* = 7.9 Hz, 1H), 7.08 (s, 1H), 6.54 (s, 1H), 5.60 (m, 1H), 3.73 (t, *J* = 7.5 Hz, 1H), 3.50 (dd, *J* = 11.6, 7.1 Hz, 1H), 3.40 (m, 1H), 3.31 (s, 3H), 3.18 (dd, *J* = 16.8, 9.2 Hz, 1H), 2.15 (m, 2H). ^{13}C NMR (100 MHz, CDCl_3) δ 157.6, 152.2, 150.5, 148.6, 138.7, 133.2, 130.7, 127.5, 122.8, 121.0, 103.5, 101.9, 54.4, 49.1, 47.2, 32.5, 28.4. HRMS (ESI) calcd for $\text{C}_{17}\text{H}_{19}\text{N}_6\text{O}_4\text{S}$: 403.1188. Obsd: 403.1184. $[\alpha]_{\text{D}} -41.1^\circ$ (*c* 1.24, CHCl_3).

(R)-N-Methyl-N-(1-((4-nitrophenyl)sulfonyl)pyrrolidin-3-yl)-7H-pyrrolo[2,3-d]pyrimidin-4-amine, 89

Yield: 95.3 mg (74.0%). 99.1% purity by HPLC. ^1H NMR (400 MHz, CDCl_3) δ 10.99 (s, 1H), 8.42 (d, $J = 8.6$ Hz, 2H), 8.22 (s, 1H), 8.05 (d, $J = 8.6$ Hz, 2H), 7.09 (d, $J = 2.1$ Hz, 1H), 6.52 (d, $J = 2.6$ Hz, 1H), 5.59 (dt, $J = 15.6$, 7.9 Hz, 1H), 3.70 (m, 1H), 3.51 (m, 1H), 3.38 (dd, $J = 10.2$, 7.0 Hz, 1H), 3.30 (s, 3H), 3.18 (dd, $J = 16.9$, 9.2 Hz, 1H), 2.15 (m, 2H). ^{13}C NMR (100 MHz, CDCl_3) δ 157.6, 152.2, 150.9, 150.5, 142.3, 129.0, 124.6, 120.7, 103.5, 102.1, 54.5, 49.1, 47.2, 32.5, 28.4. HRMS (ESI) calcd for $\text{C}_{17}\text{H}_{19}\text{N}_6\text{O}_4\text{S}$: 403.1188. Obsd: 403.1185. $[\alpha]_{\text{D}} -63.5^\circ$ (c 0.568, CHCl_3).

(R)-N-Methyl-N-(1-(m-tolylsulfonyl)pyrrolidin-3-yl)-7H-pyrrolo[2,3-d]pyrimidin-4-amine, 90

Yield: 101 mg (84.9%). 95.0% purity by HPLC. ^1H NMR (400 MHz, CDCl_3) δ 12.57 (s, 1H), 8.27 (s, 1H), 7.66 (d, $J = 9.2$ Hz, 2H), 7.44 (m, 2H), 7.10 (d, $J = 3.0$ Hz, 1H), 6.48 (d, $J = 2.7$ Hz, 1H), 5.58 (dt, $J = 14.9$, 7.4 Hz, 1H), 3.62 (t, $J = 7.5$ Hz, 1H), 3.44 (m, 1H), 3.33 (dd, $J = 10.2$, 6.4 Hz, 1H), 3.25 (s, 3H), 3.10 (dd, $J = 16.9$, 9.1 Hz, 1H), 2.44 (s, 3H), 2.14 (dd, $J = 9.7$, 5.3 Hz, 1H), 2.03 (m, 1H). ^{13}C NMR (100 MHz, CDCl_3) δ 157.4, 152.0, 150.2, 139.4, 135.5, 133.8, 129.0, 128.1, 124.9, 120.9, 103.3, 101.6, 54.3, 49.2, 47.1, 32.0, 28.4, 21.4. HRMS (ESI) calcd for $\text{C}_{18}\text{H}_{22}\text{N}_5\text{O}_2\text{S}$: 372.1494. Obsd: 372.1495. $[\alpha]_{\text{D}} -39.6^\circ$ (c 3.34, CHCl_3).

(R)-N-Methyl-N-(1-tosylpyrrolidin-3-yl)-7H-pyrrolo[2,3-d]pyrimidin-4-amine, 91

Yield: 87.4 mg (73.5%). 99.4% purity by HPLC. ^1H NMR (400 MHz, CDCl_3) δ 12.57 (s, 1H), 8.26 (s, 1H), 7.73 (d, $J = 6.8$ Hz, 2H), 7.35 (d, $J = 7.1$ Hz, 2H), 7.10 (s, 1H), 6.48 (s, 1H), 5.58 (m, 1H), 3.61 (d, $J = 7.6$ Hz, 1H), 3.41 (t, $J = 9.0$ Hz, 1H), 3.31 (dd, $J = 8.7$, 6.2 Hz, 1H), 3.25 (s, 3H), 3.08 (dd, $J = 16.3$, 7.7 Hz, 1H), 2.44 (s, 3H), 2.13 (s, 1H), 2.04 (dd, $J = 18.2$, 9.9 Hz, 1H). ^{13}C NMR (100 MHz, CDCl_3) δ 157.4, 151.9, 150.2, 143.8, 132.5, 129.8, 127.8,

120.8, 103.2, 101.6, 54.2, 49.2, 47.0, 32.0, 28.3, 21.5. HRMS (ESI) calcd for $C_{18}H_{22}N_5O_2S$: 372.1494. Obsd: 372.1490. $[\alpha]_D -41.5^\circ$ (c 3.24, $CHCl_3$).

(R)-N-(1-((4-Methoxyphenyl)sulfonyl)pyrrolidin-3-yl)-N-methyl-7H-pyrrolo[2,3-d]pyrimidin-4-amine, 92

Yield: 107 mg (86.2%). 100% purity by HPLC. 1H NMR (400 MHz, $CDCl_3$) δ 12.56 (s, 1H), 8.27 (s, 1H), 7.79 (d, $J = 6.6$ Hz, 2H), 7.10 (s, 1H), 7.02 (d, $J = 6.6$ Hz, 2H), 6.48 (s, 1H), 5.58 (s, 1H), 3.87 (s, 3H), 3.59 (t, $J = 8.5$ Hz, 1H), 3.40 (t, $J = 9.0$ Hz, 1H), 3.31 (d, $J = 6.3$ Hz, 1H), 3.25 (s, 3H), 3.08 (m, 1H), 2.14 (s, 1H), 2.03 (m, 1H). ^{13}C NMR (100 MHz, $CDCl_3$) δ 163.1, 157.4, 151.9, 150.2, 129.9, 127.1, 120.8, 114.3, 103.2, 101.6, 55.6, 54.2, 49.2, 47.0, 32.0, 28.3. HRMS (ESI) calcd for $C_{18}H_{22}N_5O_3S$: 388.1443. Obsd: 388.1441. $[\alpha]_D -37.5^\circ$ (c 4.03, $CHCl_3$).

(R)-N-Methyl-N-(1-((4-(trifluoromethyl)phenyl)sulfonyl)pyrrolidin-3-yl)-7H-pyrrolo[2,3-d]pyrimidin-4-amine, 93

Yield: 99.2 mg (72.9%). 99.8% purity by HPLC. 1H NMR (400 MHz, $DMSO-d_6$) δ 11.71 (s, 1H), 8.05 (m, 5H), 7.12 (s, 1H), 6.48 (s, 1H), 5.28 (dd, $J = 14.4, 7.2$ Hz, 1H), 3.51 (s, 1H), 3.43 (dd, $J = 18.2, 8.2$ Hz, 3H), 3.22 (m, 2H), 3.12 (m, 3H), 2.04 (m, 2H). ^{13}C NMR (100 MHz, $DMSO-d_6$) δ 157.2, 152.1, 150.8, 140.0, 133.2 (q, $J = 32.4$ Hz), 128.9, 127.0 (d, $J = 3.1$ Hz), 123.9 (q, $J = 272.7$ Hz), 121.5, 102.9, 101.7, 54.5, 49.1, 47.2, 32.1, 28.0. HRMS (ESI) calcd for $C_{18}H_{19}F_3N_5O_2S$: 426.1212. Obsd: 426.1204. $[\alpha]_D -29.6^\circ$ (c 3.29, $CHCl_3$).

(R)-N-Methyl-N-(1-(naphthalen-2-ylsulfonyl)pyrrolidin-3-yl)-7H-pyrrolo[2,3-d]pyrimidin-4-amine, 94

Yield: 112 mg (84.7%). 96.8% purity by HPLC. 1H NMR (400 MHz, $CDCl_3$) δ 12.57 (s, 1H), 8.43 (s, 1H), 8.21 (s, 1H), 7.97 (m, 2H), 7.91 (d, $J =$

7.9 Hz, 1H), 7.85 (d, $J = 8.6$ Hz, 1H), 7.61 (td, $J = 15.0, 7.0$ Hz, 2H), 7.02 (d, $J = 2.5$ Hz, 1H), 6.39 (d, $J = 2.6$ Hz, 1H), 5.52 (m, 1H), 3.68 (m, 1H), 3.50 (t, $J = 9.4$ Hz, 1H), 3.37 (dd, $J = 9.9, 6.7$ Hz, 1H), 3.20 (s, 3H), 3.16 (m, 1H), 2.10 (ddd, $J = 18.9, 8.3, 6.1$ Hz, 1H), 2.00 (m, 1H). ^{13}C NMR (100 MHz, CDCl_3) δ 157.4, 151.9, 150.2, 134.9, 132.8, 132.2, 129.4, 129.2, 129.1, 128.9, 127.9, 127.6, 123.0, 120.8, 103.2, 101.6, 54.3, 49.2, 47.1, 32.0, 28.3. HRMS (ESI) calcd for $\text{C}_{21}\text{H}_{22}\text{N}_5\text{O}_2\text{S}$: 408.1494. Obsd: 408.1495. $[\alpha]_{\text{D}} -40.3^\circ$ (c 3.97, CHCl_3).

(R)-N-Methyl-N-(1-(piperidin-1-ylsulfonyl)pyrrolidin-3-yl)-7H-pyrrolo[2,3-d]pyrimidin-4-amine, 95

Yield: 91.0 mg (77.8%). 98.7% purity by HPLC. ^1H NMR (400 MHz, CDCl_3) δ 12.65 (s, 1H), 8.36 (s, 1H), 7.15 (s, 1H), 6.58 (s, 1H), 5.78 (m, 1H), 3.60 (m, 2H), 3.35 (s, 3H), 3.34 (m, 2H), 3.26 (d, $J = 4.7$ Hz, 4H), 2.28 (dd, $J = 9.6, 7.4$ Hz, 1H), 2.13 (m, 1H), 1.64 (d, $J = 4.2$ Hz, 4H), 1.56 (d, $J = 3.4$ Hz, 2H). ^{13}C NMR (100 MHz, CDCl_3) δ 157.6, 152.0, 150.4, 120.9, 103.3, 101.7, 77.5, 77.2, 76.9, 54.6, 49.4, 47.3, 47.1, 32.0, 28.5, 25.5, 23.8. HRMS (ESI) calcd for $\text{C}_{16}\text{H}_{25}\text{N}_6\text{O}_2\text{S}$: 365.1760. Obsd: 365.1755. $[\alpha]_{\text{D}} +13.7^\circ$ (c 3.06, CHCl_3).

(R)-N-Methyl-N-(1-(morpholinosulfonyl)pyrrolidin-3-yl)-7H-pyrrolo[2,3-d]pyrimidin-4-amine, 96

Yield: 47.0 mg (40.2%). 96.8% purity by HPLC. ^1H NMR (400 MHz, CDCl_3) δ 12.37 (s, 1H), 8.35 (s, 1H), 7.15 (s, 1H), 6.58 (s, 1H), 5.79 (m, 1H), 3.76 (m, 4H), 3.65 (m, 2H), 3.38 (m, 2H), 3.36 (s, 3H), 3.28 (m, 4H), 2.27 (dt, $J = 10.4, 8.5$ Hz, 1H), 2.16 (m, 1H). ^{13}C NMR (100 MHz, CDCl_3) δ 157.7, 152.2, 150.5, 121.0, 103.5, 101.8, 66.5, 54.7, 49.4, 47.6, 46.5, 32.2, 28.6. HRMS (ESI) calcd for $\text{C}_{15}\text{H}_{23}\text{N}_6\text{O}_3\text{S}$: 367.1552. Obsd: 367.1547. $[\alpha]_{\text{D}} +12.9^\circ$ (c 1.53, CHCl_3).

***In vitro* enzyme assays and kinase profiling**

All enzyme inhibition assay including kinase profiling results were obtained by commercially available kinase binding activity assay, KinaseProfiler™ services (Eurofins Scientific, UK).⁸³ All kinase binding activity assays were performed at K_m values for ATP. The 50% inhibitory concentration (IC_{50}) of each compound was determined with GraphPad Prism software. The kinome tree of the inhibition percentages of 323 kinases at the 10 μM concentration for (**R**)-**6c** and **12a** was drawn by R. Najmanovich's Kinome Render web accessible tool.⁷⁸

Cell-based functional assays

Phosphorylation of STAT6

THP-1 cells were purchased from ATCC (ATCC TIB-202) and then grown in RPMI-1640 medium (Hyclone) containing 10% fetal bovine serum (FBS) (Hyclone) and 1% penicillin/streptomycin (Hyclone). Cells were pretreated with the indicated compound at 8 concentrations over a 3-fold serial dilution series (0 – 10 μM), 30 μM and 50 μM at 37 °C for 1 h. Cells were then stimulated with IL-4 (10 ng/mL) (Peprotech) at 37 °C for 60 min and fixed in Cytofix/Cytoperm (BD Biosciences) buffer. Thereafter, they were permeabilization in Phosflow perm buffer III (BD Biosciences) on ice for 30 min. After blocking with Fc blocking reagent (Miltenyi Biotec), cells were stained with PE-conjugated mouse anti-human pSTAT6 antibody (BD Phosflow) on ice for 30 min. pSTAT6 was detected by flow cytometry (Beckman, Gallios) after washing three times. All experiments were repeated at least twice to confirm the reproducibility. The 50% inhibitory concentration (IC_{50}) of each compound was determined with GraphPad Prism software.

Proliferation of Ba/F3 cells

Ba/F3 cells are dependent on IL-3 for proliferation. Thus, Ba/F3 cells

were grown and maintained in RPMI containing 10% FBS, mouse IL-3 (Peprotech), and 1% penicillin/streptomycin. Ba/F3 cell lines expressing TEL-JAK1, TEL-JAK2, TEL-JAK3, and TEL-TYK2 are independent of IL-3 for proliferation. These cell lines were grown and maintained in RPMI-1640 medium containing 10% FBS and antibiotics without IL-3. For the cell proliferation assay, each cell line (1×10^4 /well) was grown in a 96-well plate overnight and then treated with the indicated compound at 10 concentrations over a 3-fold serial dilution series (0 – 10 μ M). The cell proliferation was analyzed using the Cell Counting Kit-8 (CCK8) (Dojindo Laboratories) according to the manufacturer's instructions. All experiments were performed twice and the mean 50% inhibitory concentrations (IC_{50}) of each compound were determined with GraphPad Prism software.

Human whole blood tests

The 10 mM stock solutions of test articles in dimethyl sulfoxide were prepared. The solutions of test articles at desired concentrations were obtained through the dilution of stock solutions with 4% dimethyl sulfoxide solution. In a 1.75 mL Eppendorf tube, 90 μ L of human whole blood was placed and it was treated with 5 μ L of sample solution at the desired concentration. The human whole blood tube was incubated at 37 °C for 45 minutes. For the activation of JAK1 or JAK2 signals, 5 μ L of IL-6 or GM-CSF, respectively, was added to the human whole blood tube. It was incubated at 37 °C for 15 minutes. To the blood tube was added 900 μ L of lysis/fix buffer solution which was warmed at 37 °C and then it was placed at 37 °C for 20 minutes. The blood tube was centrifuged with a 500 xg force at 4 °C for 8 minutes. After removing the supernatant, 1 mL of wash buffer (500 mL of Dulbecco's phosphate-buffered saline + 0.5 g of bovine serum albumin + 0.5 g of sodium azide) was added to the tube. Then it was centrifuged with a 500 xg force at 4 °C for 8 minutes. The above washing process was carried out once more. After removing the

supernatant, 400 μ L of BD phosflow perm buffer cooled at ice bath was added and it was vortexed. The it was placed at ice bath for 30 minutes. The tube was centrifuged with a 500 xg force at 4 °C for 8 minutes. Antibody solutions were prepared: 5.5 mL of BD pharmingen staining buffer + 110 μ L of Anti-Human CD4 + 55 μ L of pSTAT1 antibody for IL-6/JAK1/pSTAT1 signaling and 5.5 mL of BD pharmingen staining buffer + 110 μ L of Anti-Human CD33 + 55 μ L of pSTAT5 antibody for GM-CSF/JAK2/pSTAT5 signaling. After removing the supernatant in the blood tube, 250 μ L of antibody solution was added and then the tube was placed at 4 °C for overnight. It was analyzed with fluorescence-activated cell sorting (FACS) method.

***In vitro* ADME assays**

All *in vitro* ADME, including plasma stability, plasma protein binding, liver microsomal stability, and Caco-2 permeability assays, and hERG assays were performed by commercially available services at the New Drug Development Center, Daegu-Gyeongbuk Medical Innovation Foundation, South Korea and Drug Discovery Platform Technology Group, Korea Research Institute of Chemical Technology, South Korea.

Plasma stability assay

Human or rat plasma was treated with test articles at 10 μ M concentration. Procaine and diltiazem were used for positive controls. The plasma tubes were incubated at 37 °C for 0, 30, and 120 minutes. Acetonitrile including internal standard, chlorpropamide, was added to the tube, which was vortexed and centrifuged with a power of 14,000 rpm at 4 °C. After the centrifugation, the supernatant was analysed by LC-MS/MS, Nexera XR system (Shimadzu, Japan) with TSQ vantage triple quadruple (Thermo, USA). The column was Kinetex XB-C18 column (2.1x100 mm, 2.6 μ m particle size;

Phenomenex, USA) and the obtained data were analysed in Xcalibur program (version 1.6.1).

Plasma protein binding test

Rapid equilibrium dialysis (RED) method was used for plasma protein binding test. Positive controls were dexamethasone and warfarin. Human or rat plasma was treated with test articles at 10 μ M concentration. The same volumes of the treated plasma and phosphate-buffered saline (PBS, pH 7.4) were placed in RED chamber. The chamber was incubated at 37 °C for 4 hours. The same volumes of the incubated plasma and buffer were sampled and the same volumes of buffer and blank plasma were added, respectively. Acetonitrile including internal standard, chlorpropamide, was added to each sample tube, which was vortexed and centrifuged with a power of 14,000 rpm at 4 °C. After the centrifugation, the supernatant was analysed by LC-MS/MS, Nexera XR system (Shimadzu, Japan) with TSQ vantage triple quadrupole (Thermo, USA). The column was Kinetex XB-C18 column (2.1x100 mm, 2.6 μ m particle size; Phenomenex, USA) and the obtained data were analysed in Xcalibur program (version 1.6.1).

Liver microsomal stability test

The liver microsome of human, dog, rat, or mouse (0.5 mg/mL), 0.1 M phosphate buffer, and a test article at 1 μ M concentration were placed in a tube. Positive control was verapamil. The tube was incubated at 37 °C for 5 minutes. NADPH regeneration system solution was added to the tube, which were incubated at 37 °C for 30 minutes. Acetonitrile including internal standard, chlorpropamide, was added to the tube, which was vortexed and centrifuged with a power of 14,000 rpm at 4 °C. After the centrifugation, the supernatant was analysed by LC-MS/MS, Nexera XR system (Shimadzu, Japan) with TSQ vantage triple quadrupole (Thermo, USA). The column was Kinetex XB-C18

column (2.1x100 mm, 2.6 μ m particle size; Phenomenex, USA) and the obtained data were analysed in Xcalibur program (version 1.6.1).

Caco-2 permeability assay

In a 12-well transwell, 1×10^6 cells of Caco-2 cells (ATCC® HTB-37™) were seeded and they were grown for 3 weeks. Test article was diluted to 25 μ M concentration with transport buffer (10 mM glucose, 4 mM sodium bicarbonate, and 1 mM 4-(2-hydroxyethyl)-1-piperazineethanesulfonic acid in Hank's balanced salt solution, pH 7.4). Positive controls were caffeine, ofloxacin, and atenolol. Of apical and basolateral chamber, test article was added to one chamber and then transport buffer was added to the other. During 60-minute incubation at 37 °C, samples from each chamber were taken every 15 minutes. The samples were diluted to 5 μ M concentration with acetonitrile including internal standard, chlorpropamide. the samples were analysed by LC-MS/MS, Nexera XR system (Shimadzu, Japan) with TSQ vantage triple quadruple (Thermo, USA). The column was Kinetex XB-C18 column (2.1x100 mm, 2.6 μ m particle size; Phenomenex, USA) and the obtained data were analysed in Xcalibur program (version 1.6.1).

CYP inhibition test

A cocktail of human liver microsomes (0.25 mg/mL), 0.1 M phosphate buffer, each substrate for CYP₄₅₀ isozymes, and test article at 0 or 10 μ M concentration was incubated at 37 °C for 5 minutes. The cocktails are as follows: Cocktail A, phenacetin 50 μ M + coumarin 2.5 μ M + *S*-mephenytoin 100 μ M + dextromethorphan 5 μ M + midazolam 2.5 μ M; Cocktail B, bupropion 50 μ M + aminodaquine 2.5 μ M + tolbutamide 100 μ M + chlorzoxazone 50 μ M. Then NADPH generation system solution was added and it was incubated at 37 °C for 15 minutes again. After the incubation, the reaction was quenched with acetonitrile including chlorphopamide as an internal standard. It was centrifuged with a power of 14,000 rpm at 4 °C. After

the centrifugation, the supernatant was analysed by LC-MS/MS, Nexera XR system (Shimadzu, Japan) with TSQ vantage triple quadruple (Thermo, USA). The column was Kinetex XB-C18 column (2.1x100 mm, 2.6 μ m particle size; Phenomenex, USA) and the obtained data were analysed in Xcalibur program (version 1.6.1).

Human ether-a-go-go related gene (hERG) potassium channel assay

hERG assay was performed with automated planar patch clamp method in PatchXpress® 7000A (Molecular Devices, LLC., USA). HERG – HEK293 cells ($2 - 4 \times 10^6$ cells) were placed in a 384 well-plate. Amphotericin B solution was added for perforated patch clamp and then it was placed for 10 minutes. To measure hERG normal current, The HEK293 cell membrane was held at -80 mV, and the current of potassium channel was measured while voltage was changed as follows: -40 mV for 100 milliseconds (ms), +40 mV for 500 ms, and -50 mV for 2 seconds. After measuring normal current with the mentioned method, the HEK293 cells were treated with test article solution at desired concentration. After 5 minutes, the current of potassium channel treated with test article was measured with the aforementioned method.

Pharmacokinetic study

Beagle dogs (10 – 12 kg), Sprague Dawley rats (7 – 8 weeks old) and ICR mice (7 – 8 weeks old) were kept in an environmentally controlled breeding room (25 ± 2 °C, $60 \pm 5\%$ humidity, 12h dark/light cycle) with free access to food and water. All groups consisted of four males fed freely for intravenous tests, but had fasted for 16 hours beforehand per oral tests. The dosages for intravenous and per oral tests in dogs, rats, and mice were 5 and 3 mg/kg, 5 and 10 mg/kg, and 5 and 10 mg/kg, respectively. The free base form of (**R**)-**6c** or **12a** was clearly solved under the vehicle condition of 10% ethanol

and 90% PEG400 so the dose volume of 1 mL/kg is for intravenous administration. For oral administration, it became the suspension in corn oil, which has the 5 mL/kg dose volume. The salt forms include hydrochloride, citrate, and tartrate, which were clearly solved in 100% saline so that their dose volumes became 250 and 2500 μ L/kg for IV and PO, respectively. After their administrations, the blood samplings were performed at 0.08, 0.25, 0.5, 1, 2, 4, 6, 8, 12 and 24 hours for IV and at 0.25, 0.5, 1, 2, 4, 6, 8, 12, and 24 hours for PO. 20 μ L of the sampled plasma was diluted with 180 μ L of acetonitrile at an internal standard. It was then vortexed and centrifuged under 15000 rpm at 4 °C. After the centrifugation, the supernatant was analyzed by LC-MS/MS, Nexera XR system (Shimadzu, Japan) with TSQ vantage triple quadrupole (Thermo, USA). The column was Kinetex XB-C18 column (2.1x100 mm, 2.6 μ m particle size; Phenomenex, USA) and pharmacokinetic parameters were obtained by the non-compartmental analysis model in Phoenix WinNonlin 6.4 version (Pharsight, USA). The animal care and procedure of this study were approved by the Animal Research Care Committee of New Drug Development Center, Daegu-Gyeongbuk Medical Innovation Foundation.

Mouse collagen-induced arthritis

Male DBA1/J mice (6 weeks old) were purchased from Japan SLC, Inc and all mice were housed in specific pathogen-free (SPF) conditions with free access to food and water. After 7 days of acclimation, mice were immunized with 0.1 mL of 1:1 mixture of type II collagen emulsion (2 mg/mL) and complete Freund's adjuvant by subcutaneous injection at 1.5 cm distal from the tail base. After 21 days, immunized mice were boosted by another injection with 0.1 mL of type II collagen emulsion and incomplete Freund's adjuvant. The emulsions were prepared according to manufacturer's instruction.⁸⁴ When all mice indicated signs of arthritis, treatment with test articles and assessment of arthritis were initiated (day 1). The immunized and boosted mice were

randomized into 6 treatment groups ($n = 10$ each) and same-aged naïve mice were assigned to a normal group ($n = 5$). All test articles or vehicle were orally administered once daily and the clinical arthritis scores were assessed twice weekly for 18 days. Corn oil was used as a vehicle and all test articles were suspended in vehicle. The test article doses were 25, 50, and 100 mg/kg/day for **(R)-6c**, 100 mg/kg/day for **12a**, 100 mg/kg/day for filgotinib, and 50 mg/kg/day for tofacitinib citrate. Paw volumes were measured by LE7500 plethysmometer (Panlab, Spain) on days 1 and 15. The severity of each paw was evaluated and scored according to criteria where 0 = normal; 0.5 = redness of the toe, but not swollen; 1 = one toe inflamed and swollen; 2 = more than one toe, but entire paw, inflamed and swollen, or mild swelling of entire paw; 3 = entire paw inflamed and swollen; and 4 = very inflamed and swollen paw or ankylosed paw.⁸⁵ The clinical arthritis score was represented by the total scores of each paw. On day 19, all individuals were sacrificed and autopsies were performed. Serum cytokines including IL-1 β , IL-6, MCP-1, and TNF- α were measured by ELISA kits (ProcartaPlex Mix and Match customized, Mouse 5 plex, BMS). For the histopathological studies, the right hind paws of each mouse were fixed by 10% formalin solution and the hematoxylin-eosin staining was performed on the ankle and third digit of the paw. The histopathological score was semiquantitatively measured according to criteria where 0 = normal; 1 = infiltration of inflammatory cells; 2 = synovial hyperplasia and pannus formation; and 3 = bone erosion and destruction.⁸⁶ The obtained images were analyzed by iSolution EL ver 9.1 (IMT i-solution Inc., Canada) and the micro-CT analyses of all individuals were performed by viviCT 80 micro-CT (SCANCO Medical, Switzerland) to measure bone surface/volume ratio. Student's *t*-test or one-way analysis of variance test was performed to determine statistically significant differences. The data for clinical arthritis scores were statistically analyzed by the Kruskal-Wallis test or Mann-Whitney test where a significant difference was defined as $P < 0.05$. The experimental protocol of

the mouse study was approved by the Animal Research Care Committee of Gyeonggi Biocenter (Approval No. 2015-11-0019).

Rat adjuvant-induced arthritis

AIA was induced in SPF Lewis LEW/SsNSlc rats (Japan SLC Inc., Japan). After 2 weeks of acclimation, 10 week old rats were immunized by the subcutaneous injection of 0.1 mL of complete Freund's adjuvant containing 10 mg/mL of heat-killed mycobacterium (Chondrex, Inc., USA) at a 2.0 cm distal from the rat tail base. After 12 days of immunization (day 1), the rats were randomized into 6 treatment groups (n = 10 each) and received test articles or vehicles alone once daily for 14 days. Same-aged naïve mice were assigned to a normal group (n = 5). Corn oil was used as a vehicle and test article doses were 5, 10, and 20 mg/kg/day for (**R**)-**6c**, 20 mg/kg/day for **12a**, 20 mg/kg/day for filgotinib, and 10 mg/kg/day for tofacitinib citrate. The clinical arthritis score and paw thicknesses were evaluated twice weekly for 14 days. The criteria for the clinical arthritis score are 0 = normal; 1 = mild edema or erythema; 2 = moderate edema; 3 = severe edema; and 4 = ankylosis. The paw thicknesses were measured by electric caliper CD-15CPX (Mitutoyo Corp., Japan). Kruskal-Wallis test or one-way analysis of variance test was performed to determine statistically significant differences, which were defined as $P < 0.05$. The experimental protocol of the rat study was approved by the Animal Research Care Committee of Qu-BEST BIO, Co., Ltd. (Approval No. QBSIACUC-A17001).

Acknowledgement

This research was performed with the DGMIF Drug Development Center and supported by the Bio & Medical Technology Development Program through the National Research Foundation of Korea (NRF); funded by the Ministry of Science, ICT & Future Planning (2014M3A9D9033717).

References

1. Stoll, J. G.; Yasothan, U., Rheumatoid arthritis market. *Nat Rev Drug Discov* **2009**, 8 (9), 693-694.
2. Mount, C.; Featherstone, J., Rheumatoid arthritis market. *Nat Rev Drug Discov* **2005**, 4 (1), 11-12.
3. Deane, K. D.; El-Gabalawy, H., Pathogenesis and prevention of rheumatic disease: focus on preclinical RA and SLE. *Nat Rev Rheumatol* **2014**, 10 (4), 212-228.
4. Jacques, P.; Van den Bosch, F., Emerging therapies for rheumatoid arthritis. *Expert Opinion on Emerging Drugs* **2013**, 18 (2), 231-244.
5. Emery, P., Rheumatoid arthritis in 2014: Exciting times for RA research. *Nat Rev Rheumatol* **2015**, 11 (2), 69-70.
6. Meier, F. M. P.; Frerix, M.; Hermann, W.; Müller-Ladner, U., Current immunotherapy in rheumatoid arthritis. *Immunotherapy* **2013**, 5 (9), 955-974.
7. Burmester, G. R.; Feist, E.; Dorner, T., Emerging cell and cytokine targets in rheumatoid arthritis. *Nat Rev Rheumatol* **2014**, 10 (2), 77-88.
8. Neumann, E.; Khawaja, K.; Muller-Ladner, U., G protein-coupled receptors in rheumatology. *Nat Rev Rheumatol* **2014**, 10 (7), 429-436.
9. Müller, S.; Knapp, S., Targeting kinases for the treatment of inflammatory diseases. *Expert Opinion on Drug Discovery* **2010**, 5 (9), 867-881.
10. Kelly, V.; Genovese, M., Novel small molecule therapeutics in rheumatoid arthritis. *Rheumatology* **2013**, 52 (7), 1155-1162.
11. Buer, J. K., A history of the term “DMARD”. *Inflammopharmacology* **2015**, 23 (4), 163-171.
12. Doan, T.; Massarotti, E., Rheumatoid Arthritis: An Overview of New and Emerging Therapies. *The Journal of Clinical Pharmacology* **2005**, 45 (7), 751-762.
13. O'Dell, J. R., Therapeutic Strategies for Rheumatoid Arthritis. *New England Journal of Medicine* **2004**, 350 (25), 2591-2602.
14. Detert, J.; Klaus, P., Biologic monotherapy in the treatment of rheumatoid arthritis. *Biologics : Targets & Therapy* **2015**, 9, 35-43.

15. Mócsai, A.; Kovács, L.; Gergely, P., What is the future of targeted therapy in rheumatology: biologics or small molecules? *BMC Medicine* **2014**, *12* (1), 43.
16. Wilks, A. F., Two putative protein-tyrosine kinases identified by application of the polymerase chain reaction. *Proceedings of the National Academy of Sciences* **1989**, *86* (5), 1603-1607.
17. Darnell, J.; Kerr, I.; Stark, G., Jak-STAT pathways and transcriptional activation in response to IFNs and other extracellular signaling proteins. *Science* **1994**, *264* (5164), 1415-1421.
18. Shuai, K.; Liu, B., Regulation of JAK-STAT signalling in the immune system. *Nat Rev Immunol* **2003**, *3* (11), 900-911.
19. Ghoreschi, K.; Laurence, A.; O'Shea, J. J., Janus kinases in immune cell signaling. *Immunological Reviews* **2009**, *228* (1), 273-287.
20. Changelian, P. S.; Flanagan, M. E.; Ball, D. J.; Kent, C. R.; Magnuson, K. S.; Martin, W. H.; Rizzuti, B. J.; Sawyer, P. S.; Perry, B. D.; Brissette, W. H.; McCurdy, S. P.; Kudlacz, E. M.; Conklyn, M. J.; Elliott, E. A.; Koslov, E. R.; Fisher, M. B.; Strelevitz, T. J.; Yoon, K.; Whipple, D. A.; Sun, J.; Munchhof, M. J.; Doty, J. L.; Casavant, J. M.; Blumenkopf, T. A.; Hines, M.; Brown, M. F.; Lillie, B. M.; Subramanyam, C.; Shang-Poa, C.; Milici, A. J.; Beckius, G. E.; Moyer, J. D.; Su, C.; Woodworth, T. G.; Gaweco, A. S.; Beals, C. R.; Littman, B. H.; Fisher, D. A.; Smith, J. F.; Zagouras, P.; Magna, H. A.; Saltarelli, M. J.; Johnson, K. S.; Nelms, L. F.; Des Etages, S. G.; Hayes, L. S.; Kawabata, T. T.; Finco-Kent, D.; Baker, D. L.; Larson, M.; Si, M.-S.; Paniagua, R.; Higgins, J.; Holm, B.; Reitz, B.; Zhou, Y.-J.; Morris, R. E.; O'Shea, J. J.; Borie, D. C., Prevention of Organ Allograft Rejection by a Specific Janus Kinase 3 Inhibitor. *Science* **2003**, *302* (5646), 875-878.
21. Meyer, D. M.; Jesson, M. I.; Li, X.; Elrick, M. M.; Funckes-Shippy, C. L.; Warner, J. D.; Gross, C. J.; Dowty, M. E.; Ramaiah, S. K.; Hirsch, J. L.; Saabye, M. J.; Barks, J. L.; Kishore, N.; Morris, D. L., Anti-inflammatory activity and neutrophil reductions mediated by the JAK1/JAK3 inhibitor, CP-690,550, in rat adjuvant-induced arthritis. *Journal of Inflammation* **2010**, *7* (1), 41.
22. Dowty, M. E.; Jesson, M. I.; Ghosh, S.; Lee, J.; Meyer, D. M.; Krishnaswami, S.; Kishore, N., Preclinical to Clinical Translation of Tofacitinib, a Janus Kinase Inhibitor, in Rheumatoid Arthritis. *Journal of Pharmacology and*

Experimental Therapeutics **2014**, 348 (1), 165-173.

23. Feist, E.; Burmester, G. R., Small molecules targeting JAKs—a new approach in the treatment of rheumatoid arthritis. *Rheumatology* **2013**, 52 (8), 1352-1357.

24. Bannwarth, B.; Kostine, M.; Poursac, N., A pharmacokinetic and clinical assessment of tofacitinib for the treatment of rheumatoid arthritis. *Expert Opinion on Drug Metabolism & Toxicology* **2013**, 9 (6), 753-761.

25. Kremer, J. M.; Bloom, B. J.; Breedveld, F. C.; Coombs, J. H.; Fletcher, M. P.; Gruben, D.; Krishnaswami, S.; Burgos-Vargas, R.; Wilkinson, B.; Zerbini, C. A. F.; Zwillich, S. H., The safety and efficacy of a JAK inhibitor in patients with active rheumatoid arthritis: Results of a double-blind, placebo-controlled phase IIa trial of three dosage levels of CP-690,550 versus placebo. *Arthritis & Rheumatism* **2009**, 60 (7), 1895-1905.

26. US Food and Drug Administration Center for drug evaluation and research, Application number: 203214Orig1s000, Approval letter.

27. Neubauer, H.; Cumano, A.; Müller, M.; Wu, H.; Huffstadt, U.; Pfeffer, K., Jak2 Deficiency Defines an Essential Developmental Checkpoint in Definitive Hematopoiesis. *Cell* **93** (3), 397-409.

28. Levy, D. E.; Loomis, C. A., STAT3 Signaling and the Hyper-IgE Syndrome. *New England Journal of Medicine* **2007**, 357 (16), 1655-1658.

29. Park, S. O.; Wamsley, H. L.; Bae, K.; Hu, Z.; Li, X.; Choe, S.-w.; Slayton, W. B.; Oh, S. P.; Wagner, K.-U.; Sayeski, P. P., Conditional Deletion of Jak2 Reveals an Essential Role in Hematopoiesis throughout Mouse Ontogeny: Implications for Jak2 Inhibition in Humans. *PLOS ONE* **2013**, 8 (3), e59675.

30. Tefferi, A., JAK inhibitors for myeloproliferative neoplasms: clarifying facts from myths. *Blood* **2012**, 119 (12), 2721-2730.

31. Pardanani, A.; Gotlib, J. R.; Jamieson, C.; Cortes, J. E.; Talpaz, M.; Stone, R. M.; Silverman, M. H.; Gilliland, D. G.; Shorr, J.; Tefferi, A., Safety and Efficacy of TG101348, a Selective JAK2 Inhibitor, in Myelofibrosis. *Journal of Clinical Oncology* **2011**, 29 (7), 789-796.

32. Riese, R. J.; Krishnaswami, S.; Kremer, J., Inhibition of JAK kinases in patients with rheumatoid arthritis: scientific rationale and clinical outcomes. *Best Practice & Research Clinical Rheumatology* **2010**, 24 (4), 513-526.

33. European Medicines Agency Refusal of the marketing authorisation for Xeljanz (tofacitinib), EMA/248755/2013, EMEA/H/C/002542. http://www.ema.europa.eu/docs/en_GB/document_library/Summary_of_opinion_-_Initial_authorisation/human/002542/WC500142485.pdf.
34. Dymock, B. W.; Yang, E. G.; Chu-Farseeva, Y.; Yao, L., Selective JAK inhibitors. *Future Medicinal Chemistry* **2014**, *6* (12), 1439-1471.
35. Boyle, D. L.; Soma, K.; Hodge, J.; Kavanaugh, A.; Mandel, D.; Mease, P.; Shurmur, R.; Singhal, A. K.; Wei, N.; Rosengren, S.; Kaplan, I.; Krishnaswami, S.; Luo, Z.; Bradley, J.; Firestein, G. S., The JAK inhibitor tofacitinib suppresses synovial JAK1-STAT signalling in rheumatoid arthritis. *Annals of the Rheumatic Diseases* **2015**, *74* (6), 1311-1316.
36. Menet, C. J.; Fletcher, S. R.; Van Lommen, G.; Geney, R.; Blanc, J.; Smits, K.; Jouannigot, N.; Deprez, P.; van der Aar, E. M.; Clement-Lacroix, P.; Lepescheux, L.; Galien, R.; Vayssiere, B.; Nelles, L.; Christophe, T.; Brys, R.; Uhring, M.; Ciesielski, F.; Van Rompaey, L., Triazolopyridines as Selective JAK1 Inhibitors: From Hit Identification to GLPG0634. *Journal of Medicinal Chemistry* **2014**, *57* (22), 9323-9342.
37. Van 't Klooster, G. A. E.; Brys, R. C. X.; Van Rompaey, L. J. C.; Namour, F. S. Aminotriazolopyridine for use in the treatment of inflammation, and pharmaceutical compositions thereof. WO2013189771A1, 2013.
38. Menet, C. J. M.; Van Rompaey, L. J. C.; Fletcher, S. R.; Blanc, J.; Jouannigot, N.; Hodges, A. J.; Smits, K. K. Novel triazolopyridine compounds as JAK kinase inhibitors useful for the treatment of degenerative and inflammatory diseases and their preparation. WO2010010190A1, 2010.
39. Menet, C. J. M.; Smits, K. K. Preparation of N-(triazolopyridinyl)carboxamides as JAK kinase inhibitors and useful in treatment of diseases. WO2010149769A1, 2010.
40. Namour, F.; Diderichsen, P. M.; Cox, E.; Vayssière, B.; Van der Aa, A.; Tasset, C.; Van't Klooster, G., Pharmacokinetics and Pharmacokinetic/Pharmacodynamic Modeling of Filgotinib (GLPG0634), a Selective JAK1 Inhibitor, in Support of Phase IIB Dose Selection. *Clinical Pharmacokinetics* **2015**, *54* (8), 859-874.
41. Namour, F.; Desrivot, J.; Van der Aa, A.; Harrison, P.; Tasset, C.; van't

Klooster, G., Clinical Confirmation that the Selective JAK1 Inhibitor Filgotinib (GLPG0634) has a Low Liability for Drug-drug Interactions. *Drug Metabolism Letters* **2016**, *10* (1), 38-48.

42. Westhovens, R.; Taylor, P. C.; Alten, R.; Pavlova, D.; Enríquez-Sosa, F.; Mazur, M.; Greenwald, M.; Van der Aa, A.; Vanhoutte, F.; Tasset, C.; Harrison, P., Filgotinib (GLPG0634/GS-6034), an oral JAK1 selective inhibitor, is effective in combination with methotrexate (MTX) in patients with active rheumatoid arthritis and insufficient response to MTX: results from a randomised, dose-finding study (DARWIN 1). *Annals of the Rheumatic Diseases* **2017**, *76* (6), 998.

43. Kavanaugh, A.; Kremer, J.; Ponce, L.; Cseuz, R.; Reshetko, O. V.; Stanislavchuk, M.; Greenwald, M.; Van der Aa, A.; Vanhoutte, F.; Tasset, C.; Harrison, P., Filgotinib (GLPG0634/GS-6034), an oral selective JAK1 inhibitor, is effective as monotherapy in patients with active rheumatoid arthritis: results from a randomised, dose-finding study (DARWIN 2). *Annals of the Rheumatic Diseases* **2017**, *76* (6), 1009.

44. Vanhoutte, F.; Mazur, M.; Voloshyn, O.; Stanislavchuk, M.; Van der Aa, A.; Namour, F.; Galien, R.; Meuleners, L.; van 't Klooster, G., Efficacy, Safety, Pharmacokinetics, and Pharmacodynamics of Filgotinib, a Selective JAK-1 Inhibitor, After Short-Term Treatment of Rheumatoid Arthritis: Results of Two Randomized Phase IIa Trials. *Arthritis & Rheumatology* **2017**, *69* (10), 1949-1959.

45. Wishart, N.; Argiriadi, M. A.; Calderwood, D. J.; Ericsson, A. M.; Fiamengo, B. A.; Frank, K. E.; Friedman, M.; George, D. M.; Goedken, E. R.; Josephsohn, N. S.; Li, B. C.; Morytko, M. J.; Stewart, K. D.; Voss, J. W.; Wallace, G. A.; Wang, L.; Woller, K. R. Novel tricyclic compounds as JAK3 inhibitors and their preparation and use in the treatment of immunological and oncological diseases. WO2011068881A1, 2011.

46. Mohamed, M.-E. F.; Camp, H. S.; Jiang, P.; Padley, R. J.; Asatryan, A.; Othman, A. A., Pharmacokinetics, Safety and Tolerability of ABT-494, a Novel Selective JAK 1 Inhibitor, in Healthy Volunteers and Subjects with Rheumatoid Arthritis. *Clinical Pharmacokinetics* **2016**, *55* (12), 1547-1558.

47. Genovese, M. C.; Smolen, J. S.; Weinblatt, M. E.; Burmester, G. R.; Meerwein, S.; Camp, H. S.; Wang, L.; Othman, A. A.; Khan, N.; Pangan, A. L.; Jungerwirth, S., Efficacy and Safety of ABT-494, a Selective JAK-1 Inhibitor, in a Phase IIb Study in Patients With Rheumatoid Arthritis and an Inadequate Response to

Methotrexate. *Arthritis & Rheumatology* **2016**, 68 (12), 2857-2866.

48. Kremer, J. M.; Emery, P.; Camp, H. S.; Friedman, A.; Wang, L.; Othman, A. A.; Khan, N.; Pangan, A. L.; Jungerwirth, S.; Keystone, E. C., A Phase IIb Study of ABT-494, a Selective JAK-1 Inhibitor, in Patients With Rheumatoid Arthritis and an Inadequate Response to Anti-Tumor Necrosis Factor Therapy. *Arthritis & Rheumatology* **2016**, 68 (12), 2867-2877.

49. Mohamed, M.-E. F.; Jungerwirth, S.; Asatryan, A.; Jiang, P.; Othman, A. A., Assessment of effect of CYP3A inhibition, CYP induction, OATP1B inhibition, and high-fat meal on pharmacokinetics of the JAK1 inhibitor upadacitinib. *British Journal of Clinical Pharmacology* **2017**, 83 (10), 2242-2248.

50. Vollenhoven, R. F. v.; Layton, M.; Kahl, L.; Schifano, L.; Hachulla, E.; Machado, D.; Staumont-Sallé, D.; Patel, J., DRESS syndrome and reversible liver function abnormalities in patients with systemic lupus erythematosus treated with the highly selective JAK-1 inhibitor GSK2586184. *Lupus* **2015**, 24 (6), 648-649.

51. Kahl, L.; Patel, J.; Layton, M.; Binks, M.; Hicks, K.; Leon, G.; Hachulla, E.; Machado, D.; Staumont-Sallé, D.; Dickson, M.; Condreay, L.; Schifano, L.; Zamuner, S.; Vollenhoven, R. F. v.; on behalf of the, J. A. K. S. T., Safety, tolerability, efficacy and pharmacodynamics of the selective JAK1 inhibitor GSK2586184 in patients with systemic lupus erythematosus. *Lupus* **2016**, 25 (13), 1420-1430.

52. Ludbrook, V. J.; Hicks, K. J.; Hanrott, K. E.; Patel, J. S.; Binks, M. H.; Wyres, M. R.; Watson, J.; Wilson, P.; Simeoni, M.; Schifano, L. A.; Reich, K.; Griffiths, C. E. M., Investigation of selective JAK1 inhibitor GSK2586184 for the treatment of psoriasis in a randomized placebo-controlled phase IIa study. *British Journal of Dermatology* **2016**, 174 (5), 985-995.

53. De Vries, L. C. S.; Ludbrook, V. J.; Hicks, K. J.; D'Haens, G. R., GSK2586184, a JAK1 selective inhibitor, in two patients with ulcerative colitis. *BMJ Case Reports* **2017**, 2017.

54. Huang, T.; Xue, C.-B.; Wang, A.; Kong, L.; Ye, H. F.; Yao, W.; Rodgers, J. D.; Shepard, S.; Wang, H.; Shao, L.; Li, H.-Y.; Li, Q. Preparation of piperidin-4-yl azetidine derivatives as JAK1 inhibitors. WO2011112662A1, 2011.

55. Zhang, Y.; Warren, M. S.; Zhang, X.; Diamond, S.; Williams, B.; Punwani, N.; Huang, J.; Huang, Y.; Yeleswaram, S., Impact on Creatinine Renal Clearance by the Interplay of Multiple Renal Transporters: A Case Study with

INCB039110. *Drug Metabolism and Disposition* **2015**, 43 (4), 485.

56. Bissonnette, R.; Luchi, M.; Fidelus-Gort, R.; Jackson, S.; Zhang, H.; Flores, R.; Newton, R.; Scherle, P.; Yeleswaram, S.; Chen, X.; Menter, A., A randomized, double-blind, placebo-controlled, dose-escalation study of the safety and efficacy of INCB039110, an oral janus kinase 1 inhibitor, in patients with stable, chronic plaque psoriasis. *Journal of Dermatological Treatment* **2016**, 27 (4), 332-338.

57. Mascarenhas, J. O.; Talpaz, M.; Gupta, V.; Foltz, L. M.; Savona, M. R.; Paquette, R.; Turner, A. R.; Coughlin, P.; Winton, E.; Burn, T. C.; O'Neill, P.; Clark, J.; Hunter, D.; Assad, A.; Hoffman, R.; Verstovsek, S., Primary analysis of a phase II open-label trial of INCB039110, a selective JAK1 inhibitor, in patients with myelofibrosis. *Haematologica* **2017**, 102 (2), 327.

58. Brown, M. F.; Fenwick, A. E.; Flanagan, M. E.; Gonzales, A.; Johnson, T. A.; Kaila, N.; Mitton-Fry, M. J.; Strohbach, J. W.; Tenbrink, R. E.; Trzuppek, J. D.; Unwalla, R. J.; Vazquez, M. L. Pyrrolo[2,3-d]pyrimidine derivatives as inhibitors of janus-related kinases (JAK) and their preparation. WO2014128591A1, 2014.

59. Coffman, K. J.; Duerr, J. M.; Kaila, N.; Parikh, M. D.; Reese, M. R.; Samad, T.; Sciabola, S.; Tuttle, J. B.; Vazquez, M. L.; Verhoest, P. R. Preparation of pyrrolo[2,3-d]pyrimidine derivatives and their use as Janus kinase inhibitors. CA2899888A1, 2016.

60. Menet, C. J.; Mammoliti, O.; López-Ramos, M., Progress toward JAK1-selective inhibitors. *Future Medicinal Chemistry* **2015**, 7 (2), 203-235.

61. Menet, C. J. M.; Van Rompaey, L. J. C.; Fletcher, S. R.; Blanc, J.; Jouannigot, N.; Hodges, A. J.; Smits, K. K. Novel compounds useful for the treatment of degenerative and inflammatory diseases. 28. January 2010, 2010.

62. Gras, J., Filgotinib. Tyrosine-protein kinase JAK1 inhibitor, Treatment of rheumatoid arthritis, Treatment of Crohn's disease. *Drugs of the Future* **2014**, 39 (8), 547-551.

63. Van Rompaey, L.; Galien, R.; van der Aar, E. M.; Clement-Lacroix, P.; Nelles, L.; Smets, B.; Lepescheux, L.; Christophe, T.; Conrath, K.; Vandeghinste, N.; Vayssiere, B.; De Vos, S.; Fletcher, S.; Brys, R.; van 't Klooster, G.; Feyen, J. H. M.; Menet, C., Preclinical Characterization of GLPG0634, a Selective Inhibitor of JAK1, for the Treatment of Inflammatory Diseases. *The Journal of Immunology* **2013**, 191 (7), 3568-3577.

64. Norman, P., Selective JAK inhibitors in development for rheumatoid arthritis. *Expert Opinion on Investigational Drugs* **2014**, 23 (8), 1067-1077.
65. Filgotinib Versus Placebo in Adults With Active Rheumatoid Arthritis (RA) Who Have an Inadequate Response to Biologic Disease-modifying Anti-rheumatic Drug(s) (DMARDs) Treatment. (2016). Retrieved from <http://clinicaltrials.gov/ct2> (Identification No. NCT02873936).
66. Filgotinib Alone and in Combination With Methotrexate (MTX) in Adults With Moderately to Severely Active Rheumatoid Arthritis Who Are Naive to MTX Therapy. (2016). Retrieved from <http://clinicaltrials.gov/ct2> (Identification No. NCT02886728).
67. Filgotinib in Combination With Methotrexate in Adults With Moderately to Severely Active Rheumatoid Arthritis Who Have an Inadequate Response to Methotrexate. (2016). Retrieved from <http://clinicaltrials.gov/ct2> (Identification No. NCT02889796).
68. Risks related to product development, regulatory approval and commercialization. <http://reports.glp.com/annual-report-2016/en/risk-factors/product-development-regulatory-approval-and-commercialization.html>.
69. A Study Comparing ABT-494 to Placebo and to Adalimumab in Subjects With Rheumatoid Arthritis Who Are on a Stable Dose of Methotrexate and Who Have an Inadequate Response to Methotrexate (SELECT-COMPARE). (2015). Retrieved from <http://clinicaltrials.gov/> (Identification No. NCT02629159)
70. A Study Comparing ABT-494 Monotherapy to Methotrexate (MTX) Monotherapy in Subjects With Rheumatoid Arthritis (RA) Who Have an Inadequate Response to MTX (SELECT-MONOTHERAPY). (2016). Retrieved from <http://clinicaltrials.gov/> (Identification No. NCT02706951).
71. Hodge, J. A.; Kawabata, T. T.; Krishnaswami, S.; Clark, J. D.; Telliez, J. B.; Dowty, M. E.; Menon, S.; Lamba, M.; Zwillich, S., The mechanism of action of tofacitinib - an oral Janus kinase inhibitor for the treatment of rheumatoid arthritis. *Clinical and Experimental Rheumatology* **2016**, 34 (2), 318-328.
72. Williams, N. K.; Bamert, R. S.; Patel, O.; Wang, C.; Walden, P. M.; Wilks, A. F.; Fantino, E.; Rossjohn, J.; Lucet, I. S., Dissecting Specificity in the Janus Kinases: The Structures of JAK-Specific Inhibitors Complexed to the JAK1 and JAK2

Protein Tyrosine Kinase Domains. *Journal of Molecular Biology* **2009**, 387 (1), 219-232.

73. Morris, G. M.; Huey, R.; Lindstrom, W.; Sanner, M. F.; Belew, R. K.; Goodsell, D. S.; Olson, A. J., AutoDock4 and AutoDockTools4: Automated docking with selective receptor flexibility. *Journal of Computational Chemistry* **2009**, 30 (16), 2785-2791.

74. Kimura, Y.; Atarashi, S.; Kawakami, K.; Sato, K.; Hayakawa, I., (Fluorocyclopropyl)quinolones. 2. Synthesis and Stereochemical Structure-Activity Relationships of Chiral 7-(7-Amino-5-azaspiro[2.4]heptan-5-yl)-1-(2-fluorocyclopropyl)quinolone Antibacterial Agents. *Journal of Medicinal Chemistry* **1994**, 37 (20), 3344-3352.

75. Kawakami, K.; Atarashi, S.; Kimura, Y.; Takemura, M.; Hayakawa, I., Synthesis and Antibacterial Activity of Novel Pyridobenzoxazine Analogues. *Chemical and Pharmaceutical Bulletin* **1998**, 46 (11), 1710-1715.

76. Department of Medicine, S. o. M., Indiana University, P450 Drug Interaction Table. <http://medicine.iupui.edu/clinpharm/ddis/main-table>.

77. European Medicines Agency Assessment report - Xeljanz, International non-proprietary name: tofacitinib, Procedure No. EMEA/H/C/002542/0000.

http://www.ema.europa.eu/docs/en_GB/document_library/EPAR_-_Public_assessment_report/human/002542/WC500154697.pdf.

78. Chartier, M.; Chénard, T.; Barker, J.; Najmanovich, R., Kinome Render: a stand-alone and web-accessible tool to annotate the human protein kinome tree. *PeerJ* **2013**, 1, e126.

79. Ward, K. W.; Azzarano, L. M.; Evans, C. A.; Smith, B. R., Apparent absolute oral bioavailability in excess of 100% for a vitronectin receptor antagonist (SB-265123) in rat. I. Investigation of potential experimental and mechanistic explanations. *Xenobiotica* **2004**, 34 (4), 353-366.

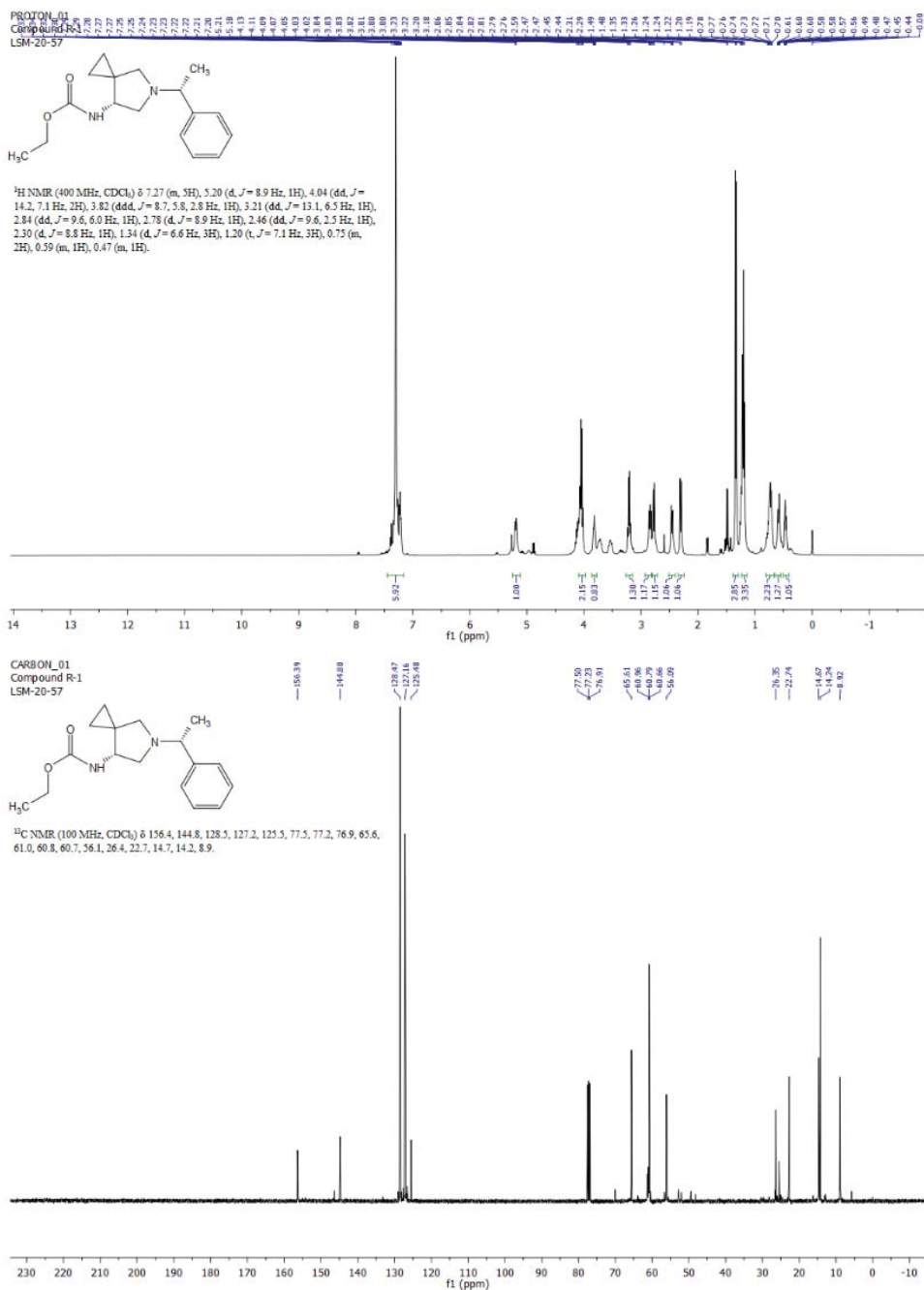
80. Weaver, R.; Riley, R. J., Identification and reduction of ion suppression effects on pharmacokinetic parameters by polyethylene glycol 400. *Rapid Communications in Mass Spectrometry* **2006**, 20 (17), 2559-2564.

81. Brand, D. D.; Latham, K. A.; Rosloniec, E. F., Collagen-induced arthritis. *Nat. Protocols* **2007**, 2 (5), 1269-1275.

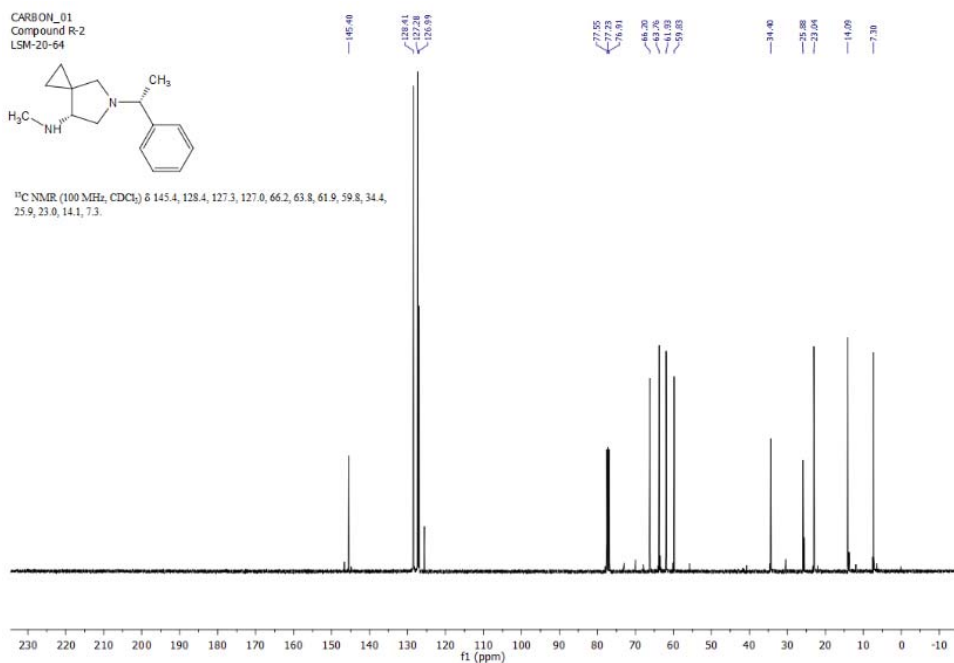
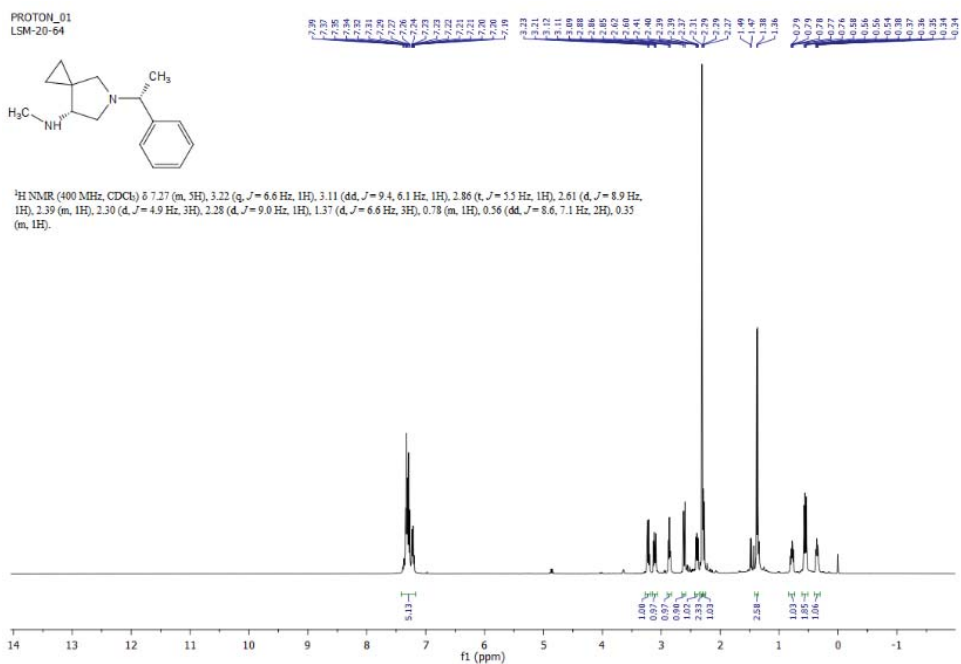
82. Whiteley, P. E.; Dalrymple, S. A., Models of Inflammation: Adjuvant-Induced Arthritis in the Rat. In *Current Protocols in Pharmacology*, John Wiley & Sons, Inc.: 2001.
83. Eurofins Protocol Guide – KinaseProfiler™ Service Assay Protocols v64.
http://www.komabiotech.co.kr/pdf/kinaseprofiler_assay_protocol_guide_eurofins_v64.pdf (accessed December 2017).
84. Protocol for the Successful Induction of Collagen-Induced Arthritis (CIA) in Mice. <https://www.chondrex.com/documents/Mouse%20CIA.pdf>.
85. CIA Induction in DBA/1 Mice. <https://hookelabs.com/protocols/pdf/CIA%20Induction%20in%20DBA1%20Mice.pdf>.
86. Sohn, K. C.; Kang, S. J.; Kim, J. W.; Kim, K. Y.; Ku, S. K.; Lee, Y. J., Effects of Calcium Gluconate, a Water Soluble Calcium Salt on the Collagen-Induced DBA/1J Mice Rheumatoid Arthritis. *Biomolecules & Therapeutics* **2013**, *21* (4), 290-298.

NMR spectra

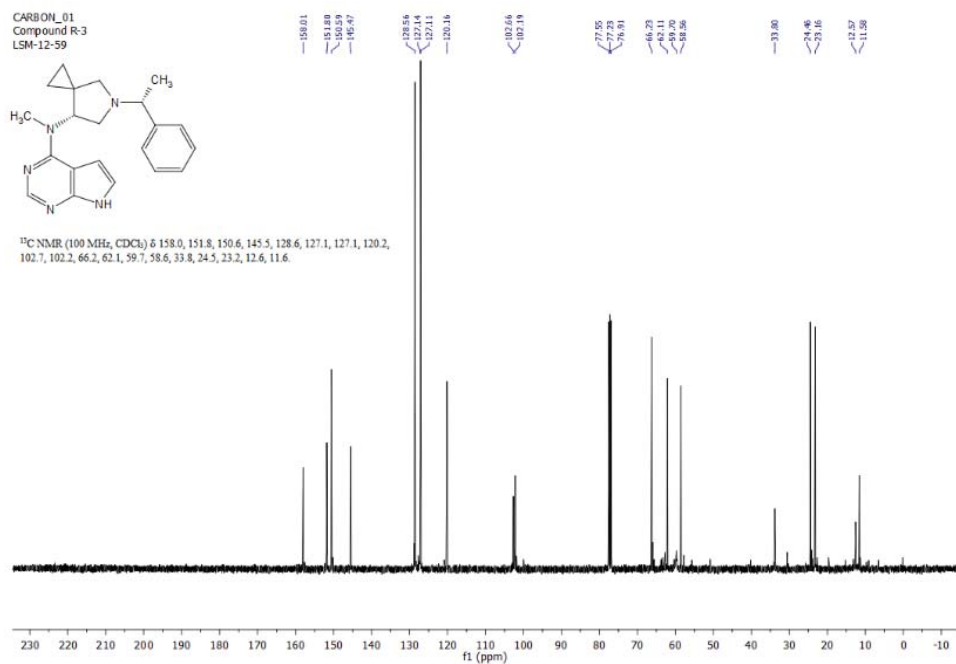
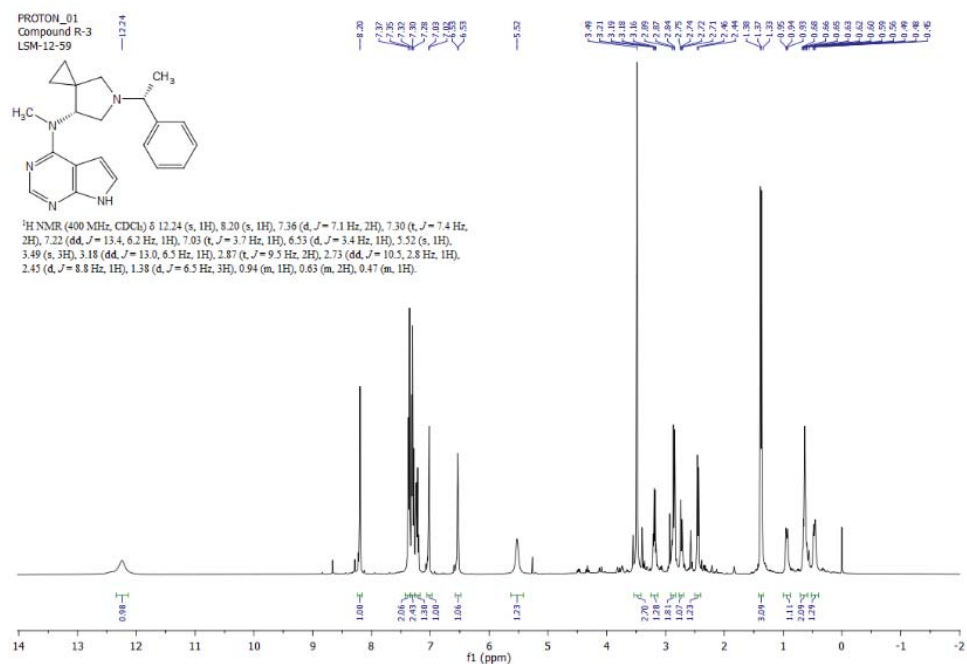
Ethyl ((R)-5-((R)-1-phenylethyl)-5-azaspiro[2.4]heptan-7-yl)carbamate, (R)-2c



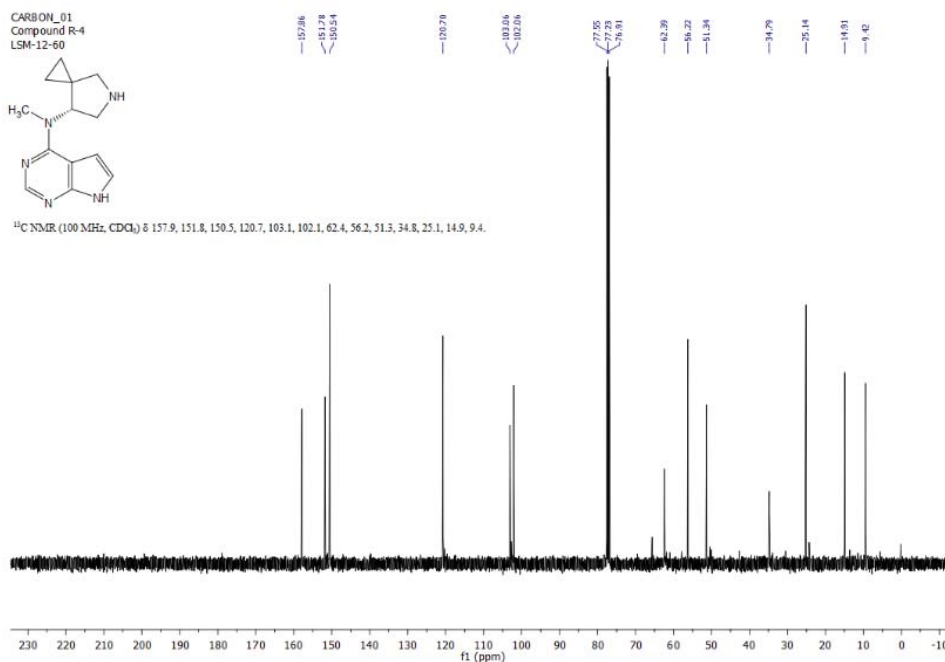
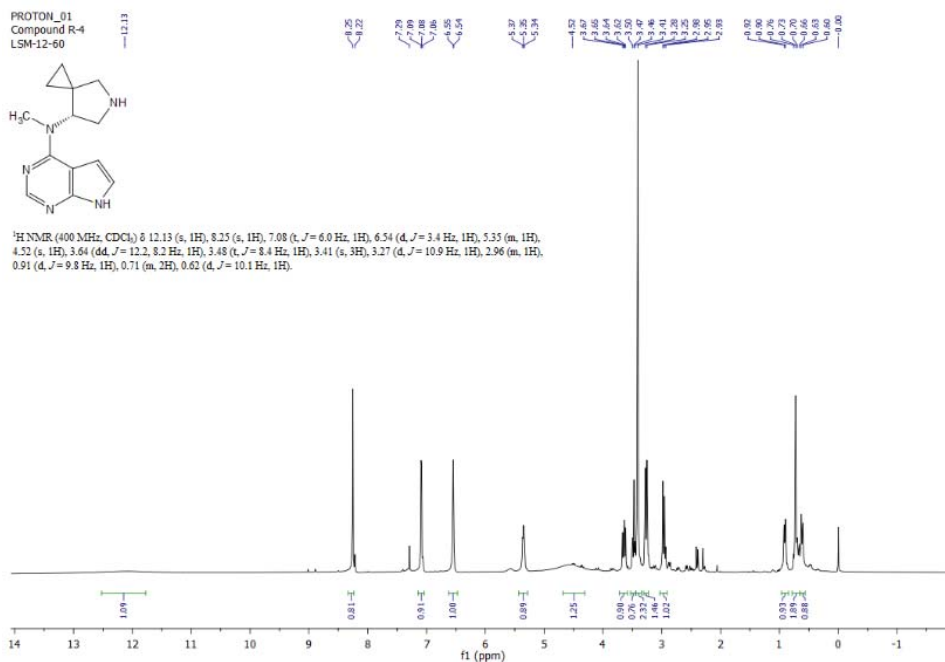
(R)-*N*-Methyl-5-((*R*)-1-phenylethyl)-5-azaspiro[2.4]heptan-7-amine, (*R*)-**3c**



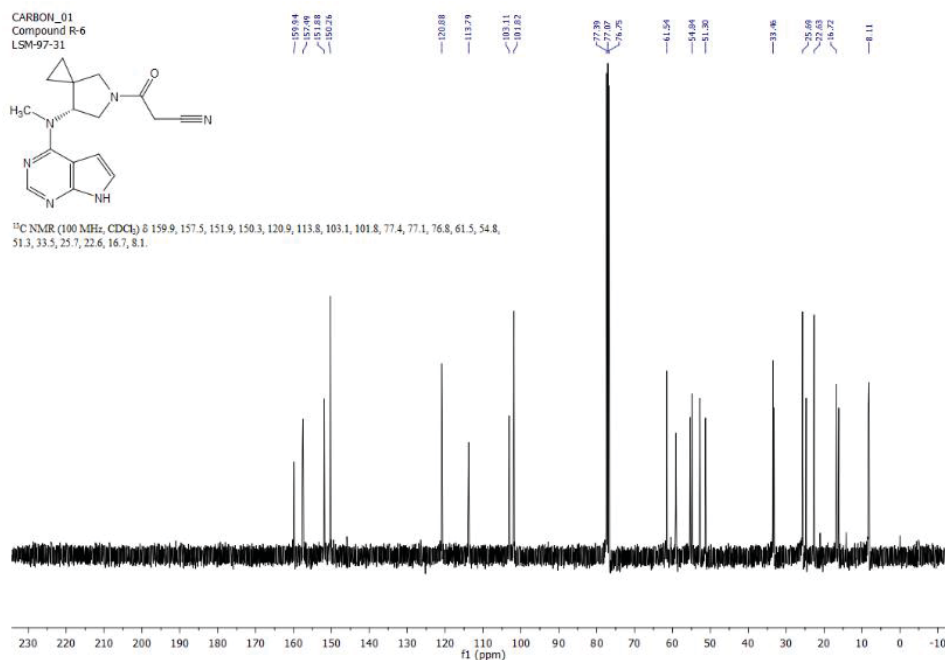
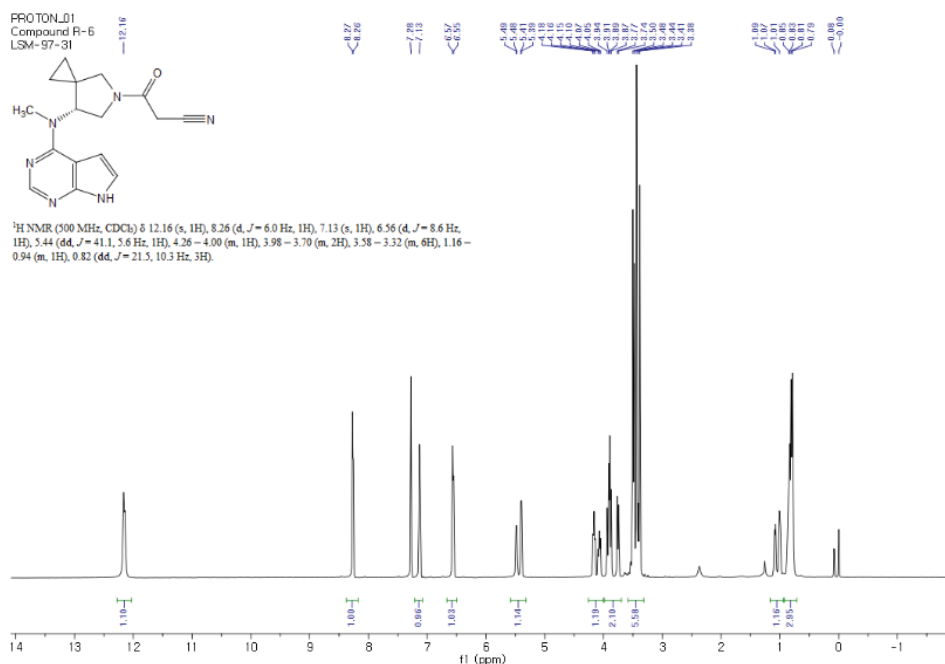
N-Methyl-*N*-((*R*)-5-((*R*)-1-phenylethyl)-5-azaspiro[2.4]heptan-7-yl)-7*H*-pyrrolo[2,3-*d*]pyrimidin-4-amine, (**R**)-**4c**



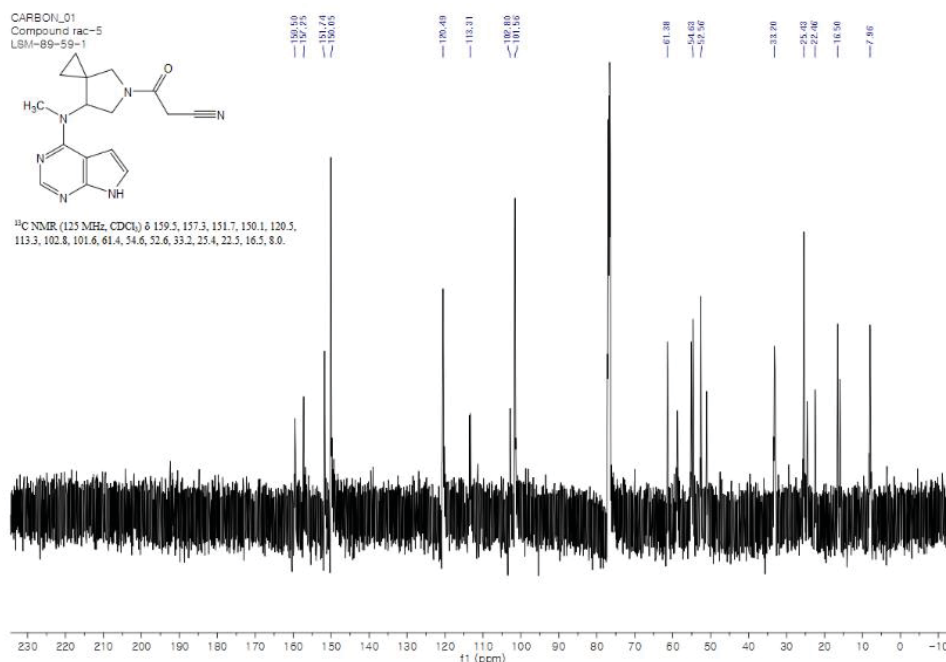
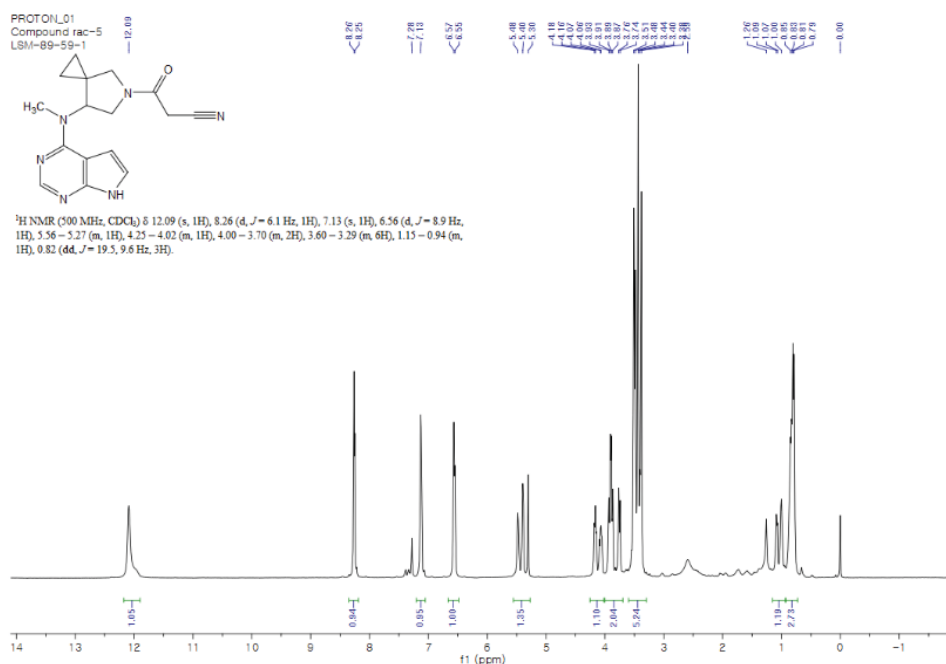
(R)-*N*-Methyl-*N*-(5-azaspiro[2.4]heptan-7-yl)-7*H*-pyrrolo[2,3-*d*]pyrimidin-4-amine,
(R)-5c



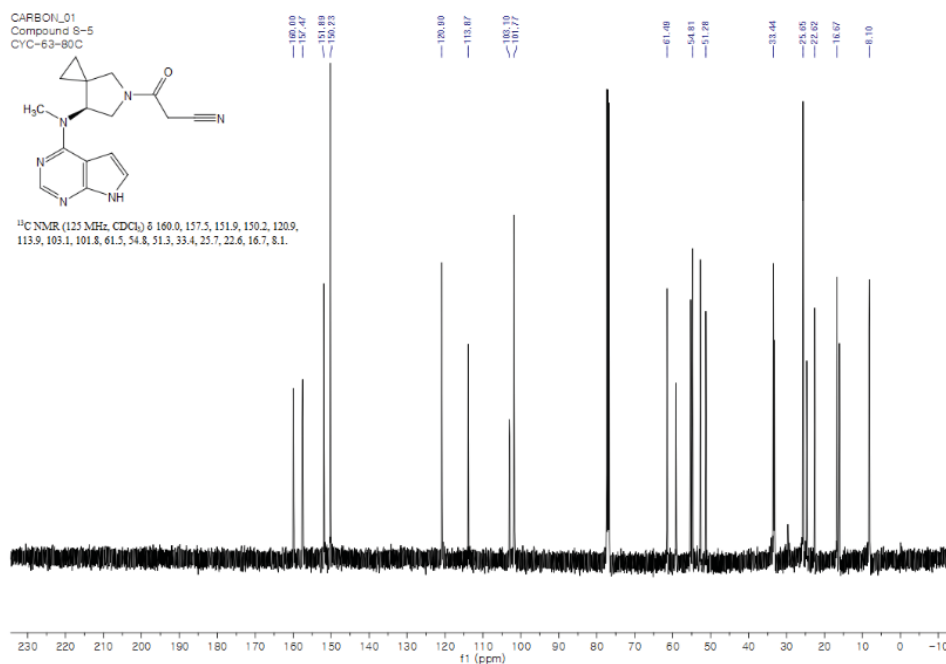
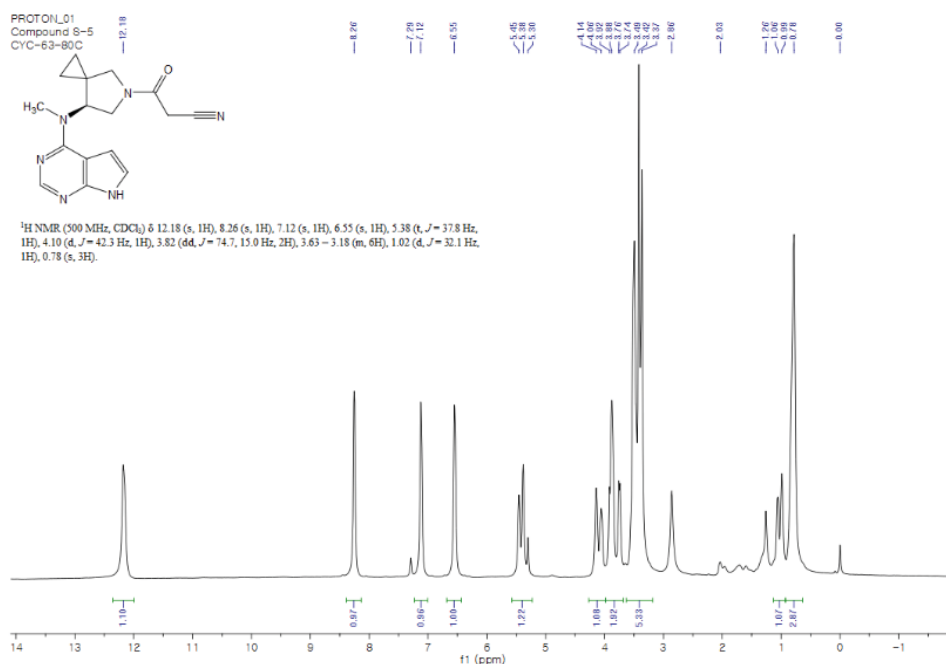
(R)-3-(7-(Methyl(7*H*-pyrrolo[2,3-*d*]pyrimidin-4-yl)amino)-5-azaspiro[2.4]heptan-5-yl)-3-oxopropanenitrile, (**R**)-**6c**



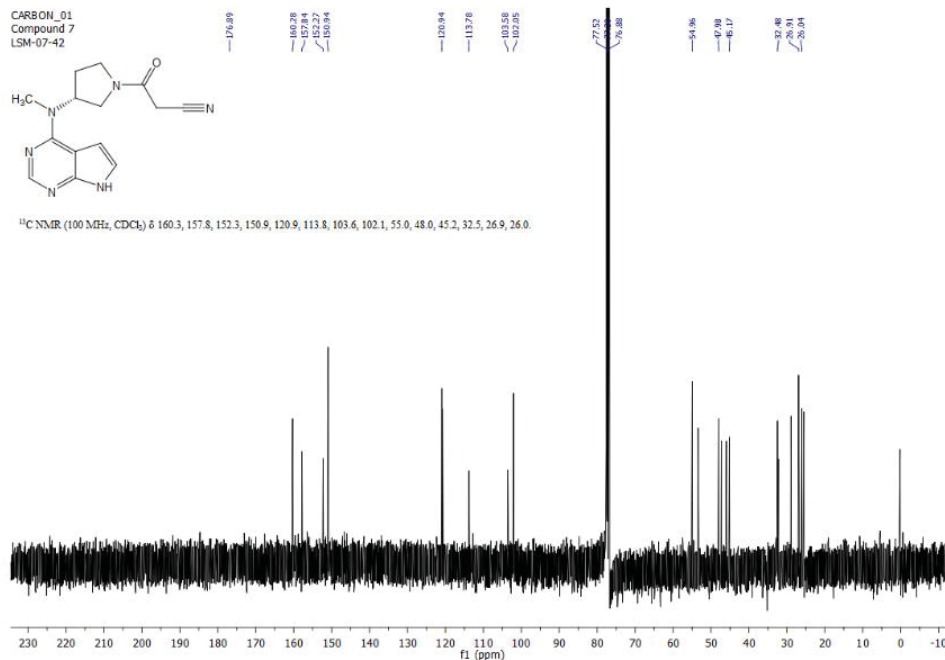
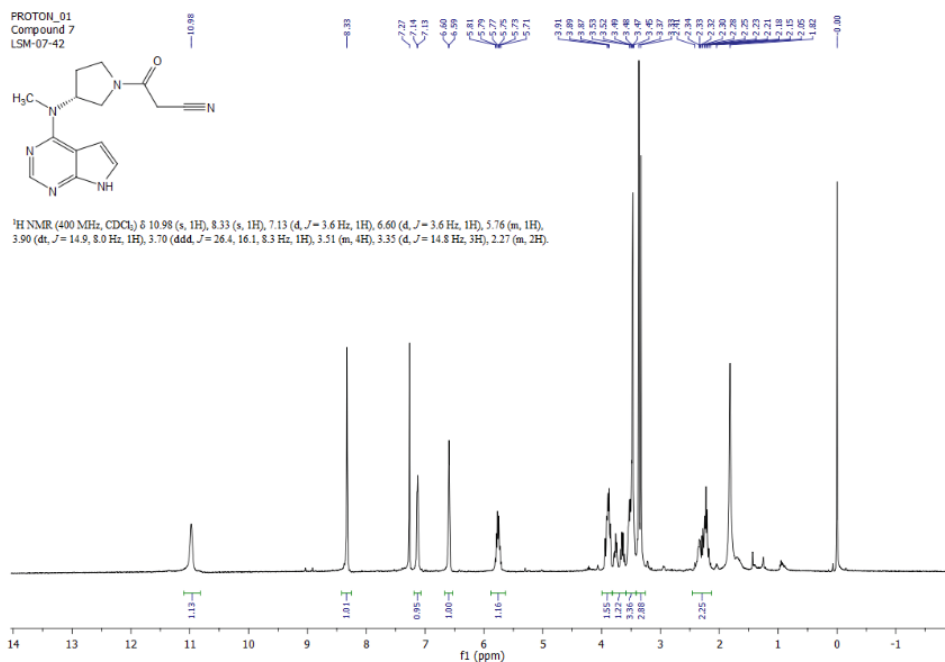
3-(7-(Methyl(7H-pyrrolo[2,3-d]pyrimidin-4-yl)amino)-5-azaspiro[2.4]heptan-5-yl)-3-oxopropanenitrile, **6c**



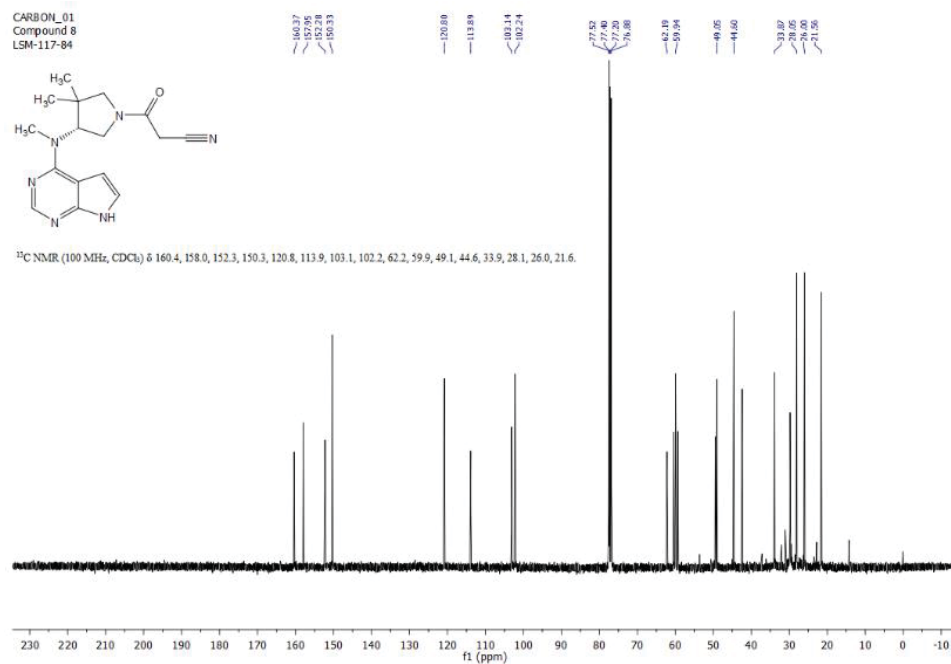
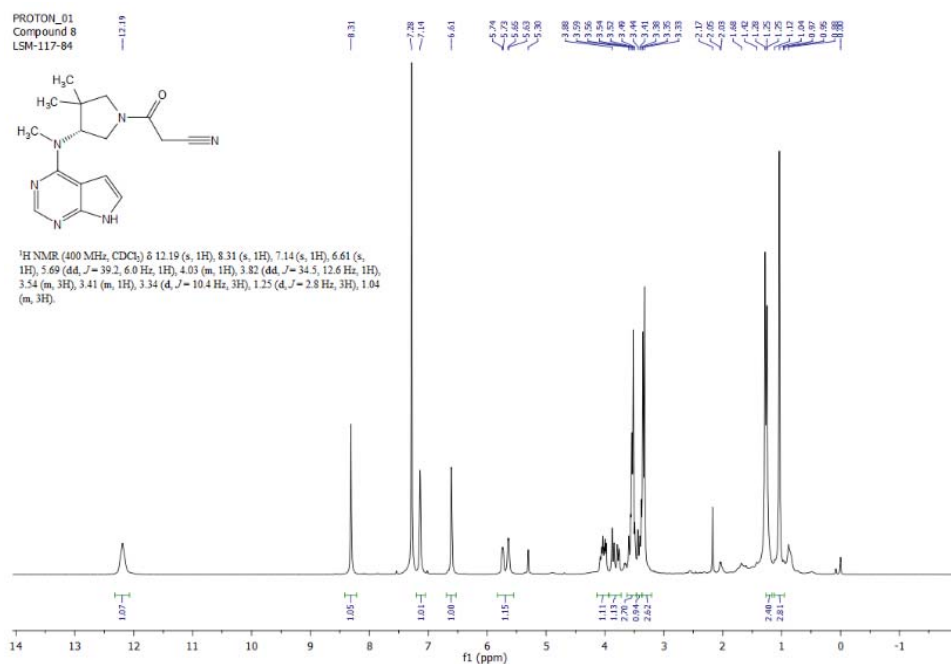
(S)-3-(7-(Methyl(7*H*-pyrrolo[2,3-*d*]pyrimidin-4-yl)amino)-5-azaspiro[2.4]heptan-5-yl)-3-oxopropanenitrile, (**S**)-**6c**



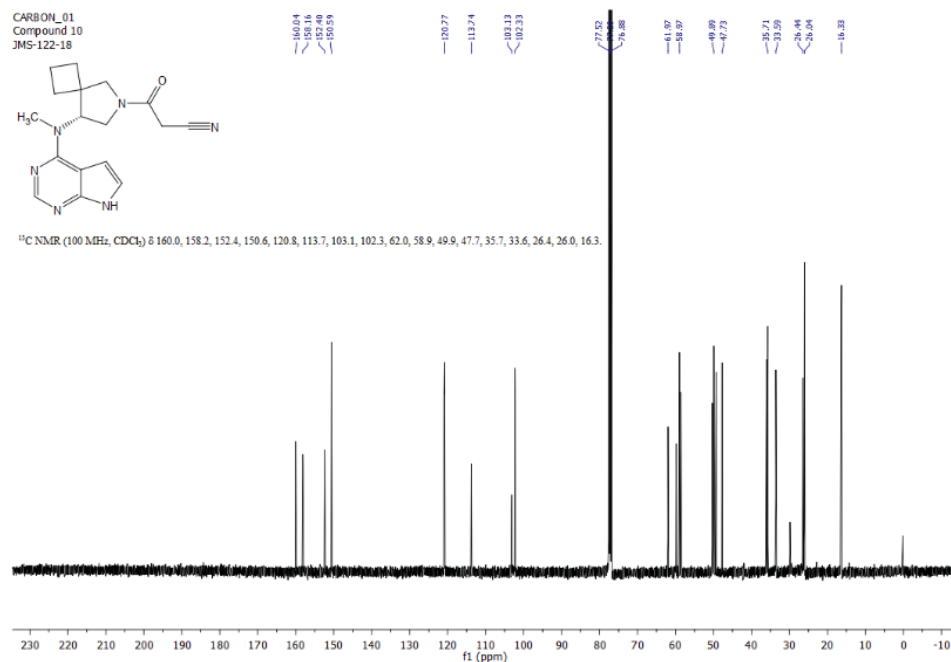
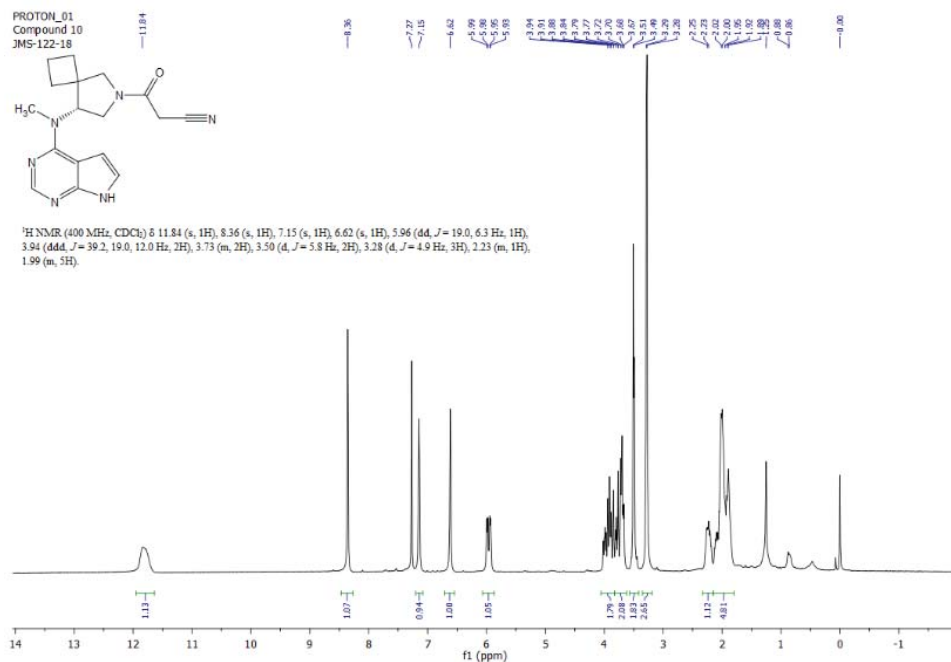
(*R*)-3-(3-(Methyl(7*H*-pyrrolo[2,3-*d*]pyrimidin-4-yl)amino)pyrrolidin-1-yl)-3-oxopropanenitrile, **12a**



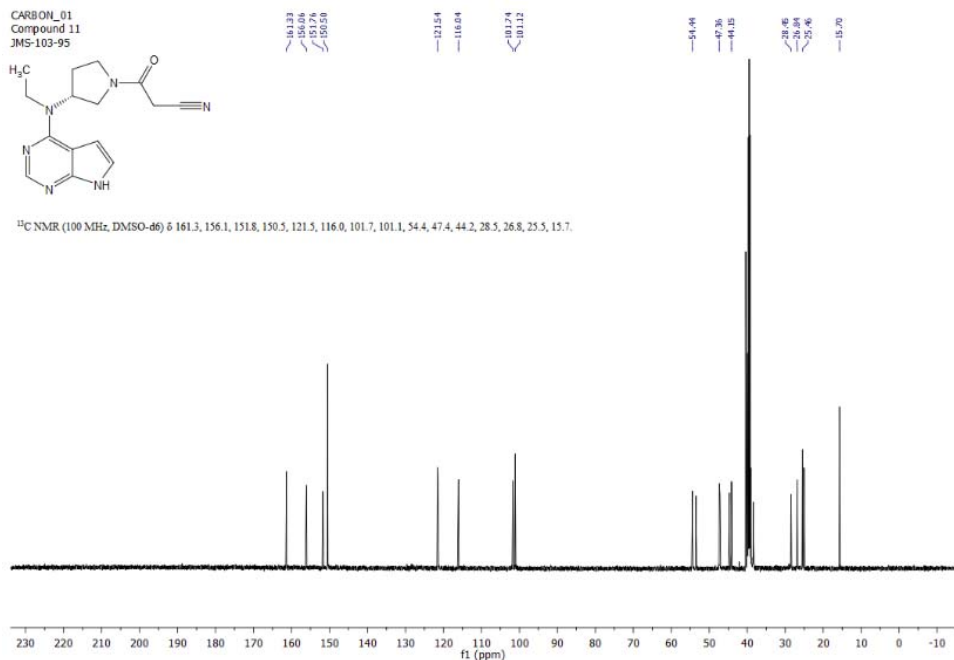
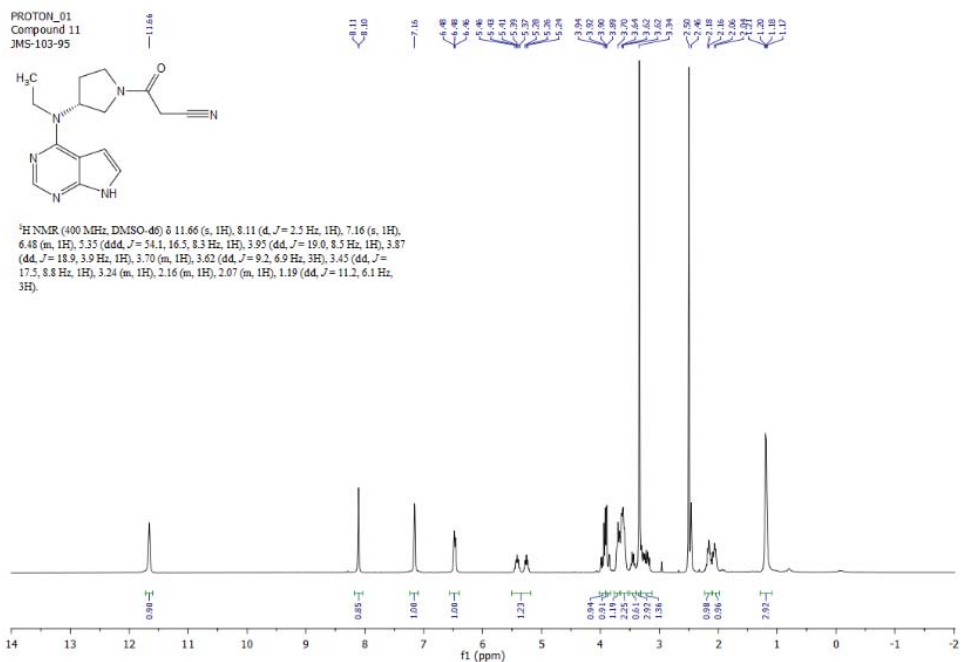
(R)-3-(3,3-Dimethyl-4-(methyl(7H-pyrrolo[2,3-d]pyrimidin-4-yl)amino)pyrrolidin-1-yl)-3-oxopropanenitrile, **12b**



(R)-3-(8-(Methyl(7H-pyrrolo[2,3-d]pyrimidin-4-yl)amino)-6-azaspiro[3.4]octan-6-yl)-3-oxopropanenitrile, **12c**



(R)-3-(3-(Ethyl(7*H*-pyrrolo[2,3-*d*]pyrimidin-4-yl)amino)pyrrolidin-1-yl)-3-oxopropanenitrile, **13**



PROTON_01
Compound 12
JMS-103-98

N#CCCC(=O)N1CC[C@H](C1)N(C2CC3C=CC=C4N=CN=C34)C2

¹H NMR (400 MHz, CDCl₃) δ 12.03 (d, *J* = 14.0 Hz, 1H), 8.35 (d, *J* = 5.1 Hz, 1H), 7.17 (d, *J* = 5.0 Hz, 1H), 6.67 (m, 1H), 5.30 (ddt, *J* = 25.0, 16.8, 8.3 Hz, 1H), 3.93 (m, 2H), 3.63 (m, 3H), 3.49 (m, 3H), 2.33 (ddt, *J* = 17.5, 12.0, 9.6 Hz, 2H), 1.18 (m, 1H), 0.69 (t, *J* = 8.9 Hz, 2H), 0.36 (m, 2H).

12.03
8.35
7.17
6.67
5.30
3.93
3.63
3.49
2.33
1.18
0.69
0.36

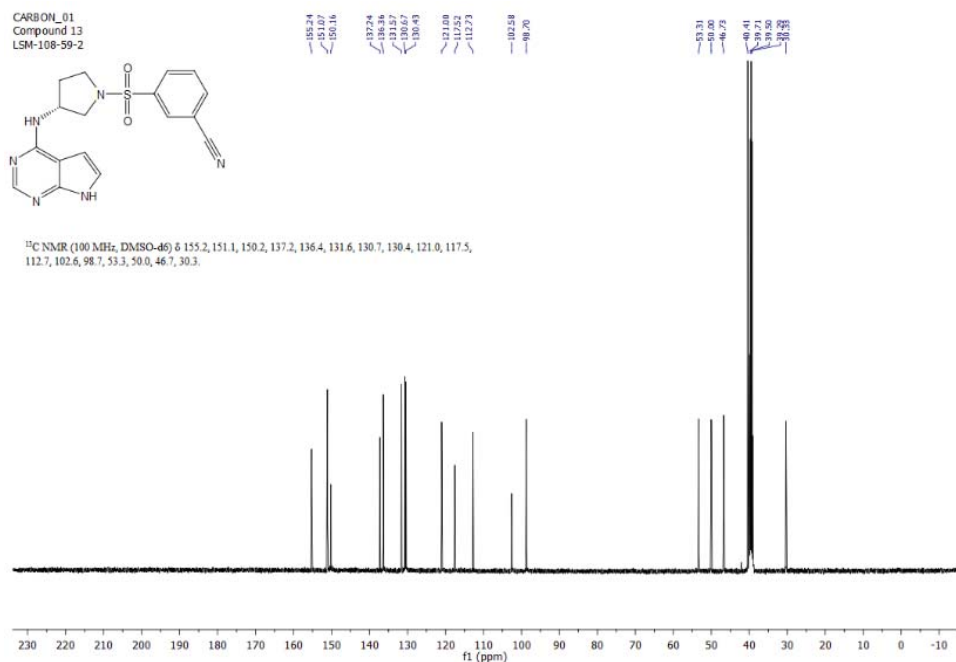
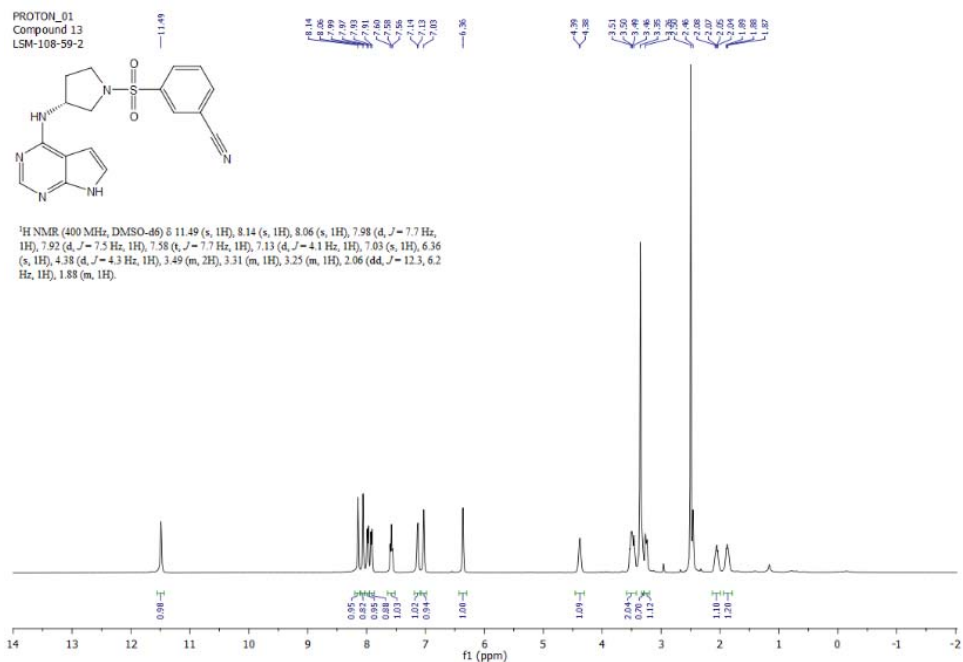
1.09
0.87
0.96
1.00
1.12
2.64
2.95
2.40
2.13
1.24
1.87
0.35

14 13 12 11 10 9 8 7 6 5 4 3 2 1 0 -1

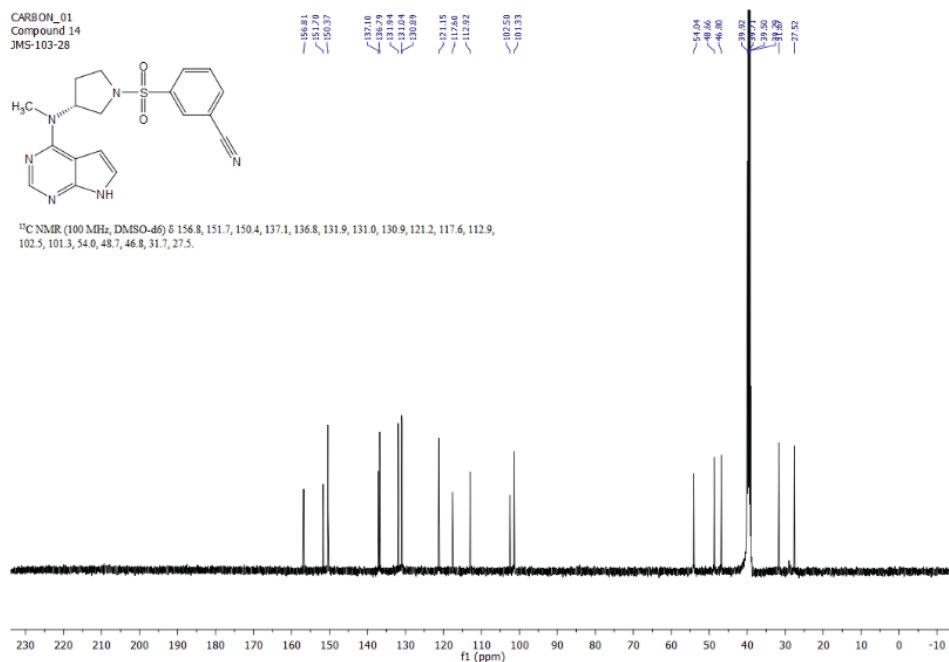
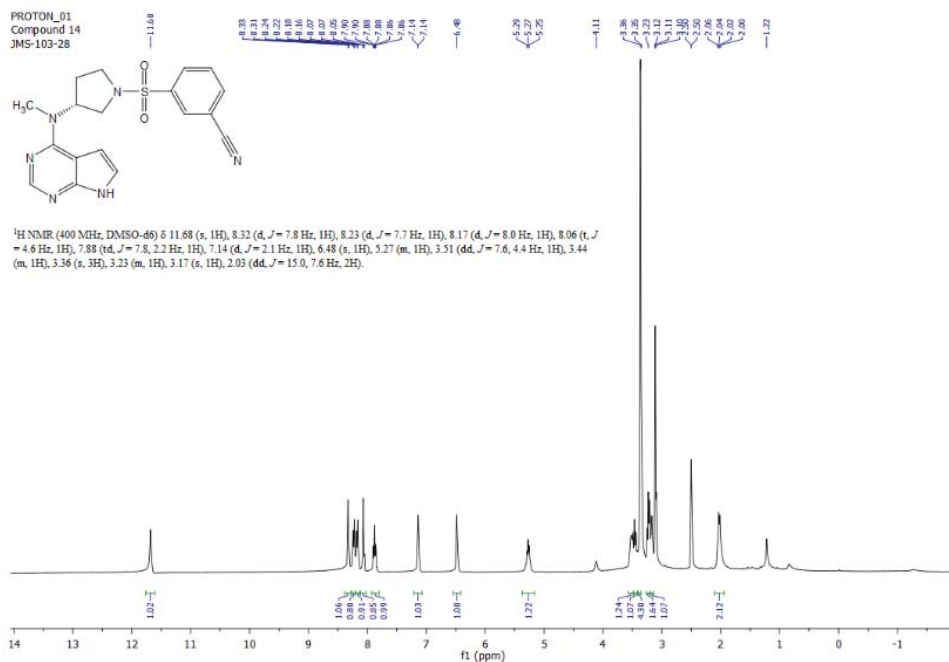
ft (ppm)



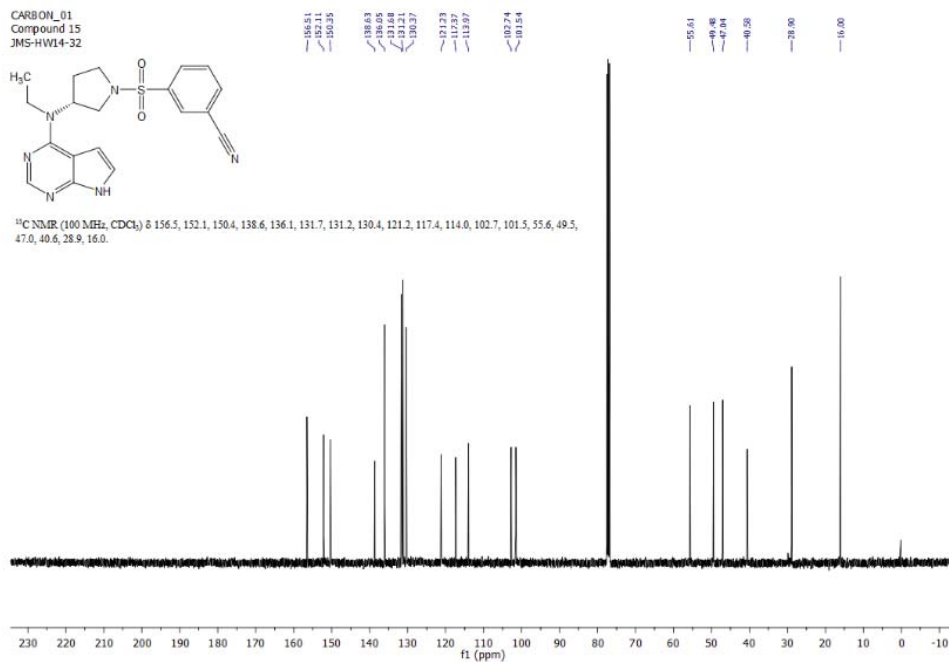
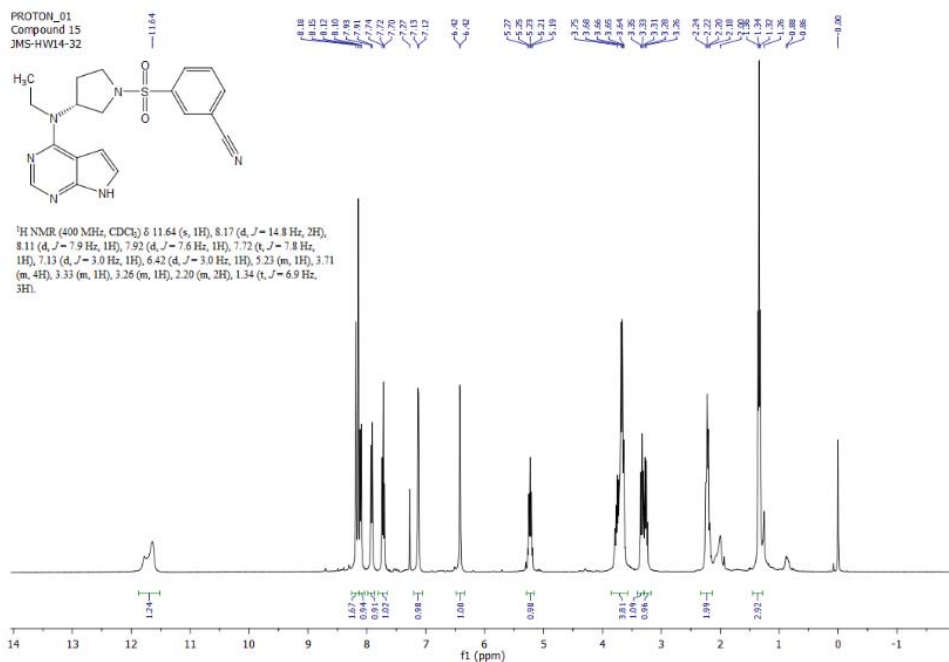
(R)-3-((3-((7H-Pyrrolo[2,3-d]pyrimidin-4-yl)amino)pyrrolidin-1-yl)sulfonyl)benzonitrile, **15**



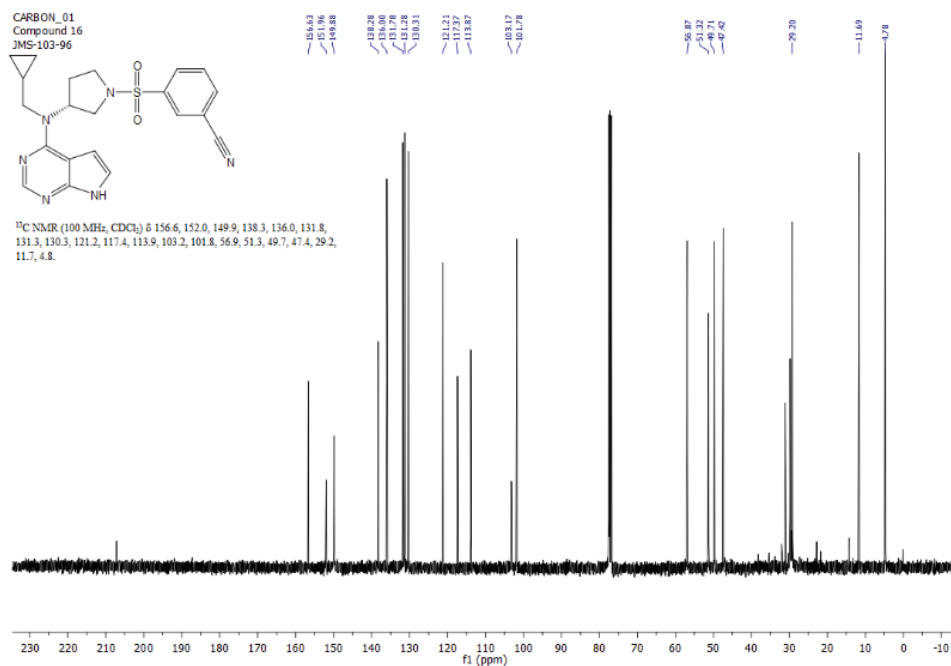
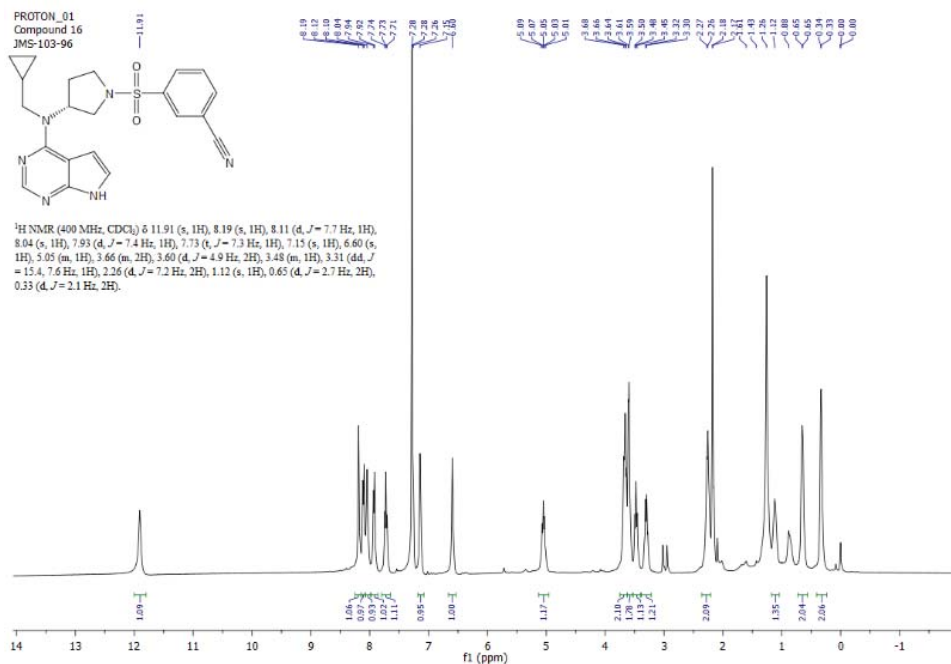
(R)-3-((3-(Methyl(7H-pyrrolo[2,3-d]pyrimidin-4-yl)amino)pyrrolidin-1-yl)sulfonyl)benzonitrile, **16**



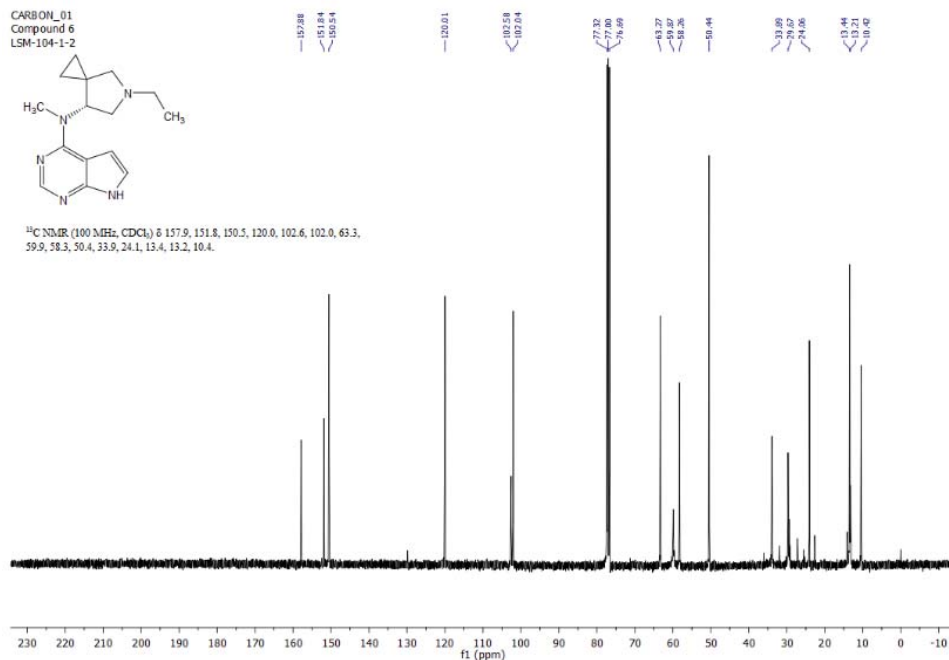
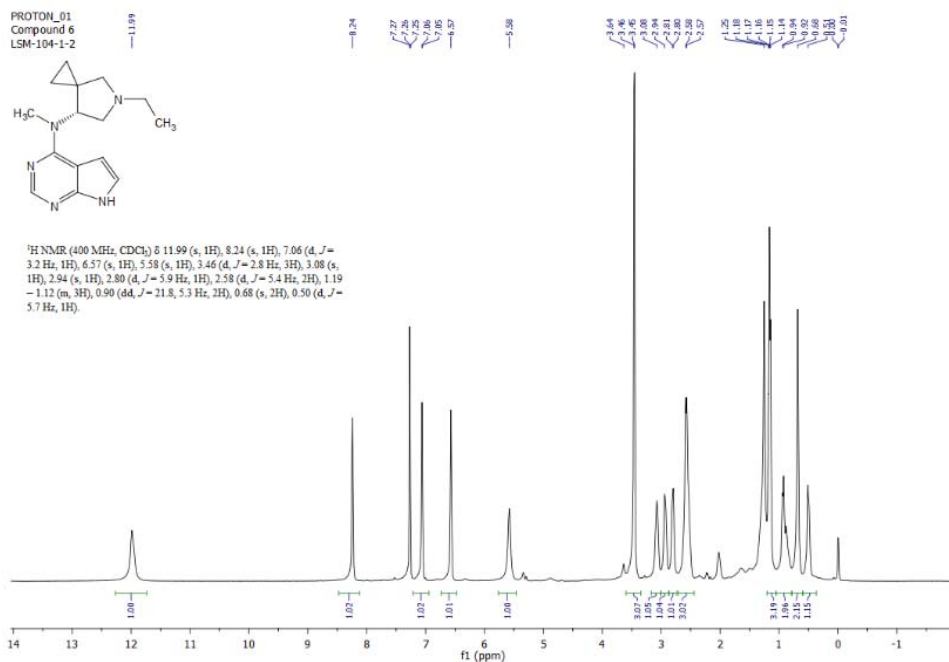
(R)-3-((3-(Ethyl(7H-pyrrolo[2,3-d]pyrimidin-4-yl)amino)pyrrolidin-1-yl)sulfonyl)benzonitrile, **17**



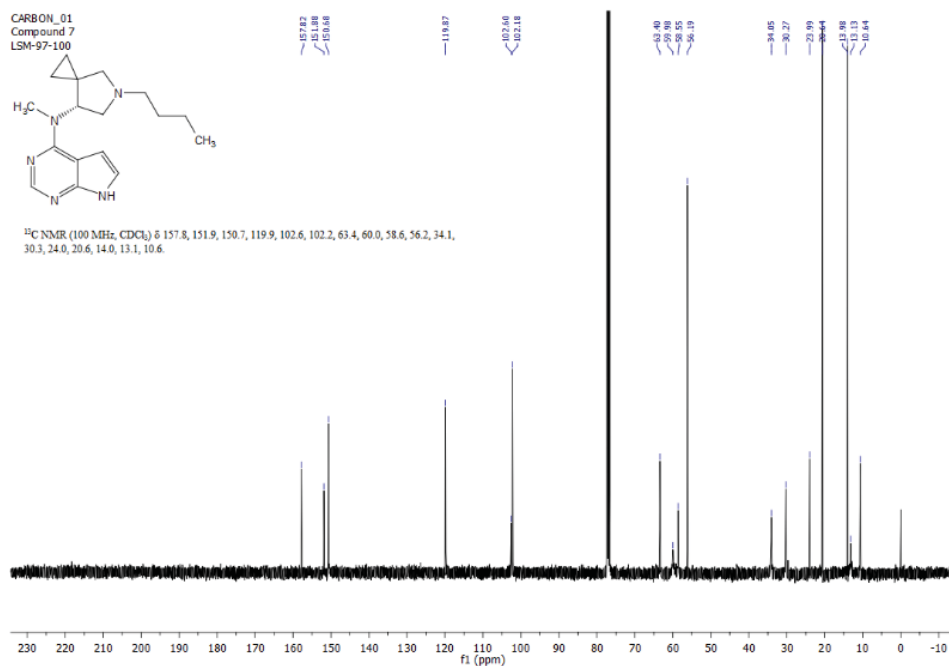
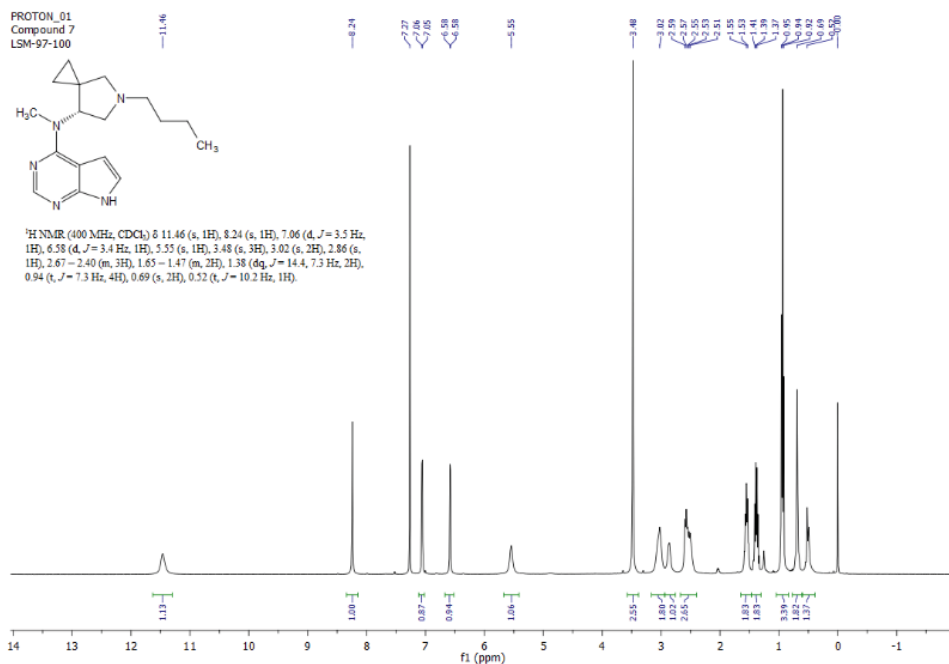
(R)-3-((3-((Cyclopropylmethyl)(7*H*-pyrrolo[2,3-*d*]pyrimidin-4-yl)amino)pyrrolidin-1-yl)sulfonyl)benzonitrile, **18**



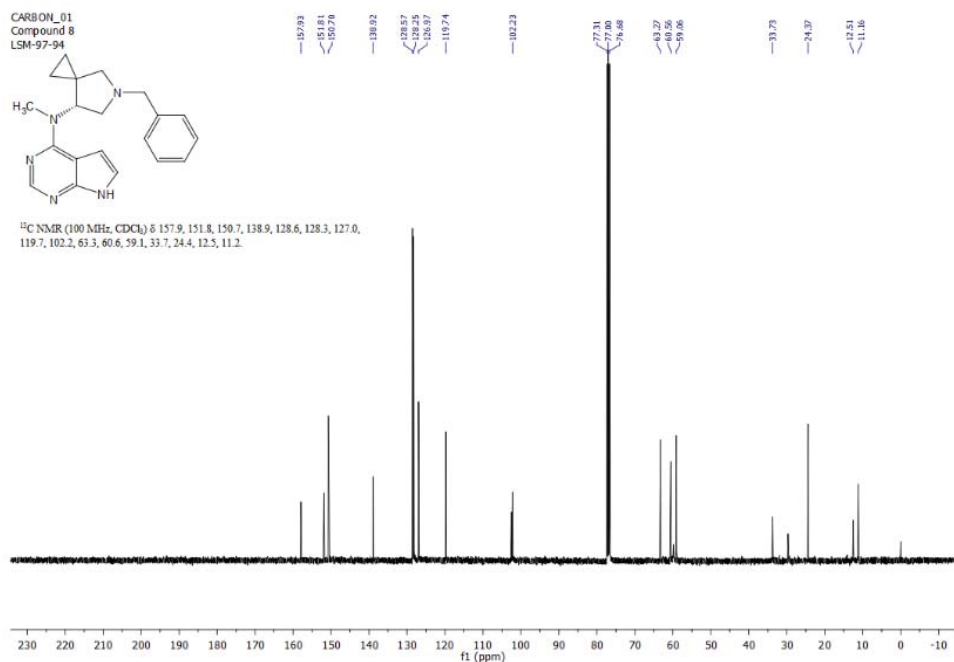
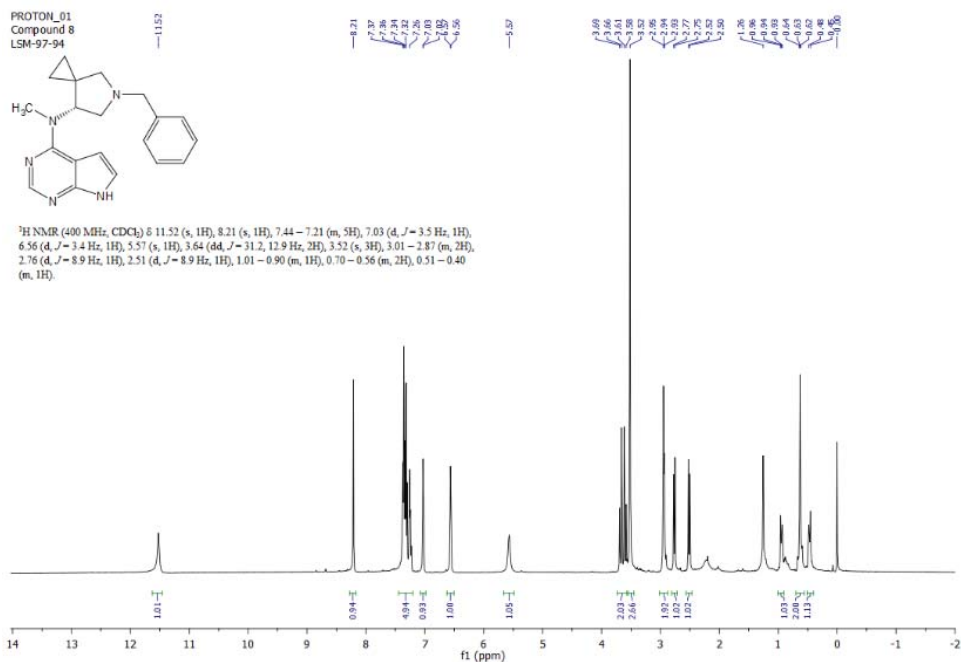
(R)-*N*-(5-Ethyl-5-azaspiro[2.4]heptan-7-yl)-*N*-methyl-7*H*-pyrrolo[2,3-*d*]pyrimidin-4-amine, **19**



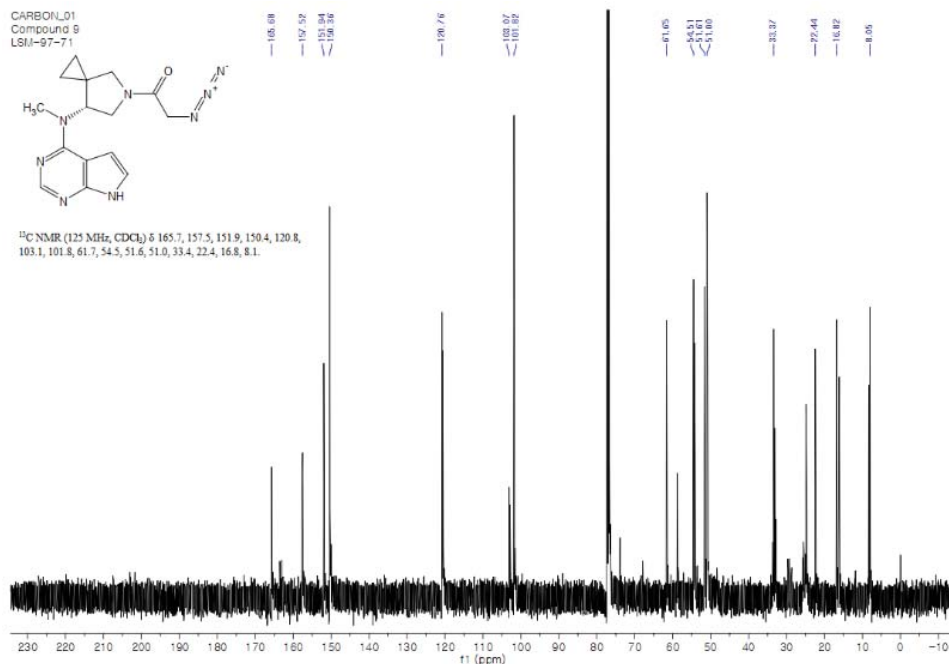
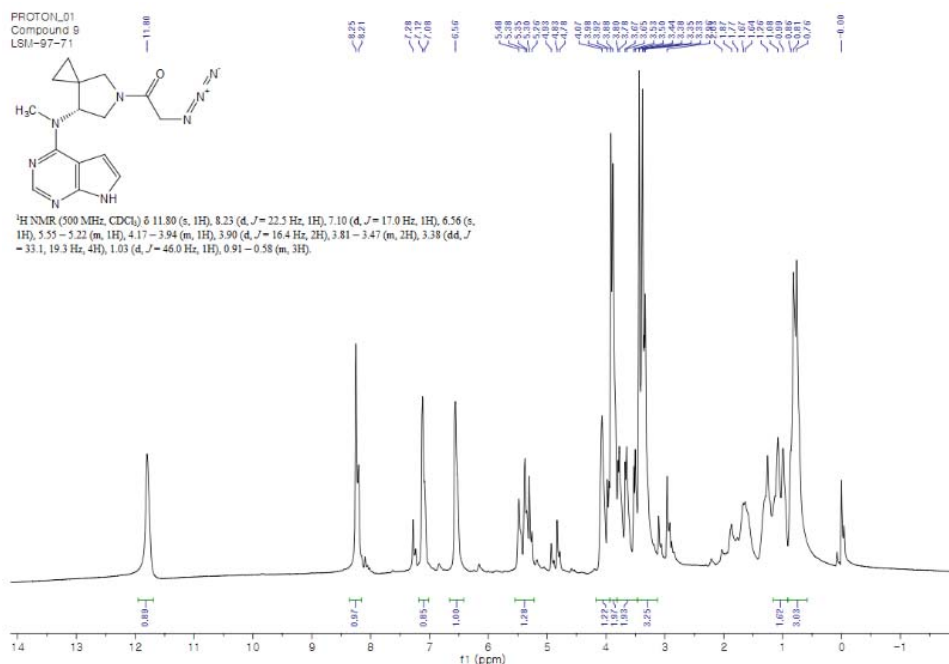
(R)-*N*-(5-Butyl-5-azaspiro[2.4]heptan-7-yl)-*N*-methyl-7*H*-pyrrolo[2,3-*d*]pyrimidin-4-amine, **20**



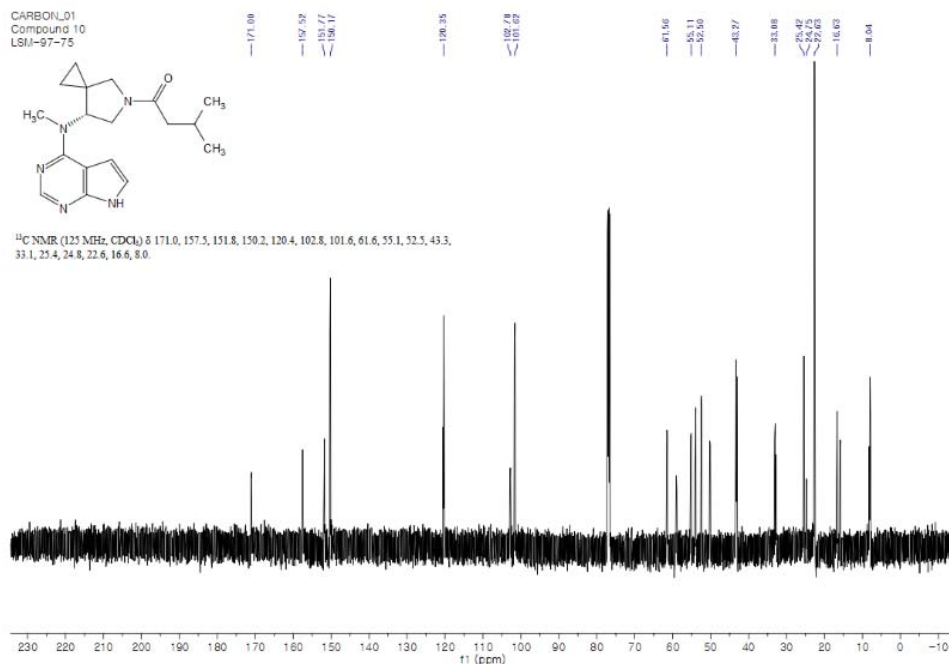
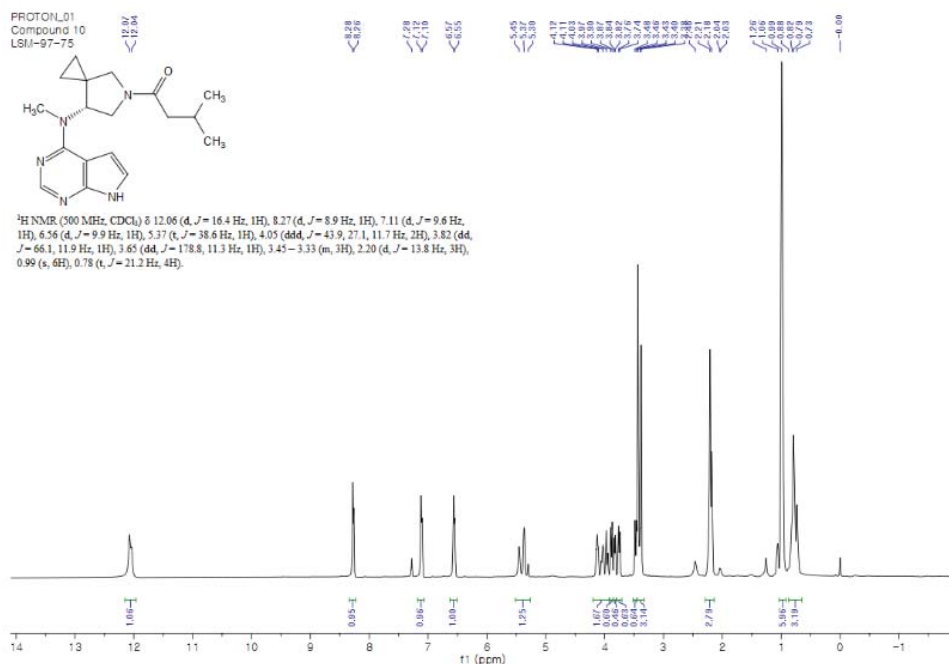
(R)-*N*-(5-Benzyl-5-azaspiro[2.4]heptan-7-yl)-*N*-methyl-7*H*-pyrrolo[2,3-*d*]pyrimidin-4-amine, **21**

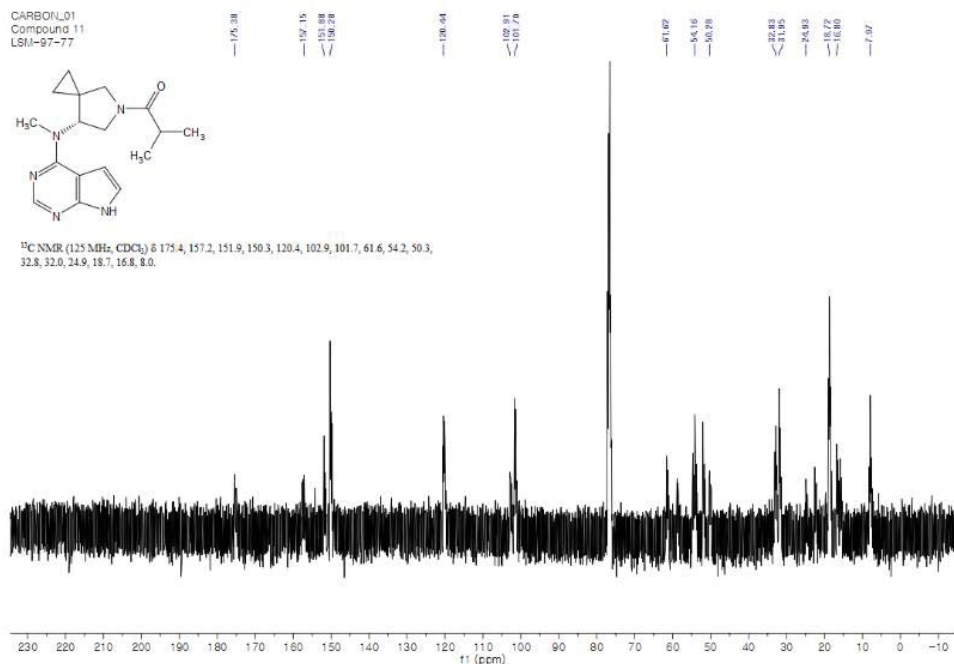


(R)-2-Azido-1-(7-(methyl(7H-pyrrolo[2,3-d]pyrimidin-4-yl)amino)-5-azaspiro[2.4]heptan-5-yl)ethan-1-one, **22**

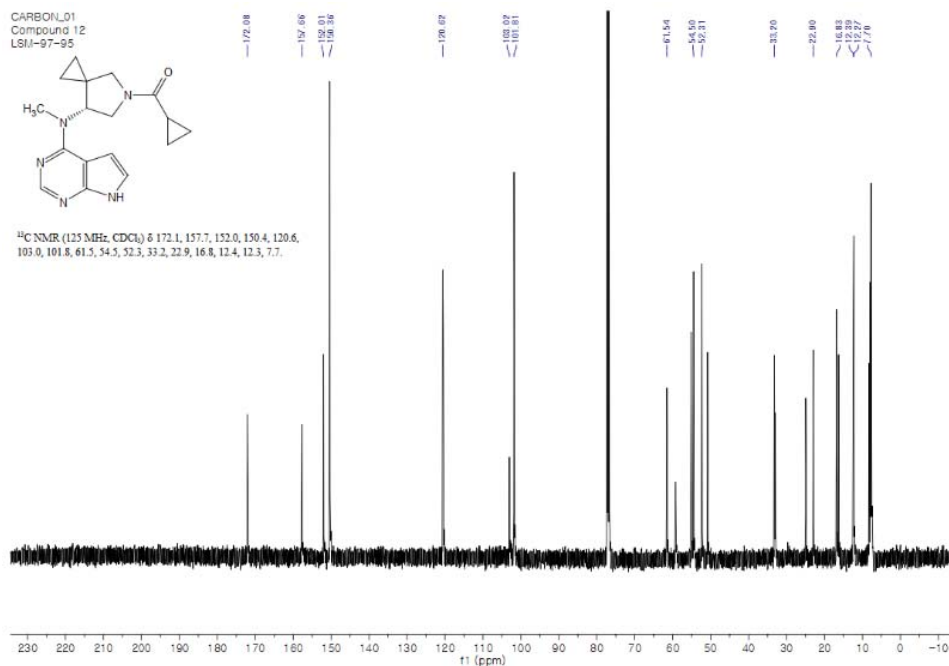
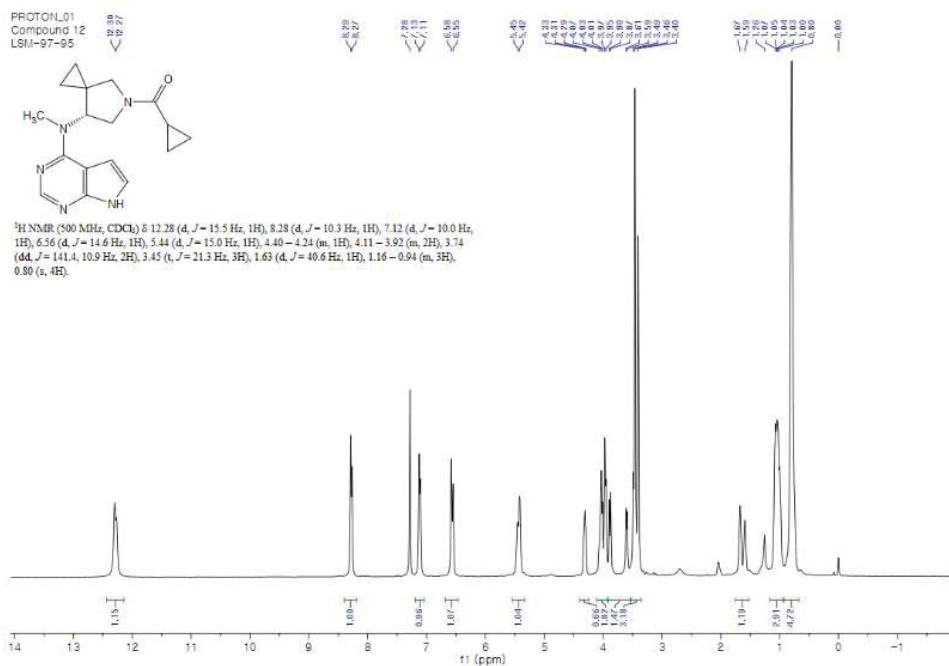


(R)-3-Methyl-1-(7-(methyl(7H-pyrrolo[2,3-d]pyrimidin-4-yl)amino)-5-azaspiro[2.4]heptan-5-yl)butan-1-one, **23**

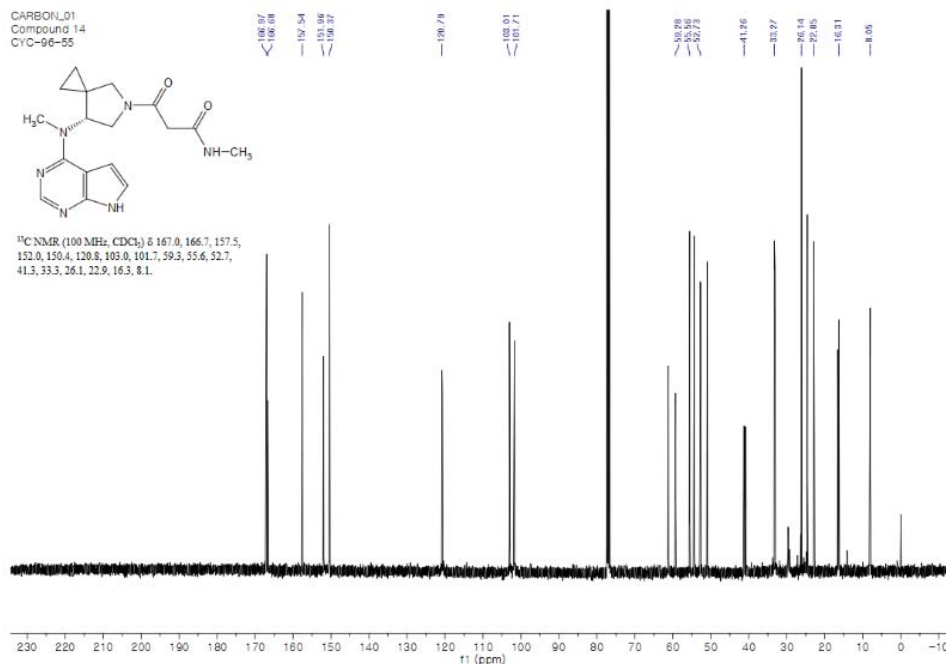
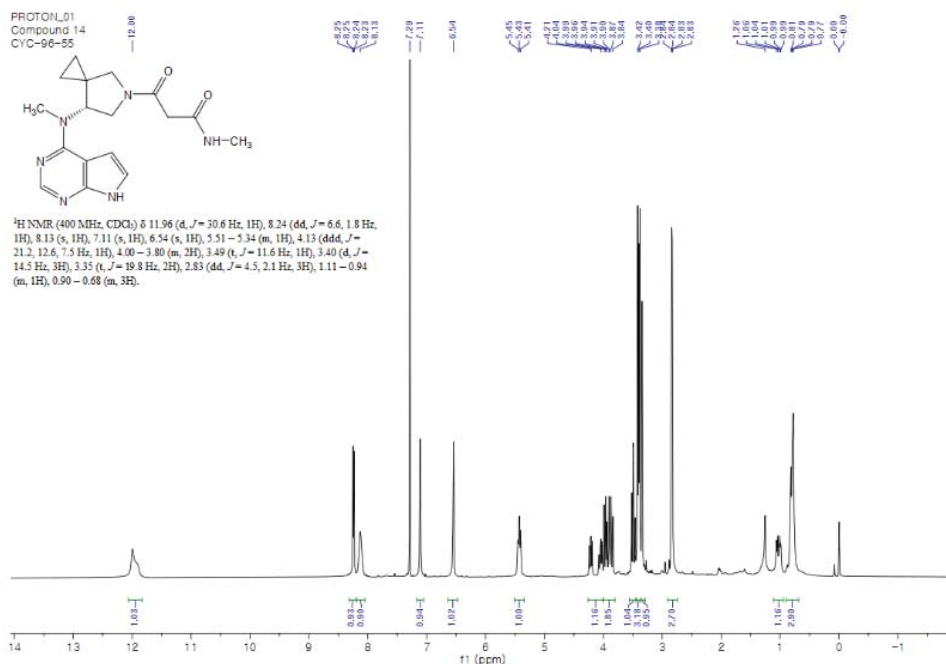




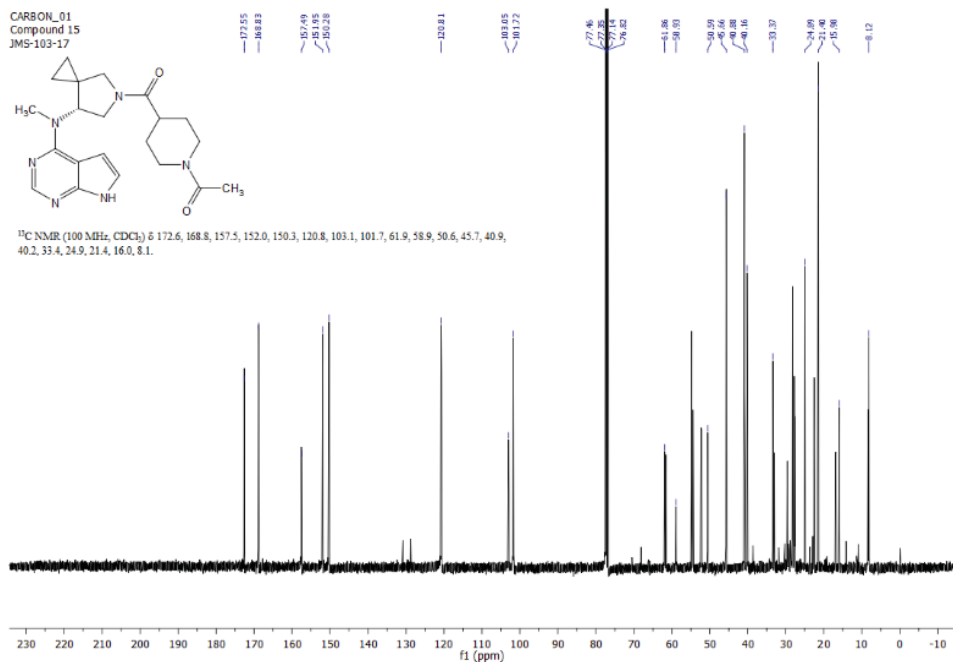
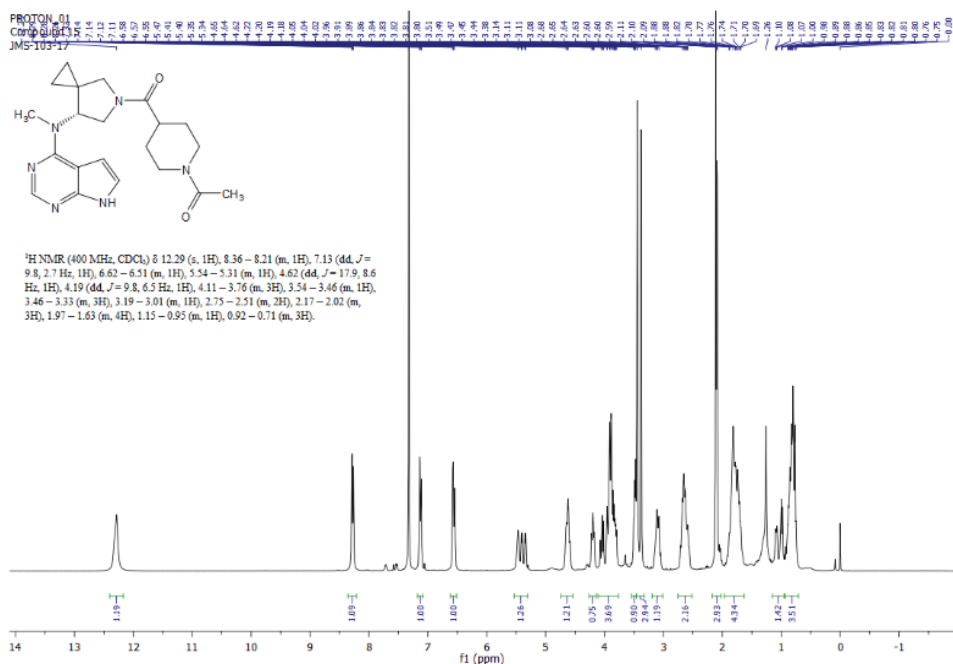
(*R*)-Cyclopropyl(7-(methyl(7*H*-pyrrolo[2,3-*d*]pyrimidin-4-yl)amino)-5-azaspiro[2.4]heptan-5-yl)methanone, **25**



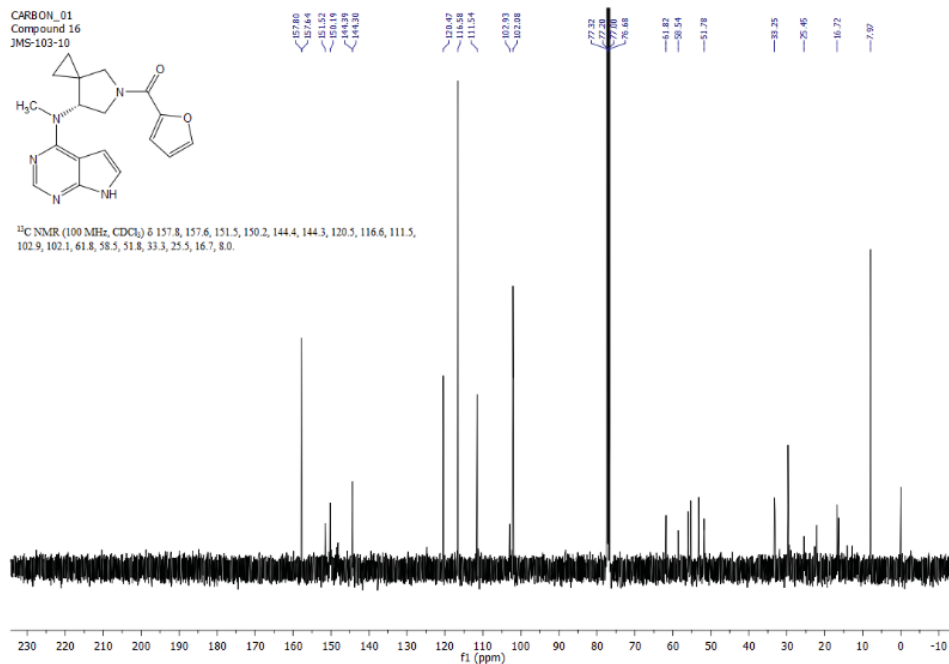
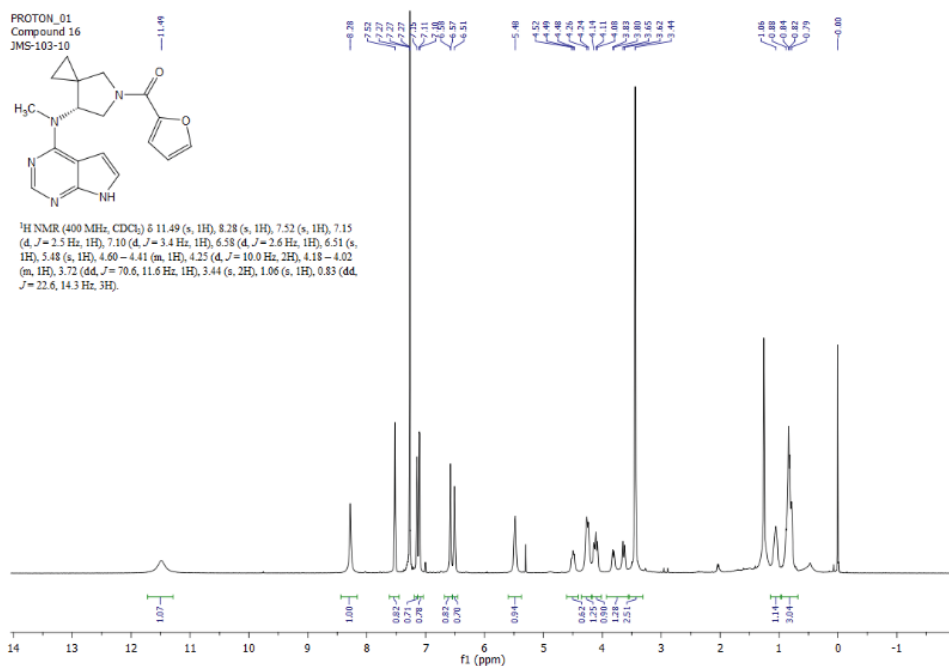
(R)-*N*-Methyl-3-(7-(methyl(7*H*-pyrrolo[2,3-*d*]pyrimidin-4-yl)amino)-5-azaspiro[2.4]heptan-5-yl)-3-oxopropanamide, 27



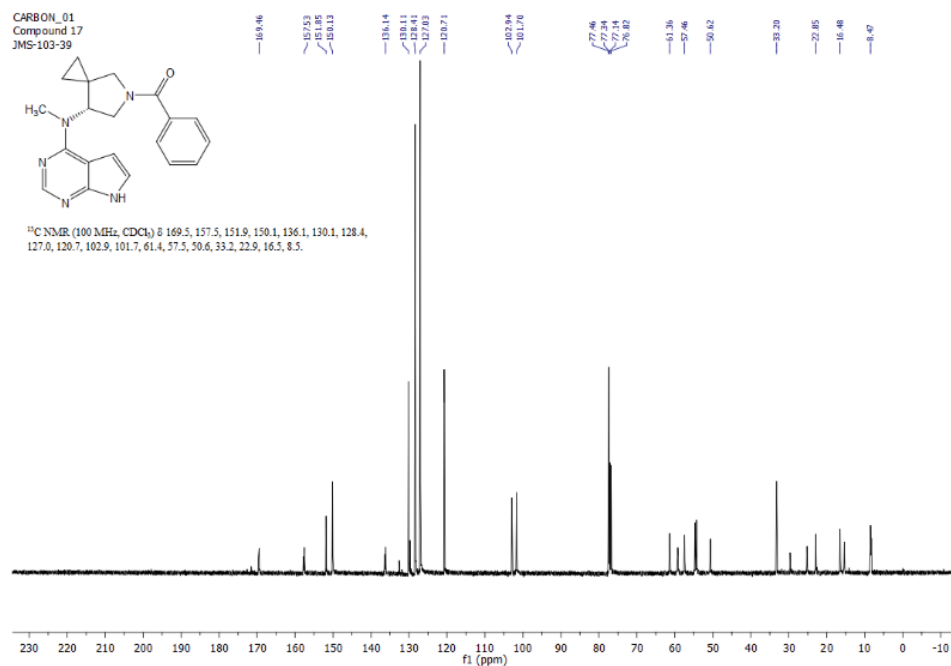
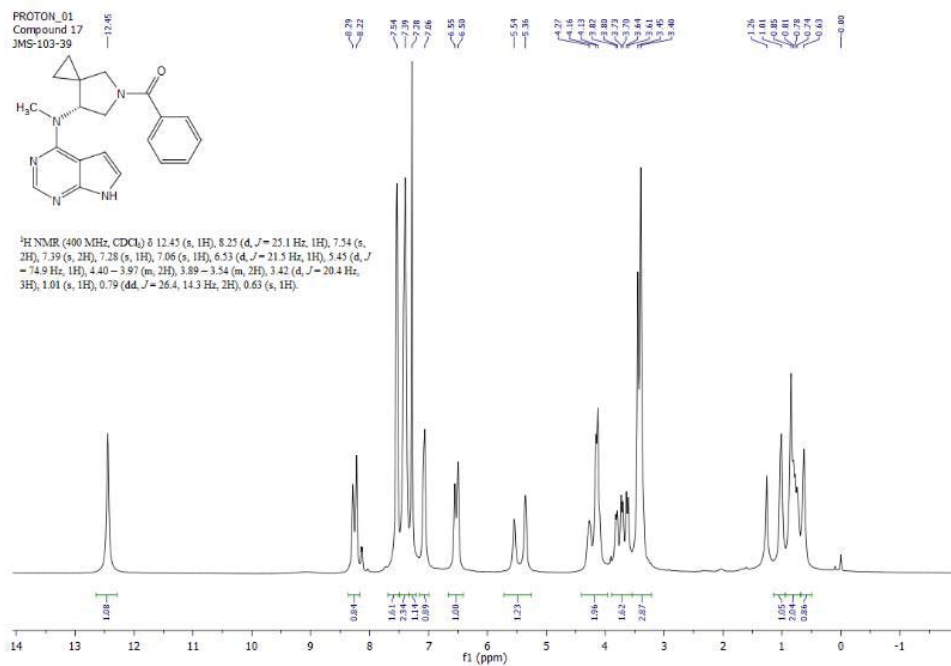
(R)-1-(4-(7-(Methyl(7H-pyrrolo[2,3-d]pyrimidin-4-yl)amino)-5-azaspiro[2.4]heptane-5-carbonyl)piperidin-1-yl)ethan-1-one, **28**



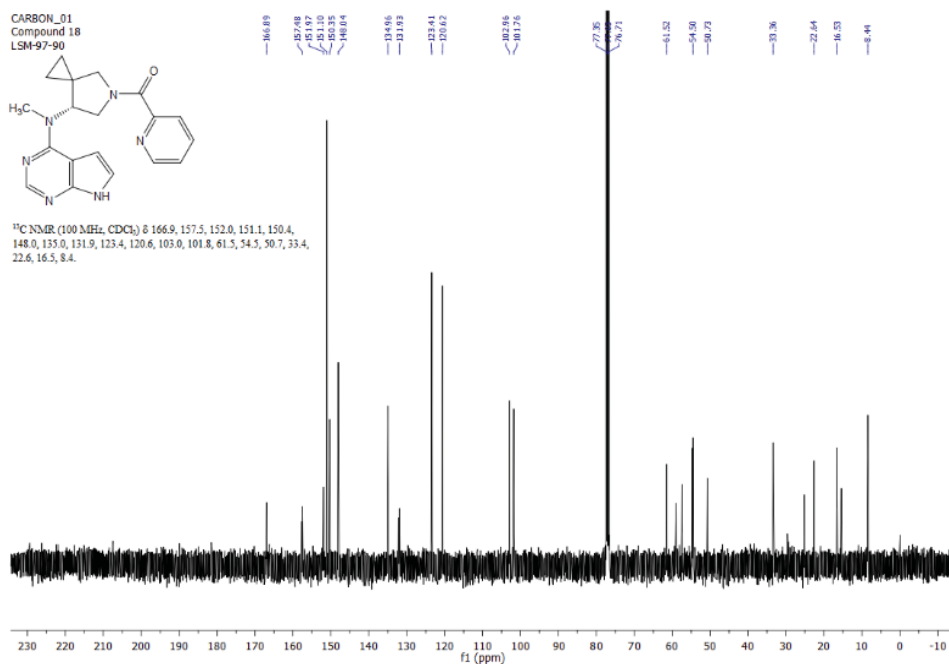
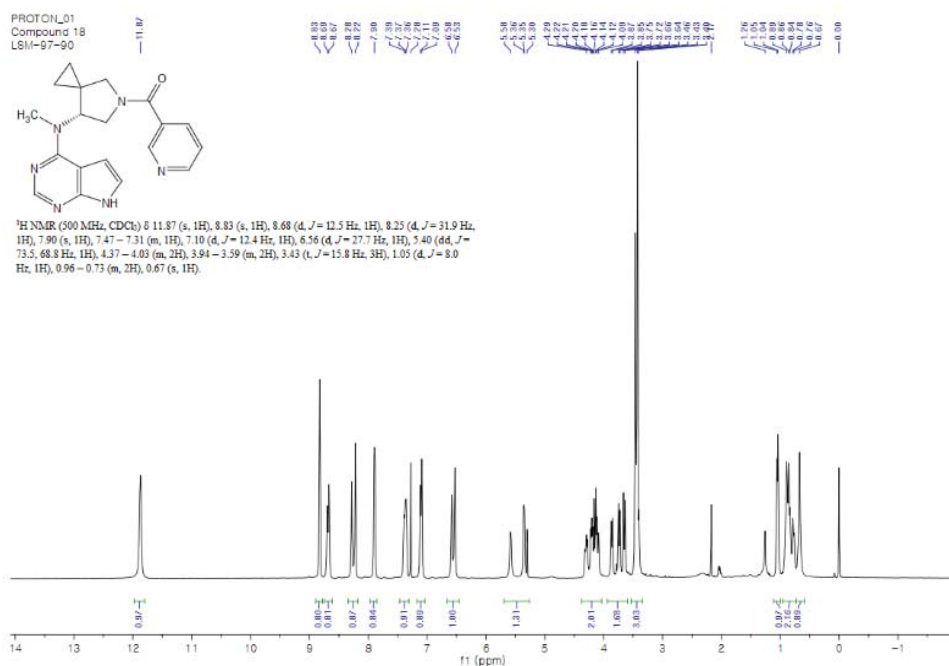
(*R*)-Furan-2-yl(7-(methyl(7*H*-pyrrolo[2,3-*d*]pyrimidin-4-yl)amino)-5-azaspiro[2.4]heptan-5-yl)methanone, **29**



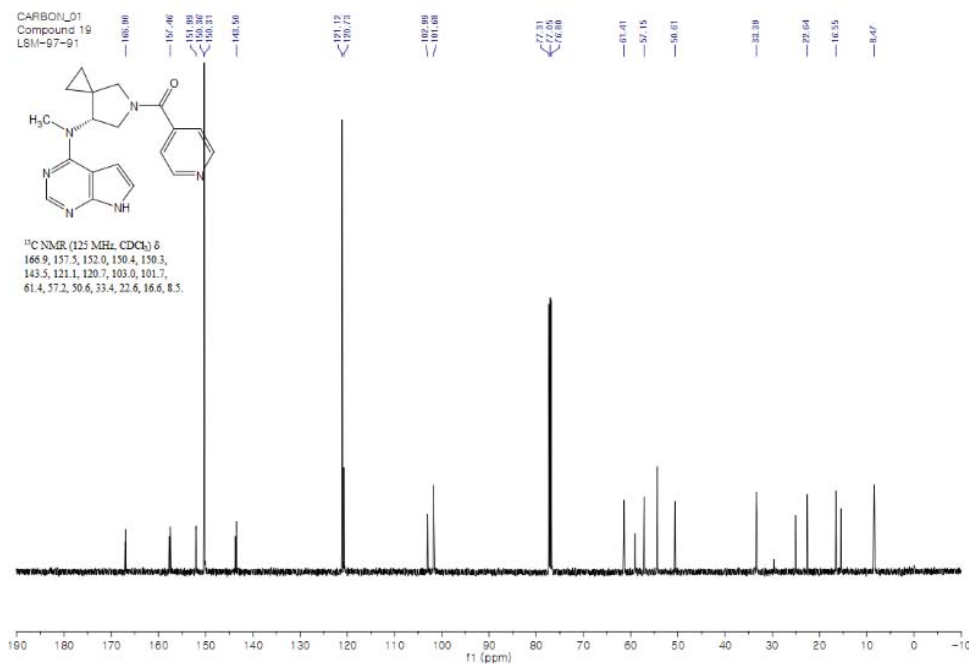
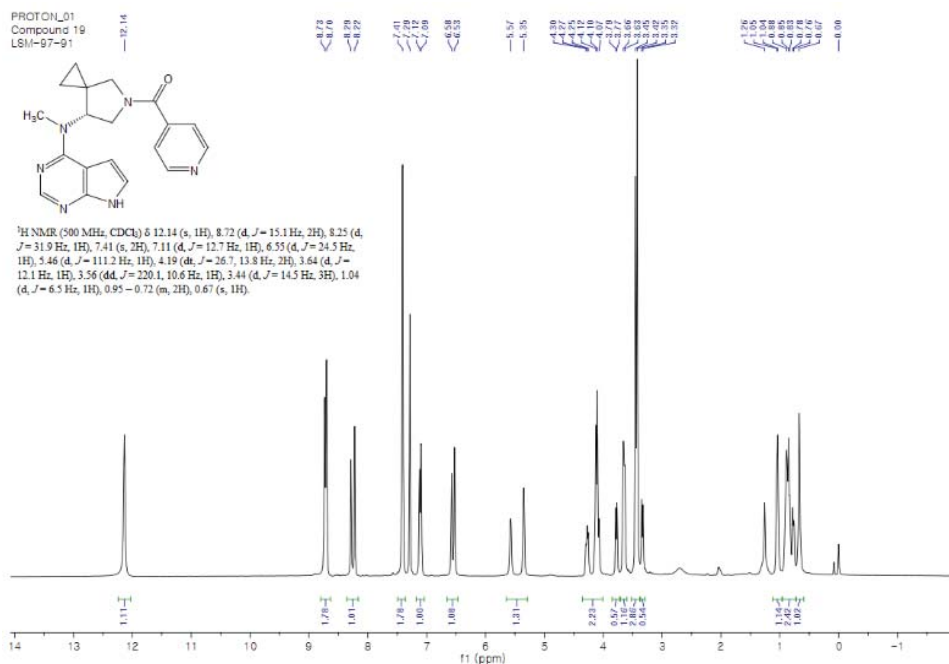
(R)-(7-(Methyl(7*H*-pyrrolo[2,3-*d*]pyrimidin-4-yl)amino)-5-azaspiro[2.4]heptan-5-yl)(phenyl)methanone, **30**



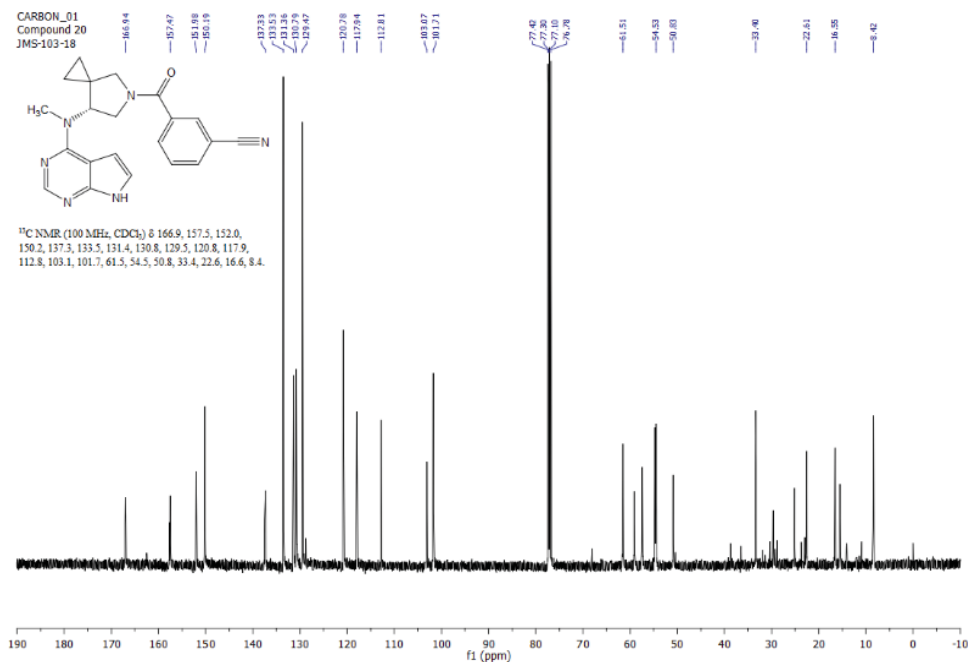
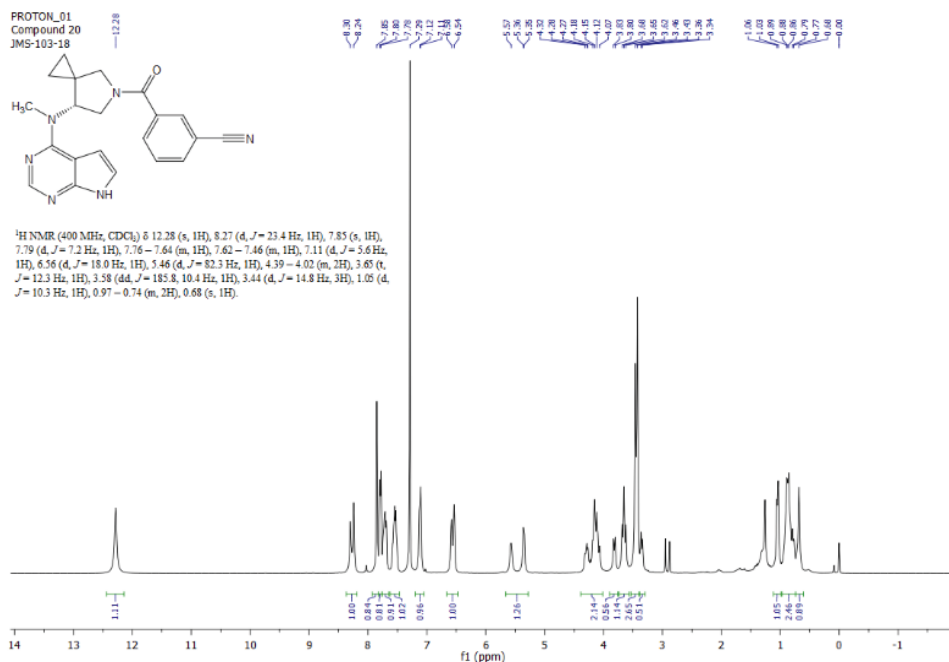
(R)-(7-(Methyl(7H-pyrrolo[2,3-d]pyrimidin-4-yl)amino)-5-azaspiro[2.4]heptan-5-yl)(pyridin-3-yl)methanone, **31**



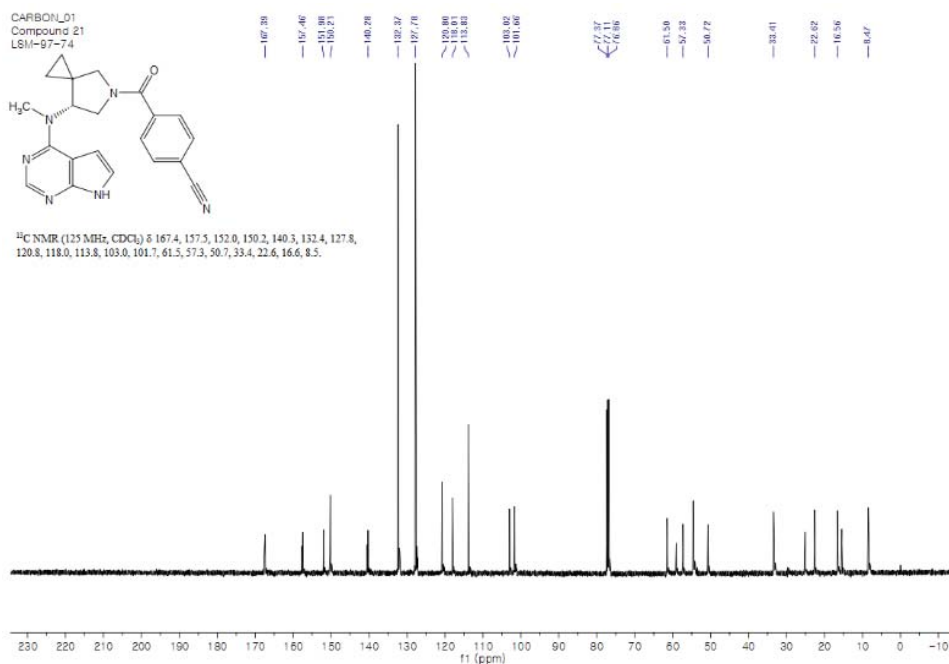
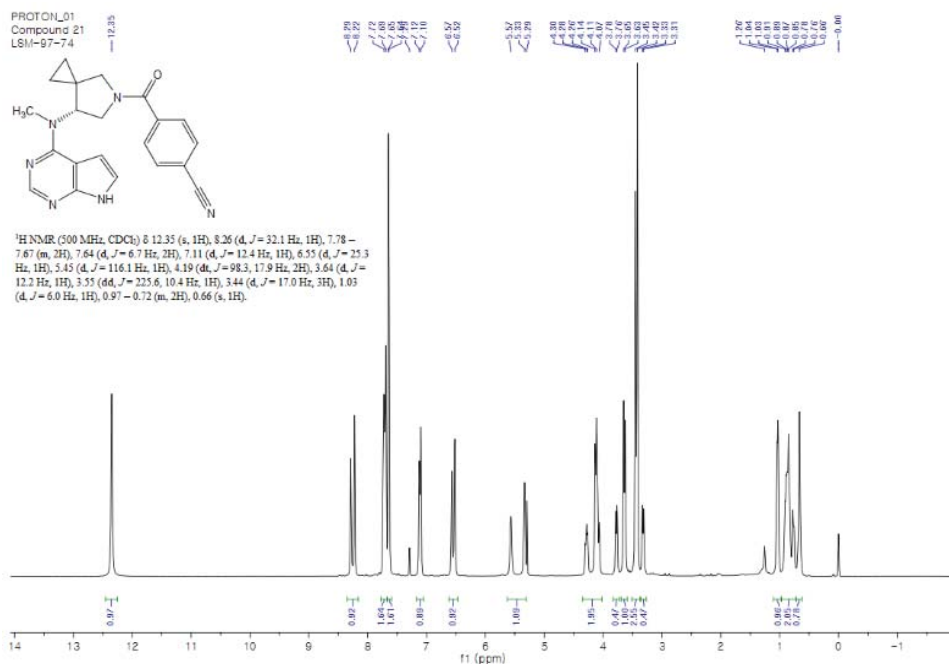
(R)-(7-(Methyl(7*H*-pyrrolo[2,3-*d*]pyrimidin-4-yl)amino)-5-azaspiro[2.4]heptan-5-yl)(pyridin-4-yl)methanone, **32**



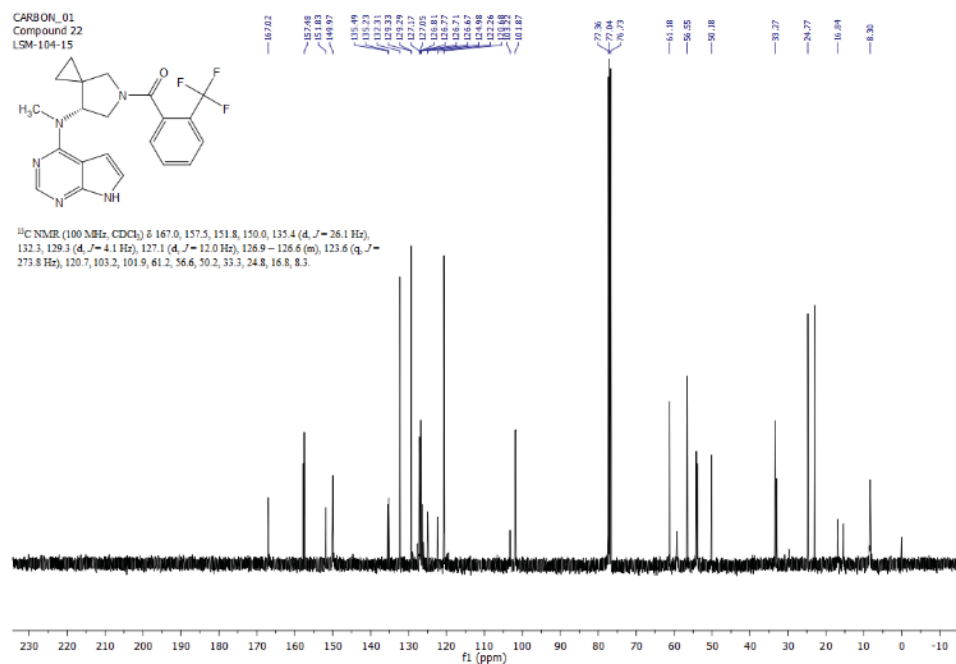
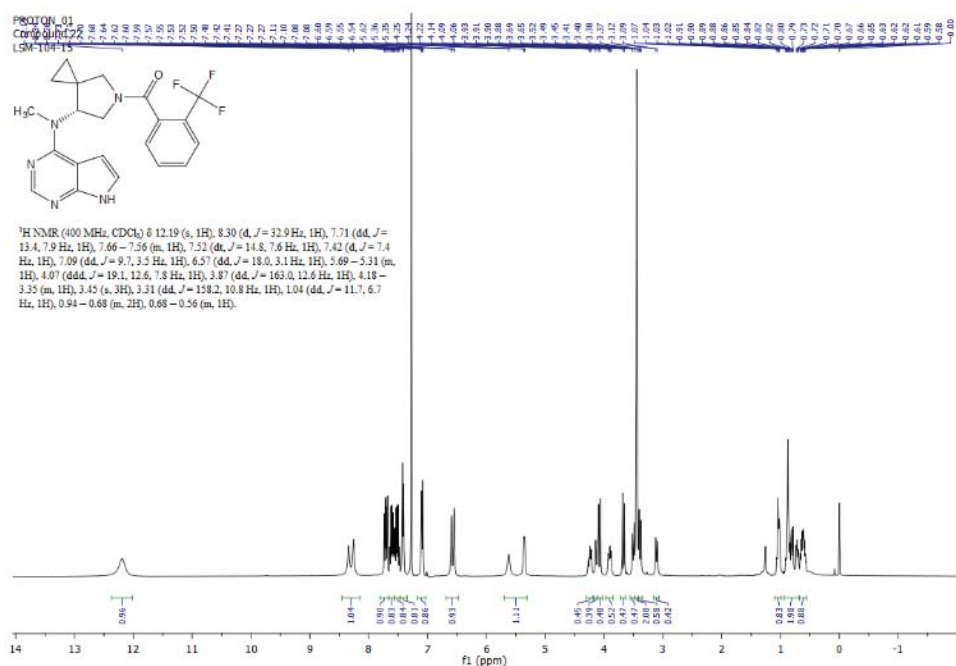
(R)-3-(7-(Methyl(7*H*-pyrrolo[2,3-*d*]pyrimidin-4-yl)amino)-5-azaspiro[2.4]heptane-5-carbonyl)benzonitrile, **33**



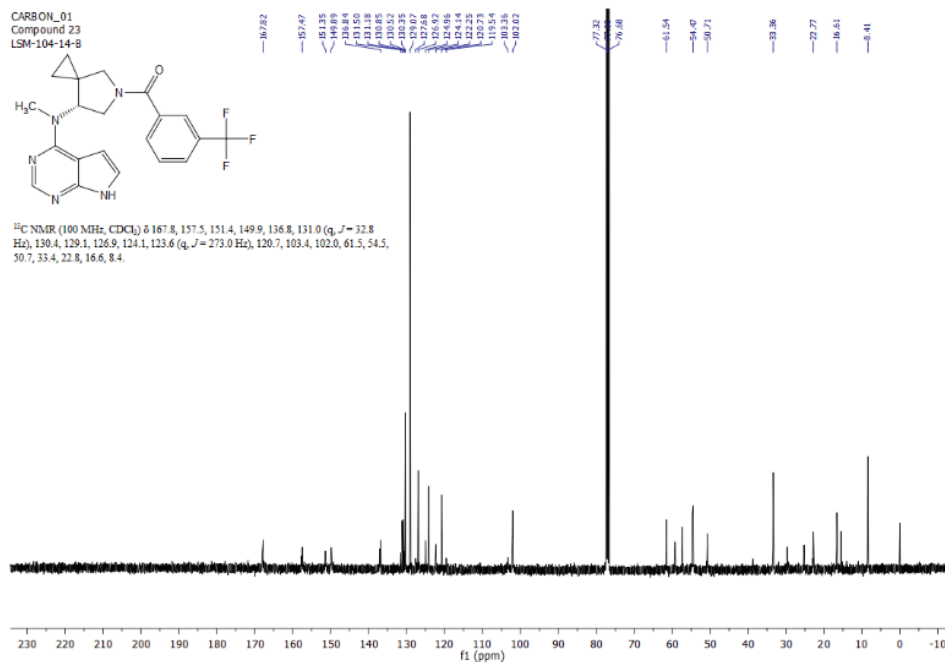
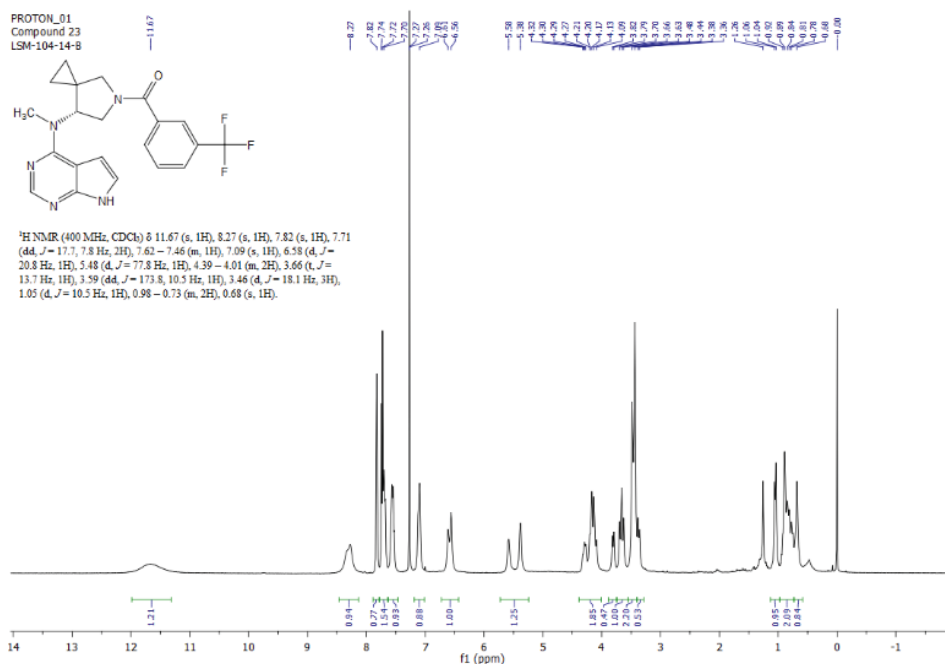
(R)-4-(7-(Methyl(7*H*-pyrrolo[2,3-*d*]pyrimidin-4-yl)amino)-5-azaspiro[2.4]heptane-5-carbonyl)benzonitrile, **34**



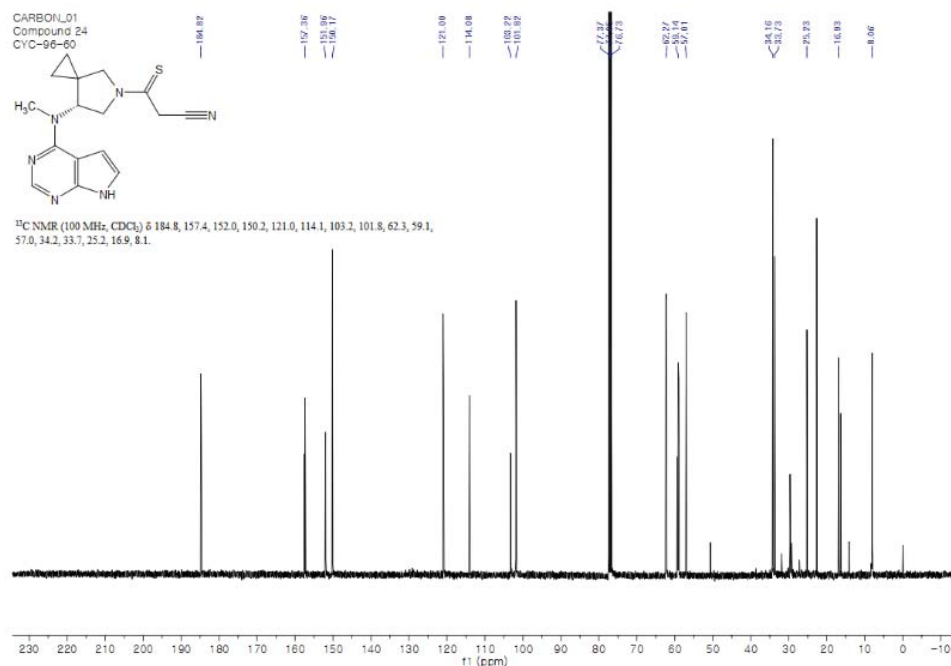
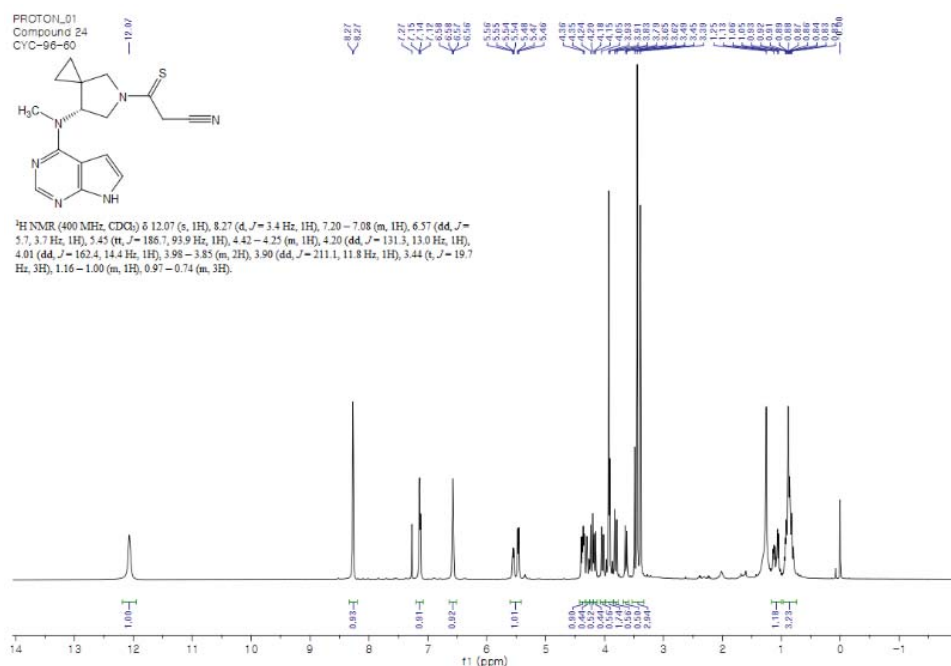
(R)-(7-(Methyl(7*H*-pyrrolo[2,3-*d*]pyrimidin-4-yl)amino)-5-azaspiro[2.4]heptan-5-yl)(2-(trifluoromethyl)phenyl)methanone, **35**



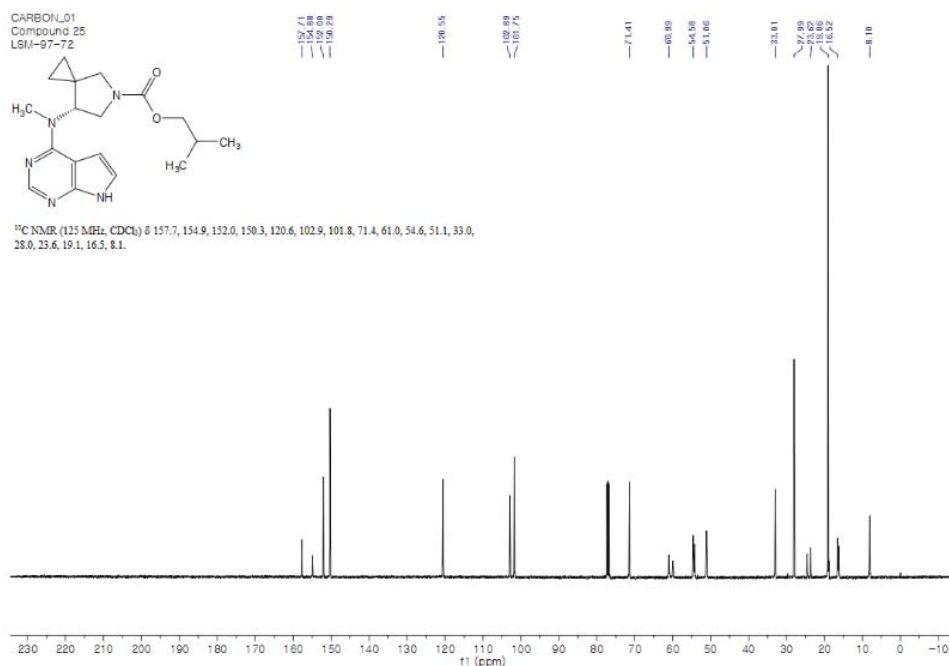
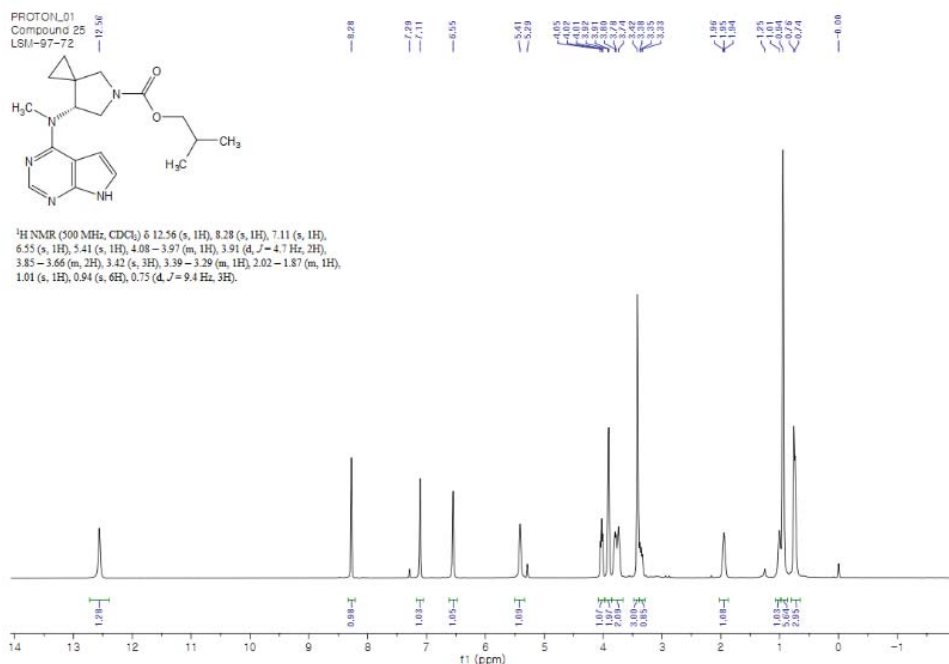
(R)-(7-(Methyl(7*H*-pyrrolo[2,3-*d*]pyrimidin-4-yl)amino)-5-azaspiro[2.4]heptan-5-yl)(3-(trifluoromethyl)phenyl)methanone, **36**



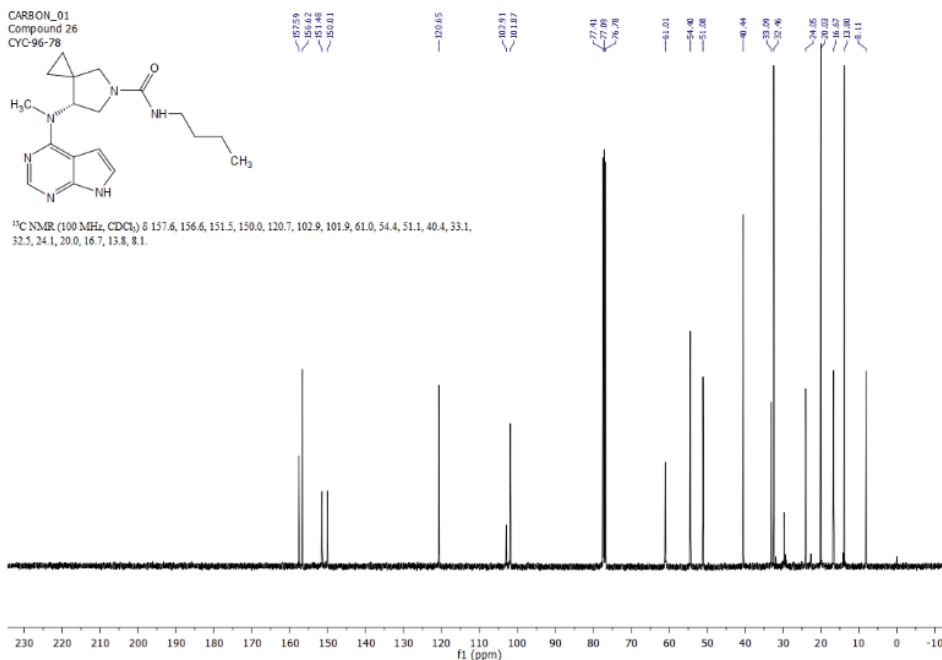
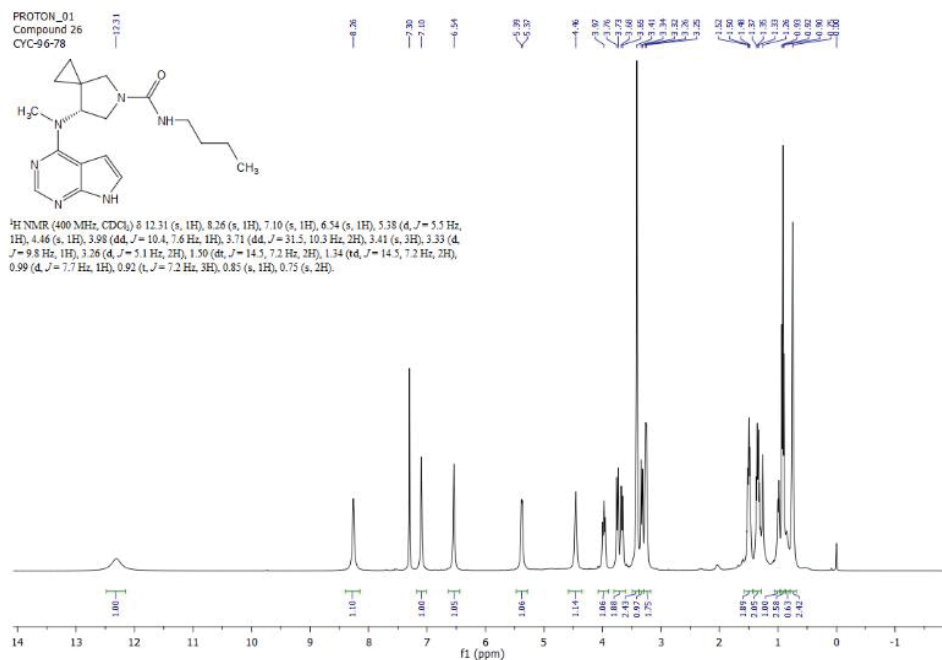
(R)-3-(7-(Methyl(7*H*-pyrrolo[2,3-*d*]pyrimidin-4-yl)amino)-5-azaspiro[2.4]heptan-5-yl)-3-thioxopropanenitrile, **37**



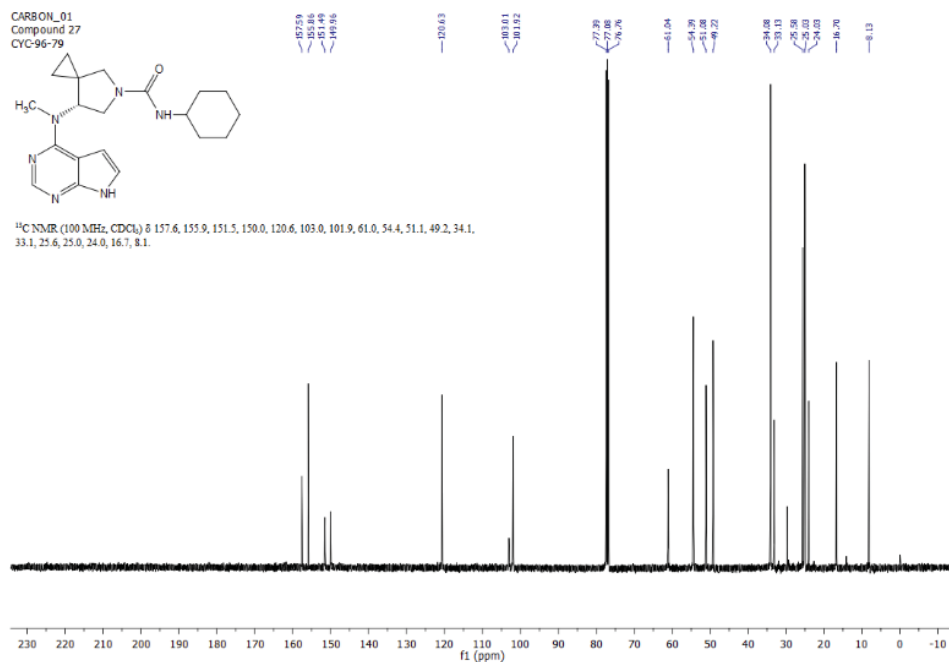
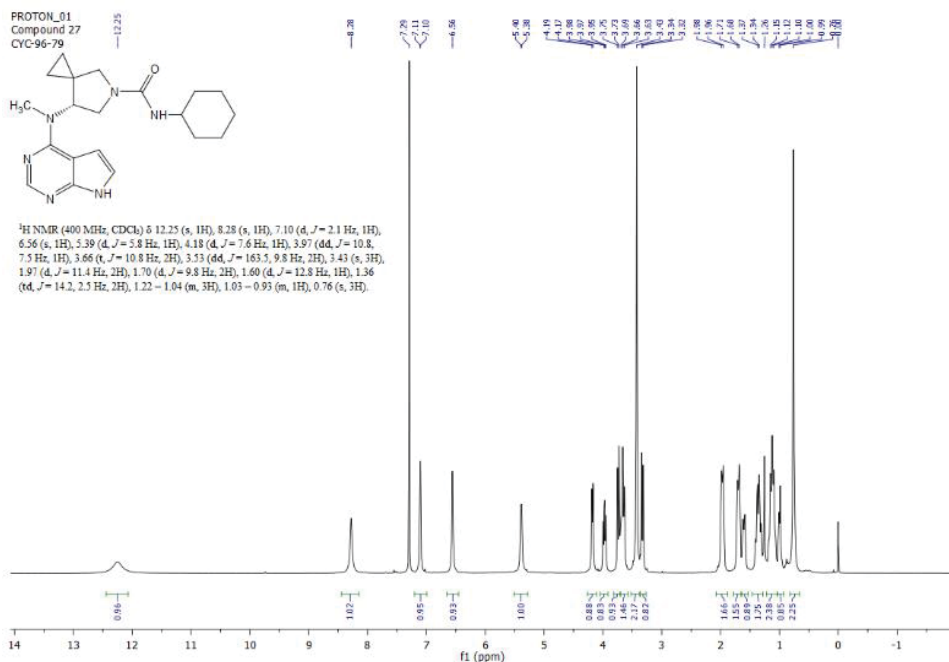
Isobutyl (R)-7-(methyl(7H-pyrrolo[2,3-d]pyrimidin-4-yl)amino)-5-azaspiro[2.4]heptane-5-carboxylate, **38**



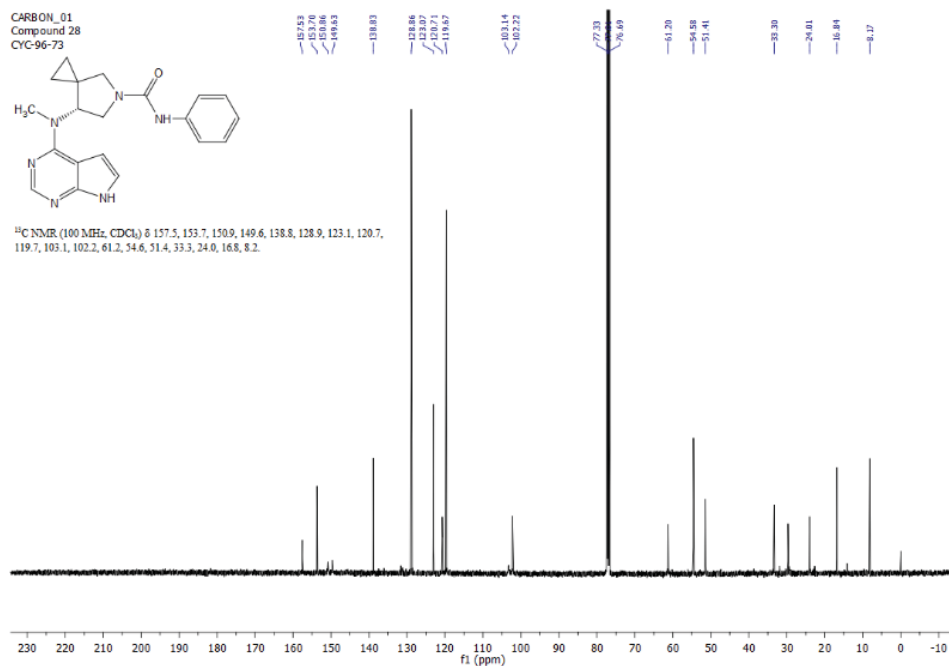
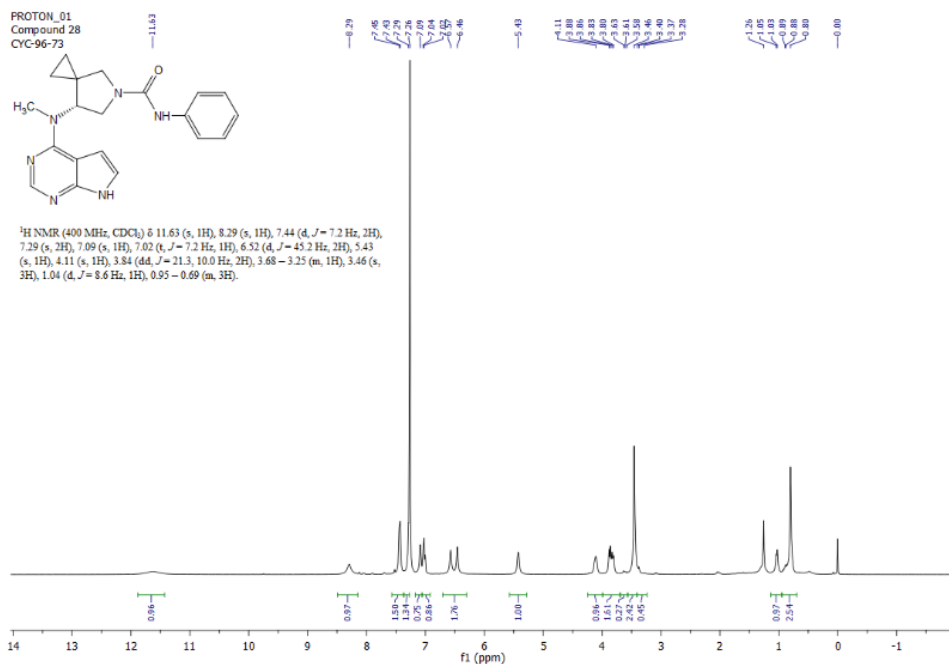
(R)-*N*-Butyl-7-(methyl(7*H*-pyrrolo[2,3-*d*]pyrimidin-4-yl)amino)-5-azaspiro[2.4]heptane-5-carboxamide, **39**



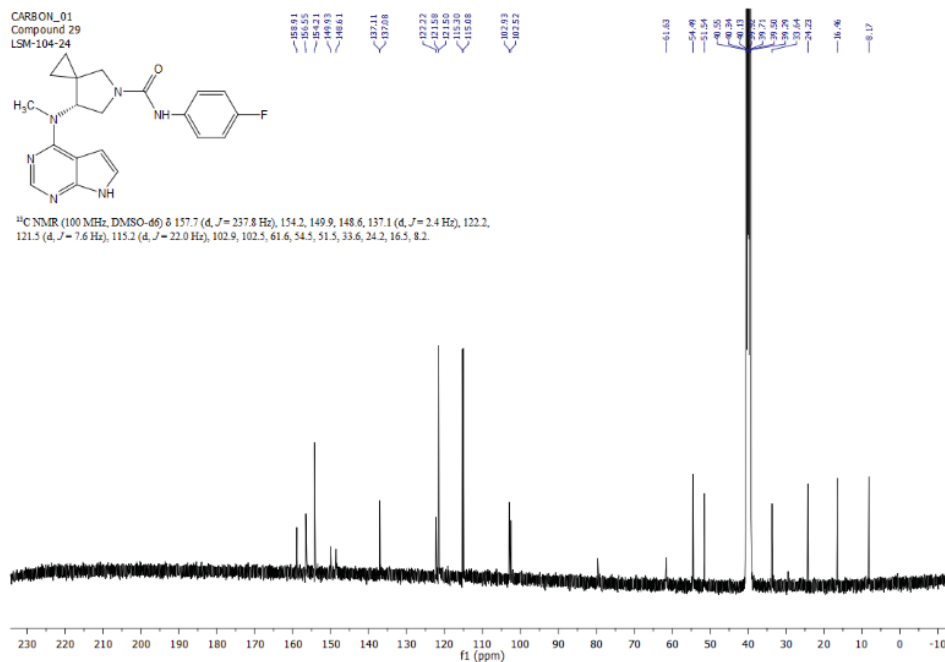
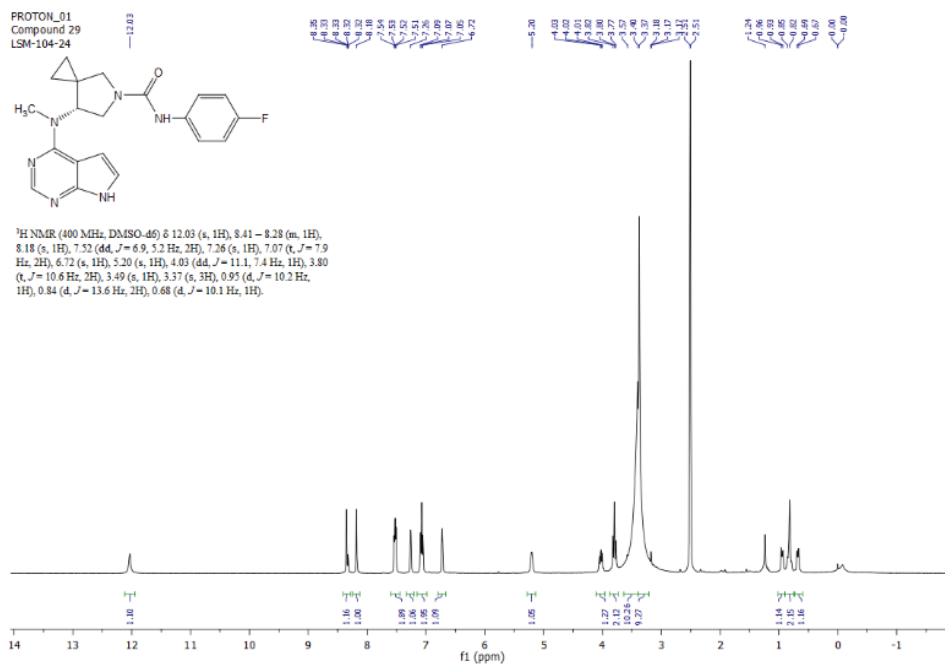
(R)-*N*-Cyclohexyl-7-(methyl(7*H*-pyrrolo[2,3-*d*]pyrimidin-4-yl)amino)-5-azaspiro[2.4]heptane-5-carboxamide, **40**



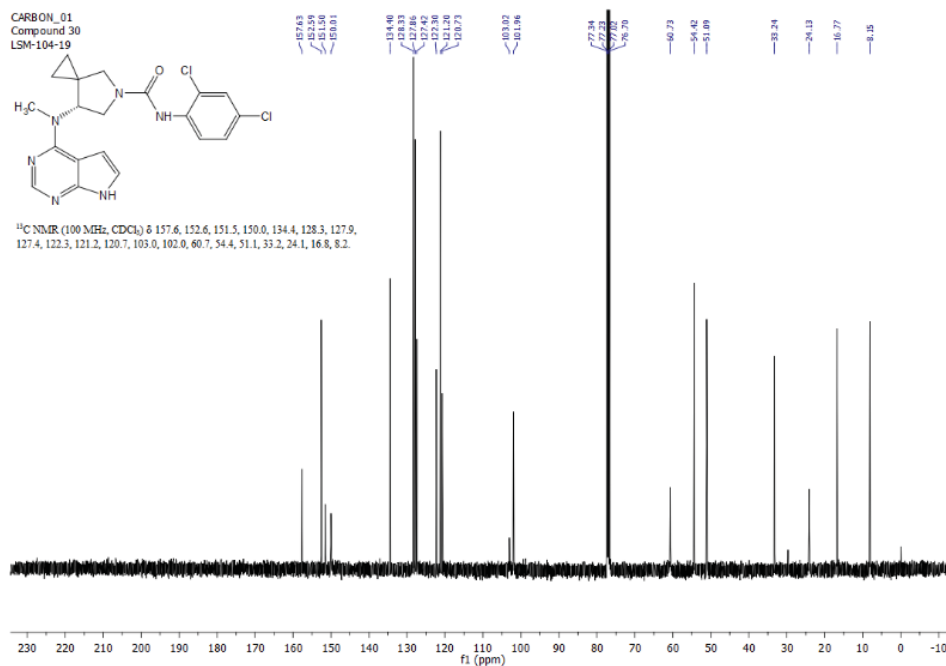
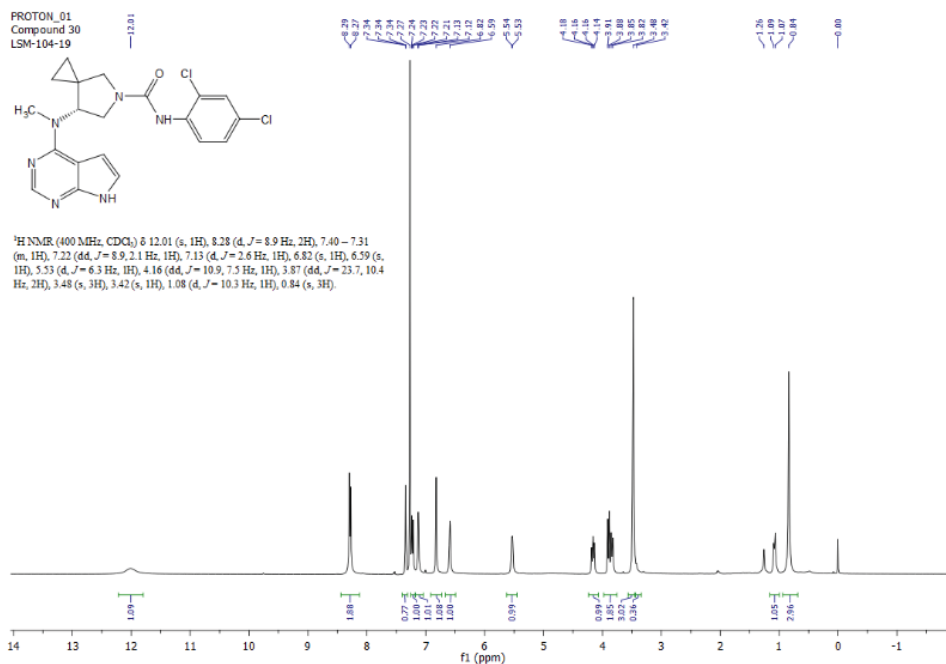
(R)-7-(Methyl(7H-pyrrolo[2,3-d]pyrimidin-4-yl)amino)-*N*-phenyl-5-azaspiro[2.4]heptane-5-carboxamide, **41**



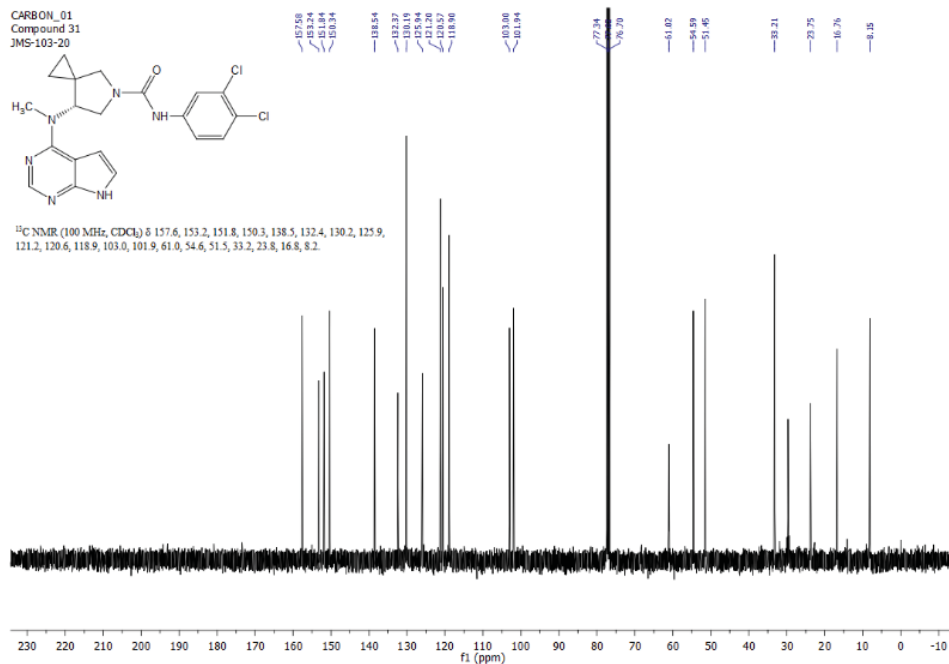
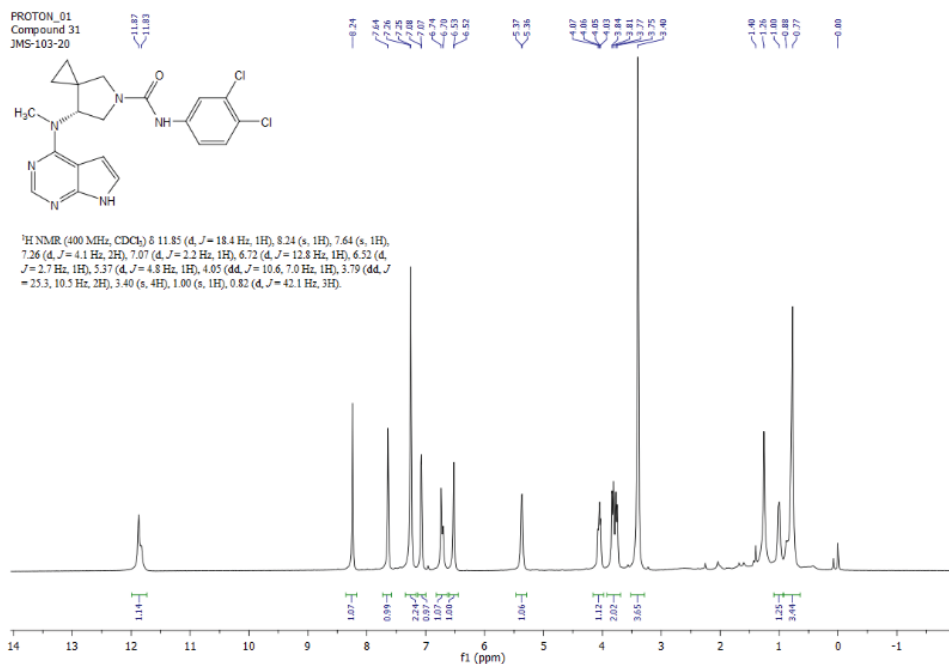
(R)-*N*-(4-Fluorophenyl)-7-(methyl(7*H*-pyrrolo[2,3-*d*]pyrimidin-4-yl)amino)-5-azaspiro[2.4]heptane-5-carboxamide, **42**



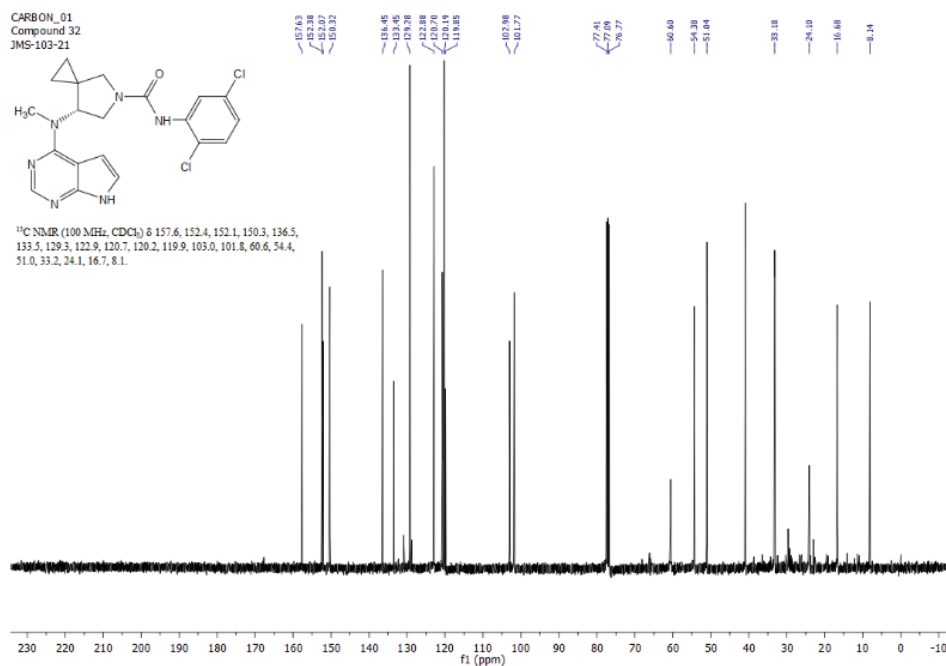
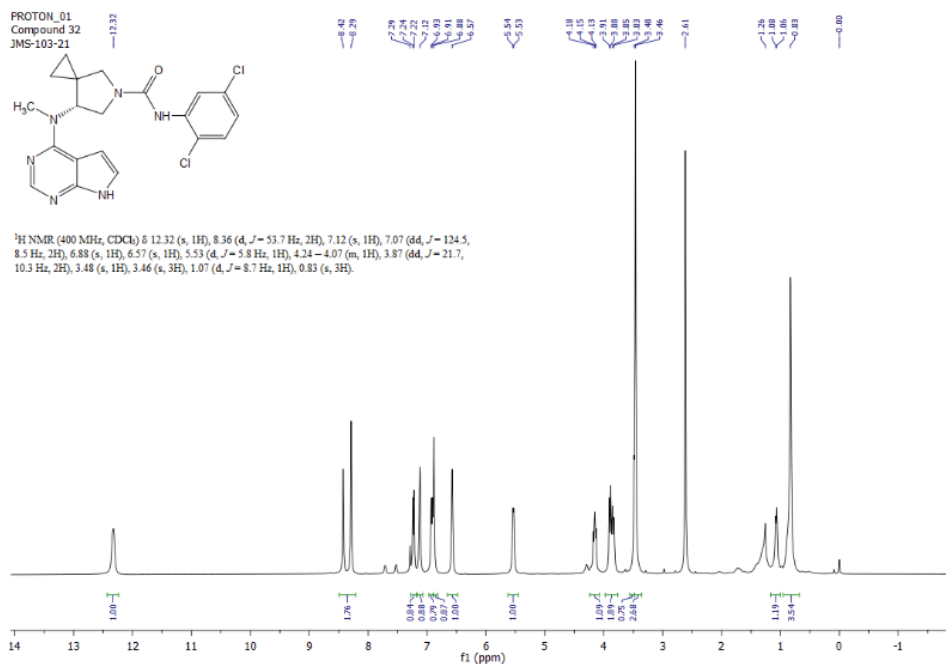
(R)-*N*-(2,4-Dichlorophenyl)-7-(methyl(7*H*-pyrrolo[2,3-*d*]pyrimidin-4-yl)amino)-5-azaspiro[2.4]heptane-5-carboxamide, **43**



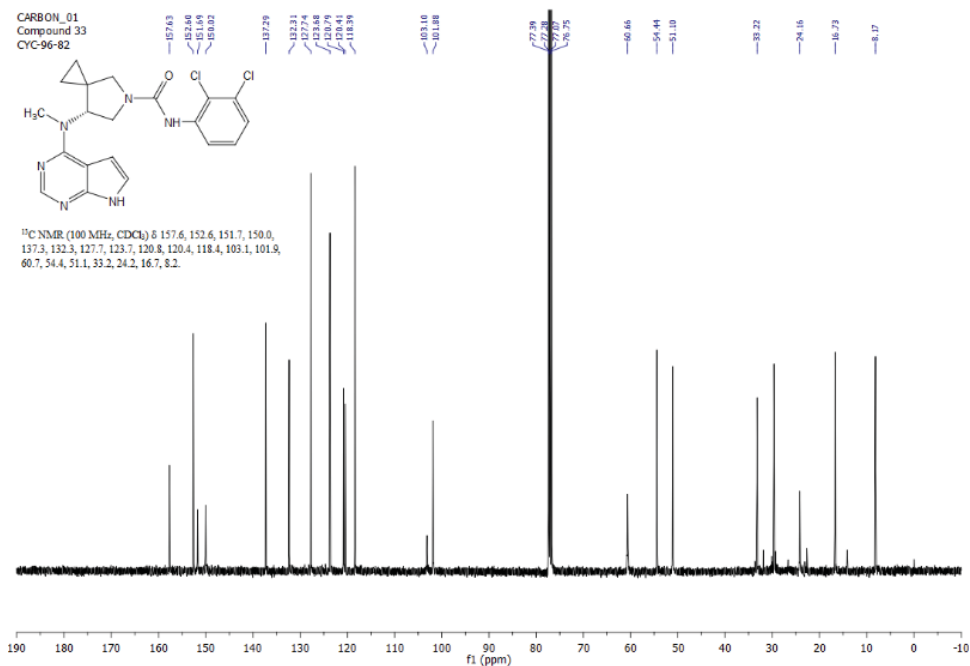
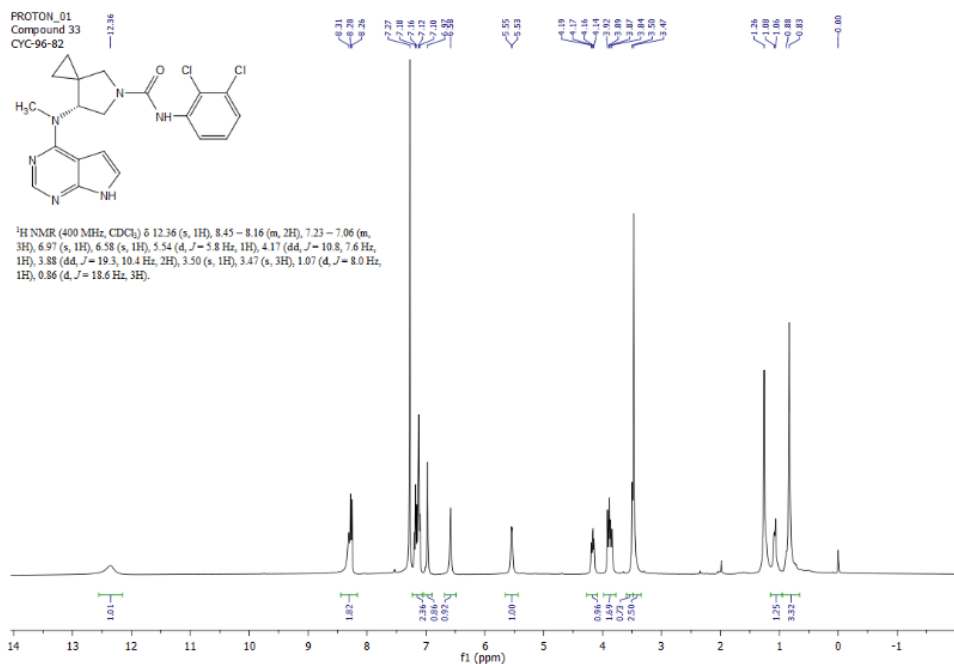
(R)-*N*-(3,4-Dichlorophenyl)-7-(methyl(7*H*-pyrrolo[2,3-*d*]pyrimidin-4-yl)amino)-5-azaspiro[2.4]heptane-5-carboxamide, **44**



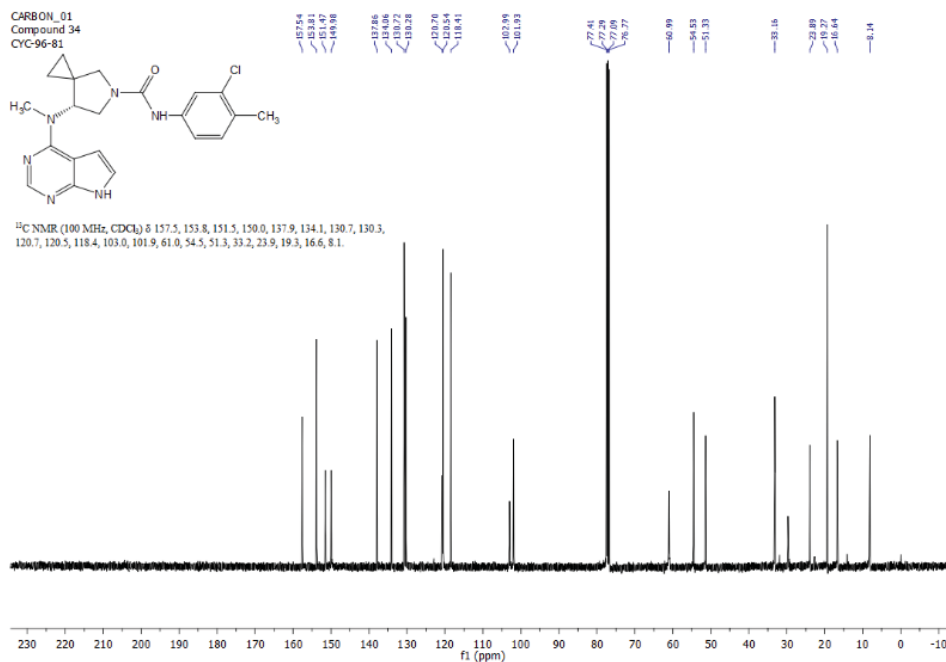
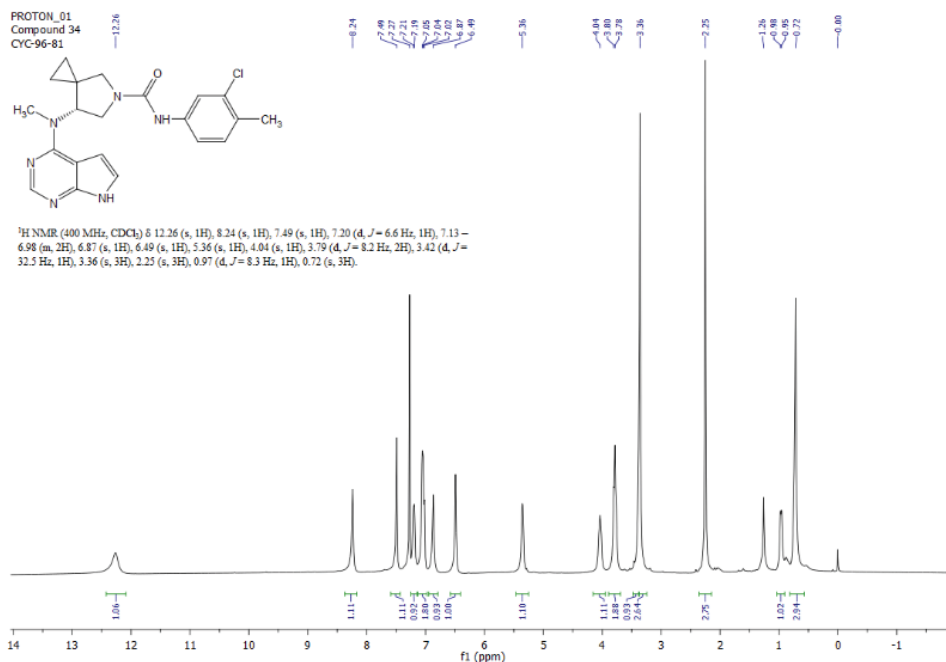
(R)-*N*-(2,5-Dichlorophenyl)-7-(methyl(7*H*-pyrrolo[2,3-*d*]pyrimidin-4-yl)amino)-5-azaspiro[2.4]heptane-5-carboxamide, **45**



(R)-*N*-(2,3-Dichlorophenyl)-7-(methyl(7*H*-pyrrolo[2,3-*d*]pyrimidin-4-yl)amino)-5-azaspiro[2.4]heptane-5-carboxamide, **46**

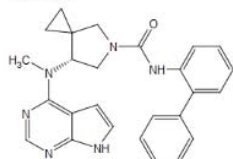


(R)-*N*-(3-Chloro-4-methylphenyl)-7-(methyl(7*H*-pyrrolo[2,3-*d*]pyrimidin-4-yl)amino)-5-azaspiro[2.4]heptane-5-carboxamide, **47**

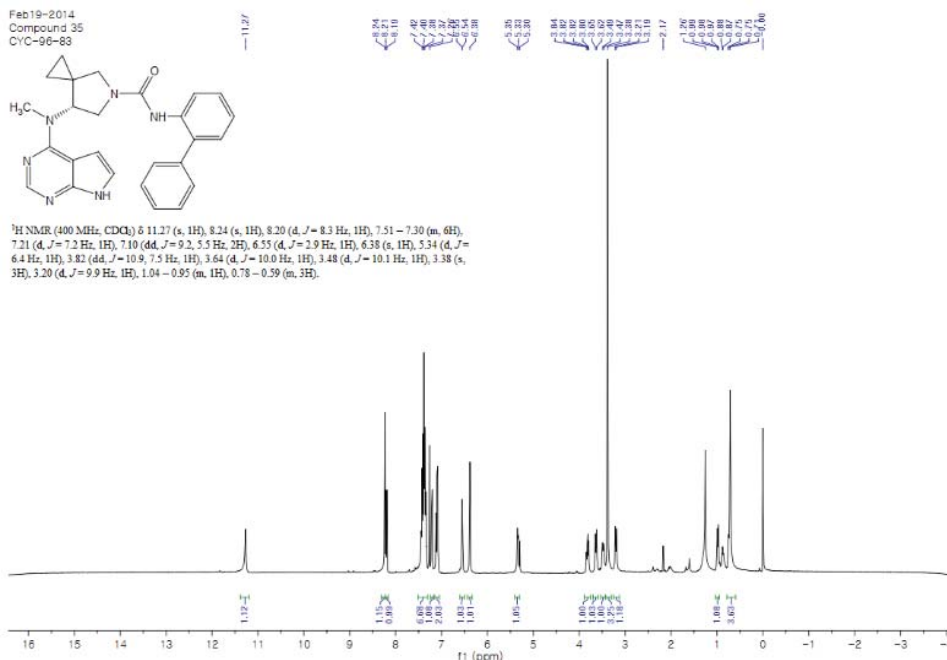


(R)-*N*-([1,1'-Biphenyl]-2-yl)-7-(methyl(7*H*-pyrrolo[2,3-*d*]pyrimidin-4-yl)amino)-5-azaspiro[2.4]heptane-5-carboxamide, **48**

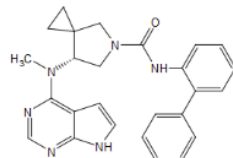
Feb19-2014
Compound 35
CVC-96-83



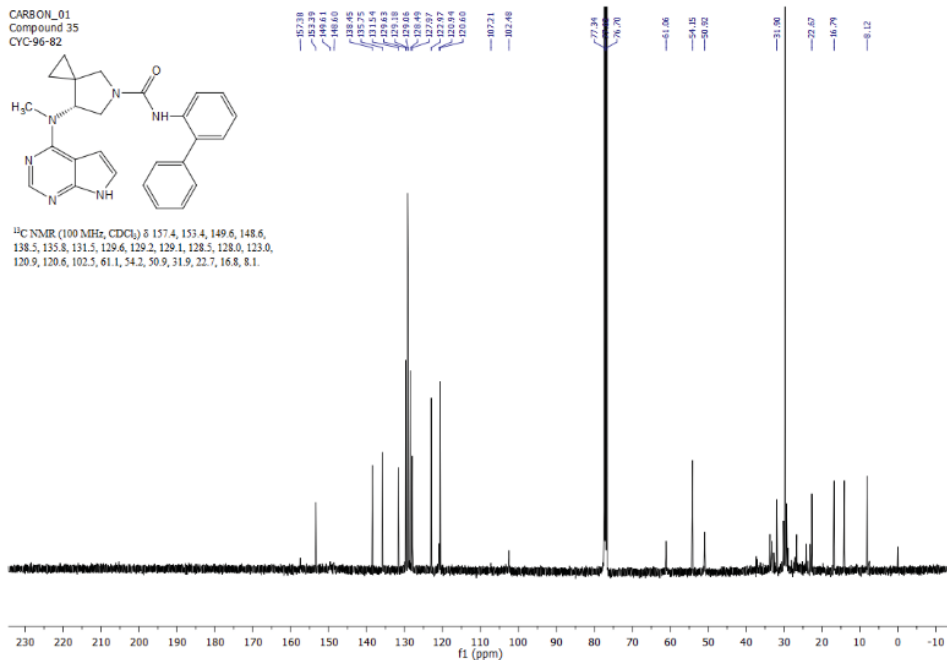
¹H NMR (400 MHz, CDCl₃) δ 11.27 (s, 1H), 8.24 (s, 1H), 8.20 (d, *J* = 8.3 Hz, 1H), 7.51–7.30 (m, 6H), 7.21 (d, *J* = 7.2 Hz, 1H), 7.10 (dd, *J* = 9.2, 5.5 Hz, 2H), 6.55 (d, *J* = 2.9 Hz, 1H), 6.38 (s, 1H), 5.34 (d, *J* = 6.4 Hz, 1H), 3.82 (dd, *J* = 10.9, 7.5 Hz, 1H), 3.64 (d, *J* = 10.0 Hz, 1H), 3.48 (d, *J* = 10.1 Hz, 1H), 3.38 (s, 3H), 3.20 (d, *J* = 9.9 Hz, 1H), 1.04–0.95 (m, 1H), 0.78–0.59 (m, 3H).



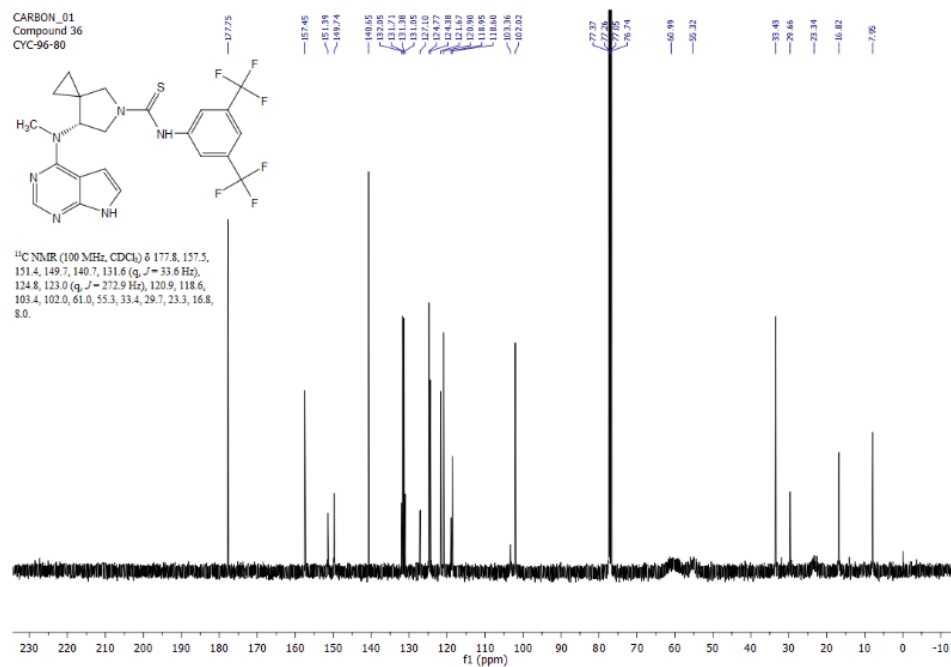
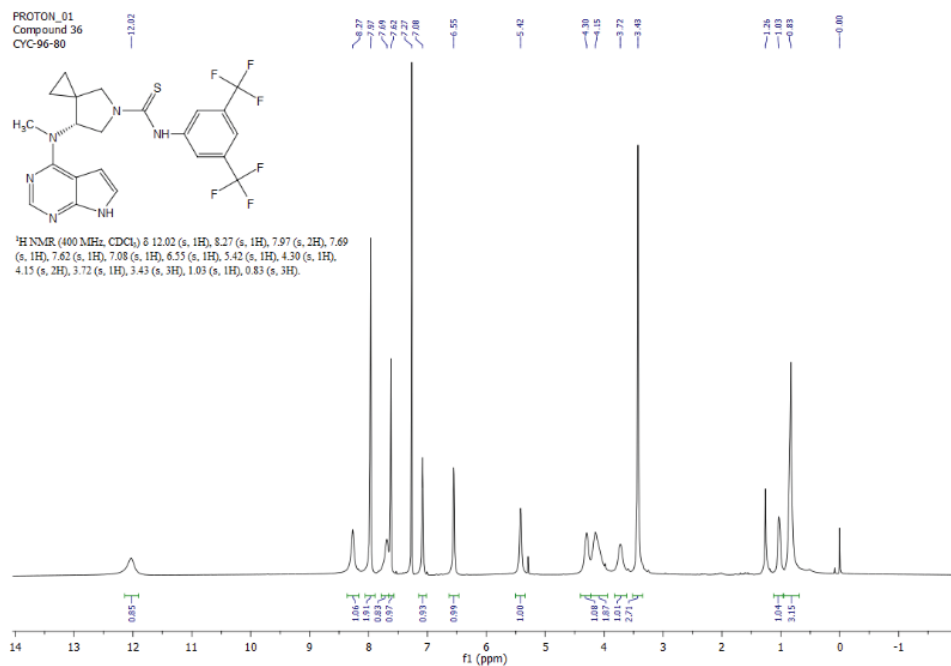
CARBON_01
Compound 35
CVC-96-82



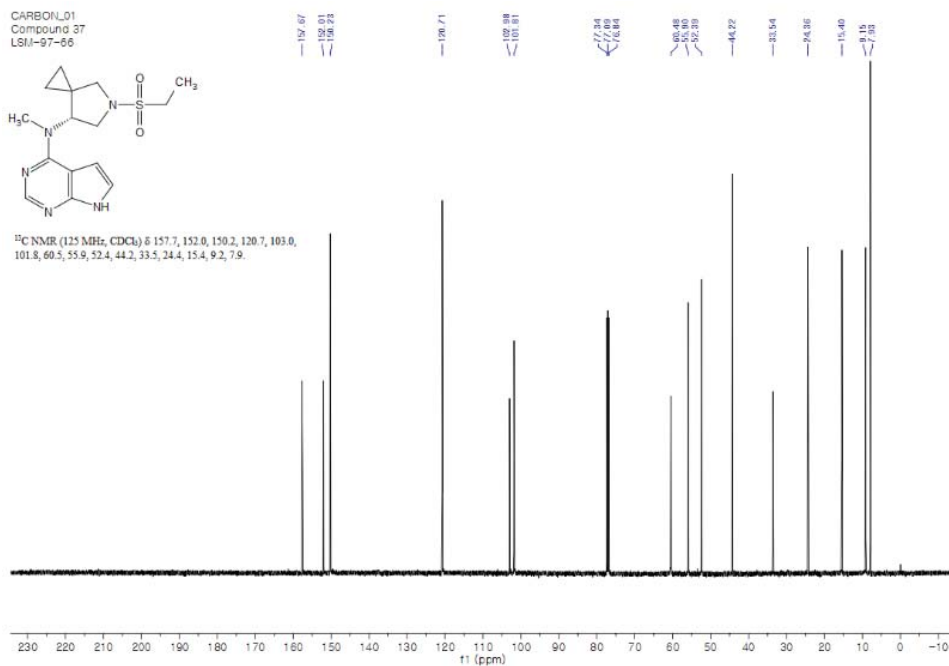
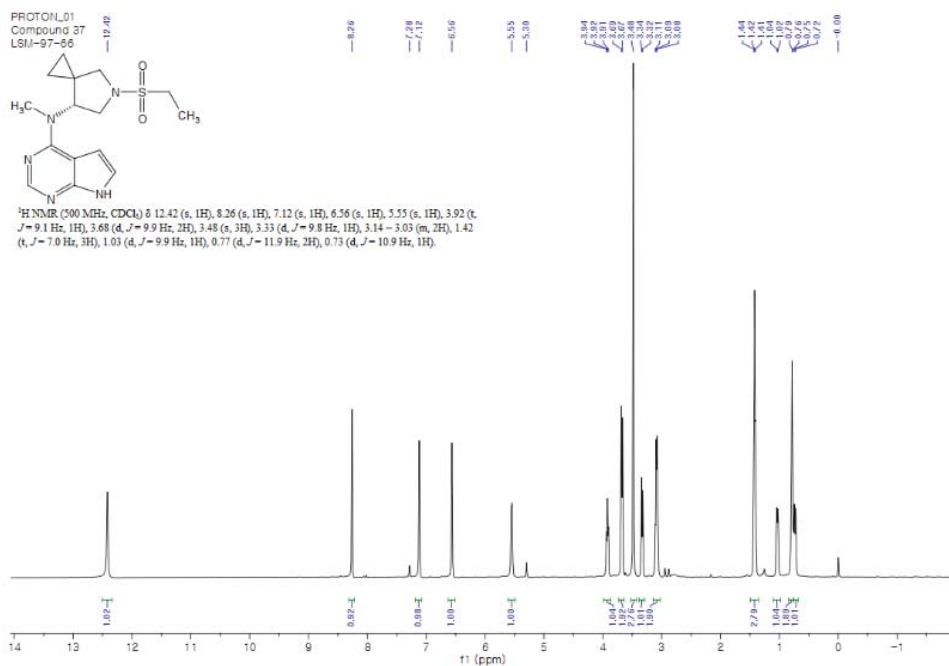
¹³C NMR (100 MHz, CDCl₃) δ 157.4, 153.4, 149.6, 148.6, 138.5, 135.8, 131.5, 129.6, 129.2, 129.1, 128.5, 128.0, 123.0, 120.9, 120.6, 102.5, 61.1, 54.2, 50.9, 31.9, 22.7, 16.8, 8.1.



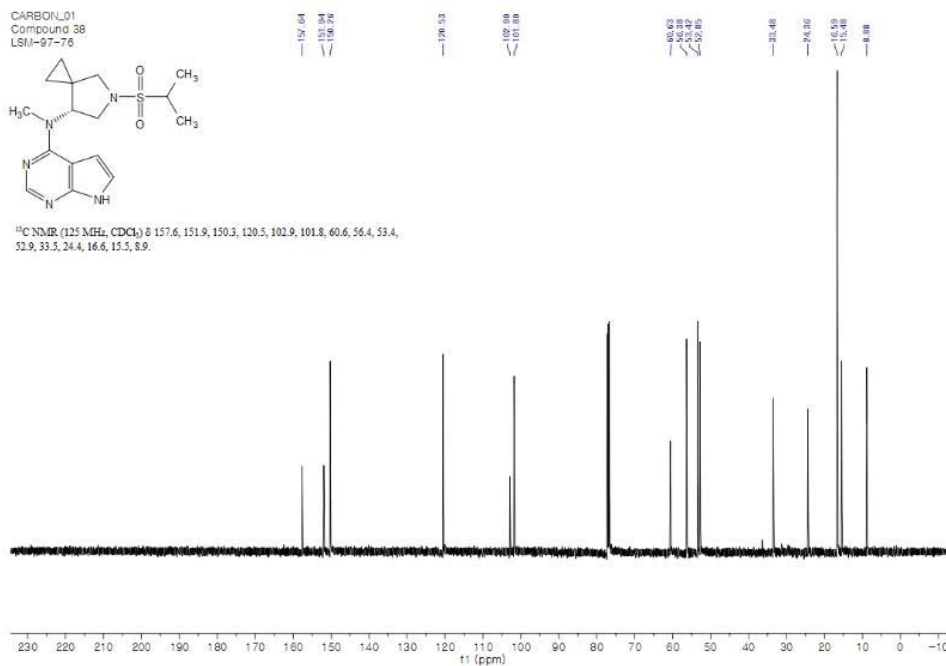
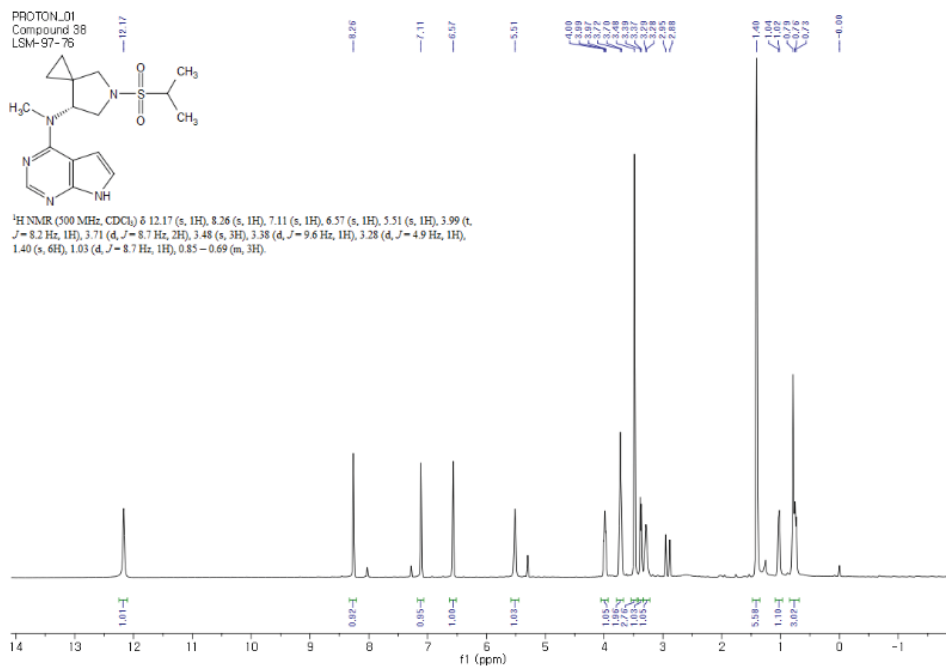
(R)-*N*-(3,5-Bis(trifluoromethyl)phenyl)-7-(methyl(7*H*-pyrrolo[2,3-*d*]pyrimidin-4-*yl*)amino)-5-azaspiro[2.4]heptane-5-carbothioamide, **49**



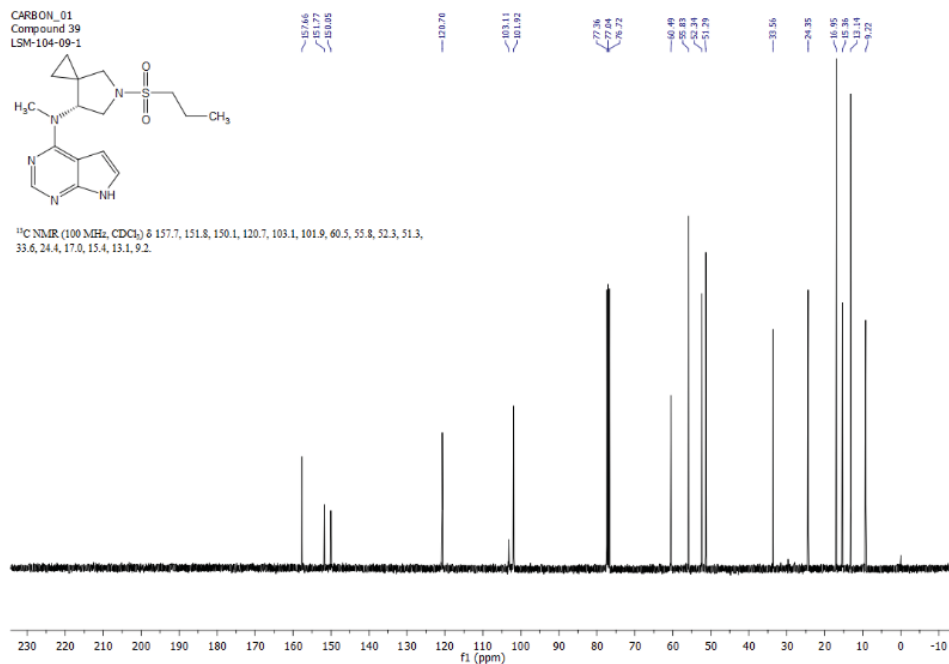
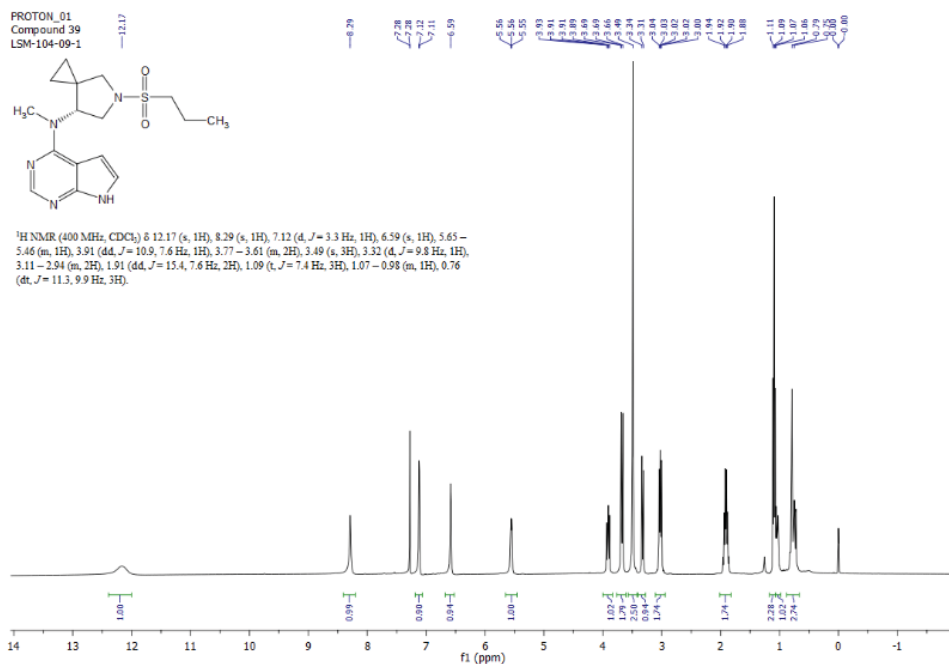
(R)-*N*-(5-(Ethylsulfonyl)-5-azaspiro[2.4]heptan-7-yl)-*N*-methyl-7*H*-pyrrolo[2,3-*d*]pyrimidin-4-amine, **50**



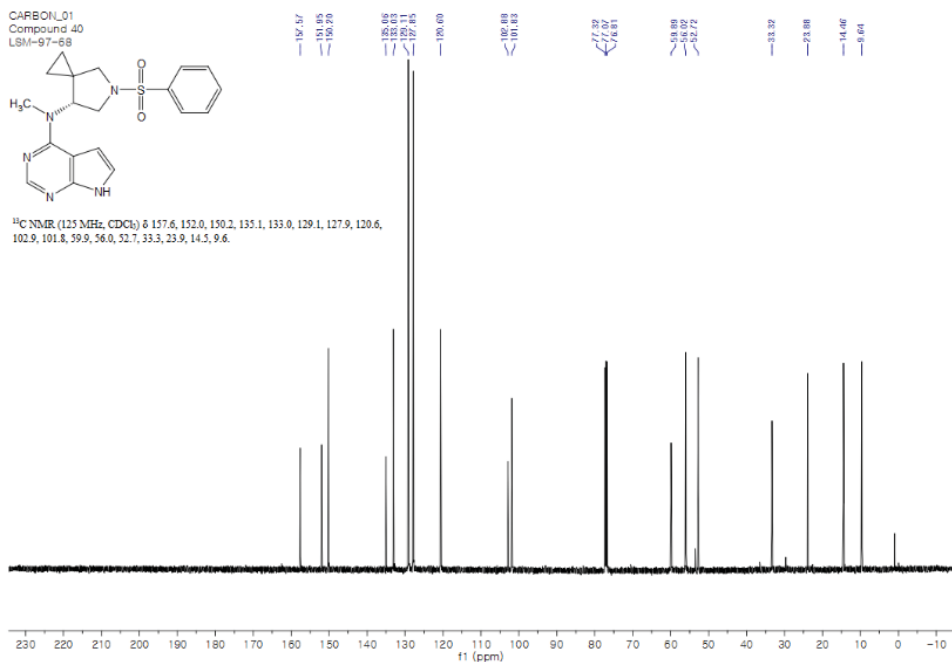
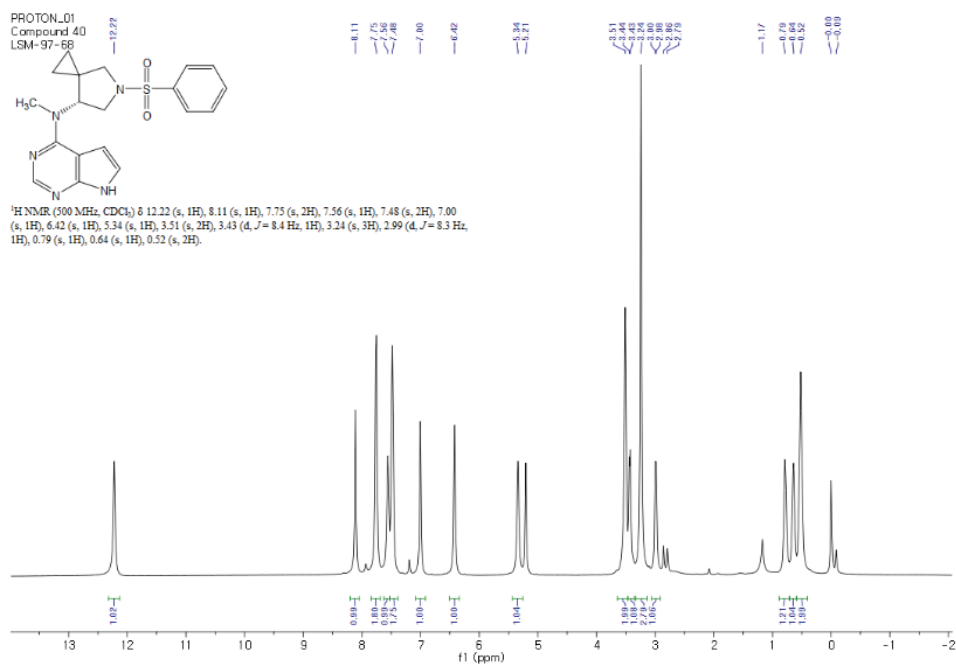
(R)-*N*-(5-(Isopropylsulfonyl)-5-azaspiro[2.4]heptan-7-yl)-*N*-methyl-7*H*-pyrrolo[2,3-*d*]pyrimidin-4-amine, **51**



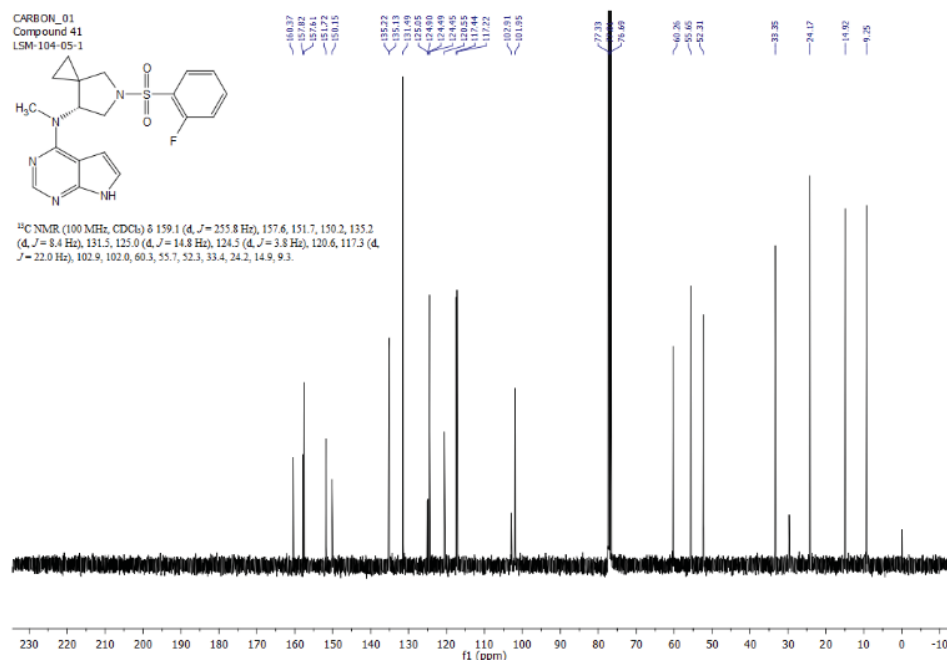
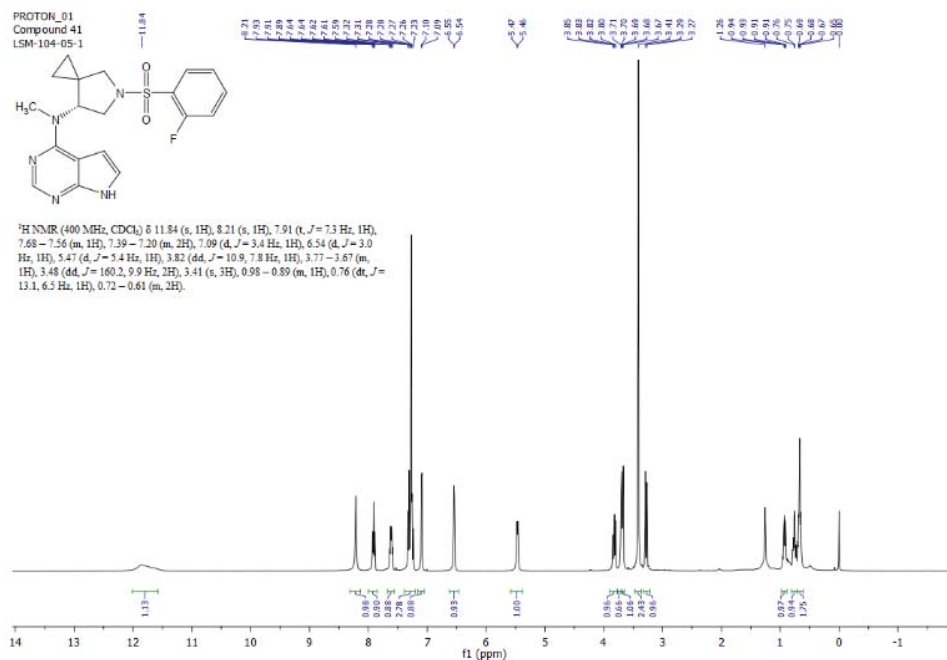
(R)-*N*-Methyl-*N*-(5-(propylsulfonyl)-5-azaspiro[2.4]heptan-7-yl)-7*H*-pyrrolo[2,3-*d*]pyrimidin-4-amine, **52**



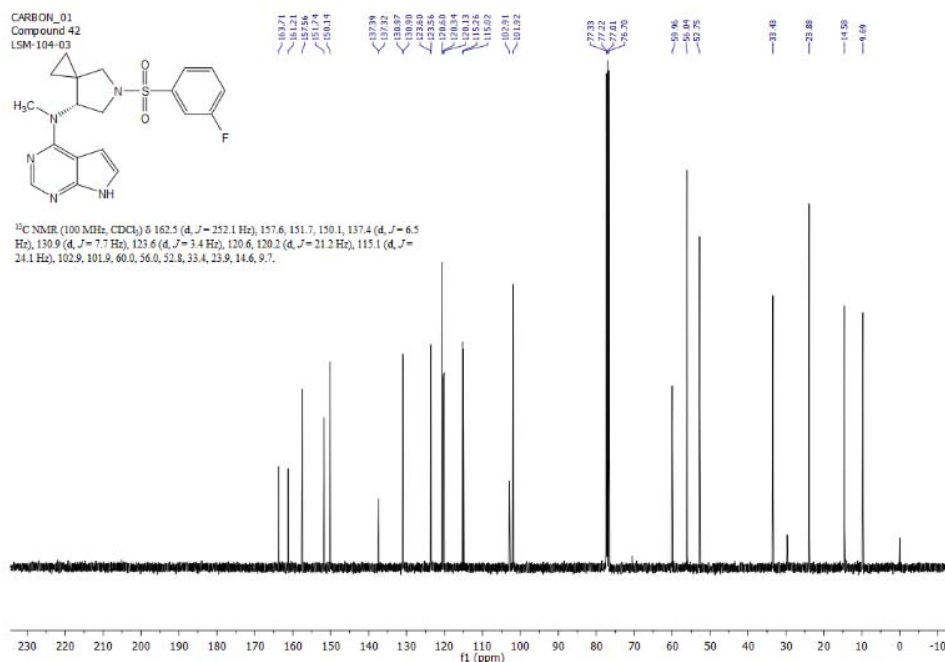
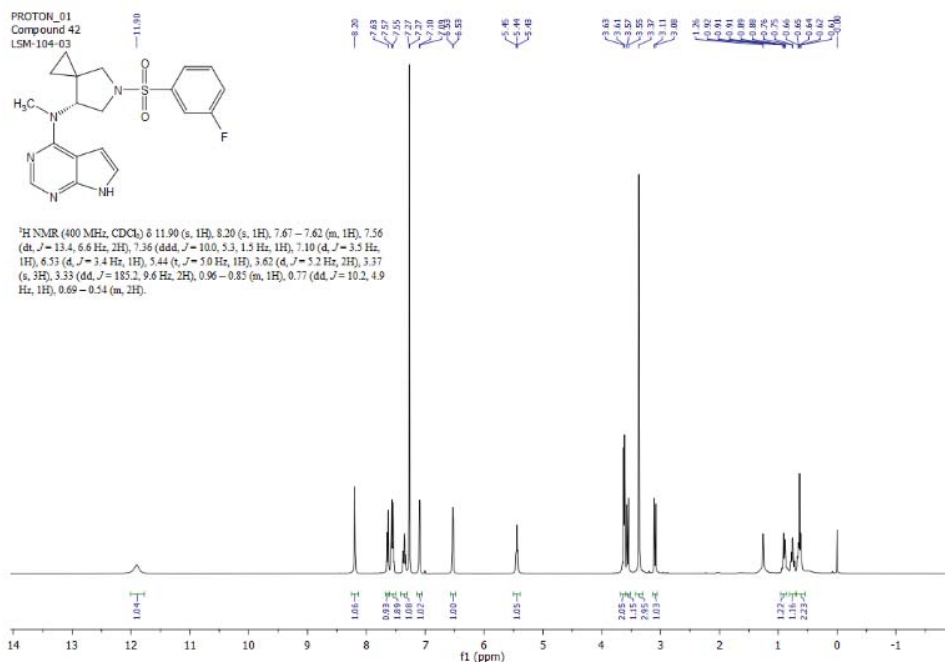
(R)-*N*-Methyl-*N*-(5-(phenylsulfonyl)-5-azaspiro[2.4]heptan-7-yl)-7*H*-pyrrolo[2,3-*d*]pyrimidin-4-amine, **53**



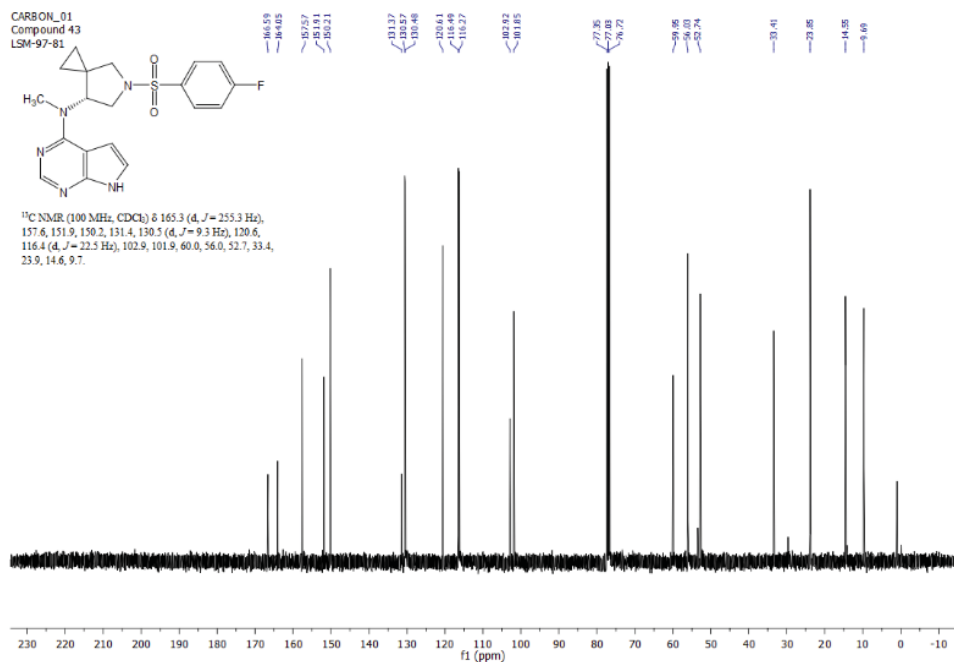
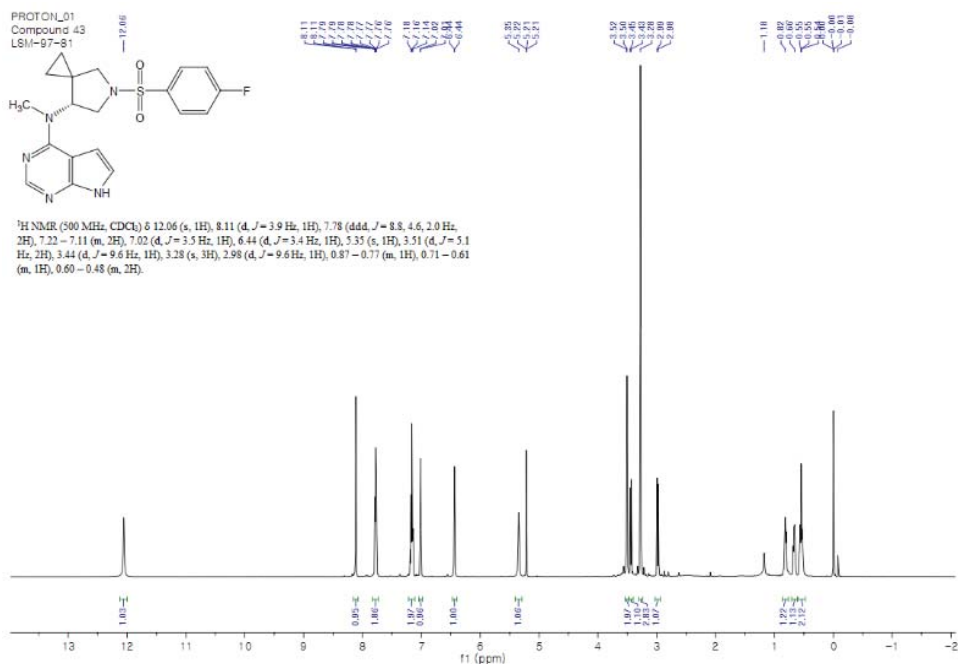
(R)-*N*-(5-((2-Fluorophenyl)sulfonyl)-5-azaspiro[2.4]heptan-7-yl)-*N*-methyl-7*H*-pyrrolo[2,3-*d*]pyrimidin-4-amine, **54**



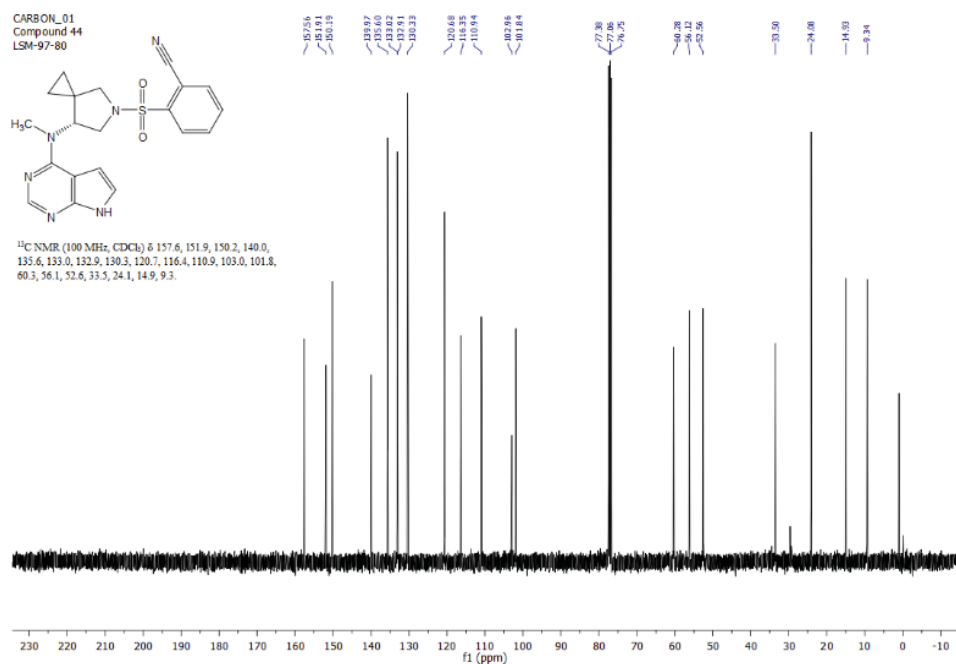
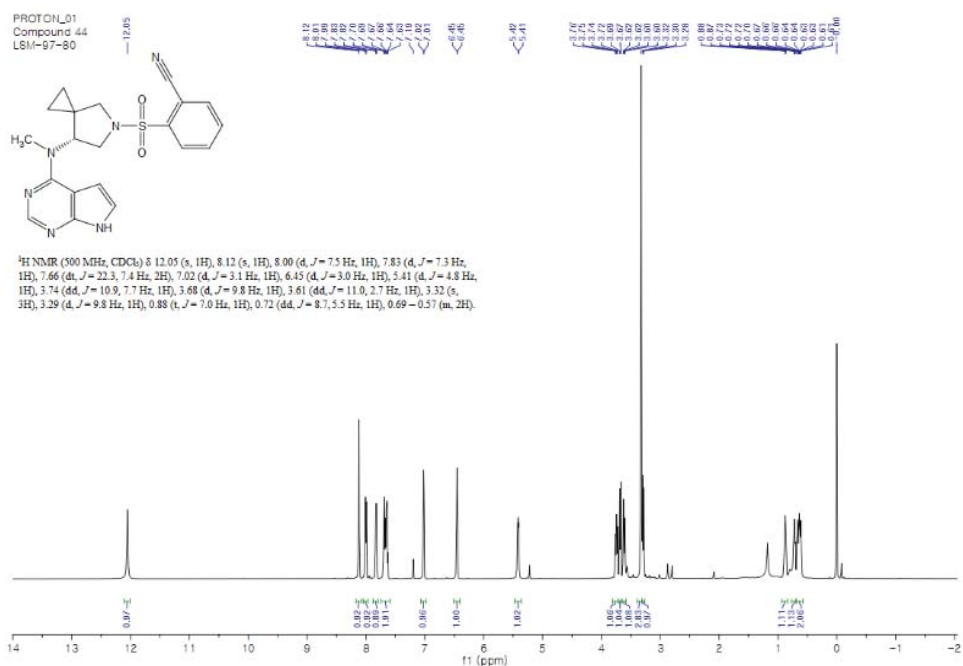
(R)-*N*-(5-((3-Fluorophenyl)sulfonyl)-5-azaspiro[2.4]heptan-7-yl)-*N*-methyl-7*H*-pyrrolo[2,3-*d*]pyrimidin-4-amine, **55**



(R)-*N*-(5-((4-Fluorophenyl)sulfonyl)-5-azaspiro[2.4]heptan-7-yl)-*N*-methyl-7H-pyrrolo[2,3-*d*]pyrimidin-4-amine, **56**

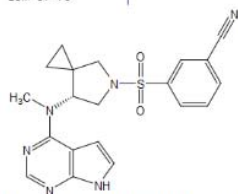


(R)-2-((7-(Methyl(7*H*-pyrrolo[2,3-*d*]pyrimidin-4-yl)amino)-5-azaspiro[2.4]heptan-5-yl)sulfonyl)benzonitrile, **57**

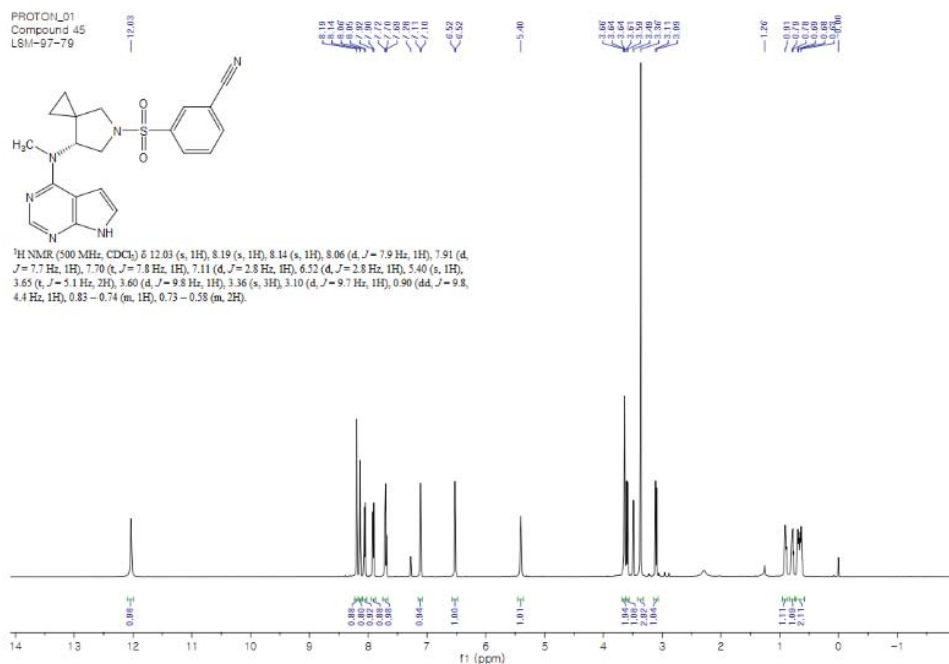


(R)-3-((7-(Methyl(7*H*-pyrrolo[2,3-*d*]pyrimidin-4-yl)amino)-5-azaspiro[2.4]heptan-5-yl)sulfonyl)benzonitrile, **58**

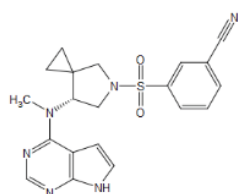
PROTON_01
Compound 45
LSM-97-79



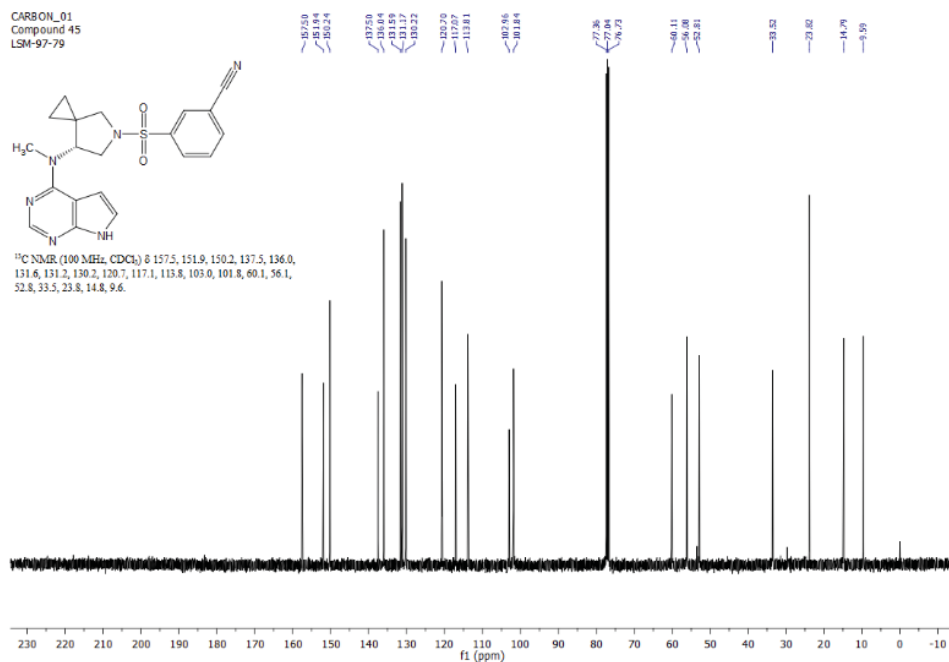
¹H NMR (500 MHz, CDCl₃) δ 12.03 (s, 1H), 8.19 (s, 1H), 8.14 (s, 1H), 8.06 (d, *J* = 7.9 Hz, 1H), 7.91 (d, *J* = 7.7 Hz, 1H), 7.70 (t, *J* = 7.8 Hz, 1H), 7.11 (d, *J* = 2.8 Hz, 2H), 6.52 (d, *J* = 2.8 Hz, 1H), 5.40 (s, 1H), 3.65 (t, *J* = 3.1 Hz, 2H), 3.60 (d, *J* = 9.8 Hz, 1H), 3.36 (s, 3H), 3.10 (d, *J* = 9.7 Hz, 1H), 0.90 (dd, *J* = 9.8, 4.4 Hz, 1H), 0.83 – 0.74 (m, 1H), 0.73 – 0.58 (m, 2H).



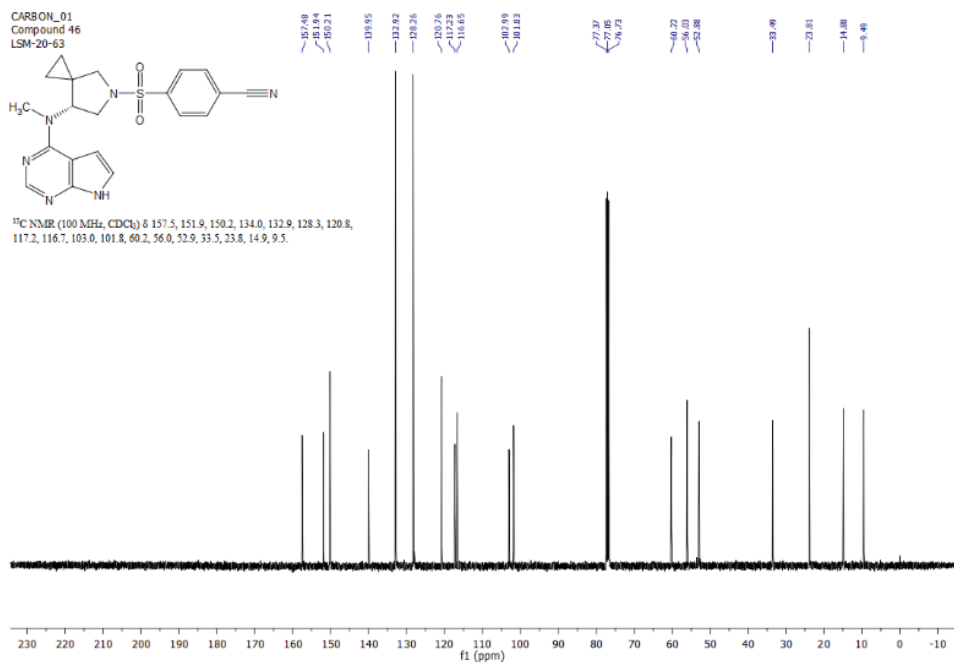
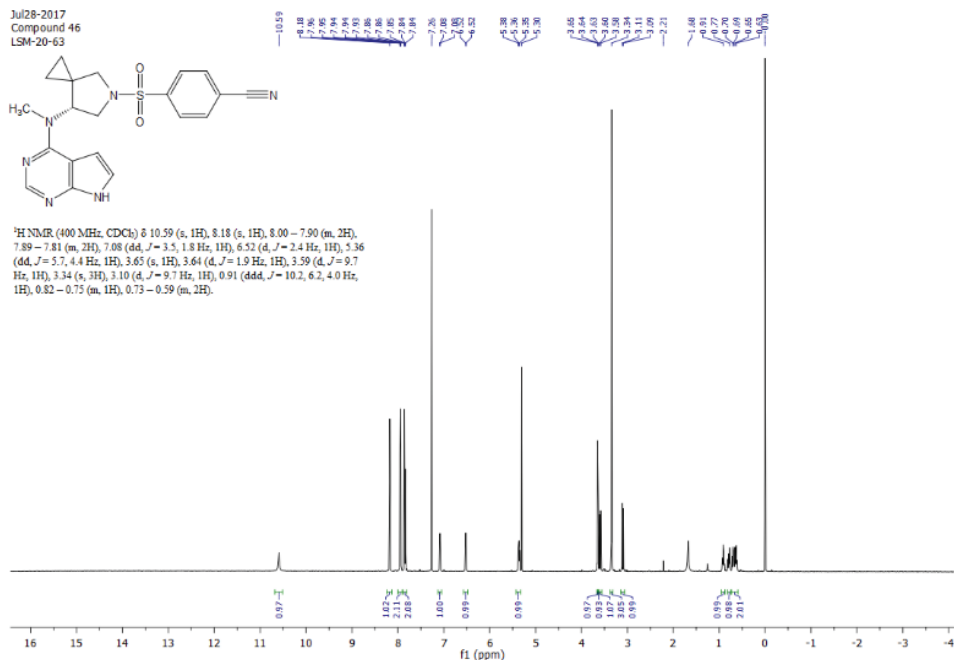
CARBON_01
Compound 45
LSM-97-79



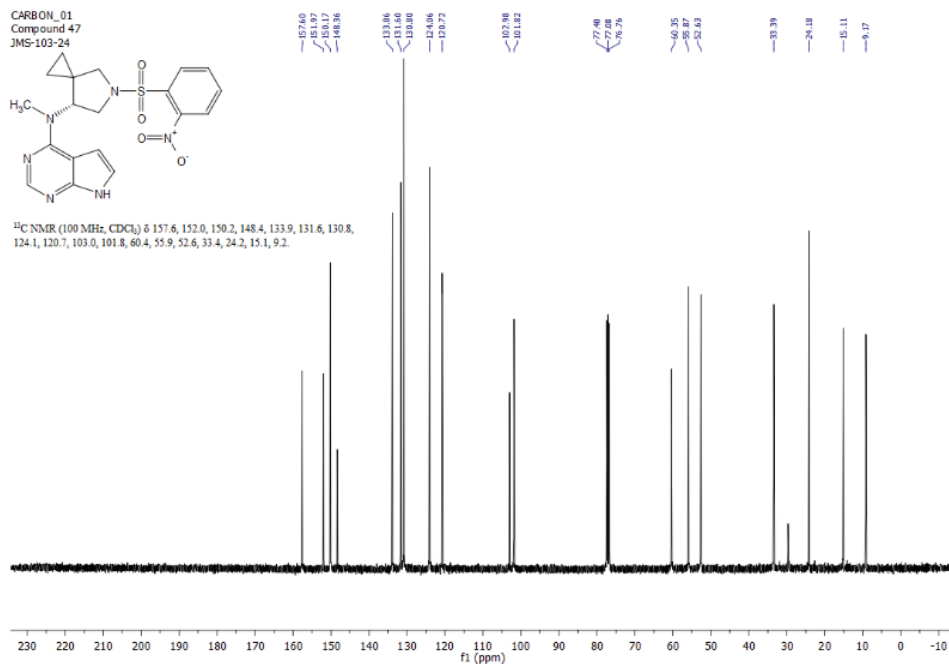
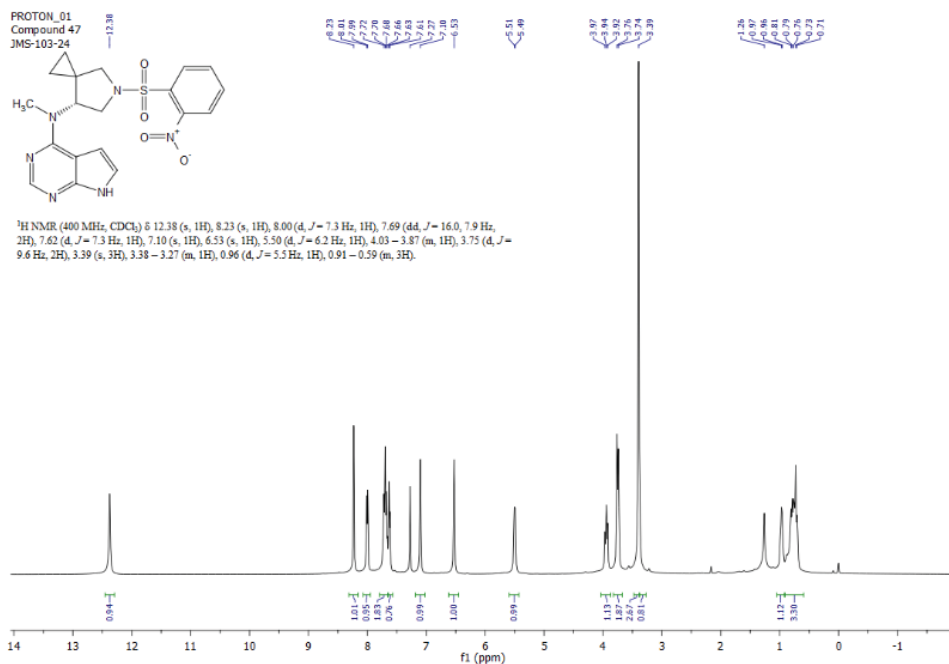
¹³C NMR (100 MHz, CDCl₃) δ 157.5, 151.9, 150.2, 137.5, 136.0, 131.6, 131.2, 130.2, 120.7, 117.1, 113.8, 103.0, 101.8, 60.1, 56.1, 52.8, 33.5, 23.8, 14.8, 9.6.



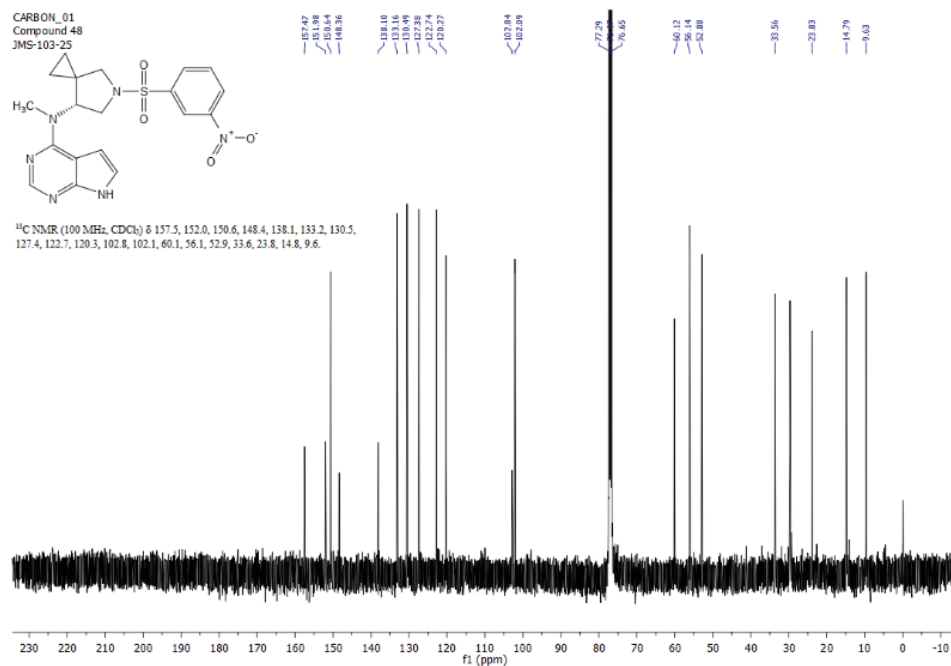
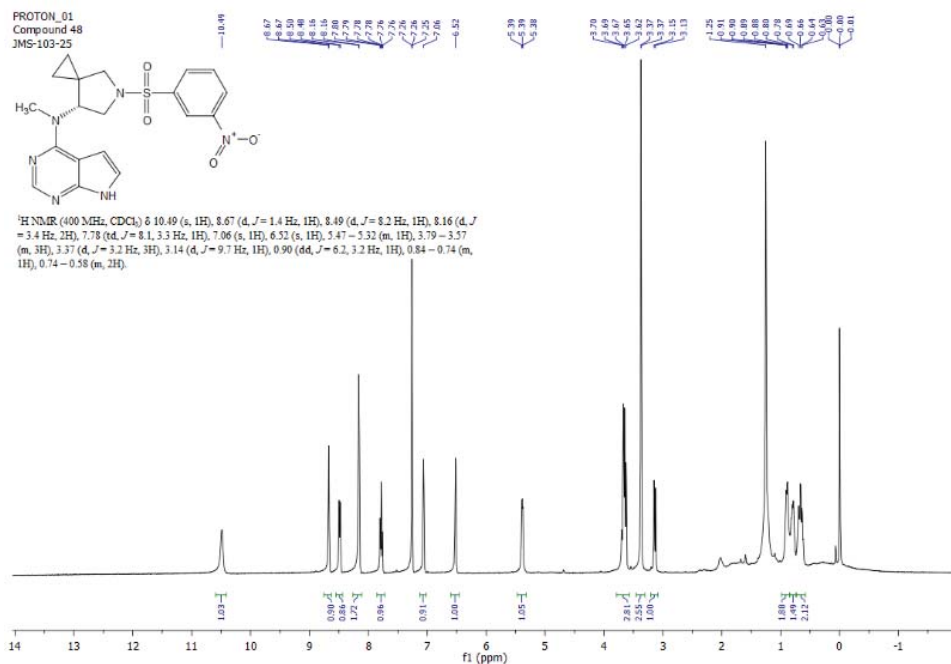
(R)-4-((7-(Methyl(7H-pyrrolo[2,3-d]pyrimidin-4-yl)amino)-5-azaspiro[2.4]heptan-5-yl)sulfonyl)benzonitrile, **59**



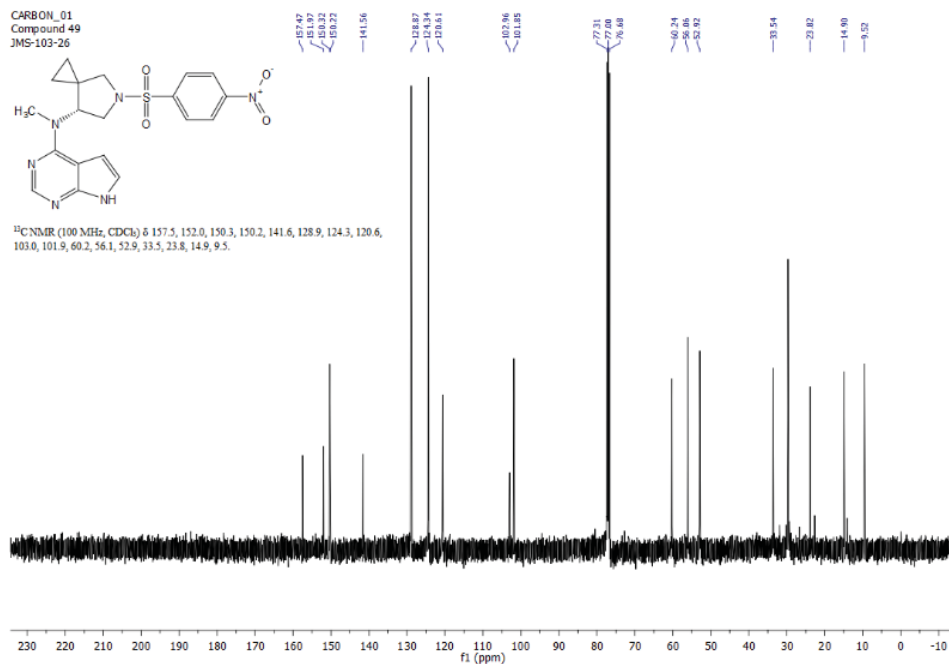
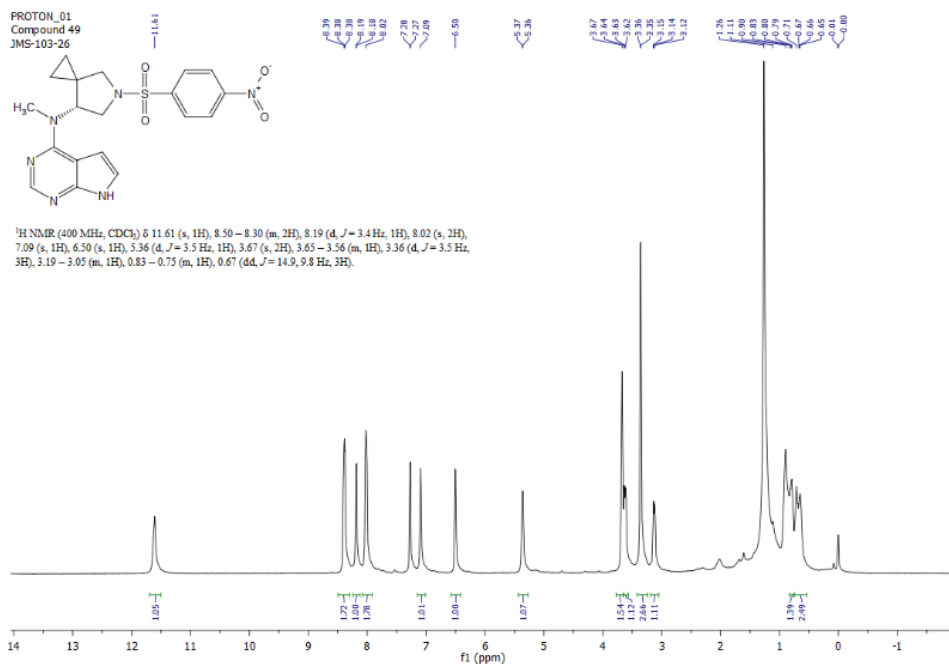
(R)-*N*-Methyl-*N*-(5-((2-nitrophenyl)sulfonyl)-5-azaspiro[2.4]heptan-7-yl)-7H-pyrrolo[2,3-*d*]pyrimidin-4-amine, **60**



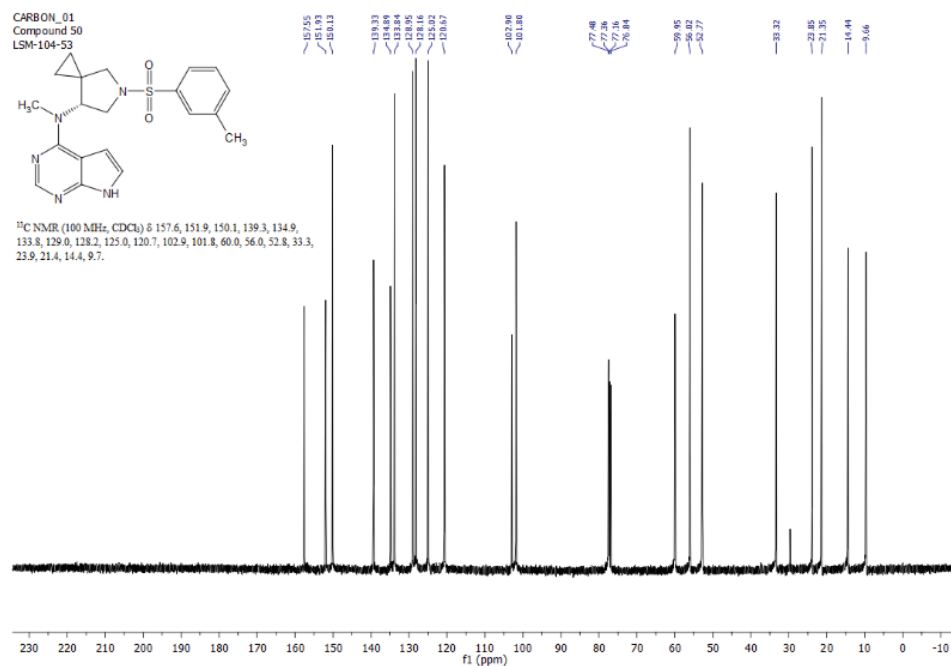
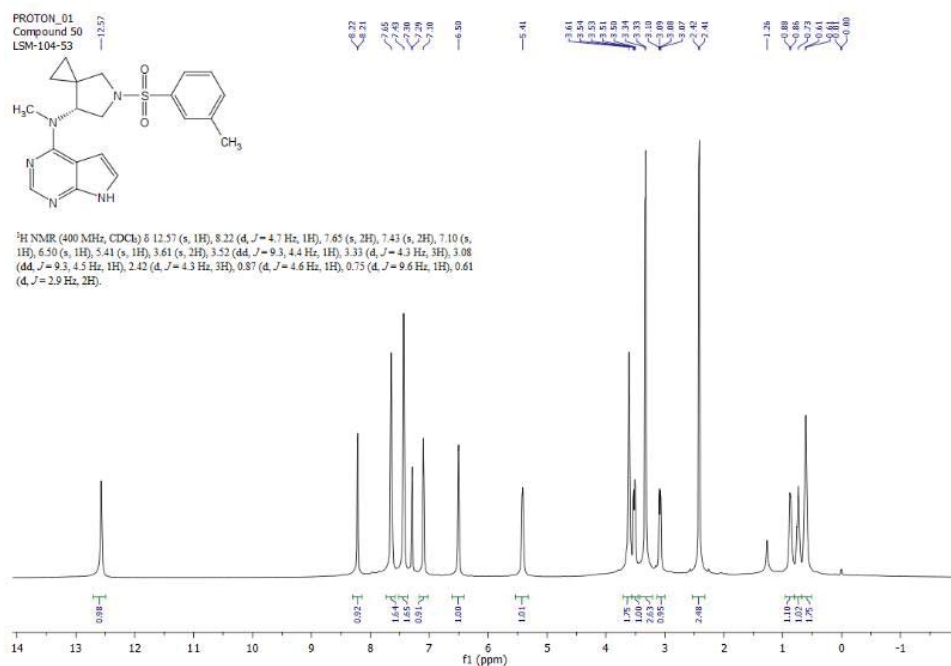
(R)-*N*-Methyl-*N*-(5-((3-nitrophenyl)sulfonyl)-5-azaspiro[2.4]heptan-7-yl)-7*H*-pyrrolo[2,3-*d*]pyrimidin-4-amine, **61**



(R)-*N*-Methyl-*N*-(5-((4-nitrophenyl)sulfonyl)-5-azaspiro[2.4]heptan-7-yl)-7*H*-pyrrolo[2,3-*d*]pyrimidin-4-amine, **62**



(R)-*N*-Methyl-*N*-(5-(*m*-tolylsulfonyl)-5-azaspiro[2.4]heptan-7-yl)-7*H*-pyrrolo[2,3-*d*]pyrimidin-4-amine, **63**



PROTON_01
Compound 51
LSM-104-06-2

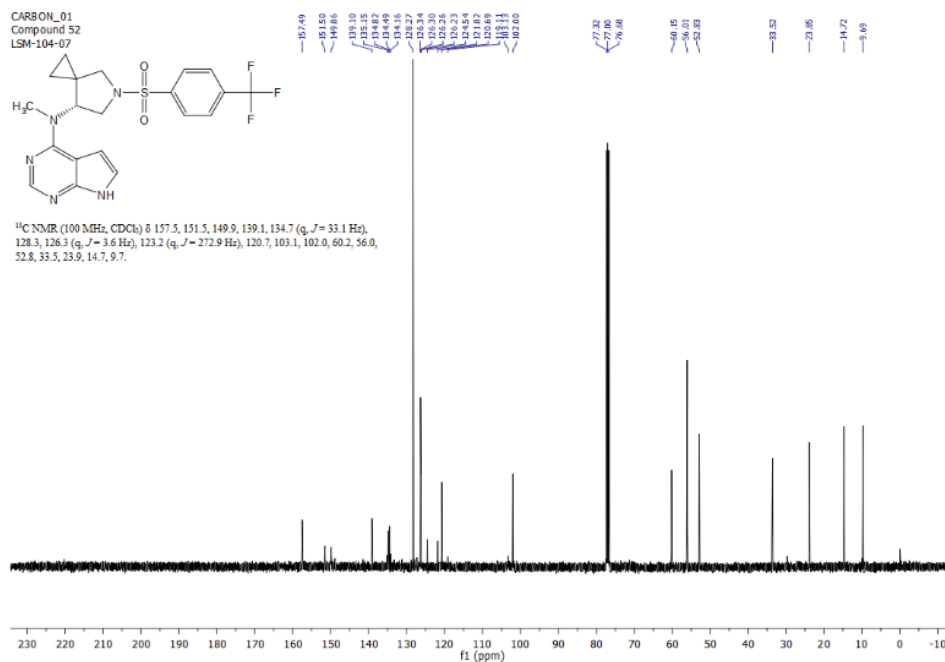
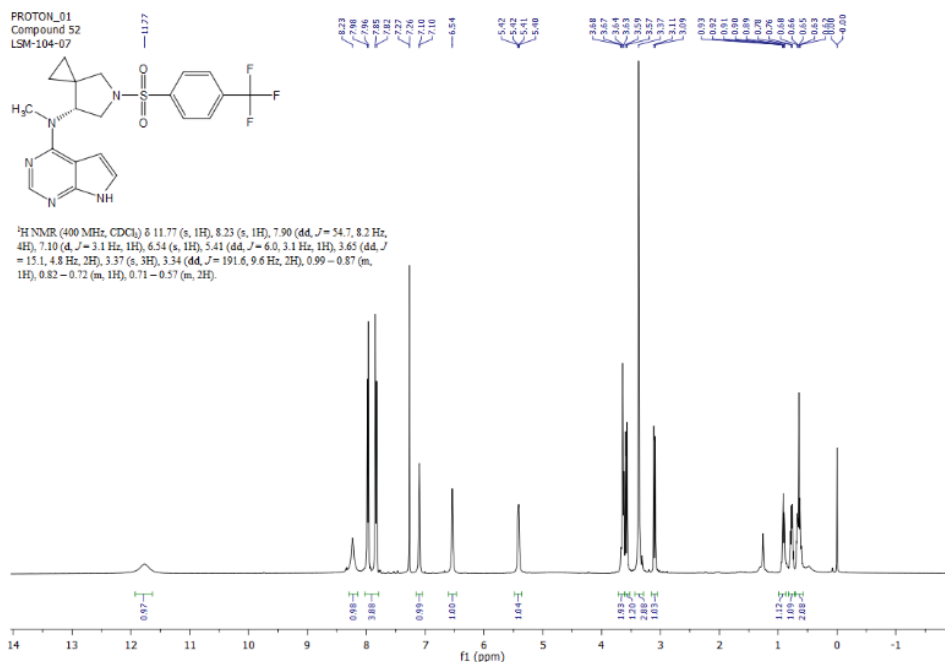
Chemical structure of Compound 51 (LSM-104-06-2) is shown, featuring a 1,2,3,4-tetrahydroquinoline ring system substituted with a methyl group and a 4-methoxyphenyl group.

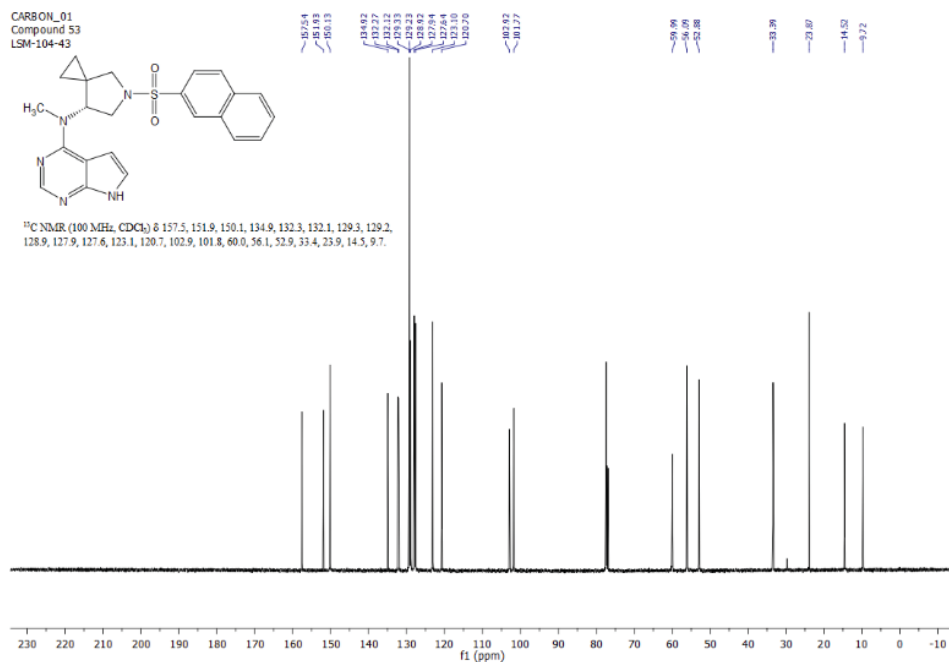
¹H NMR (400 MHz, CDCl₃) δ 11.94 (s, 1H), 8.19 (s, 1H), 7.78 (d, *J* = 8.8 Hz, 2H), 7.09 (d, *J* = 3.4 Hz, 1H), 7.02 (d, *J* = 8.8 Hz, 2H), 6.53 (d, *J* = 3.1 Hz, 1H), 5.43 (t, *J* = 4.7 Hz, 1H), 3.89 (s, 3H), 3.56 (d, *J* = 4.9 Hz, 2H), 3.36 (s, 3H), 3.27 (dd, *J* = 174.5, 9.5 Hz, 2H), 0.95 – 0.84 (m, 1H), 0.78 – 0.68 (m, 1H), 0.62 (t, *J* = 7.5 Hz, 2H).

The ¹H NMR spectrum (400 MHz, CDCl₃) is displayed, showing peaks corresponding to the structure. The x-axis represents the chemical shift (δ) in ppm, ranging from 0 to 14. Key peaks are labeled with their chemical shifts and integrations: 11.94 (s, 1H), 8.19 (s, 1H), 7.78 (d, 2H), 7.09 (d, 1H), 7.02 (d, 2H), 6.53 (d, 1H), 5.43 (t, 1H), 3.89 (s, 3H), 3.56 (d, 2H), 3.36 (s, 3H), 3.27 (dd, 2H), 0.95 – 0.84 (m, 1H), 0.78 – 0.68 (m, 1H), 0.62 (t, 2H).

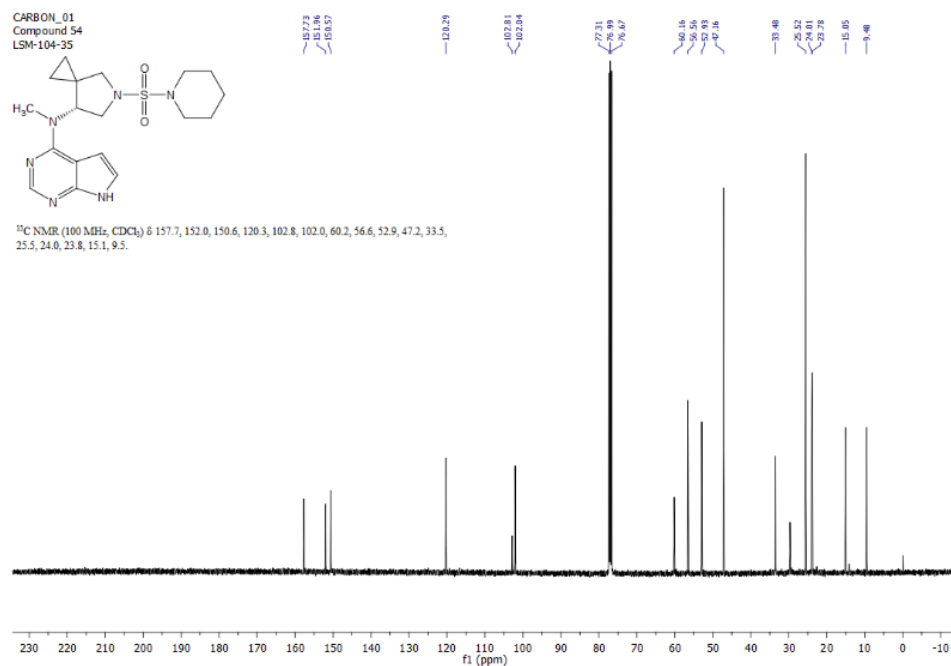
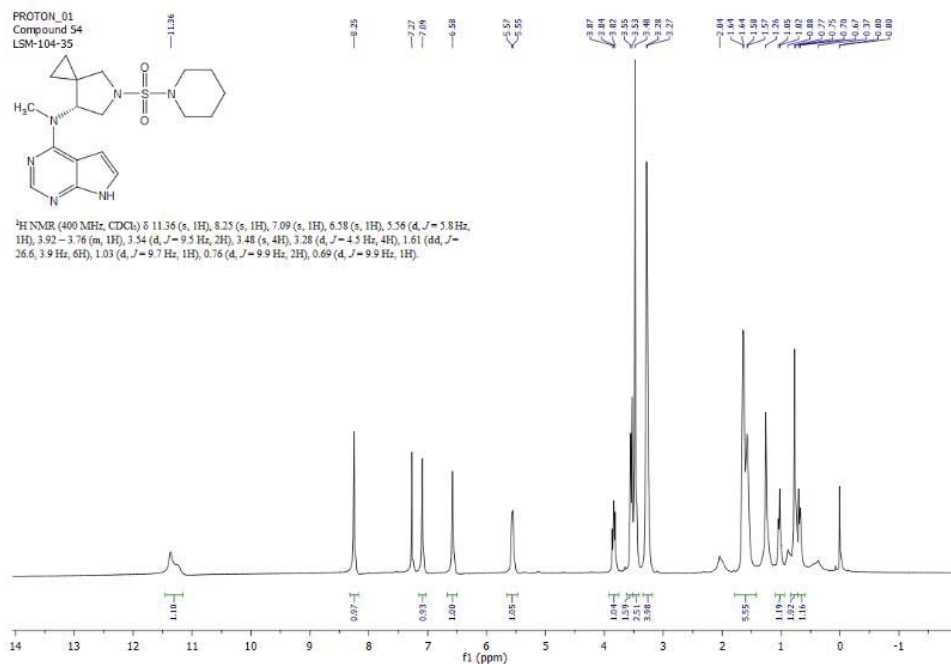


(R)-*N*-Methyl-*N*-(5-((4-(trifluoromethyl)phenyl)sulfonyl)-5-azaspiro[2.4]heptan-7-yl)-7*H*-pyrrolo[2,3-*d*]pyrimidin-4-amine, **65**

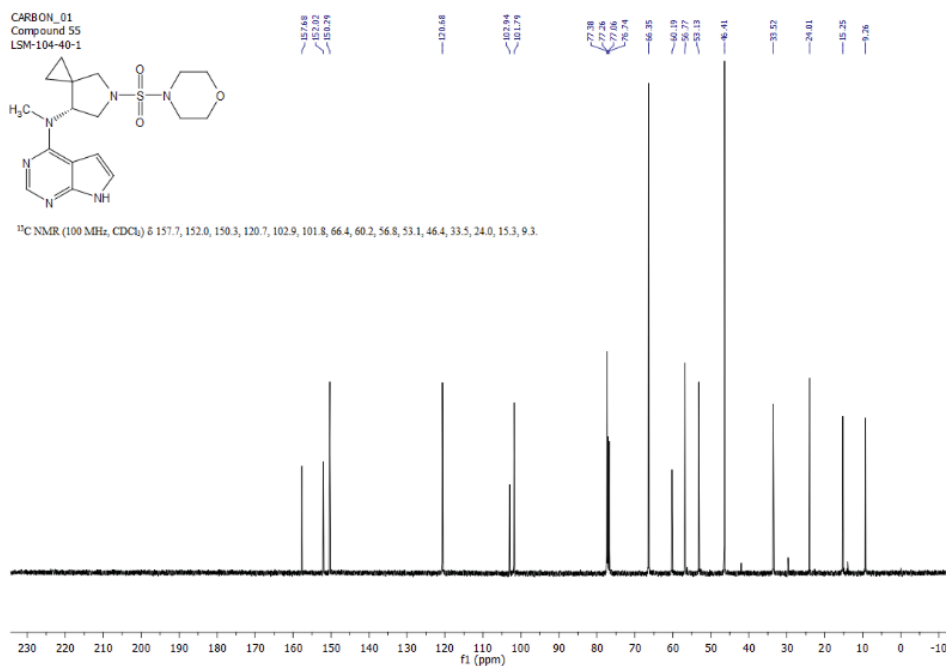
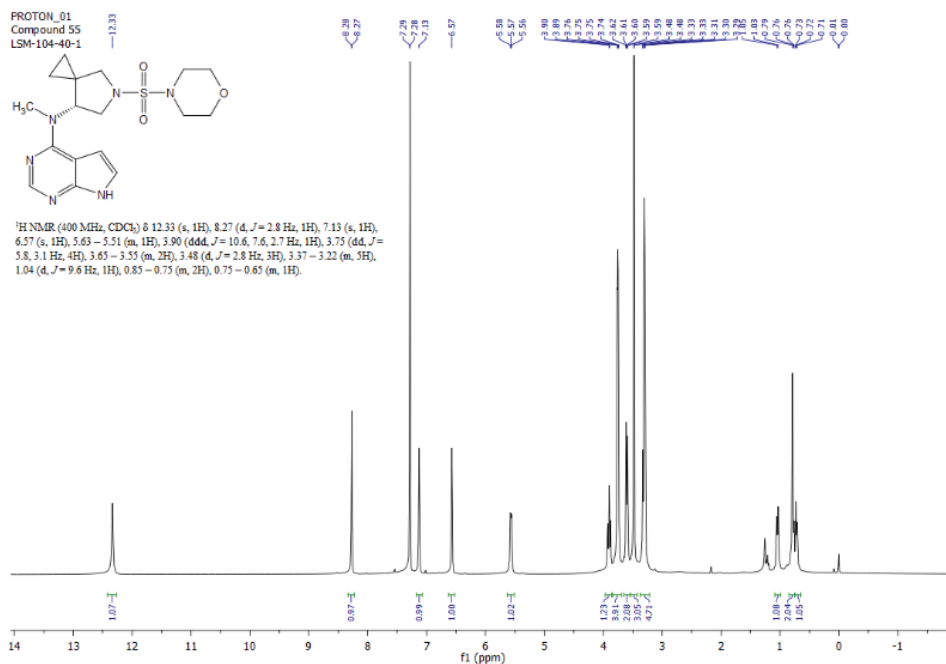




(R)-*N*-Methyl-*N*-(5-(piperidin-1-ylsulfonyl)-5-azaspiro[2.4]heptan-7-yl)-7*H*-pyrrolo[2,3-*d*]pyrimidin-4-amine, **67**



(R)-*N*-Methyl-*N*-(5-(morpholin sulfonyl)-5-azaspiro[2.4]heptan-7-yl)-7*H*-pyrrolo[2,3-*d*]pyrimidin-4-amine, **68**



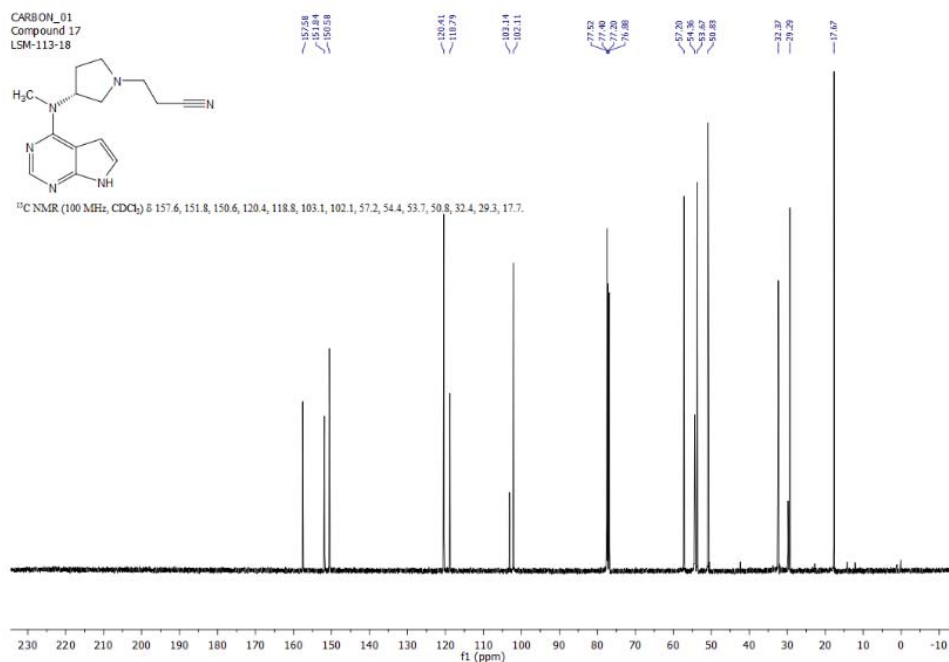
PROTON_01
Compound 17
LSM-113-18

CN1CC[C@H](C1)N(C)C2=NC3=C(N2)C=CC=C3

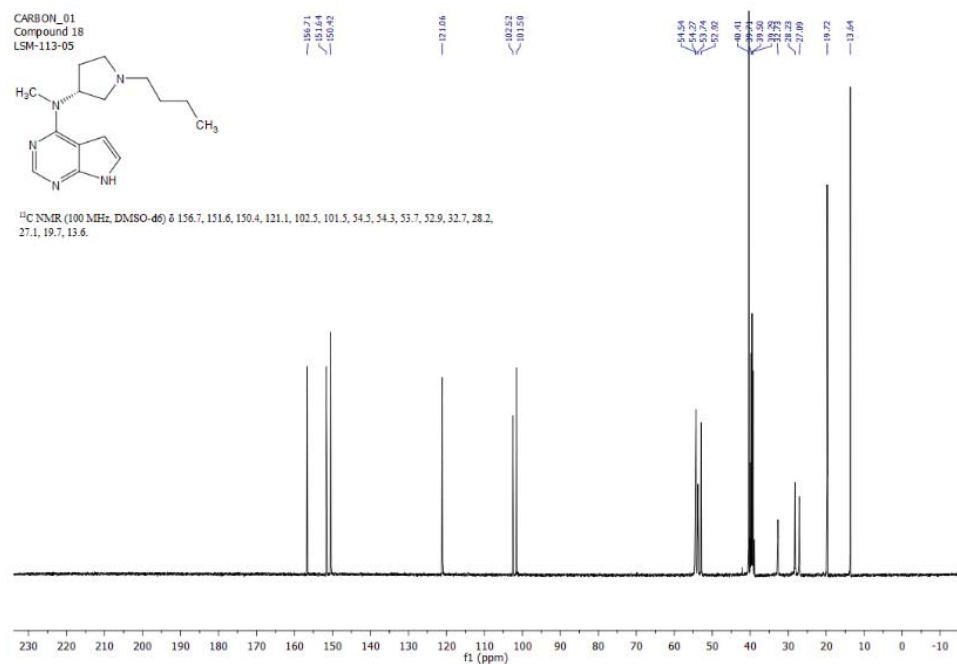
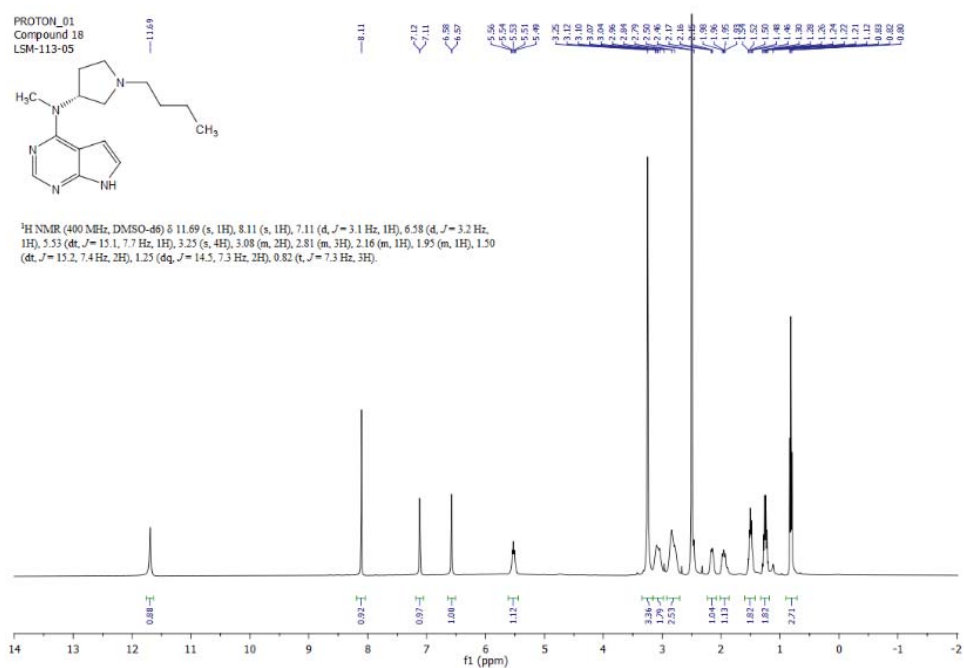
¹H NMR (400 MHz, CDCl₃) 8.32 (s, 1H), 8.32 (s, 1H), 7.10 (d, *J* = 3.4 Hz, 1H), 6.58 (d, *J* = 3.3 Hz, 1H), 5.73 (s, 1H), 3.42 (s, 3H), 3.06 (t, *J* = 7.1 Hz, 1H), 2.94 (dd, *J* = 9.9, 3.1 Hz, 1H), 2.83 (m, 1H), 2.72 (m, 1H), 2.64 (t, *J* = 9.2 Hz, 1H), 2.56 (t, *J* = 6.8 Hz, 2H), 2.34 (m, 2H), 1.93 (dt, *J* = 13.0, 10.0 Hz, 1H).

1.08 0.99 0.95 1.08 1.08 2.68 0.99 1.04 1.04 1.89 2.07 1.09

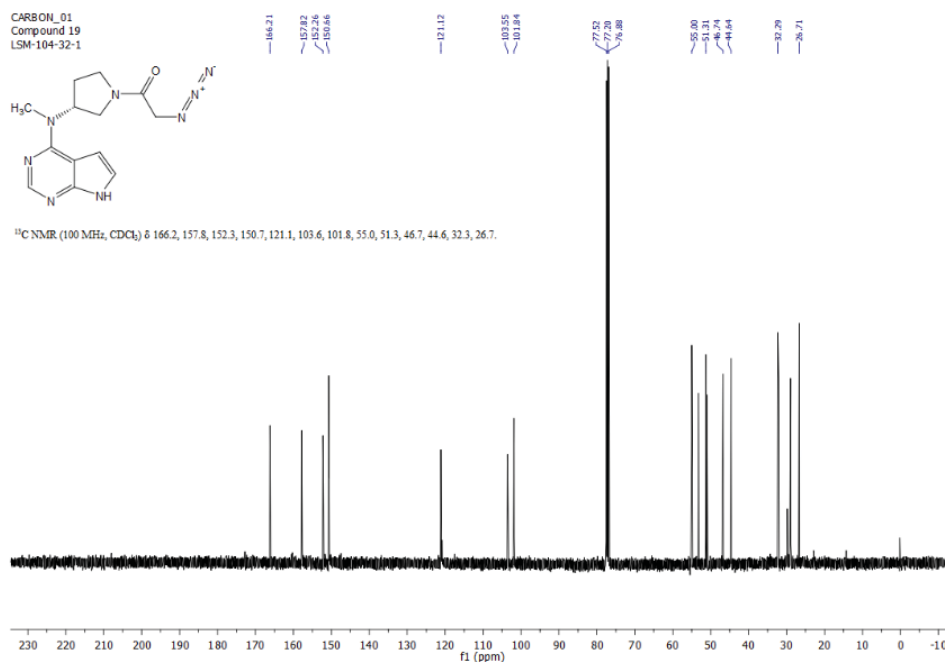
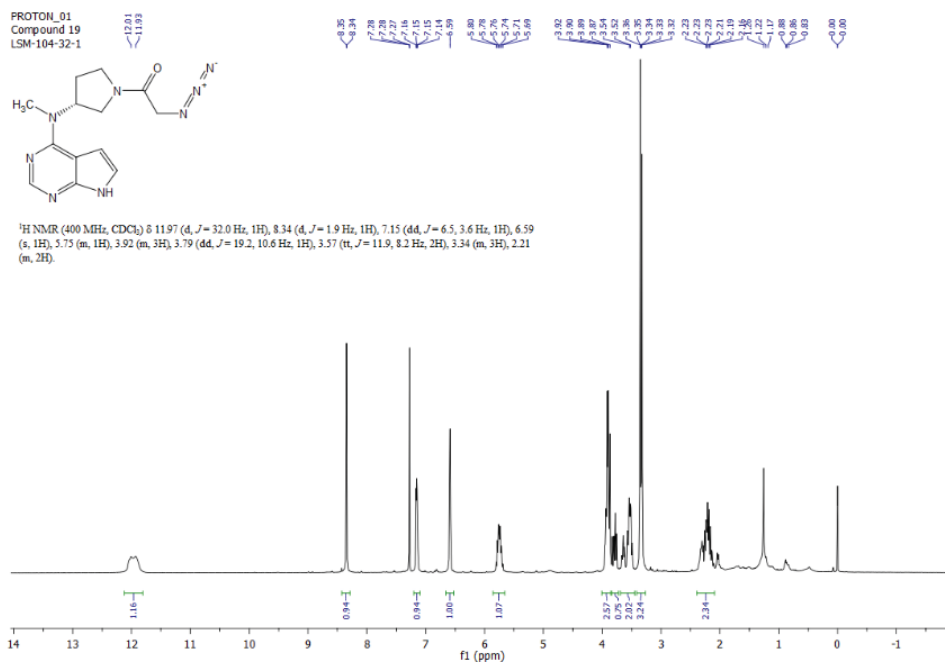
13.32 8.32 7.28 7.10 6.58 5.73 5.30 3.42 3.06 2.94 2.83 2.72 2.64 2.56 2.34 1.93 0.00



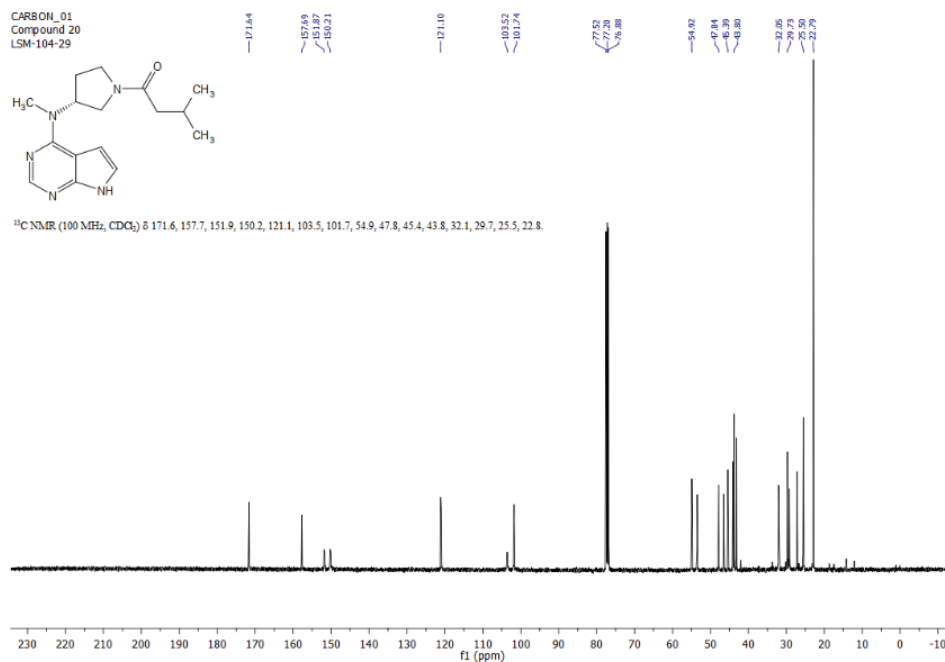
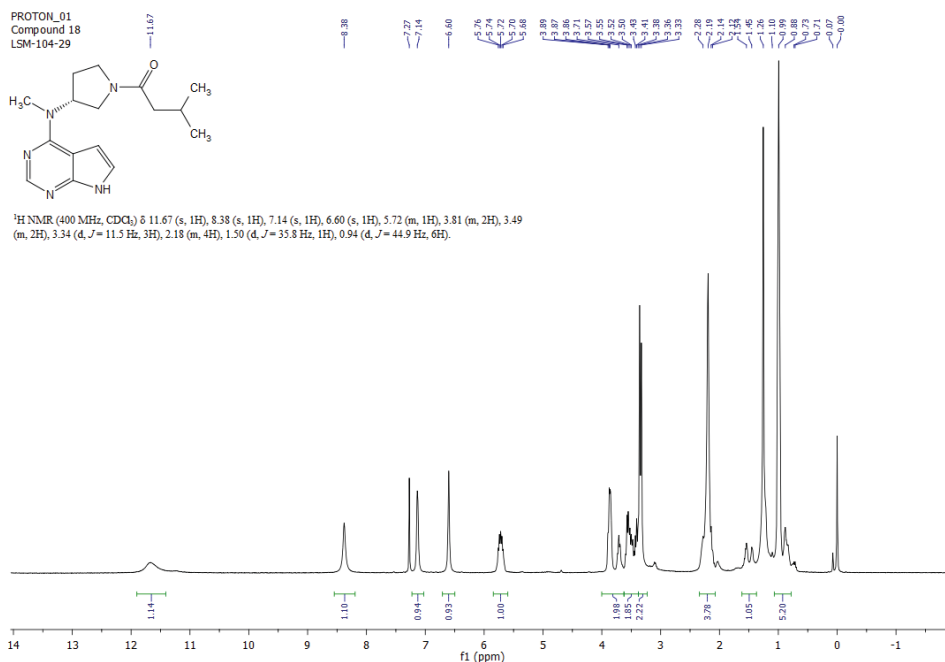
(R)-*N*-(1-Butylpyrrolidin-3-yl)-*N*-methyl-7H-pyrrolo[2,3-*d*]pyrimidin-4-amine, **70**



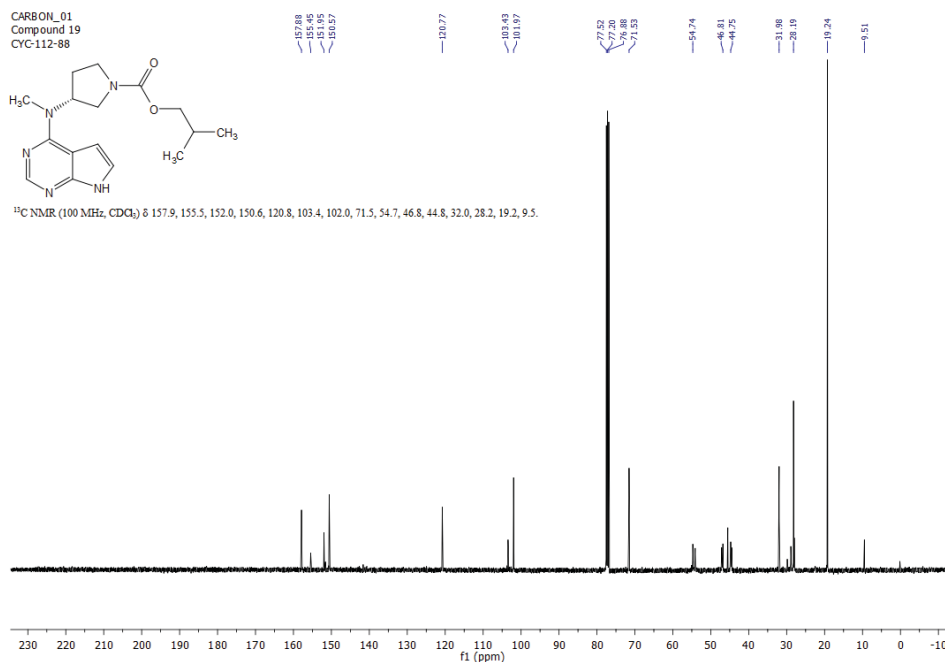
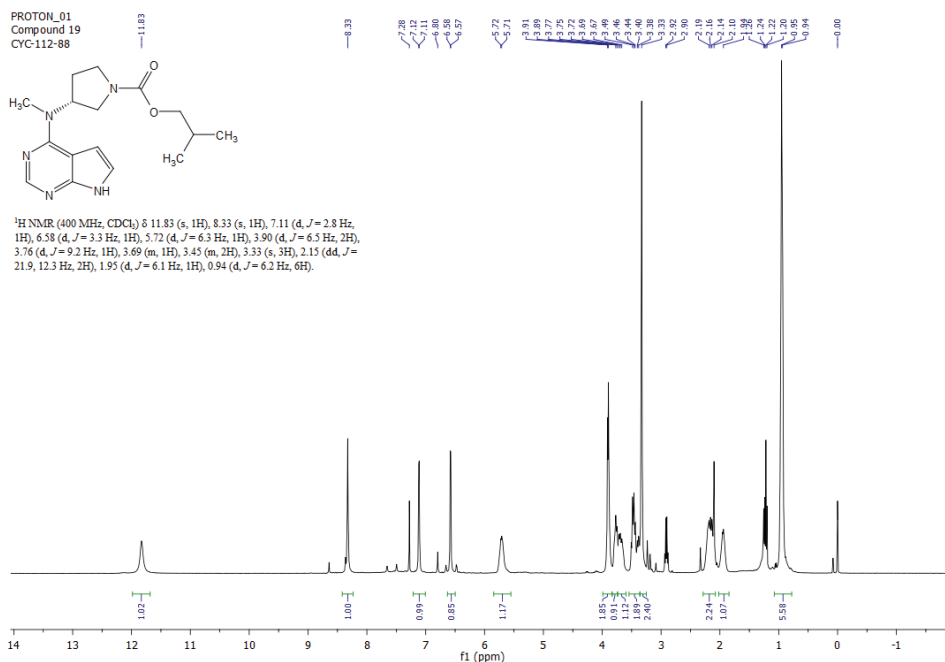
(R)-2-Azido-1-(3-(methyl(7H-pyrrolo[2,3-d]pyrimidin-4-yl)amino)pyrrolidin-1-yl)ethan-1-one, **71**



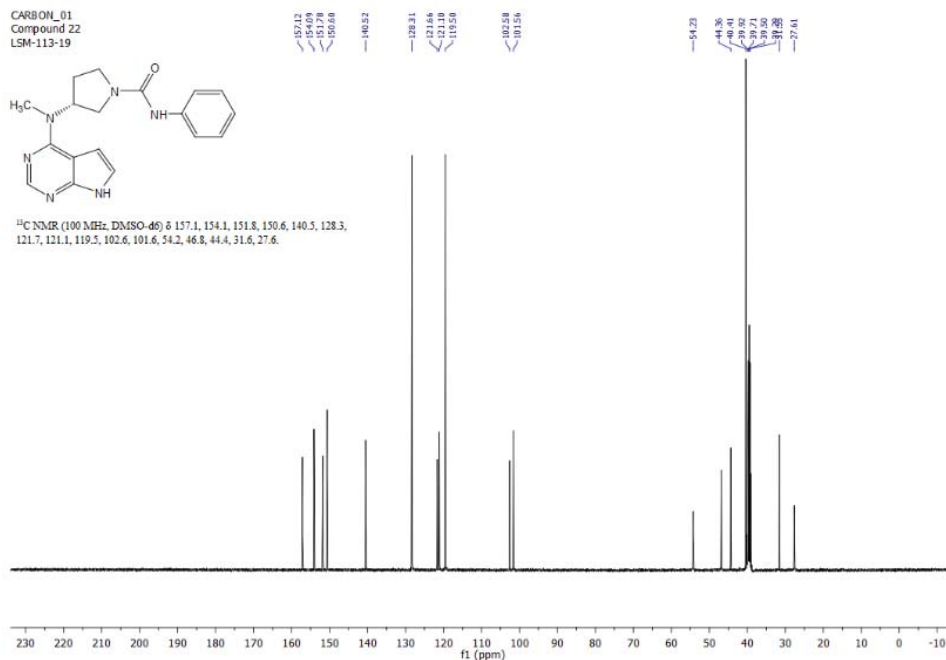
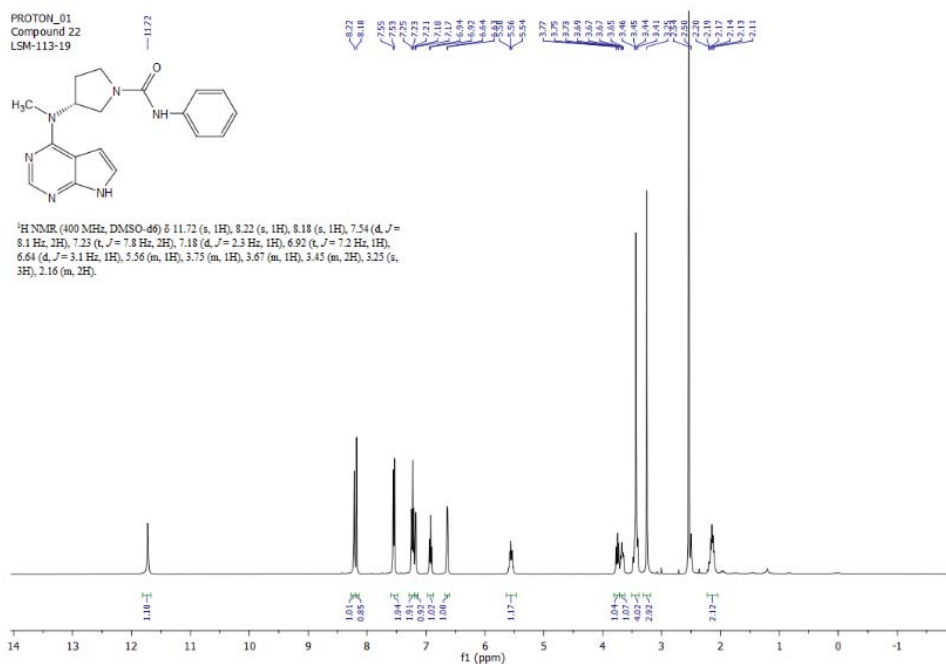
(R)-3-Methyl-1-(3-(methyl(7H-pyrrolo[2,3-d]pyrimidin-4-yl)amino)pyrrolidin-1-yl)butan-1-one, **72**



Isobutyl (R)-3-(methyl(7H-pyrrolo[2,3-d]pyrimidin-4-yl)amino)pyrrolidine-1-carboxylate, **73**



(R)-3-(Methyl(7*H*-pyrrolo[2,3-*d*]pyrimidin-4-yl)amino)-*N*-phenylpyrrolidine-1-carboxamide, **74**



PROTON_01
Compound 23
LSM-104-37

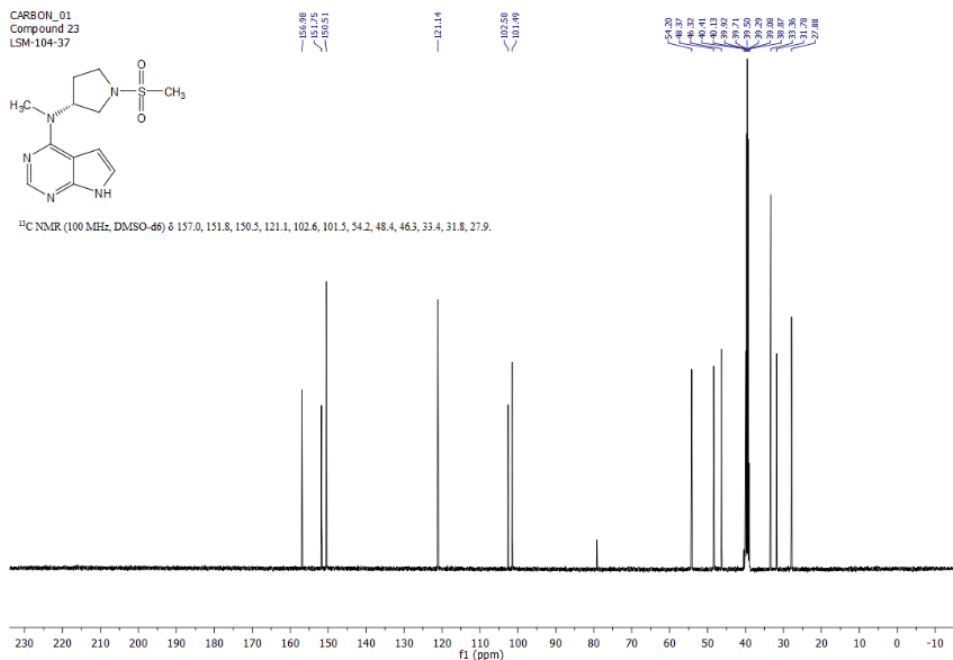
CN1CCCC1S(=O)(=O)c2cnc3c[nH]c3n2

¹H NMR (400 MHz, DMSO-d₆) δ 11.70 (s, 1H), 8.15 (d, *J* = 1.3 Hz, 1H), 7.17 (d, *J* = 2.9 Hz, 1H), 6.62 (d, *J* = 2.7 Hz, 1H), 5.58 (m, 1H), 3.52 (t, *J* = 9.0 Hz, 1H), 3.46 (m, 1H), 3.31 (dd, *J* = 17.4, 8.7 Hz, 1H), 3.23 (dd, *J* = 10.0, 4.4 Hz, 4H), 2.98 (d, *J* = 1.3 Hz, 3H), 2.14 (m, 2H).

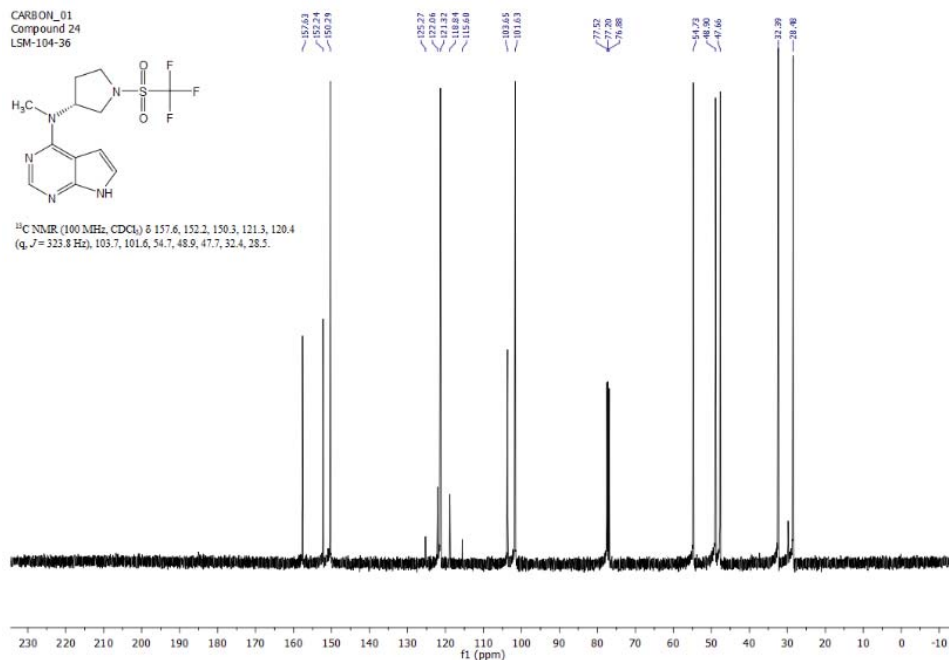
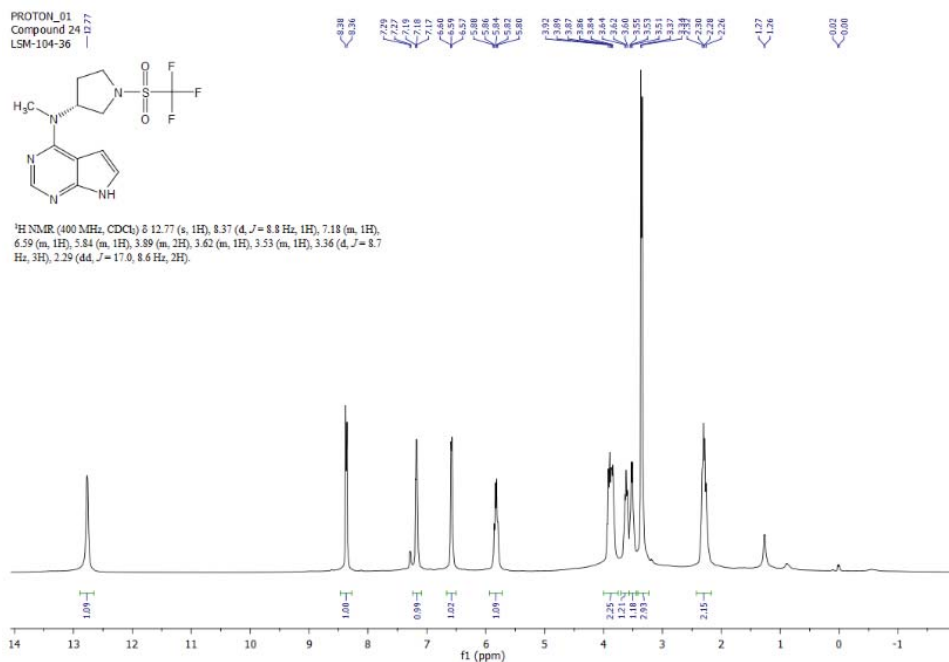
11.70
8.15
7.17
6.62
5.58
3.52
3.46
3.31
3.23
2.98
2.14

1.11
1.00
1.07
1.12
1.10
1.06
1.24
1.25
3.01
3.12
2.24

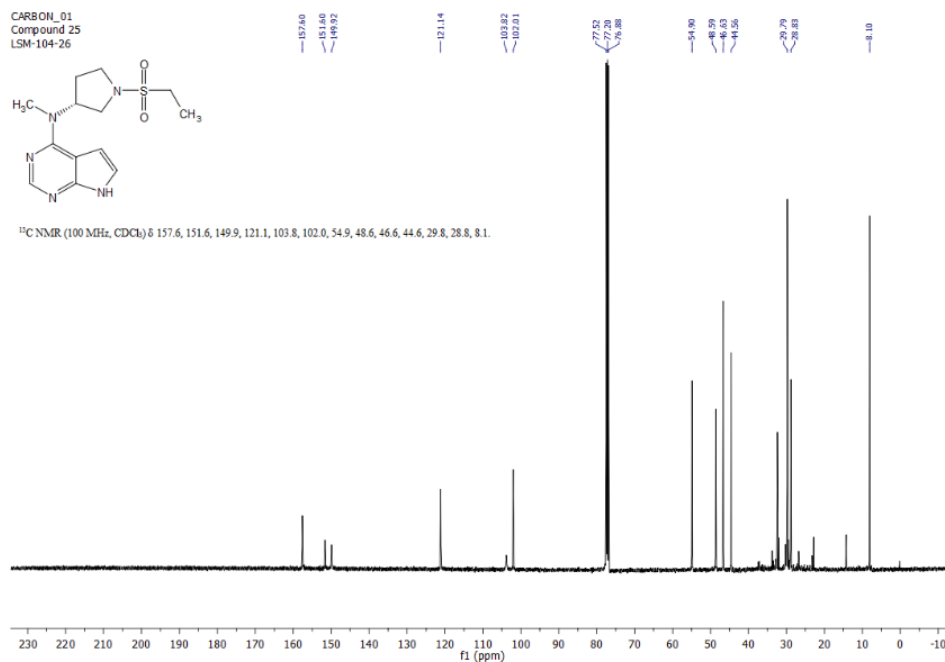
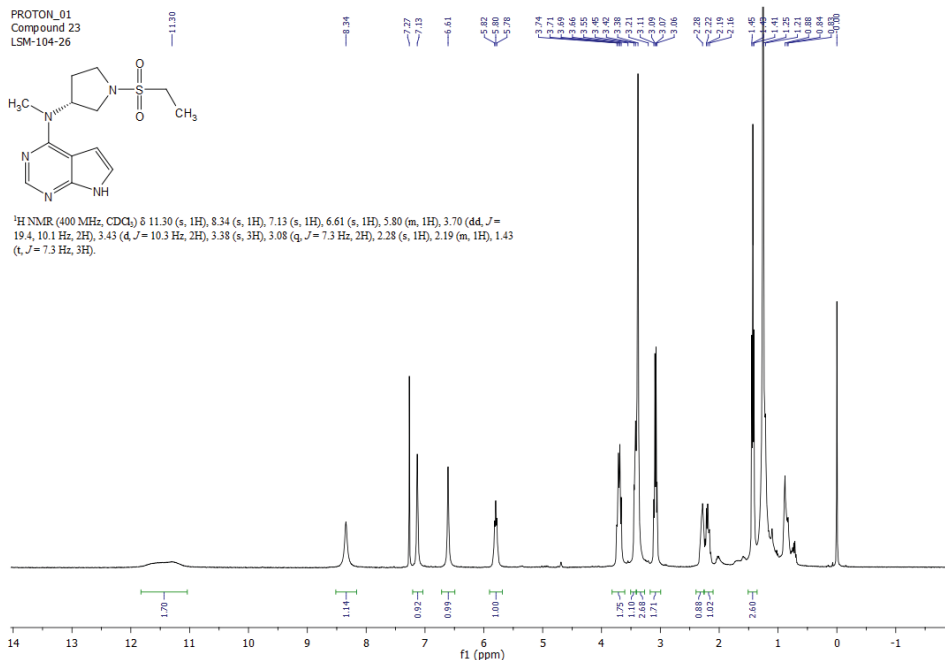
f1 (ppm)



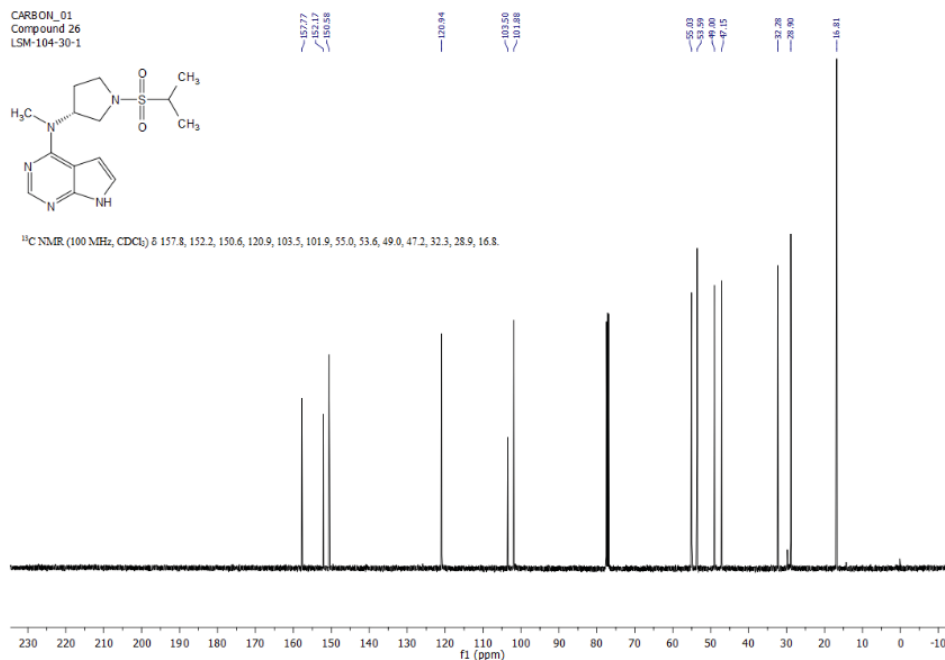
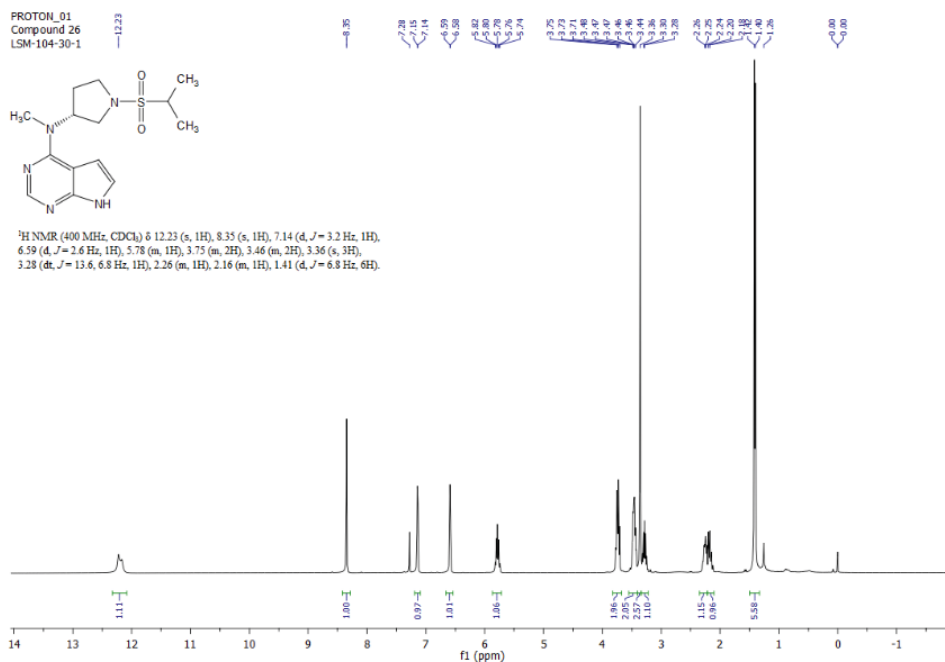
(R)-*N*-Methyl-*N*-(1-((trifluoromethyl)sulfonyl)pyrrolidin-3-yl)-7*H*-pyrrolo[2,3-*d*]pyrimidin-4-amine, **76**



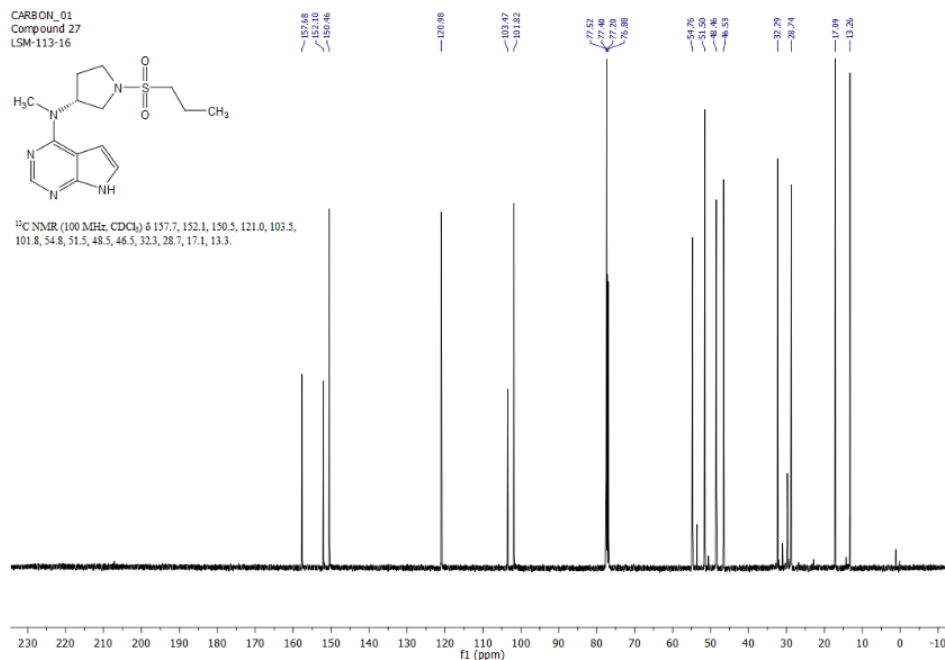
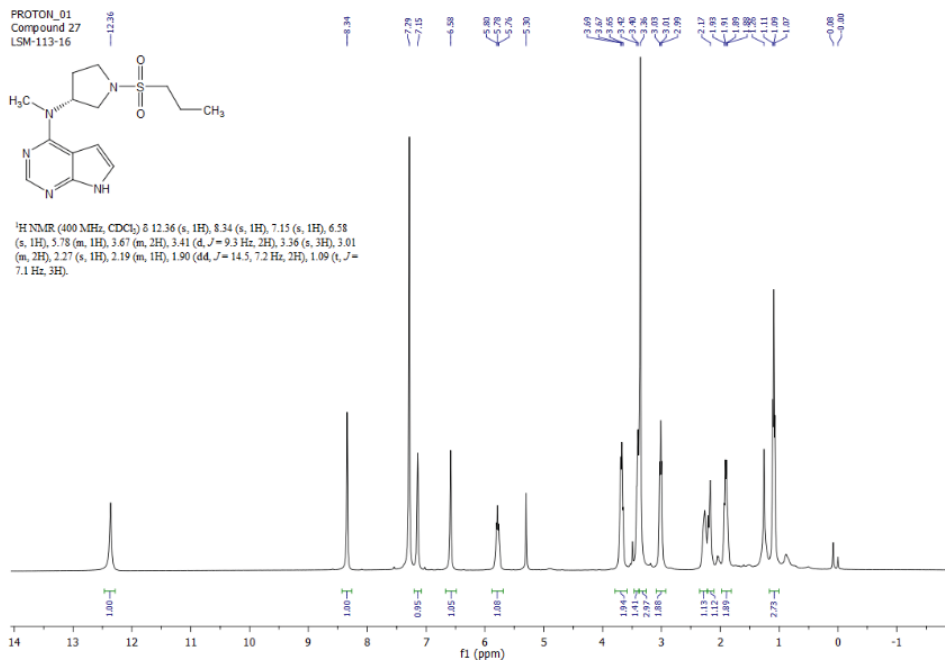
(R)-*N*-(1-(Ethylsulfonyl)pyrrolidin-3-yl)-*N*-methyl-7*H*-pyrrolo[2,3-*d*]pyrimidin-4-amine, 77



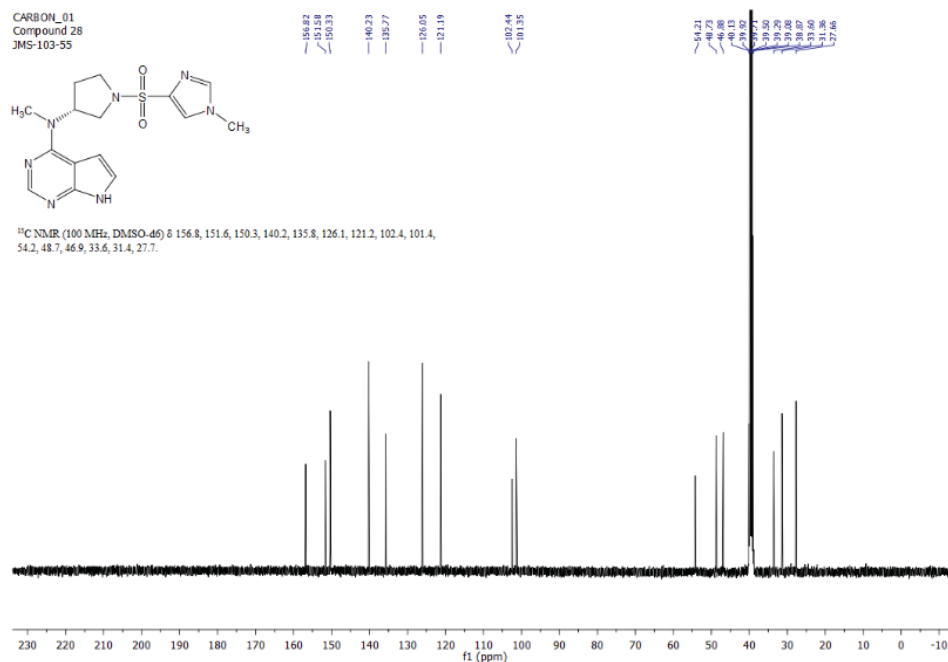
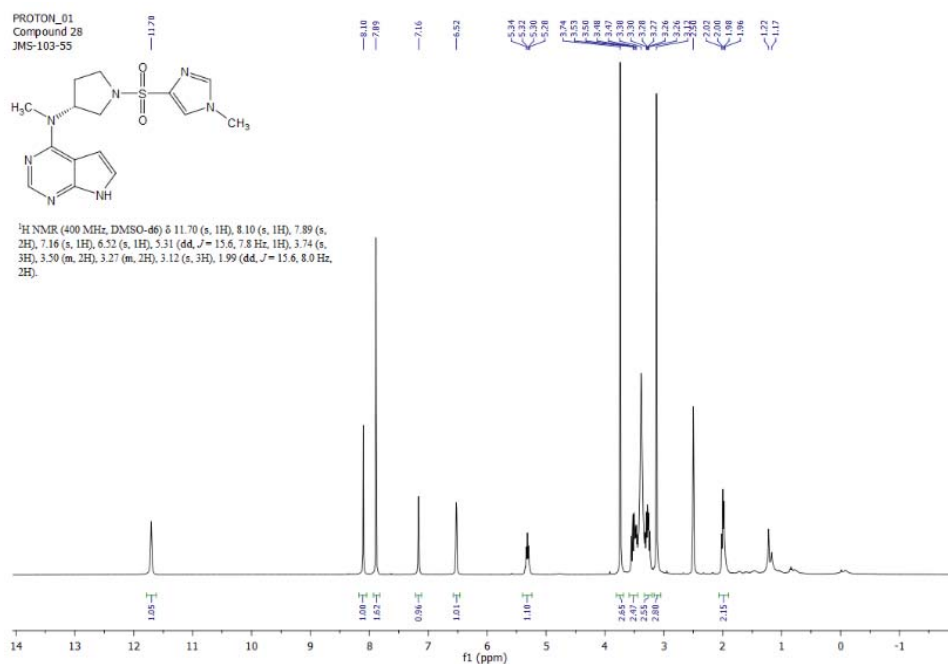
(R)-*N*-(1-(Isopropylsulfonyl)pyrrolidin-3-yl)-*N*-methyl-7*H*-pyrrolo[2,3-*d*]pyrimidin-4-amine, **78**



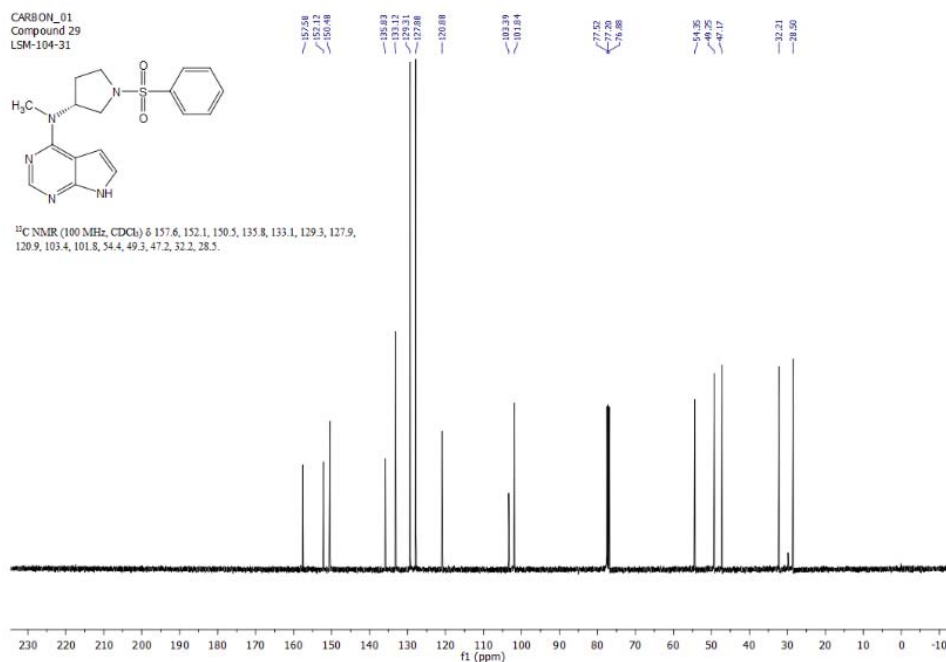
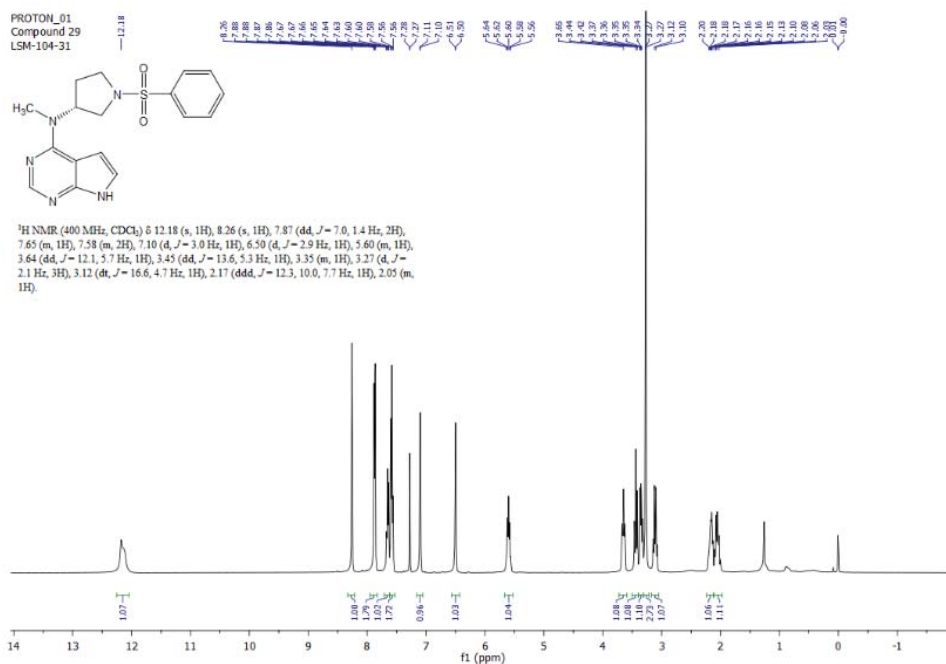
(R)-*N*-Methyl-*N*-(1-(propylsulfonyl)pyrrolidin-3-yl)-7*H*-pyrrolo[2,3-*d*]pyrimidin-4-amine, **79**



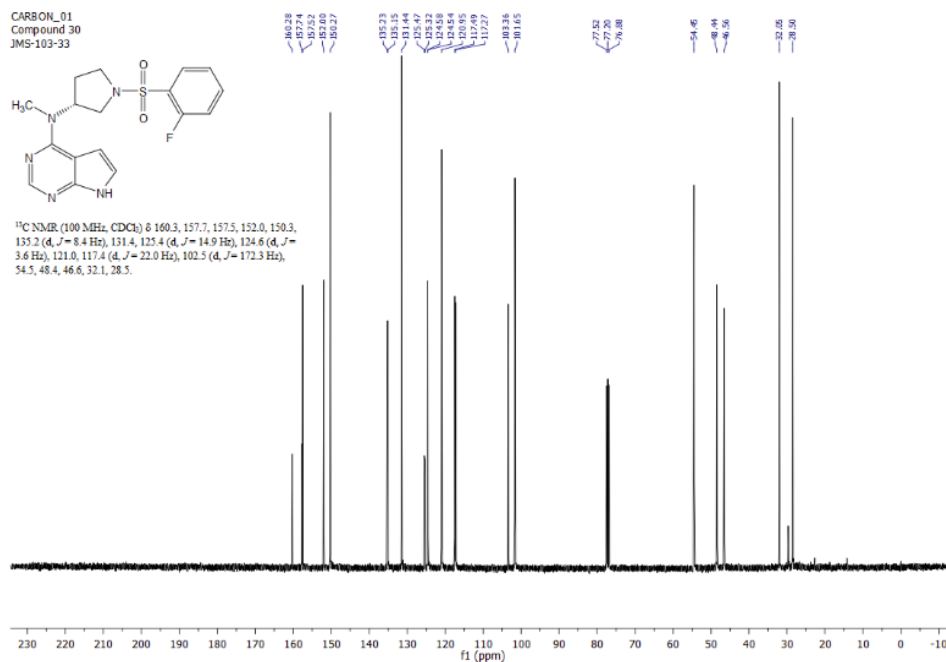
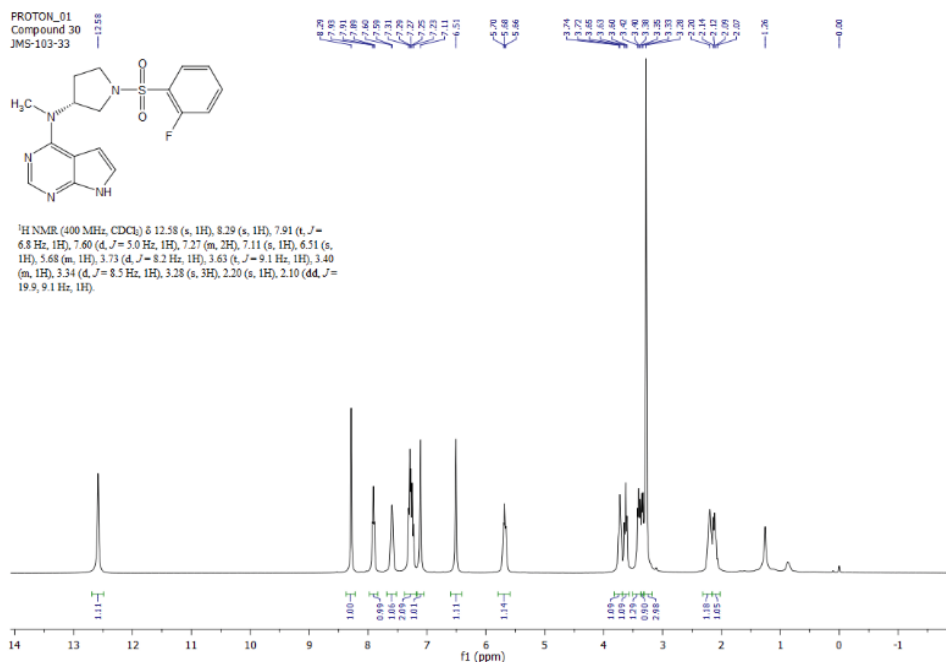
(R)-*N*-Methyl-*N*-(1-((1-methyl-1*H*-imidazol-4-yl)sulfonyl)pyrrolidin-3-yl)-7*H*-pyrrolo[2,3-*d*]pyrimidin-4-amine, **80**



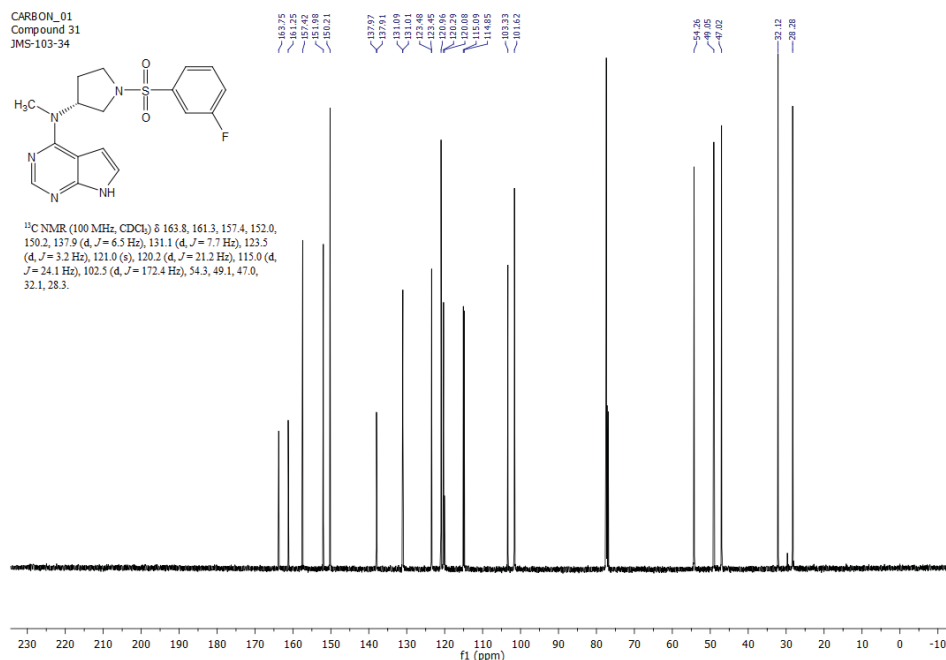
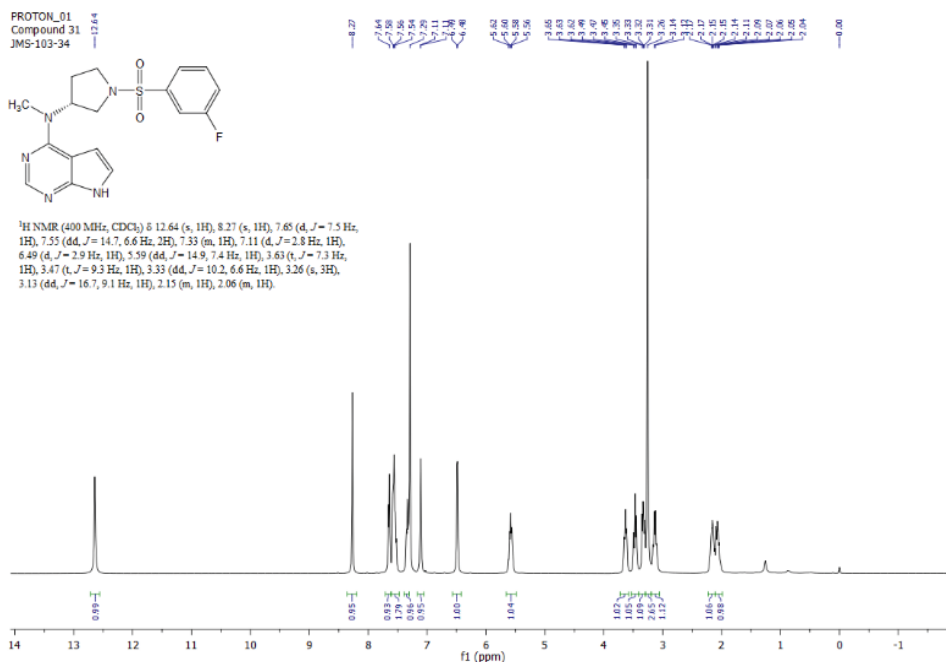
(R)-*N*-Methyl-*N*-(1-(phenylsulfonyl)pyrrolidin-3-yl)-7*H*-pyrrolo[2,3-*d*]pyrimidin-4-amine, **81**



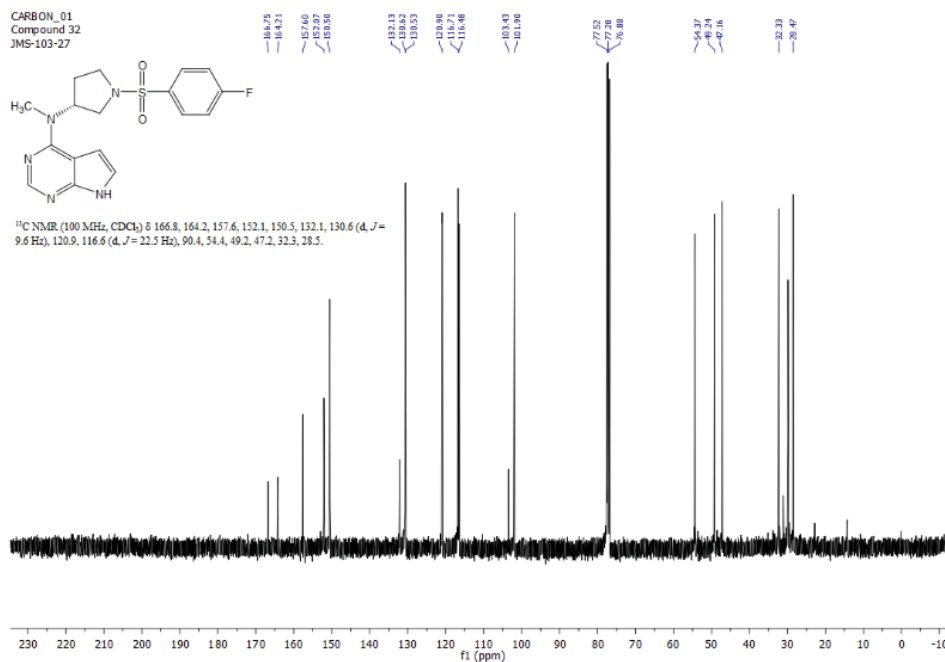
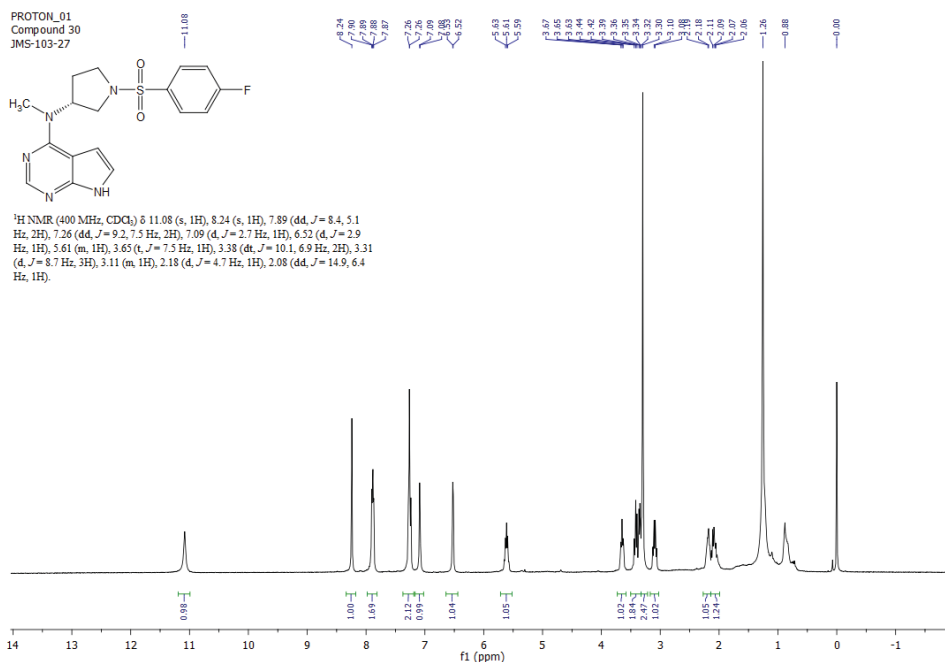
(R)-*N*-(1-((2-Fluorophenyl)sulfonyl)pyrrolidin-3-yl)-*N*-methyl-7*H*-pyrrolo[2,3-*d*]pyrimidin-4-amine, **82**



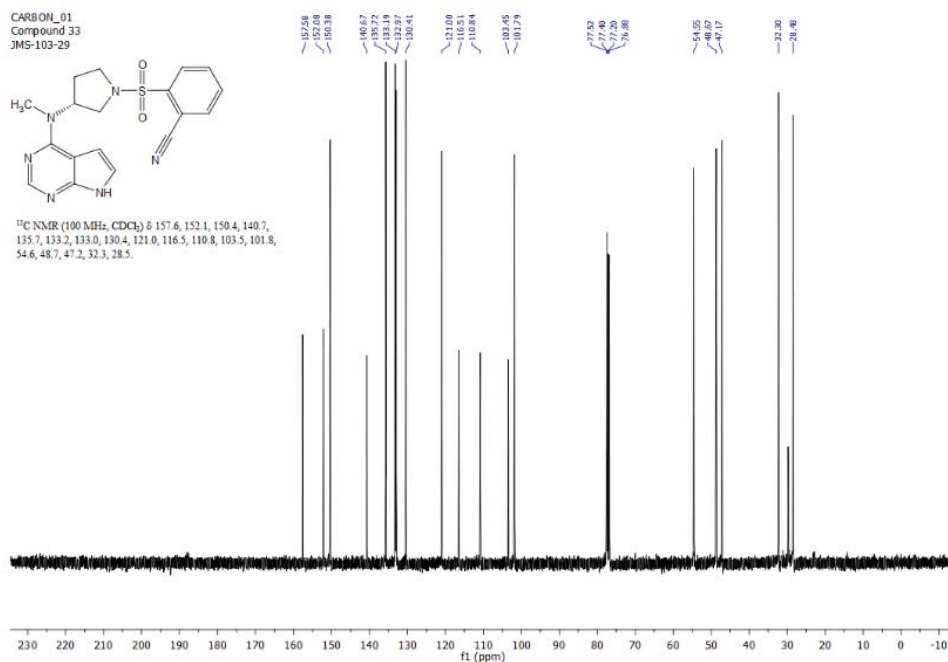
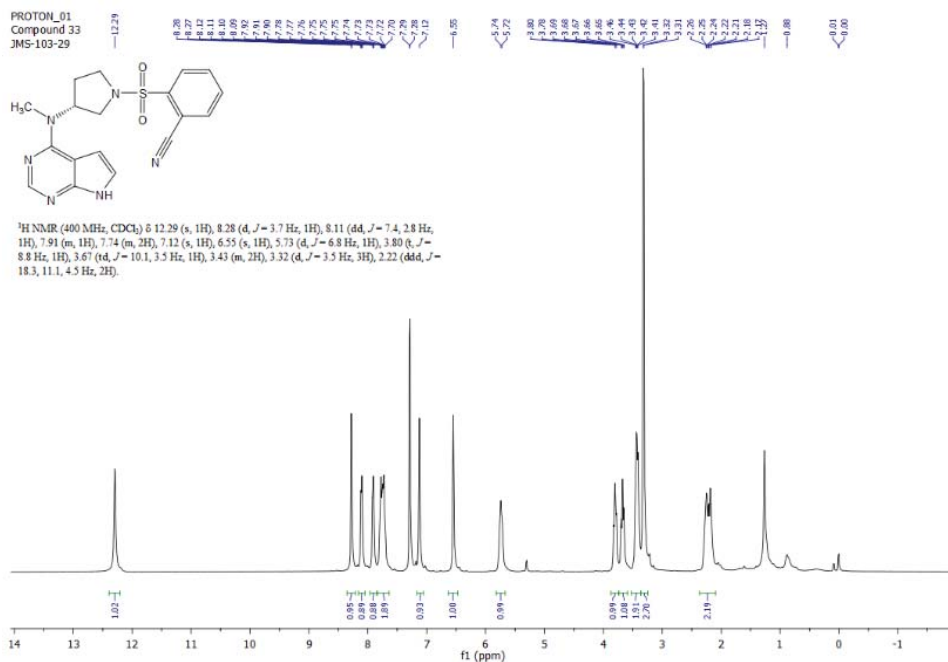
(R)-*N*-(1-((3-Fluorophenyl)sulfonyl)pyrrolidin-3-yl)-*N*-methyl-7*H*-pyrrolo[2,3-*d*]pyrimidin-4-amine, **83**



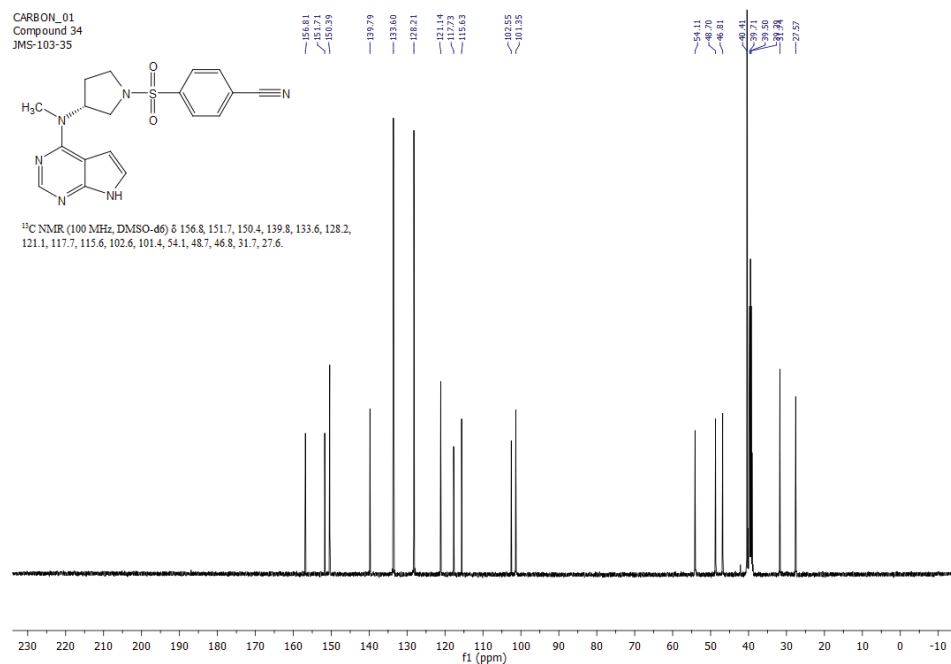
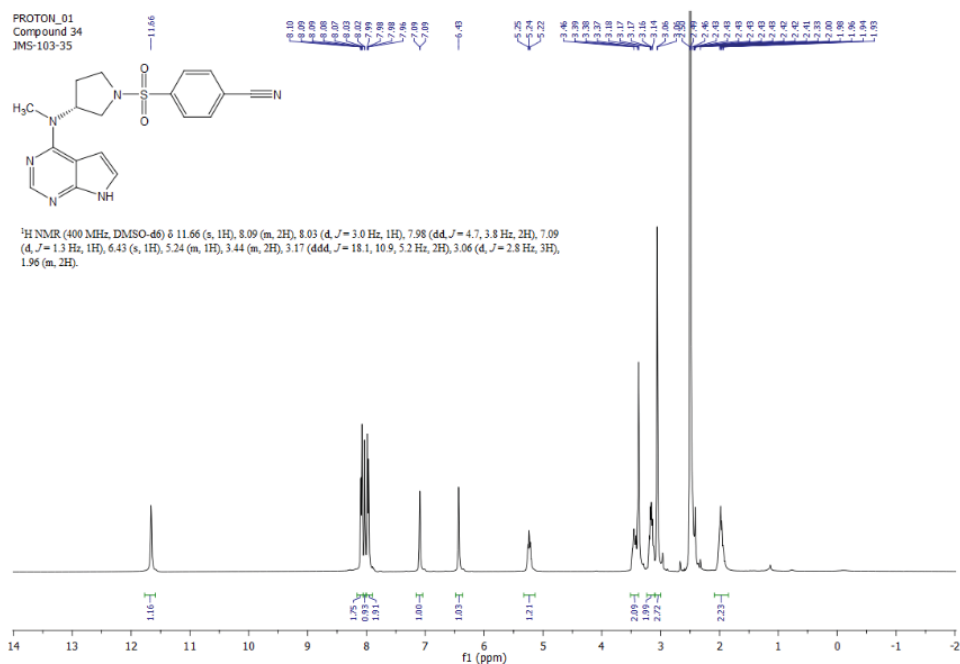
(R)-*N*-(1-((4-Fluorophenyl)sulfonyl)pyrrolidin-3-yl)-*N*-methyl-7*H*-pyrrolo[2,3-*d*]pyrimidin-4-amine, **84**



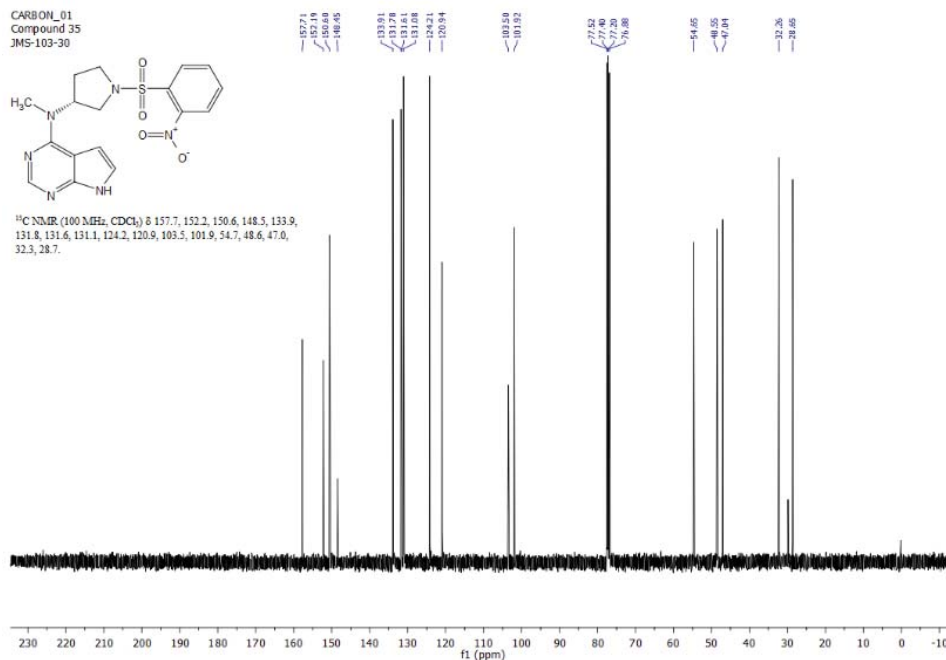
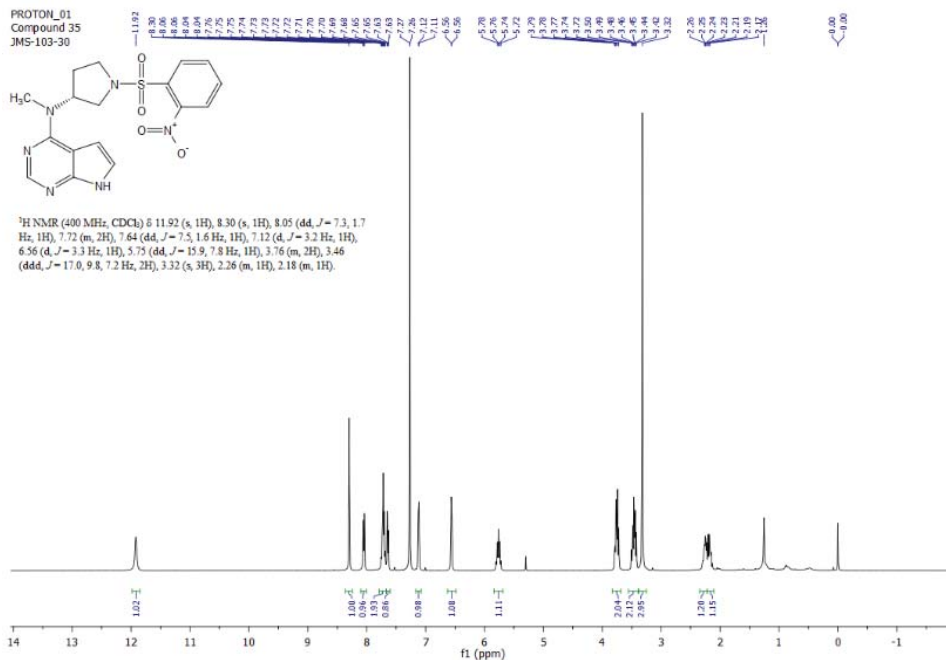
(R)-2-((3-(Methyl(7*H*-pyrrolo[2,3-*d*]pyrimidin-4-yl)amino)pyrrolidin-1-yl)sulfonyl)benzonitrile, **85**



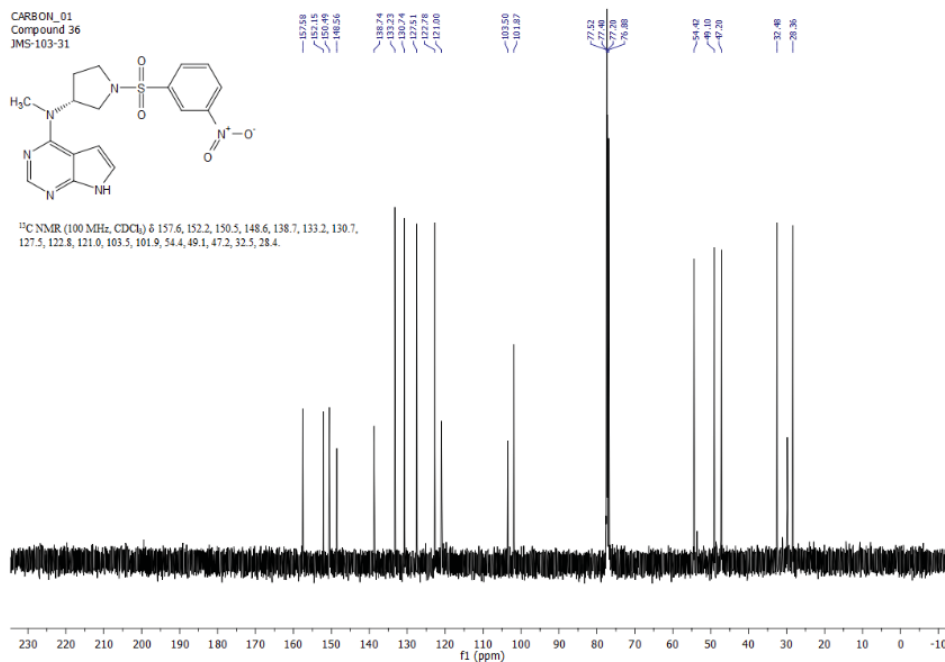
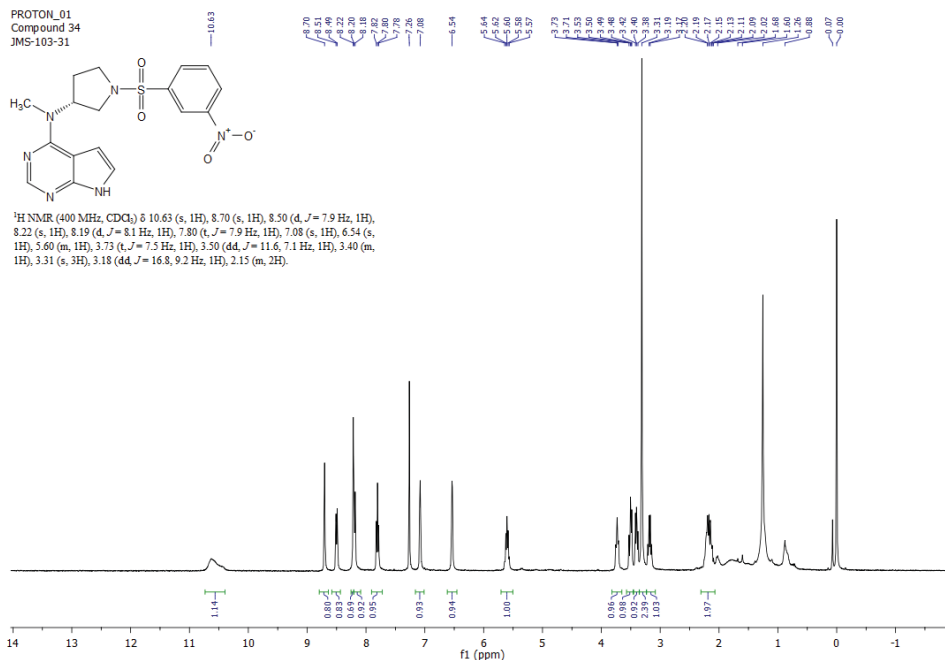
(R)-4-((3-(Methyl(7H-pyrrolo[2,3-d]pyrimidin-4-yl)amino)pyrrolidin-1-yl)sulfonyl)benzonitrile, **86**



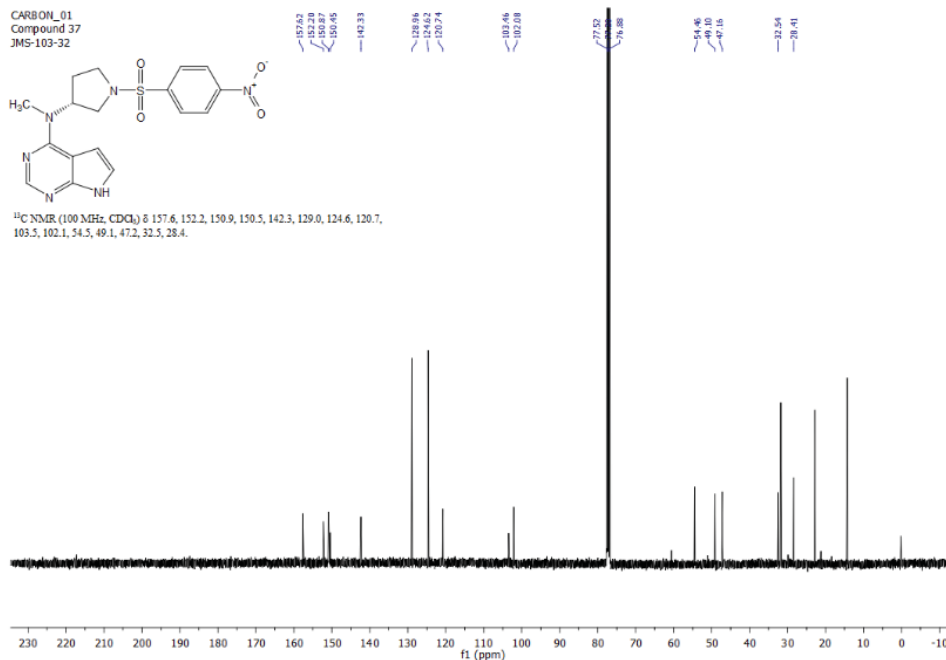
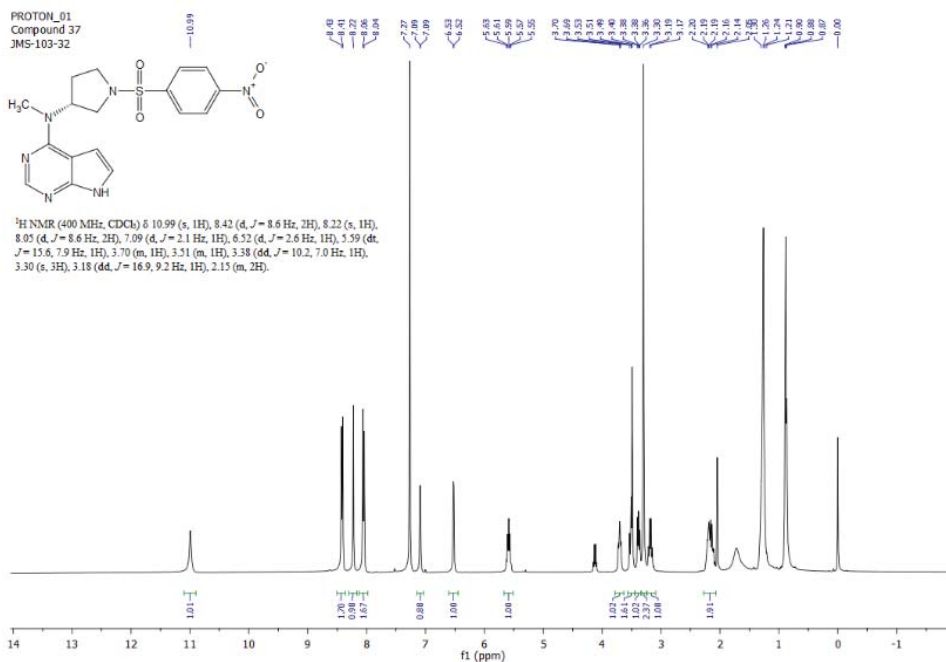
(R)-*N*-Methyl-*N*-(1-((2-nitrophenyl)sulfonyl)pyrrolidin-3-yl)-7*H*-pyrrolo[2,3-*d*]pyrimidin-4-amine, **87**



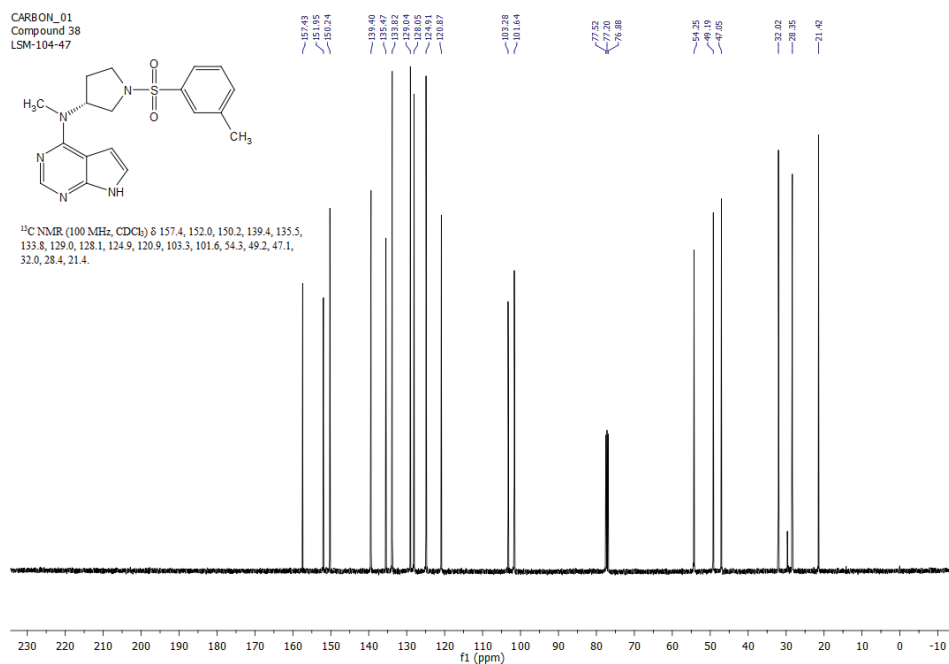
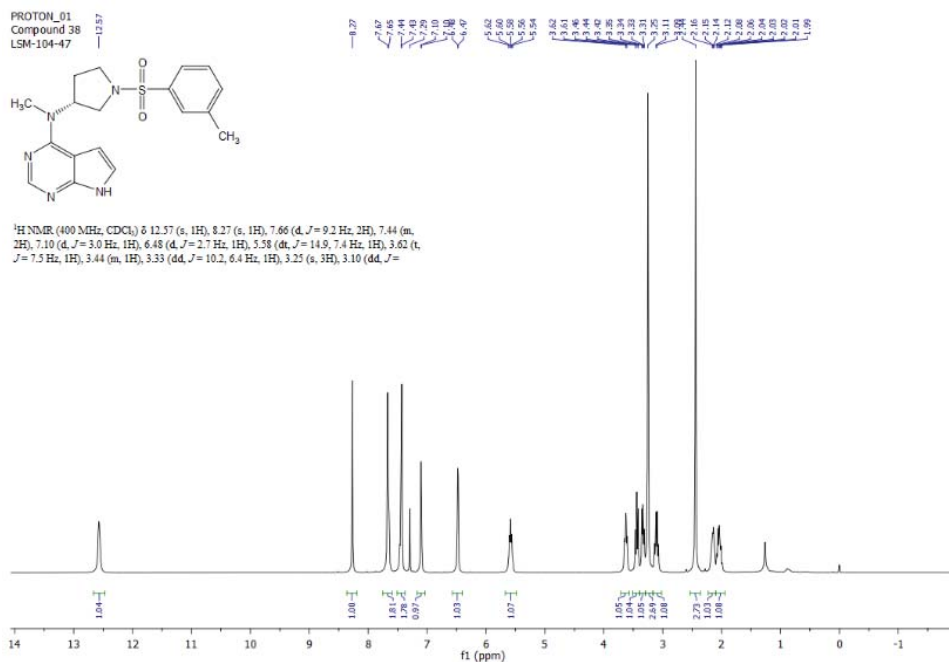
(R)-*N*-Methyl-*N*-(1-((3-nitrophenyl)sulfonyl)pyrrolidin-3-yl)-7*H*-pyrrolo[2,3-*d*]pyrimidin-4-amine, **88**



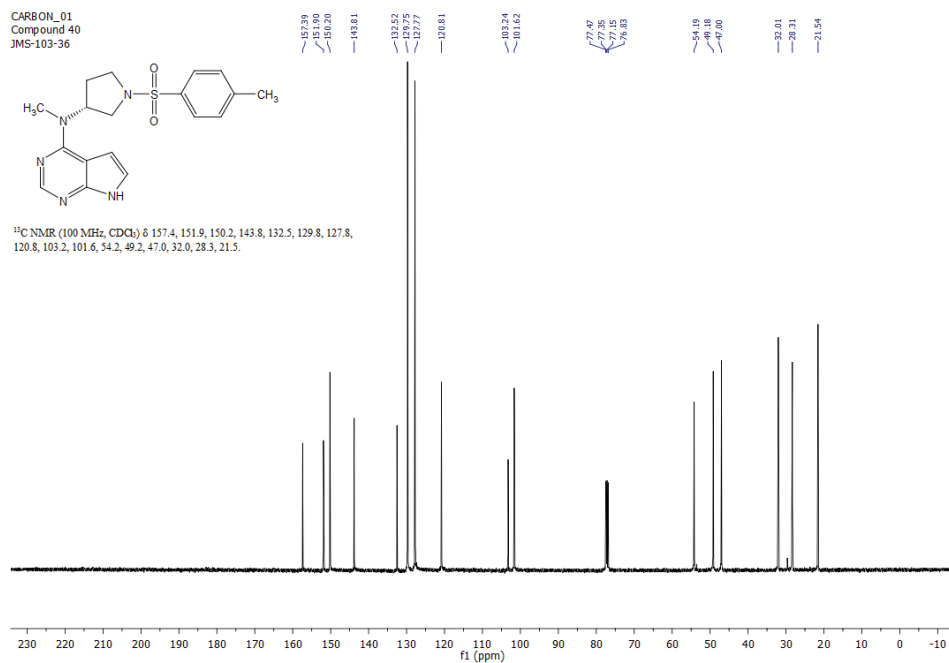
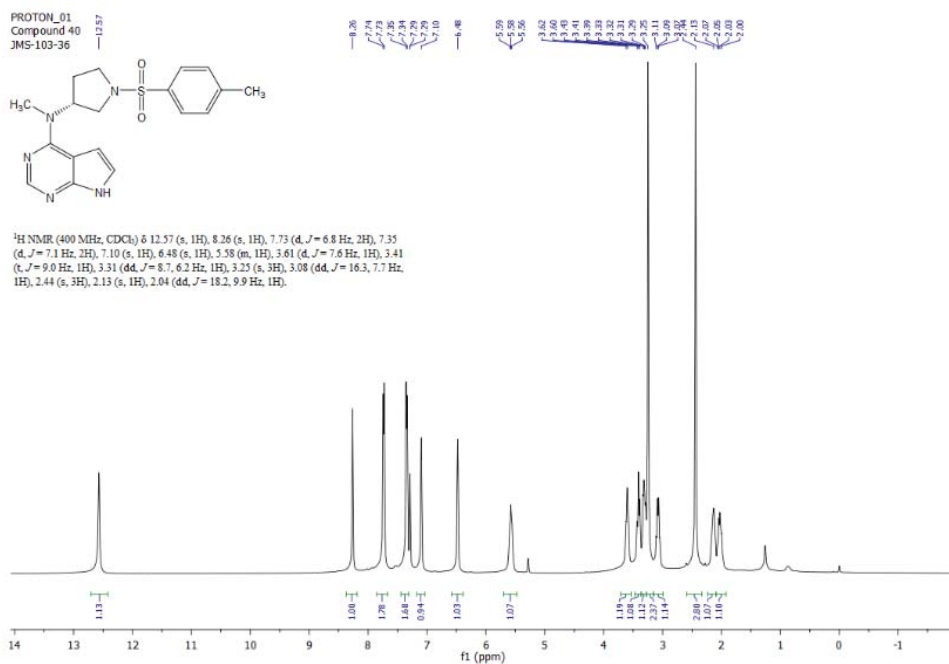
(R)-*N*-Methyl-*N*-(1-((4-nitrophenyl)sulfonyl)pyrrolidin-3-yl)-7*H*-pyrrolo[2,3-*d*]pyrimidin-4-amine, **89**



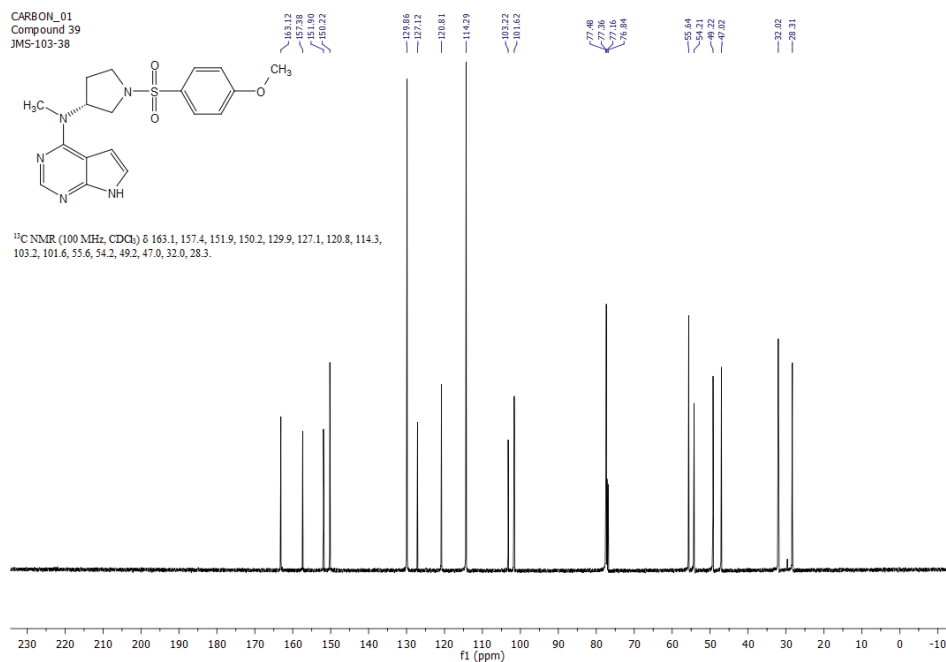
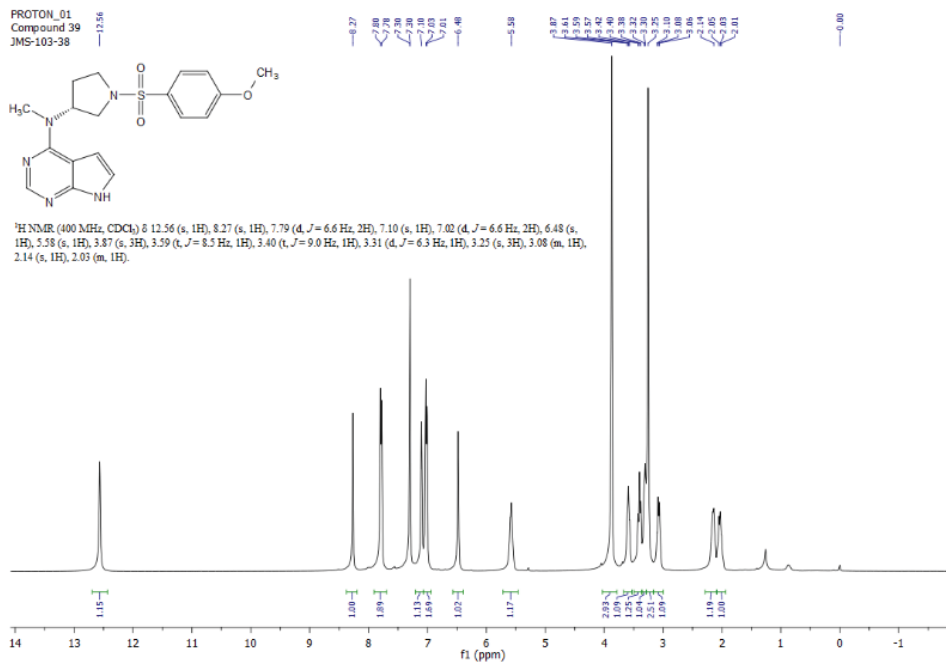
(R)-*N*-Methyl-*N*-(1-(*m*-tolylsulfonyl)pyrrolidin-3-yl)-7*H*-pyrrolo[2,3-*d*]pyrimidin-4-amine, **90**



(R)-*N*-Methyl-*N*-(1-tosylpyrrolidin-3-yl)-7*H*-pyrrolo[2,3-*d*]pyrimidin-4-amine, **91**



(R)-*N*-(1-((4-Methoxyphenyl)sulfonyl)pyrrolidin-3-yl)-*N*-methyl-7*H*-pyrrolo[2,3-*d*]pyrimidin-4-amine, **92**



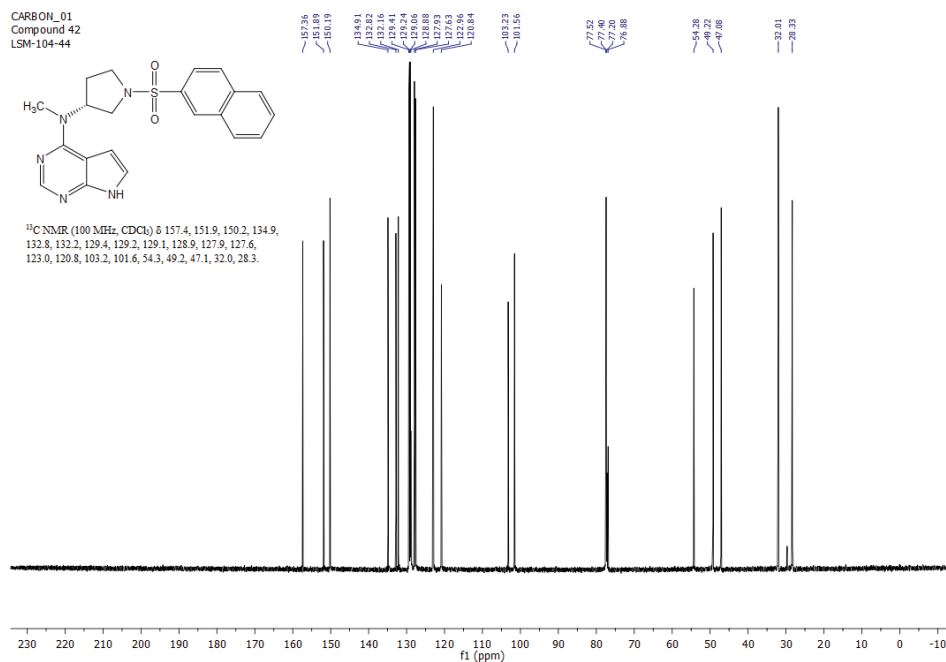
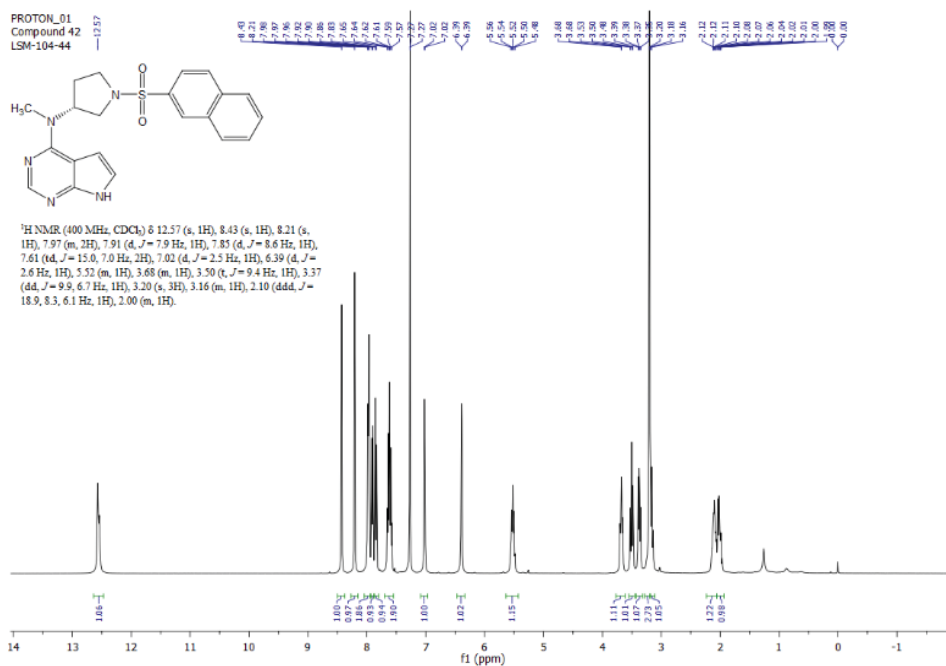
PROTON_01
Compound 41
JMS-103-37

C[C@@H]1CCCN1C2=NC3=C(N)C=CC=C3N=C2C(=O)N(C(=O)c4ccc(C(F)(F)F)cc4)C5=CC=CC=C5

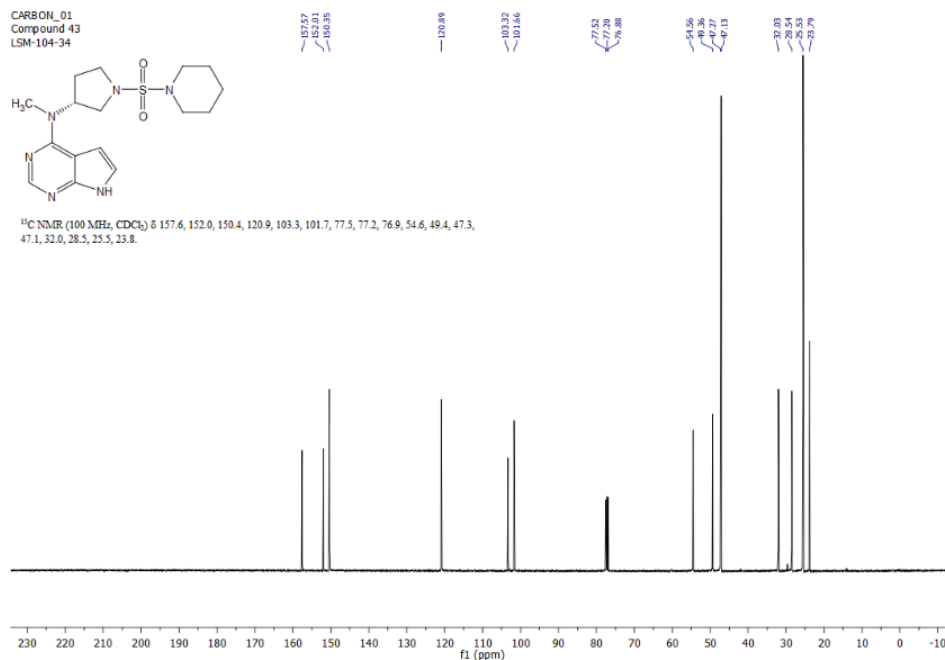
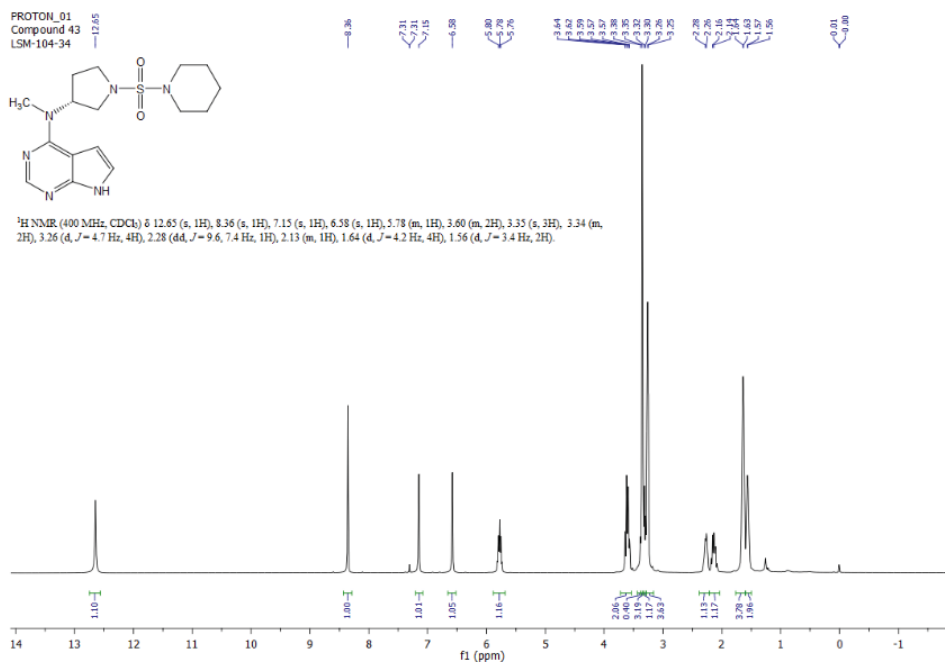
^1H NMR (400 MHz, DMSO- d_6) δ 11.71 (s, 1H), 8.05 (m, 5H), 7.12 (s, 1H), 6.48 (s, 1H), 5.28 (dd, $J = 14.4$, 7.2 Hz, 1H), 3.51 (s, 1H), 3.43 (dd, $J = 18.2$, 8.2 Hz, 3H), 3.22 (m, 2H), 3.12 (m, 3H), 2.04 (m, 2H).



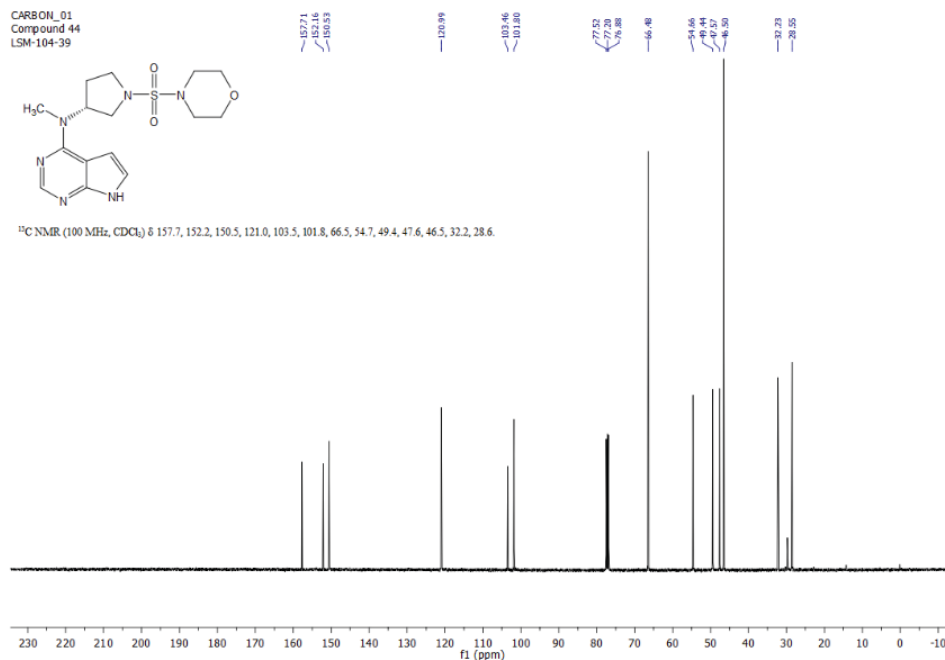
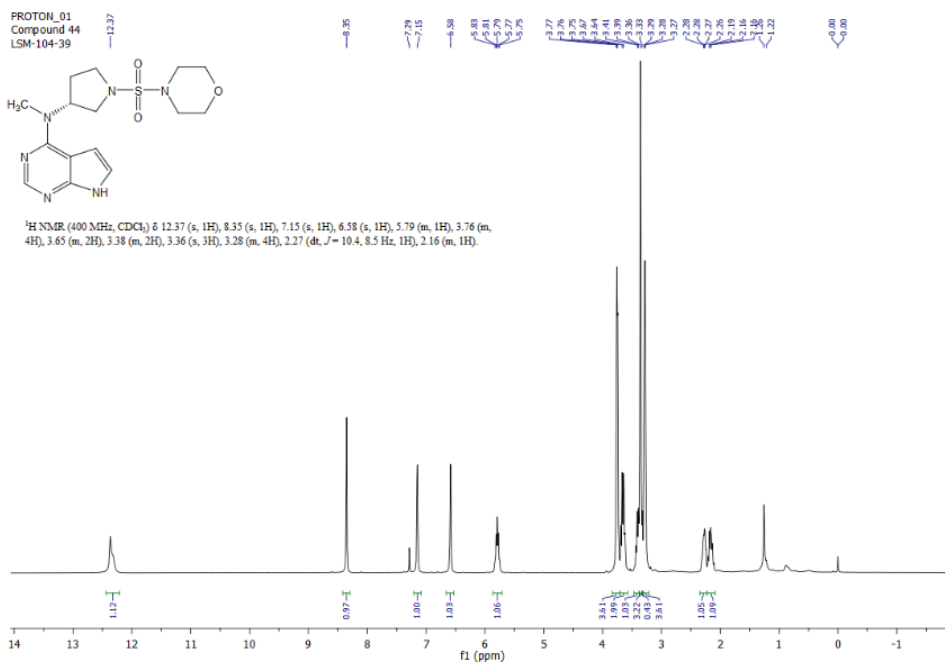
(R)-N-Methyl-N-(1-(naphthalen-2-ylsulfonyl)pyrrolidin-3-yl)-7H-pyrrolo[2,3-d]pyrimidin-4-amine, **94**



(R)-*N*-Methyl-*N*-(1-(piperidin-1-ylsulfonyl)pyrrolidin-3-yl)-7*H*-pyrrolo[2,3-*d*]pyrimidin-4-amine, **95**



(R)-*N*-Methyl-*N*-(1-(morpholinyl)sulfonyl)pyrrolidin-3-yl)-7*H*-pyrrolo[2,3-*d*]pyrimidin-4-amine, **96**



국문초록

핵심 뼈대구조로서 (*R*)-*N*-메틸-*N*-(5-아자스피로[2.4]헵탄-7-일)-7*H*-피콜로[2,3-*d*]피리미딘-4-아민을 이용하여, JAK1 선택적 억제제인 (*R*)-3-(7-(메틸(7*H*-피콜로[2,3-*d*]피리미딘-4-일)아미노)-5-아자스피로[2.4]헵탄-5-일)-3-옥소프로판니트릴 [(*R*)-**6c**]을 발굴하였다. 이 화합물의 구조적 설계는 토파시티닙의 7-디아자퓨린과 5-아자스피로[2.4]헵탄-7-아민의 조합을 기반으로 하였다. 화합물 (*R*)-**6c**은 JAK1의 IC₅₀가 8.5 nM이었고, JAK2에 대해 JAK1 선택성 지수는 48배였다. 선도물질로서 화합물 (*R*)-**6c**의 최적화를 위해 세포기반 분석, 인간 전혈 시험, 시험관 수준 ADME, hERG, 인산화효소 프로파일링, 및 약동학 시험을 진행하였다. 마우스 및 랫트 생체 시험을 통해, 화합물 (*R*)-**6c**의 CIA 및 AIA 모델에서의 효력을 확인하였다.

Key words: JAK 억제제, 류마티스 관절염, JAK1-선택적, 콜라겐-유도성 관절염 마우스 모델, adjuvant-유동성 관절염 랫트 모델